PB-230 885

REMOTE SENSING OF AIR POLLUTION IN URBAN AREAS

M. L. Streiff, et al

General Dynamics

Prepared for:

Environmental Protection Agency

August 1973

DISTRIBUTED BY:

NTIS
National Technical Information Service
U. S. DEPARTMENT OF COMMERCE
5285 Port Royal Road, Springfield Va. 22151

EPA- 650/2-73-026

REMOTE SENSING OF AIR POLLUTION IN URBAN AREAS

Reproduced from
best available copy.

by

M. L. Streiff and C. B. Ludwig

General Dynamics
Convair Aerospace Division
P. O. Box 1128
San Diego, California 92112

Contract Number 68-02-0020
Program Element No. 1A1010

EPA Project Officer: William F. Herget

Chemistry and Physics Laboratory
National Environmental Research Center
Research Triangle Park, N. C. 27711

Prepared for

OFFICE OF RESEARCH AND DEVELOPMENT
U.S. ENVIRONMENTAL PROTECTION AGENCY
Washington, D. C. 20460

August 1973

ia

This report has been reviewed by the Environmental Protection Agency and approved for publication. Approval does not signify that the contents necessarily reflect the views and policies of the Agency, nor does mention of trade names or commercial products constitute endorsement or recommendation for use.

BIBLIOGRAPHIC DATA SHEET

1. Report No. EPA-650/2-73-026

2.

PB 230 885

4. Title and Subtitle

Remote Sensing of Air Pollution in Urban Areas

5. Report Date August 1973

6.

7. Author(s) M. L. Streiff and C. B. Ludwig

8. Performing Organization Rept. No.

9. Performing Organization Name and Address

General Dynamics
Convair Aerospace Division
P. O. Box 1128
San Diego, California 92112

10. Project/Task/Work Unit No.

11. Contract/Grant No. 68-02-0020

12. Sponsoring Organization Name and Address

OFFICE OF RESEARCH AND DEVELOPMENT
U. S. ENVIRONMENTAL PROTECTION AGENCY
Washington, D. C. 20460

13. Type of Report & Period Covered

14.

15. Supplementary Notes See report EPA-R2-72-052 (GDC-DBE-72-001) for a description of the ROSE system along with preliminary field tests made in San Diego. PB 221073

16. Abstracts Remote sensing of air pollution was made using a scanning spectrometer (Rose system) and a Michelson interferometer. Both systems were for transmission measurements over nominal path lengths of 1 and 2 miles and for stack emission measurements. A comparison shows that the spectra of both instruments are of the same quality. A comparison of both instruments is made and the advantages and disadvantages are cited. In addition to the above measurements, the ROSE system alone was used to measure the pollution from an extended source (oil refinery) over a path length of 1/4 mile. All of the spectra were analyzed and a number of pollutants were identified. In the transmission measurements, the ozone and carbon monoxide concentrations as a function of time were determined. Pollutants such as CO, SO_2 and HC were identified in stack emission measurements. The analysis of molecular spectra is described. The field ruggedness and operational performance of the ROSE system was demonstrated by these test to be satisfactory. A portion of this study was supported by the General Dynamics Electro Dynamic Division (Pomona); the results of this portion of the study are reported in TM 6-125 PH-336 which is reproduced as an appendix to this report.

17. Key Words and Document Analysis. 17a. Descriptors

Air pollution
Concentration (composition)
Spectrometers
Urban areas
Sulfur dioxide
Ozone
Hydrocarbons
Optical interferometer
Carbon monoxide
Exhaust emissions
Plumes
Spectrum analysis
Tests
References
Steel mills

17b. Identifiers/Open-Ended Terms

ROSE (Remote Optical Sensing of Emission)
Area source

Reproduced by
NATIONAL TECHNICAL
INFORMATION SERVICE
U S Department of Commerce
Springfield VA 22151

17c. COSATI Field/Group 13B

18. Availability Statement

19. Security Class (This Report) UNCLASSIFIED

20. Security Class (This Page) UNCLASSIFIED

21. No. of Pages [illegible]

22. Price 12.25/1.45

FORM NTIS-35 (10-70)

USCOMM-DC 40329-P71

TABLE OF CONTENTS

Section		Page
	LIST OF FIGURES	iv
	LIST OF TABLES	vi
	SUMMARY	vii
1	INTRODUCTION	1-1
2	ANALYSIS OF MOLECULAR SPECTRA	2-1
	2.1 THE CONCEPT OF EQUIVALENT WIDTH - LABORATORY PROCEDURE	2-1
	2.2 SPECTRA OF POLLUTANTS AND ABSORPTION COEFFICIENTS	2-11
3	PERFORMANCE OF THE ROSE SYSTEM	3-1
	3.1 GENERAL	3-1
	3.2 SYSTEM NOISE	3-2
	3.3 SCINTILLATION NOISE	3-3
	3.4 SIGNAL STRENGTH	3-5
4	LONG-PATH TRANSMISSION MEASUREMENTS	4-1
	4.1 ONE MILE MEASUREMENTS	4-1
	4.2 TWO MILE MEASUREMENTS	4-15
5	EMISSION MEASUREMENTS	5-1
	5.1 STEEL MILL	5-1
	5.2 POWER STATION	5-5
	5.3 HOSPITAL INCINERATOR	5-5

TABLE OF CONTENTS

Section		Page
6	TRANSMISSION MEASUREMENTS OF EXTENDED SOURCES	6-1
7	SUPPORTING LABORATORY DATA	7-1
	7.1 DETECTOR, NOISE MEASUREMENTS	7-1
	7.2 MONOCHROMATOR CALIBRATION - TEMP. EFFECT	7-6
8	RECOMMENDATIONS	8-1
9	REFERENCES	9-1
	APPENDIX	
	I REPORT TM 6-125 Ph-336	A-0
	II MOLECULAR SPECTRA TABLES	A-49

LIST OF FIGURES

Figure Page

2-1 True Spectral Line Shape 2-3
2-2 Observed Line Shape Assuming a Triangular Slit Function 2-3
2-3 Collision Broadened Curves of Growth for Various Intensity Distributions 2-7
3-1 Relative Signals from Source and Reference Channels - One Mile Path 3-6
3-2 Calculated System Transmission 3-7
3-3 Calculated Transmission Resulting from Aberrations 3-8
4-1 7 to 13 μ Scan with One Mile Path, $\Delta\nu_{10} = 5\ \mathrm{cm}^{-1}$ 4-2
4-2 Noise at 1000 cm^{-1} with One Mile Path, $\Delta\nu_{10} = 5\ \mathrm{cm}^{-1}$ 4-3
4-3 7 to 13 μ Scan with One Mile Path, $\Delta\nu_{10} = 1\ \mathrm{cm}^{-1}$ 4-4
4-4 Noise at 1000 cm^{-1} with One Mile Path, $\Delta\nu_{10} = 1\ \mathrm{cm}^{-1}$ 4-5
4-5 7 to 13 μ I/I_o Scan with One Mile Path $\Delta\nu_{10} = 5\ \mathrm{cm}^{-1}$ 4-6
4-6 3 to 5 μ Scan with One Mile Path, $\Delta\nu_4 = 6\ \mathrm{cm}^{-1}$ 4-8
4-7 Noise at 2500 cm^{-1} with One Mile Path, $\Delta\nu_4 = 6\ \mathrm{cm}^{-1}$ 4-9
4-8 3 to 5 μ I/I_o Scan with One Mile Path, $\Delta\nu_4 = 6\ \mathrm{cm}^{-1}$ 4-10
4-9 Volz Photometer Calibration and Typical Aerosol Optical Thickness Variation in San Diego, California 4-12
4-10 Volz Photometer Measurements 4-13
4-11 Noise at 2500 cm^{-1} with Two Mile Path, $\Delta\nu_4 = 3\ \mathrm{cm}^{-1}$ 4-15
4-12 8 to 13 μ Scan with Two Mile Path, $\Delta\nu_{10} = 1\ \mathrm{cm}^{-1}$ 4-16
4-13 Ozone Concentration with Time - July 28, 1972 4-18
4-14 3 to 5 μ Scan with Two Mile Path, $\Delta\nu_4 = 3\ \mathrm{cm}^{-1}$ 4-19
4-15 Digitized Spectrum of CO Band, $\Delta\nu \sim 1.8\ \mathrm{cm}^{-1}$ 4-20
5-1 Sky Background 5-2
5-2 Coke Oven Plume Emission 5-2
5-3 Difference (Plume - Sky) 5-2
5-4 Stack Emission - Steel Mill, $\Delta\nu_4 = 9\ \mathrm{cm}^{-1}$ 5-4

LIST OF FIGURES

Figure		Page
5-5	Plume, Sky and Stack Scans Power Station Stack #3, $\Delta\nu_{10} = 3\ \mathrm{cm}^{-1}$	5-6
5-6	Difference Spectrum (Plume - Sky) Power Plant Stack #3	5-7
5-7	Plume Scan, 3 - 5 μ, Power Plant Stack #3	5-8
5-8	Variations in Plume Emission - Power Plant Stack #3	5-9
5-9	Variations of Hospital Incinerator Emission, $\nu = 2390\ \mathrm{cm}^{-1}$	5-11
5-10	Comparison of Two Scans, 3 to 5 μ, Hospital Incinerator	5-12
6-1	Comparison of CO Spectra with $\Delta\nu = 4.4\ \mathrm{cm}^{-1}$ and $1.3\ \mathrm{cm}^{-1}$	6-2
6-2	CO Spectrum at Refinery, $\Delta\nu = 1.3\ \mathrm{cm}^{-1}$	6-3
6-3	3 to 5 μ Scan at Refinery, $\Delta\nu_4 = 1.4\ \mathrm{cm}^{-1}$	6-5
6-4	Comparison of Spectra Near $3000\ \mathrm{cm}^{-1}$	6-6
6-5	7 - 13 μ Scan at Refinery $\Delta\nu_{10} = 0.65\ \mathrm{cm}^{-1}$	6-7
7-1	Waveanalyzer Measurements of Detector Noise	7-2
7-2	Analog Measurements of Noise	7-5
7-3	Divider Box Schematic	7-9

LIST OF TABLES

Table		Page
A.1	Band Strengths and Band-Averaged Absorption Coefficients and Fine Structure Parameters of Pollutants	A-49
A.2	Band Model Parameters for CO in 5 and 20 cm^{-1} Intervals	A-50
A.3	Band Model Parameters for CO_2 in 5 and 20 cm^{-1} Intervals	A-52
A.4	Band Model Parameters for SO_2 in 5 and 20 cm^{-1} Intervals	A-56
A.5	Band Model Parameters for NO_2 in 5 and 20 cm^{-1} Intervals	A-58
A.6	Band Model Parameters for NO in 5 and 20 cm^{-1} Intervals	A-60
A.7	Band Model Parameters for N_2O in 5 and 20 cm^{-1} Intervals	A-61
A.8	Band Model Parameters for NH_3 in 5 and 20 cm^{-1} Intervals	A-65
A.9	Band Model Parameters for HCHO in 5 and 20 cm^{-1} Intervals	A-69
A.10	Band Model Parameters for H_2O in 5 and 20 cm^{-1} Intervals	A-71
A.11	Band Strengths and Fine Structure Parameters of Pollutants not Included in Table D-3	A-79
A.12	Absorption Coefficients for HCl	A-80
A.13	Absorption Coefficients for HF	A-81
A.14	Absorption Coefficients for CH_4	A-82
A.15	Absorption Coefficients for C_2H_4	A-83
A.16	Absorption Coefficients for PAN	A-84
A.17	C_6H_6 Benzene	A-85
A.18	18-O_3 - Ozone	A-85

SUMMARY

Remote sensing of air pollution was made using a scanning spectrometer (ROSE system) and a Michelson interferometer. Both systems were used for transmission measurements over nominal path lengths of 1 and 2 miles and for stack emission measurements. A comparison shows that the spectra of both instruments are of the same quality. The greater throughput and multiplex advantage of the interferometer system manifests itself in the shorter time required to take the spectra, (typically, 10 sec versus 1200 sec). This time advantage is partly lost when the effort is considered which is required to reduce the interferograms to spectra by a computer. However, when an on-the-line computer is available, this effort would be greatly reduced.

In addition to the above measurements, the ROSE system alone was used to measure the pollution from an extended source (oil refinery) over a path length of 1/4 mile.

All of the spectra were analyzed and a number of pollutants were identified. In the transmission measurements, the ozone and carbon monoxide concentrations as a function of time were determined. The presence of other pollutants such as nitrogen dioxide, sulfur dioxide and several hydrocarbons is indicated. A more definite identification and determination of concentration can be made, when a computer analysis procedure is operational. In the stack emission measurements, pollutants such as carbon monoxide, sulfur dioxide and many hydrocarbons were identified.

Transmission spectra taken during hot days were influenced by scintillation noise, but much less than anticipated. Typically, a signal-to-peak-to-peak-noise ratio of 26 observed during a test at night is reduced to about 9 during a test on a hot day. Also, signal fluctuations during stack emission measurements were less than anticipated. However, this holds true only when the field-of-view is smaller

than the plume.

The field ruggedness and operational performance of the ROSE system was demonstrated by these tests to be satisfactory. A number of problems which did arise during the course of the testing were corrected either during or after the test period.

1

INTRODUCTION

Remote sensing of air pollution in the Los Angeles area with the "Remote Optical Sensing of Emission (ROSE)" system is described. The work was conducted in June, July and October 1971, under contract 68-02-0020 with the Environmental Protection Agency. A portion of the study was supported by the General Dynamics Electro Dynamic Division (Pomona); the results of this portion of the study are reported in TM 6-125 Ph-336 which is reproduced in the Appendix of this report.

A complete description of the ROSE system is presented in report EPA-R2-72-052 (GDC-DBE-72-001) along with a description of preliminary field tests made in San Diego over a path length of about 1/4 mile on June 23 and 24, 1971.

The analysis of molecular spectra is set forth in Section 2 of this report.

The performance of the ROSE system under field conditions is discussed in Section 3 of this report.

Transmission measurements are reported in Section 4 of this report. These tests were made, with a nominal one-mile path length, from June 29 to July 2, 1971, and, with a nominal two-mile path length, from July 27 to 29, 1971.

Emission tests were made of sources at three locations on successive days from July 13 to 15, 1971 inclusive: a steel mill, a power plant and a hospital incinerator. The results of these tests are reported in Section 5 of this report.

Extended source transmission measurements at an oil refinery location were made on October 20 and 21, 1971 with a path length of approximately 1/4 mile. The results of these tests are given in Section 6 of this report.

Supporting laboratory work is described in Section 7 of this report.

The program leader for these tests was Dr. C. B. Ludwig assisted by Dr. M. Griggs; they were responsible for test planning (together with government project officers), conduction of the field tests and report preparation until their departure from the company in mid-1972. M. L. Streiff assisted by C. R. Claysmith was responsible for equipment operation and modifications during and after the field tests. Mr. Streiff had principal responsibility for completion of the field test report. Mr. G. W. Ashley was in charge of the Pomona interferometer activities.

The government project officers were Mr. John S. Nader and Dr. William F. Herget. They were assisted by Dr. H. M. Barnes and Mr. R. Rollins during the field tests.

2

ANALYSIS OF MOLECULAR SPECTRA

2.1 THE CONCEPT OF EQUIVALENT WIDTH - LABORATORY PROCEDURE

The remote sensing of pollutants is presently done with scanning instruments which have a spectral resolution from 1 cm^{-1} to several wave numbers. In the case of diatomic and light polyatomic molecules, single lines can be observed with a spectral resolution of 0.1 cm^{-1}. In the case of heavier polyatomic molecules and of lower spectral resolution, a number of lines will be observed simultaneously. Thus, for the interpretation of measured spectra in terms of pollutant concentration, spectral parameters have to be known both for the single line and multiple line cases.

2.1.1 Single Line with Lorentz Shape

The total absorption over a wavenumber interval $\Delta\omega$ containing the entire line is given by the Ladenberg-Reiche function.

$$W = 2\pi\alpha x e^{-x} I_o(x) + I_1(x)) \qquad (2\text{-}1)$$

where W is the equivalent width (cm^{-1}), α is the half width at half height in cm^{-1}, I_o, I_1 are modified Bessel functions and

$$x = Su/2\pi\alpha, \qquad (2\text{-}2)$$

where S is the line strength and u is the optical path (cm-atm). The line shape for a collision broadened line is, according to Lorentz, given by

$$(W) = \frac{\alpha/\pi}{(\omega - \omega_o)^2 + \alpha^2}$$

The two parameters S and α are determined in the laboratory by making curve-of-growth measurements. It is convenient to make measurements in the two limits of small and large values of x:

$$W = Su \qquad \text{for } x < 0.02\,p \tag{2-3}$$

$$W = \text{[illegible]} \qquad \text{for } x > 12.5\,p^{-1} \tag{2-4}$$

These approx[illegible]ed the "linear" and "square root" approximations) are valid within p percent.* For instance, Equations (2-3) and (2-4) are accurate to within 5 percent when $x < 0.1$ and $x > 2.5$, respectively. Experience shows that for a reliable measurement of S three data points in the linear region should be obtained and that for a reliable measurement of the product ($S\alpha$) three data points should be obtained in the square-root region. Care must be exercised that the assumptions of the validity of these approximations are fulfilled. This is done by plotting the data points (W versus u) on logarithmic scales. In the linear region, the plot is a straight line with a slope of 1, and in the square-root region, it is also a straight line with a slope of 1/2. Between these two segments lies the "transition" region.

Experimentally, the procedure is as follows: The spectroscopic instrument with a slit function g is scanned over a single spectral line, whose true shape is shown in Figure 2-1. The true shape of the line is distorted by the slit function $g(\omega-\omega')$, and appears at the output of the instrument in the shape shown in Figure 2-2. One can show that the area under the spectral line (total absorption = equivalent width) is the same in Figure 2-1 and 2-2. That means that W is an invariant and does not depend upon the slit function of the instrument. In other words, the W determined in the laboratory with one instrument can be used to interpret the field data taken with another instrument. In mathematical terms, this fundamental fact is expressed as

---

*G. N. Plass JOSA 48 690 (1958)

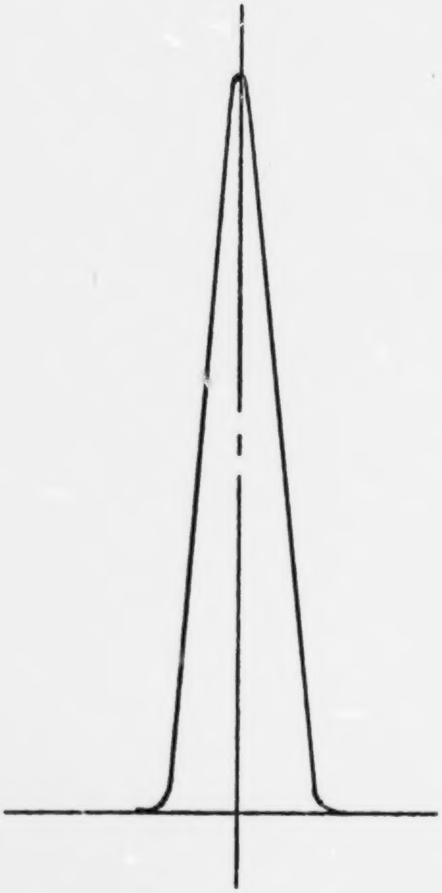

Fig. 2-1. True Spectral Line Shape

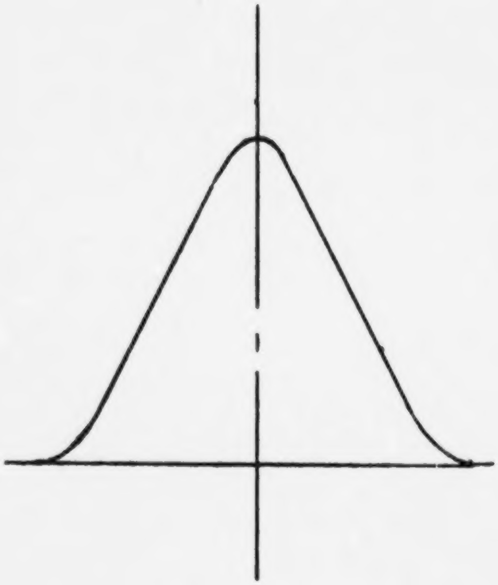

Fig. 2-2. Observed Line Shape Assuming a Triangular Slit Function

$$W = \int_{\Delta\omega} \left(1 - I^{IN}(\omega)/I_o(\omega)\right) d\,\omega \qquad (2\text{-}5)$$

$$= \int_{\Delta\omega} \left(1 - I^{OUT}(\omega)/I_o(\omega)\right) d\,\omega \qquad (2\text{-}6)$$

where $I^{IN}(\omega)$ is the "true" intensity and $I^{OUT}(\omega)$ is the "apparent" intensity as measured by the instrument, given by

$$I^{OUT}(\omega) = \int_{\Delta\omega'} I^{IN}(\omega')\,g(\omega - \omega')\,d\,\omega' \quad . \qquad (2\text{-}7)$$

When Equation (2-7) is introduced into Equation (2-6), one finds that the normalized slit function can be integrated separately, giving unit value and the equality shown in Equation (2-5) and Equation (2-6) holds.

In summary, the procedure for obtaining the laboratory data and the subsequent interpretation of field data is as follows:

1. For each single pollutant line of interest, make three laboratory measurements in the linear region of the curve-of-growth by changing u to obtain $S = W/u$, and three in the square-root region to obtain $\alpha = W^2/4\,Su$.

2. For each single pollutant line of interest, calculate by computer W as a function of u according to Equation (2-1) and electronically plot these curves-of-growth. (The linear and square-root regions are identical to the ones measured under Item 1, thus providing a consistency check.)

3. From the atmospheric spectra measured in the field, obtain W of the pollutant lines of interest according to Equation (2-6) and obtain the desired quantity u from the curve-of-growth prepared under Item 2.

4. An alternate procedure would be to store the values of S and α for each single pollutant line in the computer. After W has been measured in the field, input it together with the line identification into the computer. The computer will iterate Equation (2-1) until the proper u is found.

It is recommended that both procedures be followed. The operator in the field has a set of curves-of-growth and can thus readily obtain u. The computer analysis can be executed more accurately at a later date.

The term "pollutant lines of interest" refers to lines which can be observed in the field without interference. This will eliminate making laboratory measurements on a great number of pollutant lines. A decision of what the "pollutant lines of interest" are can be made a) theoretically, based upon existing spectra of the "clean" atmosphere and the present knowledge of pollutant line position and b) experimentally, after initial field data have been taken.

2.1.2 Multiple Lines with Lorentz Shape

If several lines contribute to the absorption in the spectral interval given by the instrument slit function, band models must be used. The most useful band model applicable to atmospheric pollutants is found to be the statistical model. In that case, the mean absorption is given by

$$1 - \bar{t} = 1 - \exp(-\bar{W}/d) \tag{2-8}$$

where $\bar{W}$ is the mean equivalent width of the lines in this interval and d is the mean line spacing. The following expressions exist for this ratio:

Equally intense lines

$$\frac{\bar{W}}{d} = \frac{2\pi\alpha}{d} \times e^{-x}\left[I_0(x) + I_1(x)\right] , \tag{2-9}$$

Exponential distribution of line intensities

$$\frac{\overline{W}}{d} = \frac{S}{d} u \left(1 + \frac{Su}{4\alpha}\right)^{-1/2} \qquad (2\text{-}10)$$

1/S distribution of line intensities

$$\frac{\overline{W}}{d} = \frac{2\alpha}{d} \left[\left(1 + \frac{Su}{\alpha}\right)^{-1/2} -1 \right] \qquad (2\text{-}11)$$

All of these expressions have the same asymptotic expressions:

$$\frac{\overline{W}}{d} \approx \frac{S}{d} u \quad \text{for} \quad \frac{Su}{\pi\alpha} \ll 1 \qquad (2\text{-}12)$$

$$\frac{\overline{W}}{d} \approx \frac{1}{d} 2 (S\alpha u)^{1/2} \quad \text{for} \quad \frac{Su}{\pi\alpha} \gg 1 \qquad (2\text{-}13)$$

In the transition region, the maximum difference in W/d is about 25% between the equally intense lines and the 1/S distribution (seeFigure 2-3).

A standard notation for the parameters S/d and α/d is

$$\frac{S}{d} = k \qquad (\text{cm}^{-1}\ \text{atm}^{-1})$$

$$\frac{\alpha}{d} = a \qquad (\text{non-dim.})$$

where k represents the average absorption coefficient and a is called the fine-structure parameter.

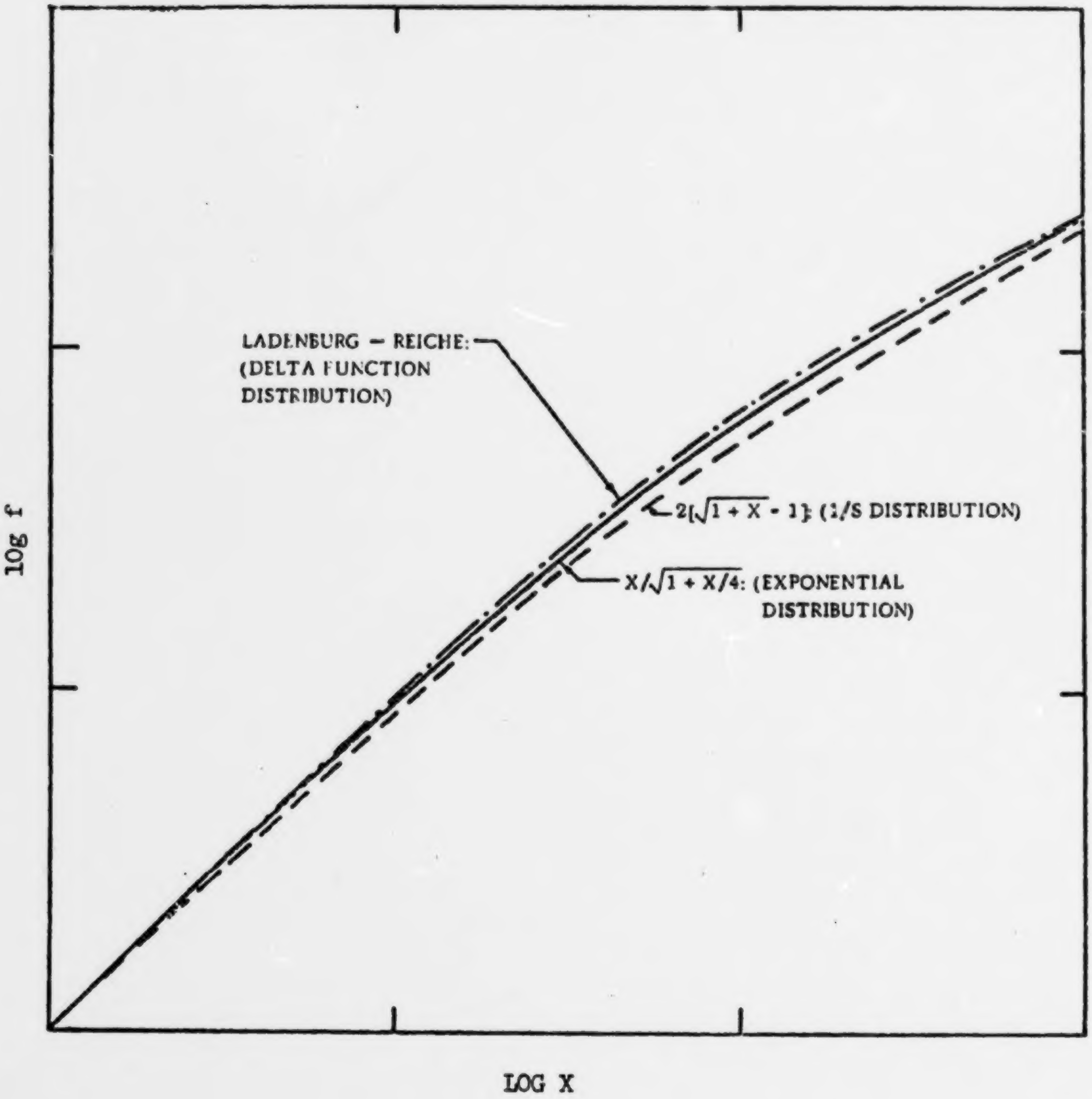

Figure 2-3. Collision-Broadened Curves of Growth for Various Intensity Distributions

The laboratory procedure is the same as previously outlined with one exception. Instead of making measurements only in the linear and square-root regions, measurements in the "transition region" are also required in order to determine which of the three models (given by Equation 2-9), (2-10), or (2-11)) applies.

If an accuracy of ± 12.5% in the transition region is deemed sufficient, the expression given by Equation (2-10) is recommended. In that case

$$-\ln t = ku \left(1 + \frac{ku}{4a}\right)^{-1/2}$$

or

$$\left(\frac{u}{-\ln t}\right)^2 = \frac{1}{k^2} + \frac{u}{4ak} \qquad (2\text{-}14)$$

Equation (2-14) is a linear relationship in u in that the observed quantity $(-u/\ln t)^2$ as a function of u is a straight line. The absorption coefficient k is determined by the intercept of this line at $u = 0$ and the slope determines the product ak. These relations were successfully employed in the determination of the curves-of-growth of hot water vapor.*

In summary, the procedure for obtaining the laboratory data and the subsequent interpretation of field data is as follows:

1. For each wavenumber interval in which a pollutant has a number of lines which are not interfered by lines from other molecules, make laboratory measurements of the curves-of-growth.

2. From the atmospheric spectra measured in the field, obtain $t(\omega) = 1 - I(\omega)/I_0(\omega)$. Determine the desired quantity u from the plots of the curves-of-growth.

---

*C. B. Ludwig Applied Optics 10 1057 (1971)

3. Using a computer, determine which of the expressions for the different line intensity distributions (Equations (2-9), (2-10), or (2-11)) is the most appropriate one. Use that expression to reduce the curves-of-growth in terms of k (ω) and a(ω) and store in memory. The values for t (ω) measured in the field are then readily reduced to u.

Again, as in the single line case, the decision of which of the spectral data are of interest can be made both theoretically and/or experimentally.

2.1.3 Laboratory Procedures

The maximum amount of data points which could be taken in the laboratory is immense. One set of measurements could be taken at room temperature, using air (mixture of N_2 and O_2) as foreign gas broadener with 1 atm total pressure. Another set of measurements could be taken at elevated temperatures, using a mixture of O_2, CO_2 and H_2O as foreign gas broadener. Considering that the diatomic and polyatomic pollutants of interest may amount to 20, that these pollutants have single or multiple infrared bands of about 200 cm^{-1}, that at least five data points are to be taken for each resolution element of 1 cm^{-1}, and that at least six points along the curve-of-growth curve are to be taken, it is easy to see that the total number of data points could run into several hundred thousand. Thus, it is imperative to limit the measurements to spectral intervals which are most useful in field work. As mentioned above, the "spectral intervals of interest" must be determined before a program of laboratory studies is initiated. This determination can be based on the theoretical knowledge of the relative location of pollutant lines with respect to the "clean" atmospheric lines and/or based on the results of field data taken by the ROSE system.

As outlined above, curve-of growth measurements are made by changing the optical thickness u at constant total pressure p_t. Since u is given by the product of cell length ℓ and partial pressure $p_p = C\, p_t$, where C is the fractional concentration and p_t is the total pressure, a change in either ℓ and/or p_p is sufficient.

However, it must be remembered that a change in p_p without a simultaneous change in C is not sufficient. In other words, a change in p_t alone does not result in independent values of transmission. This mistake has been made quite often in the past, where researchers prepared a mixture of gases in a mixing tank and added this mixture to the absorption cell at various total pressures, assuming that they had thus measured different points along the curve of growth. The fallacy of this procedure is evident if we rewrite Equation (2-10) in the following way, remembering that $a = a_o p_t$:

$$\frac{\bar{W}/d}{p_t} = \frac{-\ell n\, t}{p_t} = kC\ell \left(1 + \frac{kC\ell}{4a_o}\right)^{1/2} \tag{2-15}$$

It is clearly seen that if C and ℓ are kept constant and only p_t is changed, the right-hand side of Equation (2-15) is a constant and neither k nor a_o can be determined separately.

It is usually easier and more accurate to change the cell length ℓ rather than the concentration C. This can be done in cells which have adjustable multiple paths, such as in a White-cell arrangement.

The optical thickness to be measured in the laboratory must cover the range of the optical thickness expected in the field. Thus, for an expected concentration of 10 PPM of a given pollutant to be observed over a pathlength of 4 km, the optical thickness is 4 cm-atm. If it would be possible to use a partial pressure of 1 atm for the pollutant, a cell length of at least 4 cm must be used. However, in this case, the measurements would be made under the condition of self-broadening. The results would thus not be applicable to the atmospheric case, in which air-broadening is dominant. This is especially true for polar molecules, which may have a self-broadening coefficient (ratio of self-broadened half-width to nitrogen-broadened half-width) of the order of 10. Thus to keep the actual half-width within, say, 1% of the self-broadened value, the maximum concentration should not exceed 1000 PPM. At this concentration and 1 atm pressure, a pathlength of 40 m is required to produce an optical thickness of 4 atm-cm.

2.2 SPECTRA OF POLLUTANTS AND ABSORPTION COEFFICIENTS

The "pollutants of interest" will, to some extent, depend on the pollution monitoring task at hand. However, there are a number of pollutants of sufficiently common interest to be considered here along with the major infrared active normal atmospheric constituents, CO_2 and H_2O.

Band strenghts, band averaged absorption coefficients and fine structure parameters are given in Table A.1* and band model parameters are given in Tables A.2 through A.10* at 5 cm^{-1} and 20 cm^{-1} intervals.

Band strengths and fine structure parameters are given in Table A.11** and absorption coefficients are given in Tables A.12 through A.18** for various cm^{-1} intervals.

For details of the generation of these tables the original references given below should be consulted. Spectra of these and other pollutants are given in the open literature which are too extensive for inclusion here.

---

* Air Pollution Measurements by Satellites, C. B. Ludwig, M. Griggs, W. Malkmus and R. Bartle, NASA (in press).

** Study of Air Pollution Detection by Remote Sensors, C. B. Ludwig, R. Bartle, and M. Griggs, NASA CR 1380 (July 1969).

3

PERFORMANCE OF THE ROSE SYSTEM

3.1 GENERAL

The performance of the ROSE system has been evaluated in terms of the operation of the mechanical, optical and electronic components during the field tests. In view of the complexity of the system and, at times, unusually adverse field conditions it is considered that the system performed well.

The performance of the mechanical components of the ROSE system was excellent during the field tests which included set up at six locations and two moves from Pomona to San Diego by truck. The system proved to be rugged and was conveniently moved into position. One vendor-supplied mechanical component, the reference chopper motor bearings, failed during the emission tests. These bearings have been replaced and spares obtained for use if future trouble should develop.

The optical components of the system also performed well during the field tests. The mountings appeared to be stable and, even with severely hot ambient temperatures, no alignment problems developed. The possibility of having to shield the telescopes from direct sunlight proved to be unnecessary.

There was some difficulty with isolated electronic components believed to have been caused, in part by ambient temperatures above the design values and, in part, by non-standard voltages of portable power supplies. In particular, the reference chopper drive has been modified to make its operation more reliable. A number of wiring breaks were located and have been corrected. Subsequent to the field tests the digital coupler was modified to provide more stable operation of the digital system.

In the following sections the performance is described in terms of system noise, scintillation noise and signal strength.

3.2 SYSTEM NOISE

System noise is defined as the noise with no optical input to the system; i.e., with the optical path blocked off. Ideally, the system noise equals the detector noise but in practice other electrical components may contribute to the system noise. However, it is useful to express the system noise in terms of the detector noise.

The theoretical system noise is based on detector noise which may be calculated from

$$Vn_{\text{theo.}} = \frac{\sqrt{A\,\Delta f}\,R}{D^{*}}$$

where A = detector area - (cm^{-2})

= 0.004 cm^{2} nominally

Δf = system bandwidth - (Hz)

= 1/4 (system time constant - sec)

R = detector responsivity - (volts rms/watt rms)

D^{*} = detector specific detectivity - (cm Hz 1/2/watt)

The value of R/D^* at λ_m, the wavelength of peak response, is $12 \times 10^{4}/0.95 \times 10^{10} \sim 1.26 \times 10^{-5}$ volts/cm Hz$^{1/2}$. R and D^{*} both vary with wavelength to some extent but the ratio does not.

Using the above values the theoretical system noise at the detector is

$$Vn_{\text{theo.}} = 0.8 \times 10^{-6}\sqrt{\Delta f} = 0.8 \times 10^{-6}/\sqrt{4\tau}$$

which results in a noise voltage of about 0.4 μ volts rms for a bandwidth of 0.25 Hz (time constant = 1 sec.)

$$Vn/\sqrt{\Delta f}_{\text{theo}} = 0.8 \times 10^{-6} \text{ rms volts } /\sqrt{\text{Hz}}$$

The observed system noise is obtained by reading the peak to peak noise voltage on the recorder trace and dividing this voltage by 5 (to obtain the approximate rms value) and by the gain between the detector and the recorder and $\sqrt{\Delta f}$ to obtain the equivalent rms noise voltage per $\sqrt{Hz}$ at the detector. This system noise may then be compared to the detector noise from the above equation for the particular bandwidth (or time constant) of the test.

Analysis of the system noise data gave the following results averaged for each test.

	$V_n/\sqrt{Hz}$ (at detector)			
One mile test	1.0×10^{-6}	rms	volts	$/\sqrt{Hz}$
Emission tests	0.6-0.7	"	"	"
Two mile tests	1.1	"	"	"
Refinery tests	0.5	"	"	"

Thus the blocked off system noise is within a factor of about 1.5 of the detector noise. Considering the difficulty of noise measurement, especially with small trace deflections, it is considered that the above deviations from the detector noise value of $0.8 \times 10^{-6}/\sqrt{Hz}$ are not significant.

It should be noted that occasionally the noise exceeded the average values given above by as much as a factor of three. It is believed that these transient increases were mainly a result of electrical interference from outside the ROSE system.

Previously reported laboratory values of system noise (or zero line noise) corresponds to 0.5 to 0.8×10^{-6} rms volts $/\sqrt{Hz}$. The system noise for the San Diego field tests corresponds to about 1.2 to 1.6×10^{-6} rms volts $/\sqrt{Hz}$.

3.3 SCINTILLATION NOISE

Scintillation noise results from variable atmospheric refraction between the source and the receiver and is observed as a variation in the signal level. In the following analysis the observed signal variation is divided by the total gain, G, to normalize different gains used on different runs and is multiplied by $\sqrt{4\tau}$, where τ is the system time constant, to normalize the different time constants used. This process results in a signal noise which is referred to the detector and to unit bandwidth of

$$V_{ns}/\sqrt{Hz} = \frac{(\text{Signal Noise})\ \text{pp}\ \sqrt{4\tau}}{(5)\ (G)}$$

where the factor of 5 is again used to convert from (peak-to-peak) to rms. Only runs at constant wavenumber were used in the analysis.

For the one mile tests the values of V_{ns} $/\sqrt{Hz}$ ranged from 2 to 60 μ volts $/\sqrt{Hz}$ the average being about 17 μ volts $/\sqrt{Hz}$. No clear-cut pattern with time of day could be observed. On the first two days of testing the noise at 2500 cm^{-1} was about an order of magnitude higher than that at 1000 cm^{-1} but on later tests the signal noise at the two wavenumbers was more nearly equal. It should be noted that for the one mile test the General Dynamics/Pomona and Bendix instruments were also using the Convair source and the ROSE receiver was at the edge of the beam. This undoubtedly had the effect of increasing the signal noise.

For the two mile tests a series of runs were first made with very wide slits (S = 1000, 1500 or 2000 microns × 12 mm) for which the signal noise average was about 26 μvolts $/\sqrt{Hz}$. With narrower slits the same day and on subsequent days the signal noise varied from 1.6 to 4 μvolts $/\sqrt{Hz}$ the average being about 2.4 μ volts $/\sqrt{Hz}$. The overall average of all runs was about 16 μvolts $/\sqrt{Hz}$. The reason for the large signal noise with wide slits is not known; with the large slit width and height one would expect just the opposite since this corresponds to a slitless instrument. There was a rearrangement of the power plug on the CTI cooler cabinet after the high signal noise runs and before the low signal noise runs but it is difficult to see how this fact would influence the original noise. The ROSE receiver was set up carefully in the center of the beam for the two mile tests and, except for the early large values of signal noise, did give less noise than that observed on the one mile tests.

In the one-quarter mile tests at the refinery the signal noise ranged from 2 to 30 μvolts /$\sqrt{\text{Hz}}$ with the average being about 11 μvolts /$\sqrt{\text{Hz}}$. Again no clear cut variation with time of day was observed.

For the emission tests the signal noise varied from 0.4 to 1.6 μvolts /$\sqrt{\text{Hz}}$ which is within a factor of about two of the system noise. In these tests, of course, there is not the precise alignment requirement as there is for the transmission mode of operation.

A factor contributing to the large scintillation noise during the one mile tests was the use of a slit height equal to the theoretical image height, h_o, which was 2.3 mm for the one mile tests. Figure 3-1 shows the source and reference channel signals as a function of slit height normalized to unity for the maximum mean value of the source signal. The flattening of the source signal simply represents the fact that the source image is finite. It is readily apparent that the variation of the source signal for a given slit height depends on the value of the slit height and is a maximum near h_o. This is interpreted to be a result of vertical movement of the source image.

3.4 SIGNAL STRENGTH

The system transmission is fundamental to the calculation of the signal strength. Calculations have been made for the transmission mode of operation and the results are shown on Figure 3-2. Reflectivities for aluminum were estimated from measured values for the two telescopes which were different; thus the two curves shown represent this difference. For the emission mode of operation the transmission would be more than that shown by a factor $(1/\rho_A)^2$.

Figure 3-2 shows the transmission calculated from all known causes except aberration. The transmission from aberrations for the transmission mode of operation is shown on Figure 3-3 for a range of 0.4 km. For the emission mode of

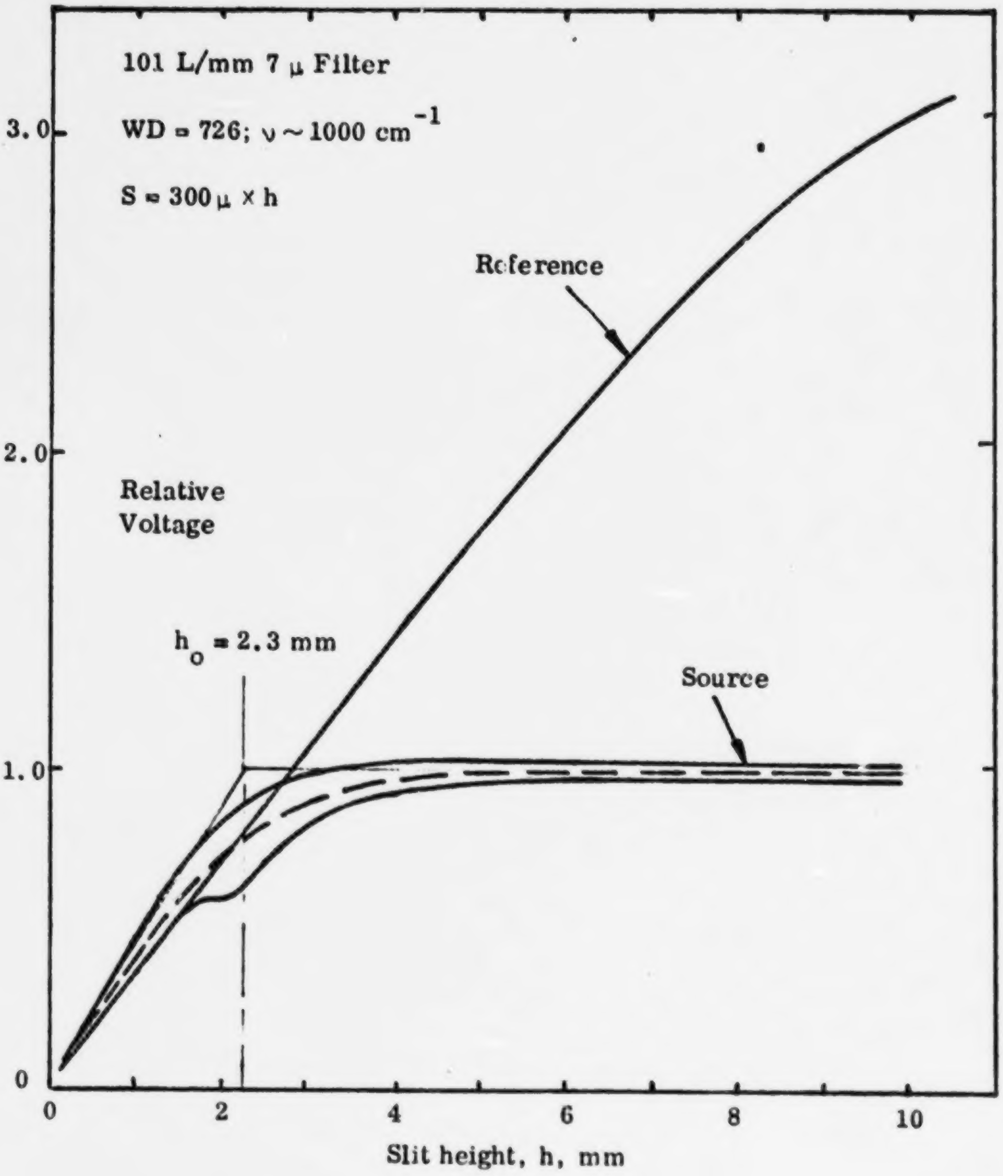

Figure 3-1. Relative Signals from Source and Reference Channels - One Mile Path

Transmission Mode of Operation

$\tau_t = \tau_c \times \rho_a^4$ (τ_c = Common Path Transmission)

$\tau_c = \tau_I^3 \times \tau_f \times \rho_a^8 \times \epsilon_{gr}$

τ_I = IRTRAN II (Entrance slit field lens, det. cass. field lens, dewar window)

τ_f = Filter transmission

ρ_a = Aluminum reflectivity

ϵ_{gr} = Grating efficiency

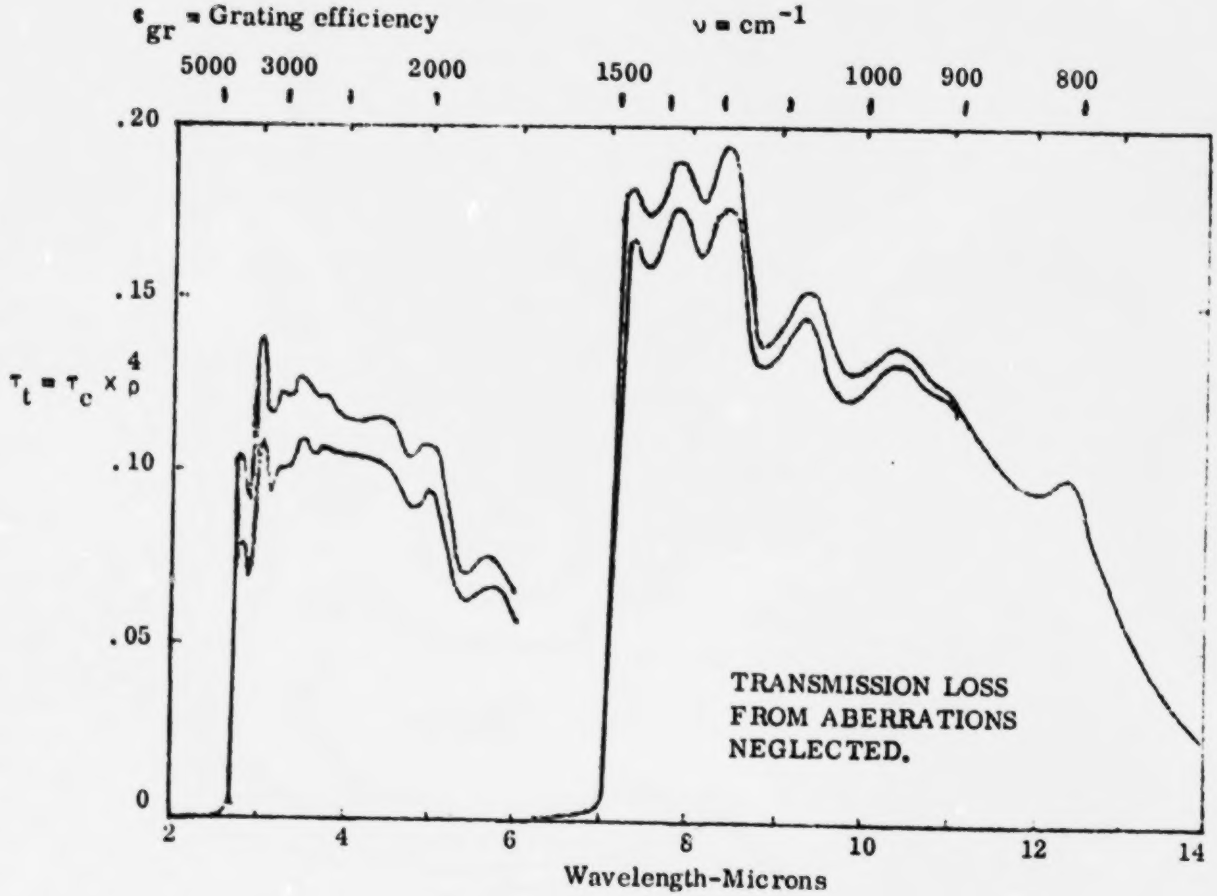

Figure 3-2. Calculated System Transmission

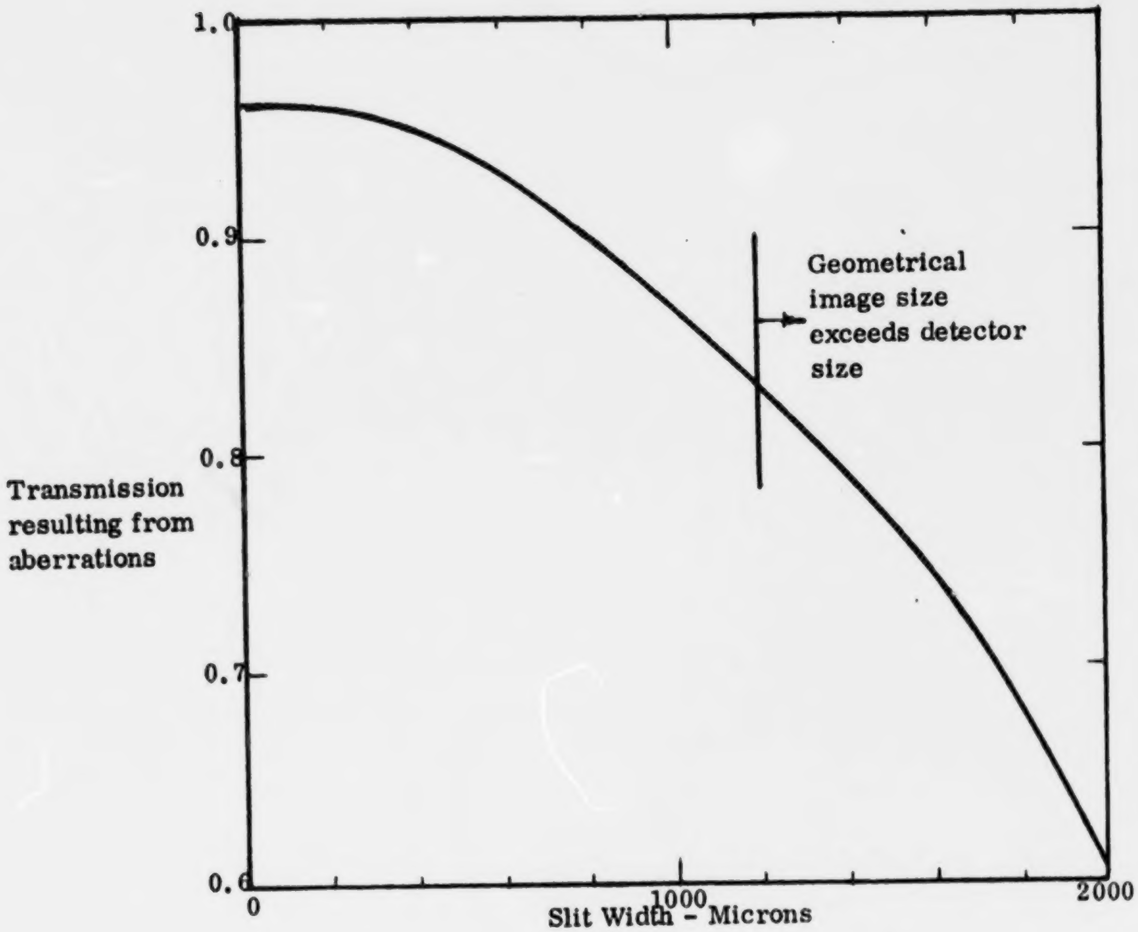

Transmission Mode of Operation Range = 0.4 km
Loss from Geometrical Image Size Exceeding Detection Size Included.

Figure 3-3. Calculated Transmission Resulting from Aberrations

operation there should be little or no transmission loss from aberrations for a uniform source field.

The signal strength in the laboratory were found to be 0.55 to 0.67 of that calculated using the above calculated transmissions (see EPA-R2-72-052 or GDCA-DBE-72-001 page 6-3). The difference between these ratios and unity represent unknown losses which may come from deviations from the calculated values of reflectivity or tranmission from aberrations or from misalignment, scattering or diffraction effects.

Signal strengths in the San Diego field tests agreed with the laboratory data (ibid page 6-7).

For the one mile tests in Pomona the signal levels were considerably below the theoretical values as a consequence of the receiver being at the edge of the beam. The signal levels as well as the signal noise showed wide variations.

The signal strength for the two mile tests at $v = 2500\ \mathrm{cm}^{-1}$ showed a range from 0.48 to 0.59 of the theoretical value with an average of 0.54. At $\nu = 1000\ \mathrm{cm}^{-1}$ the signal strength ranged from 0.37 to 0.53 of the theoretical value the average being about 0.45. These values probably are lower than those observed in San Diego at one-quarter mile because of the lower transmission of the two mile path.

For the refinery tests the signal strength was from 0.30 to 0.40 of the theoretical value. Since the path length was about one quarter mile it is suspected that the detector toroid was displaced from the optimum position during transport of the system. It is recommended that the detector toroid adjustment be checked after each move before testing (at least until experience indicates otherwise).

4

LONG PATH TRANSMISSION MEASUREMENTS

4.1 ONE-MILE MEASUREMENT

A description of the location for these tests is given in Appendix I.

As previously mentioned, these tests were influenced by scintillation noise. This noise was greater than expected. It was subsequently traced to the unfavorable position of the receiver telescope near the edge of the beam. In addition, a considerable portion of the line-of-sight was over a hot blacktop surface and one edge of the beam was close to metal lamp posts.

A typical spectrum of transmitted intensity (I) from 7.5 to 12.5 μ is shown in Figure 4-1. It was recorded with a slit width of 1500 μ, which corresponds to about 5 cm^{-1} at 1000 cm^{-1}, and a time constant of 0.1 sec. The main features are the strong absorption lines due to H_2O between 1100 and 1330 cm^{-1}, the band absorption of O_3 between 1000 and 1100 cm^{-1}, and the weak absorption lines due to H_2O between 800 and 1000 cm^{-1}. The instrument noise in this trace is very small, as can be seen at 1320 cm^{-1}, where the atmospheric transmission is reduced to zero due to strong water absorption and thus acts as a shutter. The fluctuating signal between the identified water lines notably for $\omega < 1000$ cm^{-1}, arises from the atmospheric scintillation, as can be seen from the record in Figure 4-2, which was taken at 1000 cm^{-1} for a two-minute time interval.

By increasing the spectral resolution to 1 cm^{-1}, many of the strong center lines between 1100 and 1330 cm^{-1} become better defined (see Figure 4-3). Line identification numbers were taken from Air Force Surveys in Geophysics No. 142. The increase in amplification by a factor of 10 also increases the noise in the signal, as can be seen in the record of Figure 4-4.

A typical spectrum, in which the atmospheric transmission (I/I_o) is recorded, is shown in Figure 4-5. The spectral slit width is the same as used in the recording of Figure 1, but the amplification is reduced by a factor of 2.5. The spike shown at

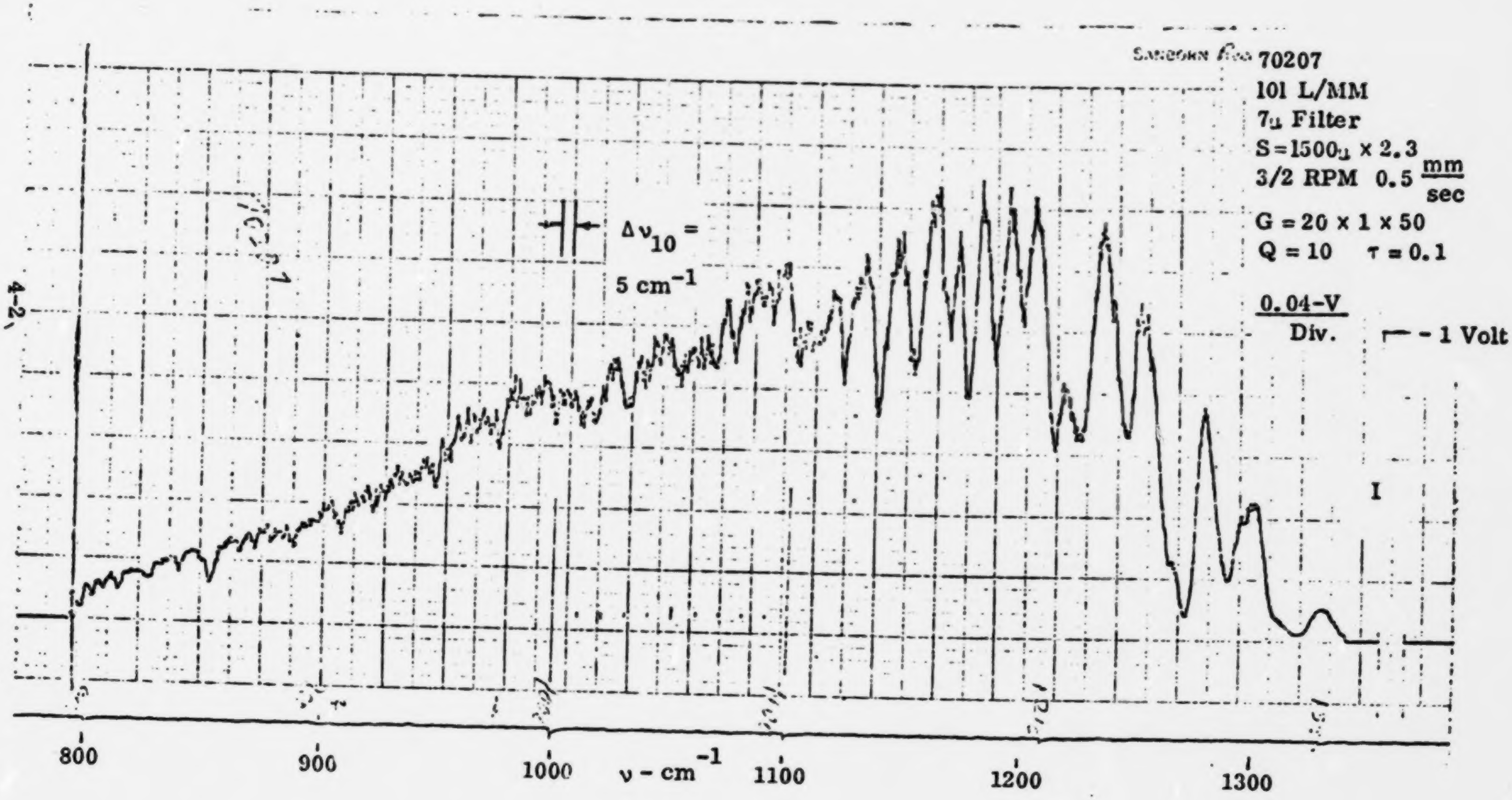

Figure 4-1. 7 to 13µ Scan with One Mile Path, $\Delta\nu_{10} = 5\ \mathrm{cm}^{-1}$

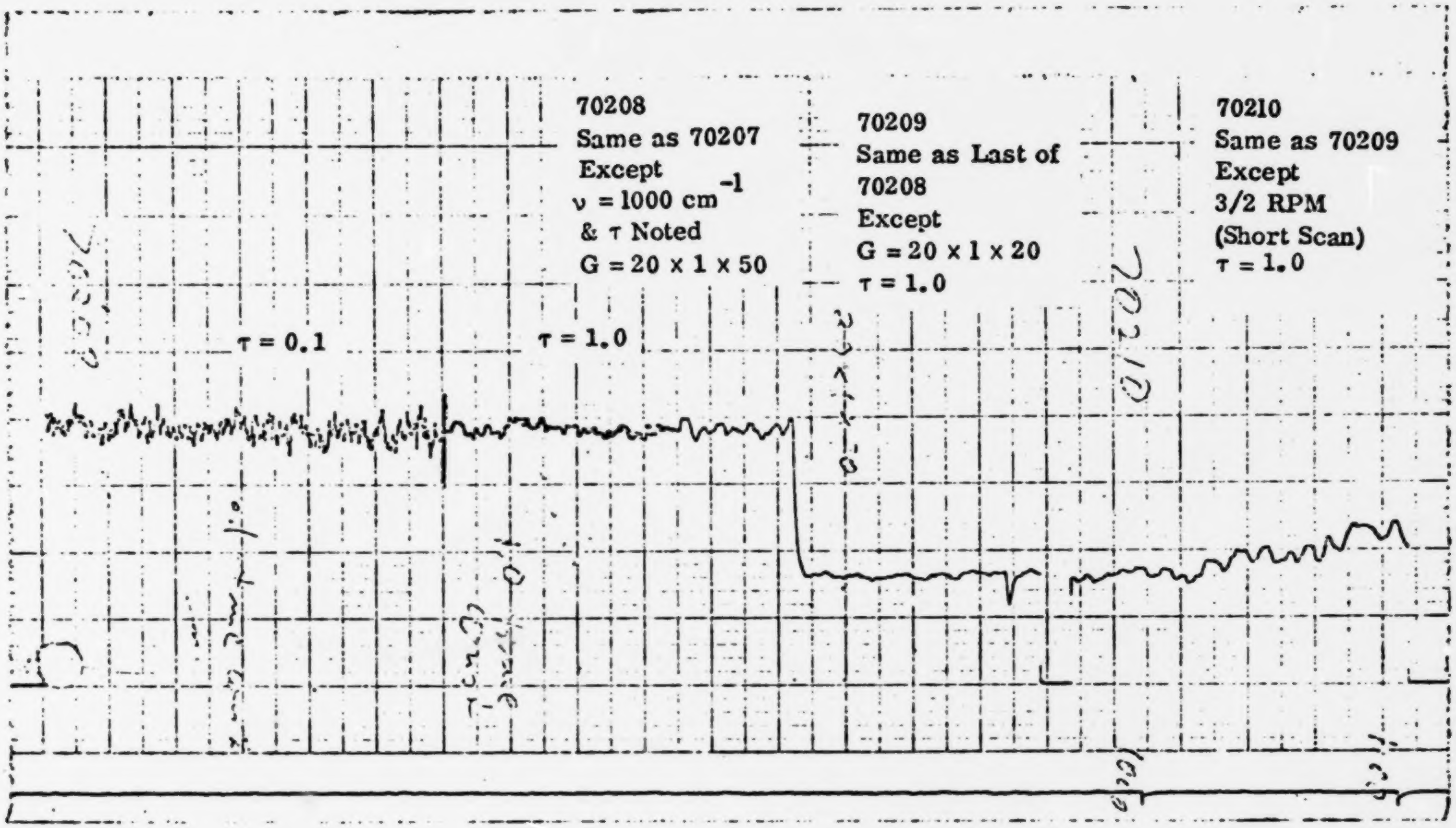

Figure 4-2. Noise at ν = 1000 cm^{-1} with One Mile Path, $\Delta\nu_{10}$ = 5 cm^{-1}

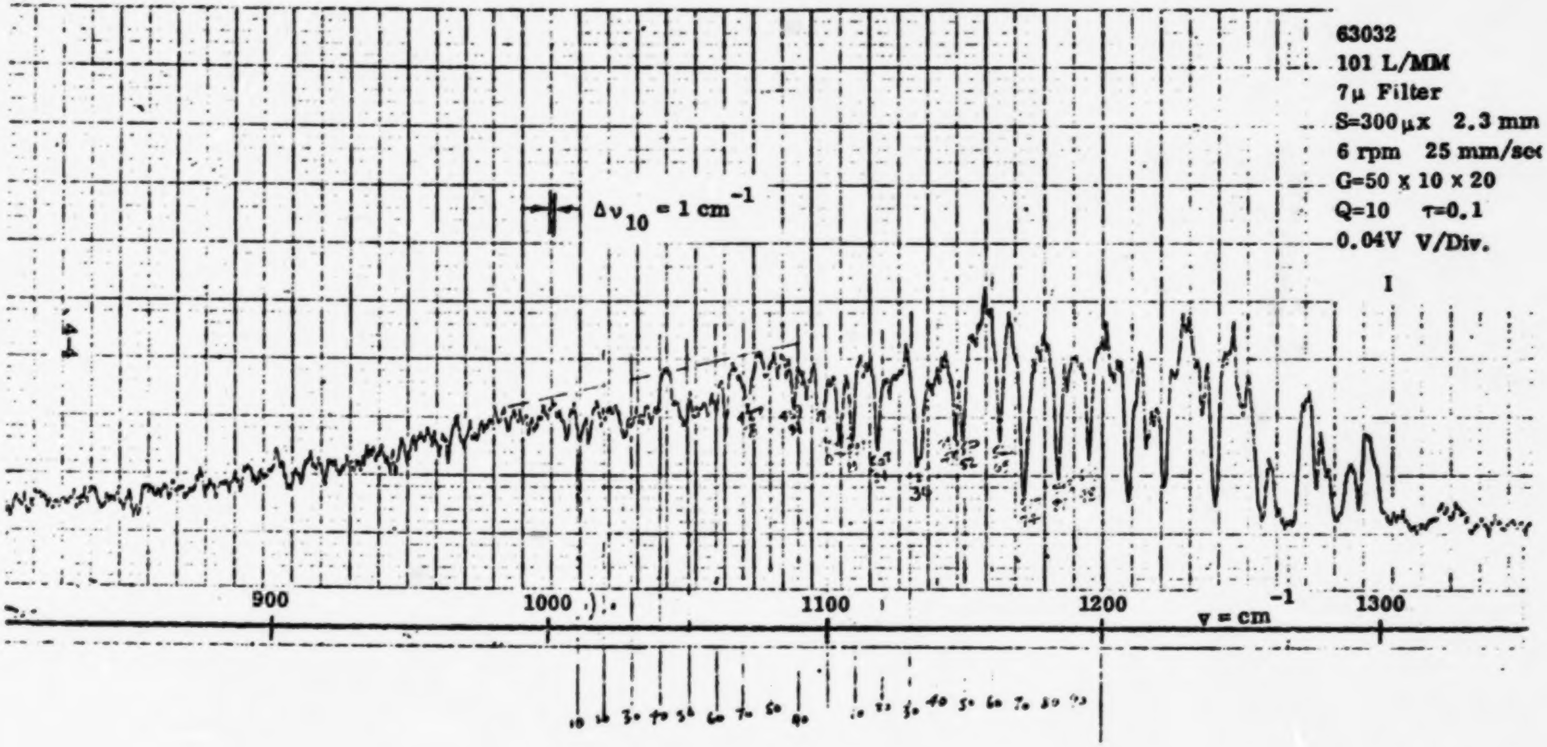

Figure 4-3. 7 to 13 μ Scan with One Mile Path, $\Delta\nu_{10} = 1\ \text{cm}^{-1}$

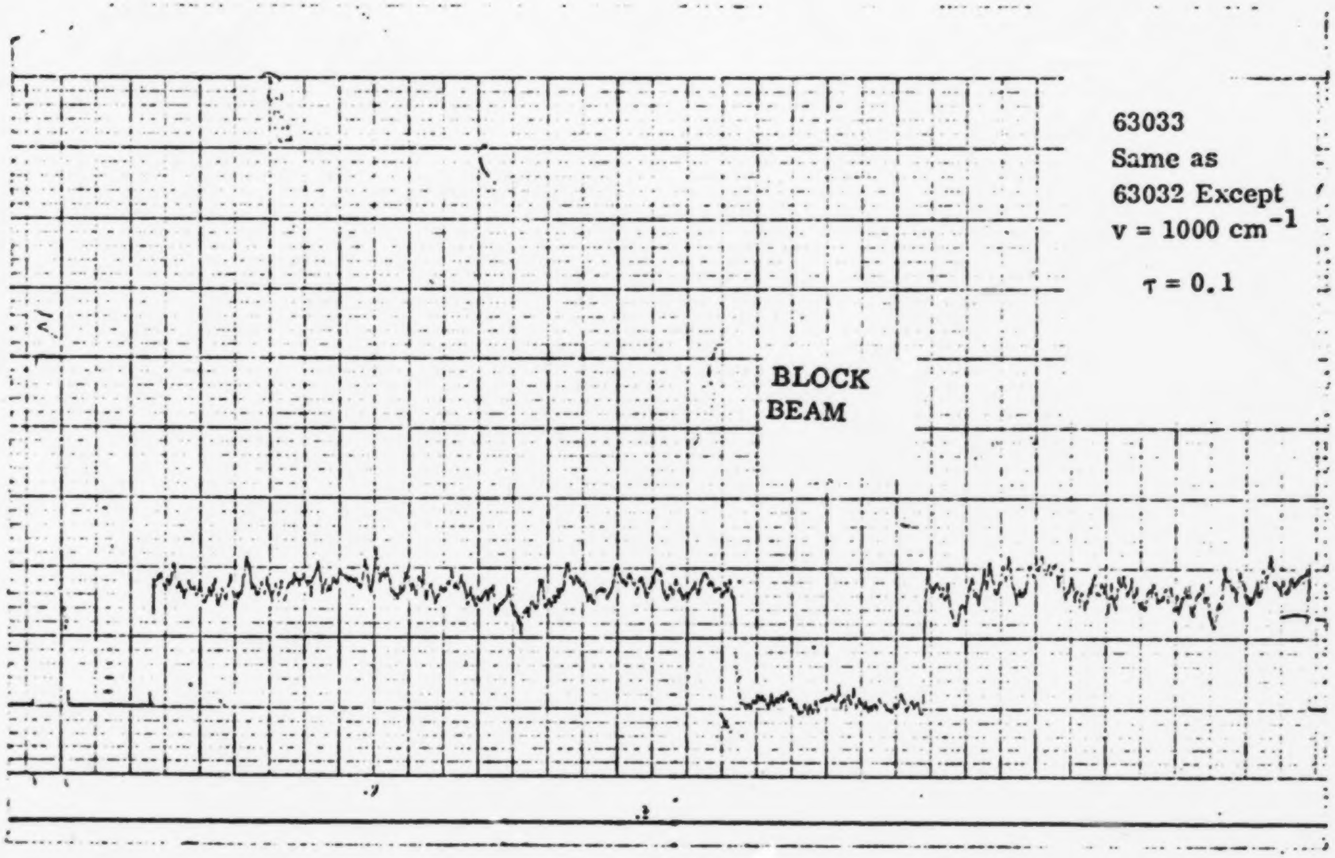

Figure 4-4. Noise at 1000 cm^{-1} with One Mile Path, $\Delta \nu_{10} = 1\ cm^{-1}$

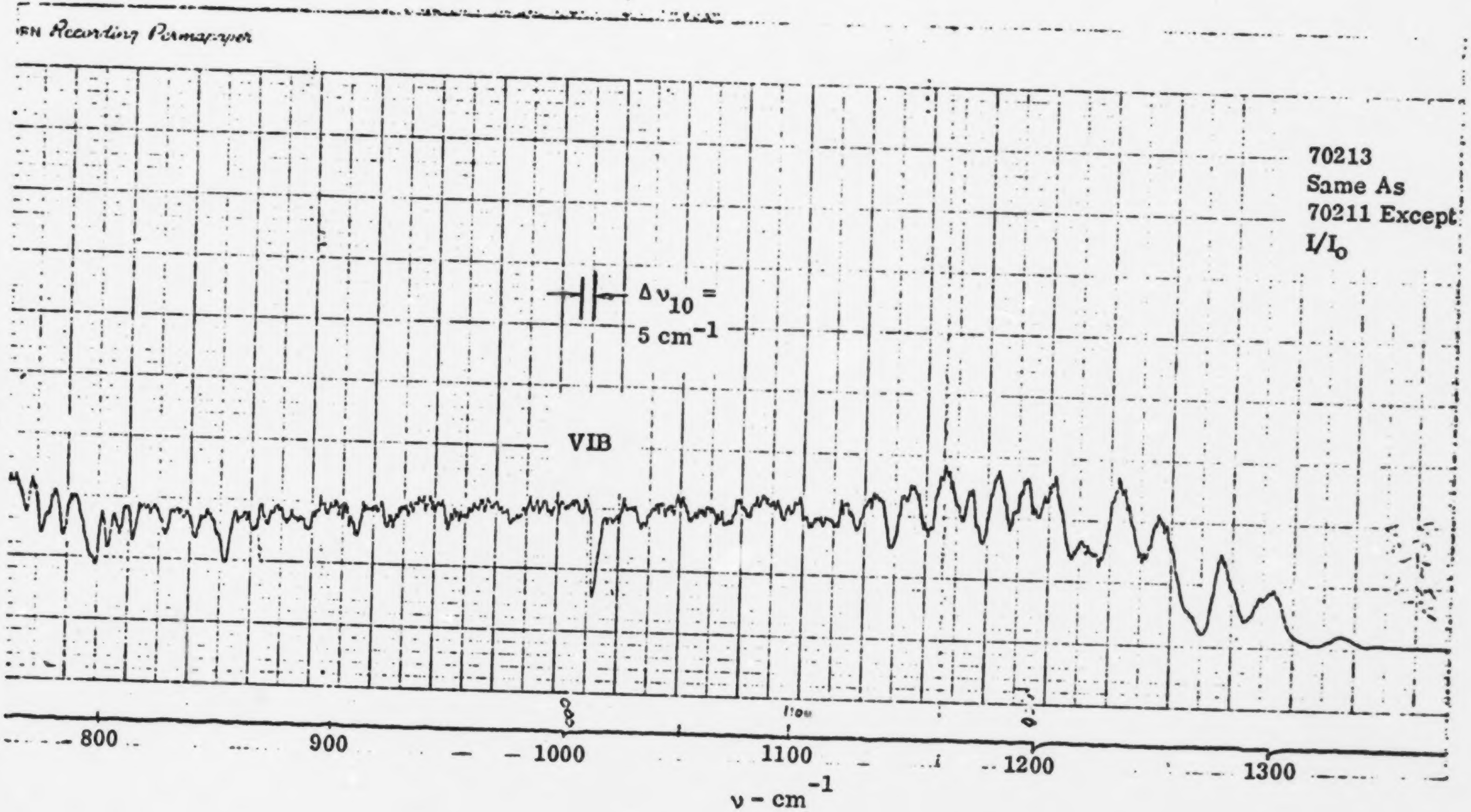

Figure 4-5. 7 to 13 μ I/I_o Scan with One Mile Path $\Delta \nu_{10} = 5\ \text{cm}^{-1}$

1010 cm^{-1} is identified as VIB ("vehicle in the beam"), an all too frequent occurrence in the measurements conducted here.

The only pollutant identified unambiguously is ozone. The quantitative analysis proceeds as follows. As has been shown in Section 2.2, the band absorption can be represented by the statistical band model. Referring to Figure 4-3, the I_o level is assumed to be the connecting line between the levels at ~ 1000 cm^{-1} and 1080 cm^{-1}. At 1055 cm^{-1} $I_o = 14.5$ and $I = 12$, thus $I/I_o = 0.83$. Using the absorption coefficient and fine structure parameter from Section 2.2, the partial pressure of ozone is calculated to be 0.12×10^{-6} atm, which corresponds to 12 pphm. This value agrees well with the hourly average value of 11 pphm recorded by the Pomona APCD station at 3 ppm (see Table I of the Appendix).

A typical spectrum of transmitted intensity from about 3 to 5 μ is shown in Figure 4-6, which was recorded with a slit width of 700 μ ($\Delta \nu_4$ at 4 μ or 2500 cm^{-1} equals 6 cm^{-1}) and a time constant of 0.1 sec. The main features are the strong water absorption between 3400 and 2900 cm^{-1}, the absorption due to HDO near 2700 cm^{-1}, the absorption due to CO_2 at 4.3 μ, due to N_2O at 2230 cm^{-1} and due to H_2O between 2200 and 2000 cm^{-1}. The amplification is the same as used in Figure 4-1. The signal at 2500 cm^{-1} shown in Figure 4-7 indicates again large fluctuations due to scintillation.

The corresponding record of atmospheric transmission (I/I_o) is shown in Figure 4-8. The unusual feature in the CO_2 absorption band between 2300 and 2400 cm^{-1} originates from the absorption in the I_o trace, which cannot be eliminated since the instrument is not flushed.

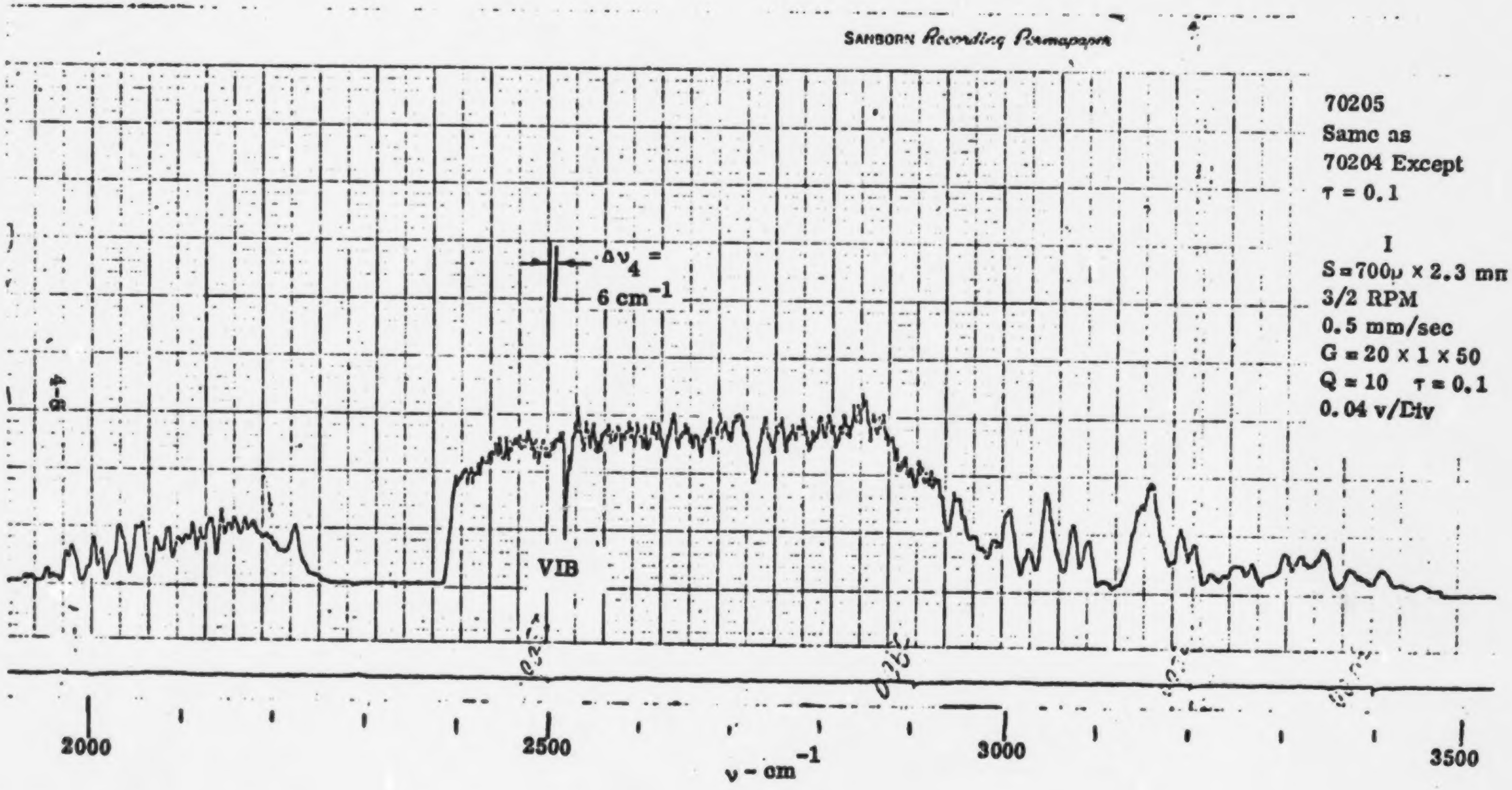

Figure 4-6. 3 to 5 μ Scan with One Mile Path, $\Delta\nu_4$ = 6 cm-1

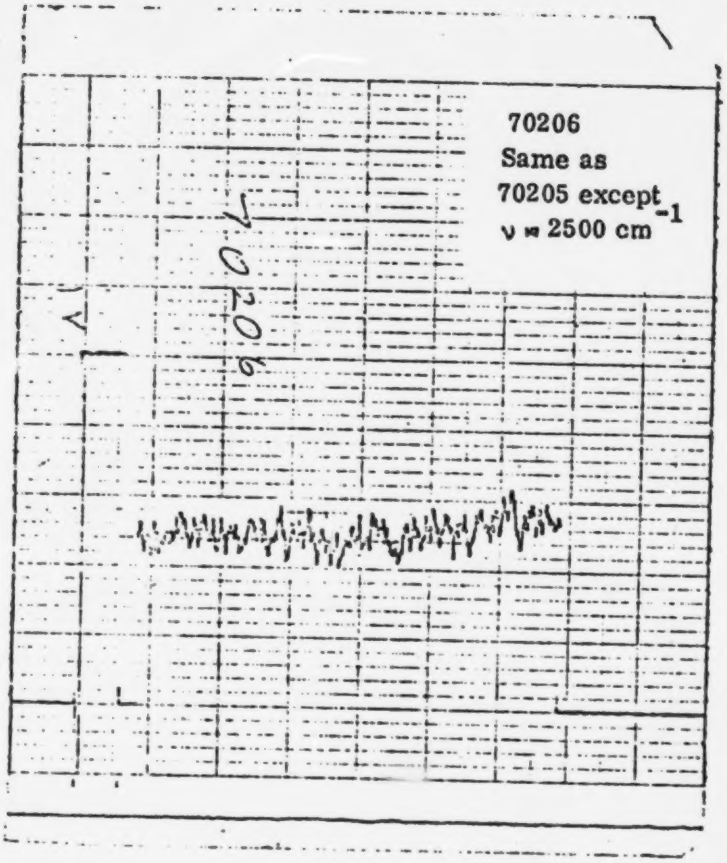

S/N ~ 3
pp

Figure 4-7. Noise at 2500 cm^{-1} with One Mile Path, $\Delta\nu_4 = 6\ \mathrm{cm}^{-1}$

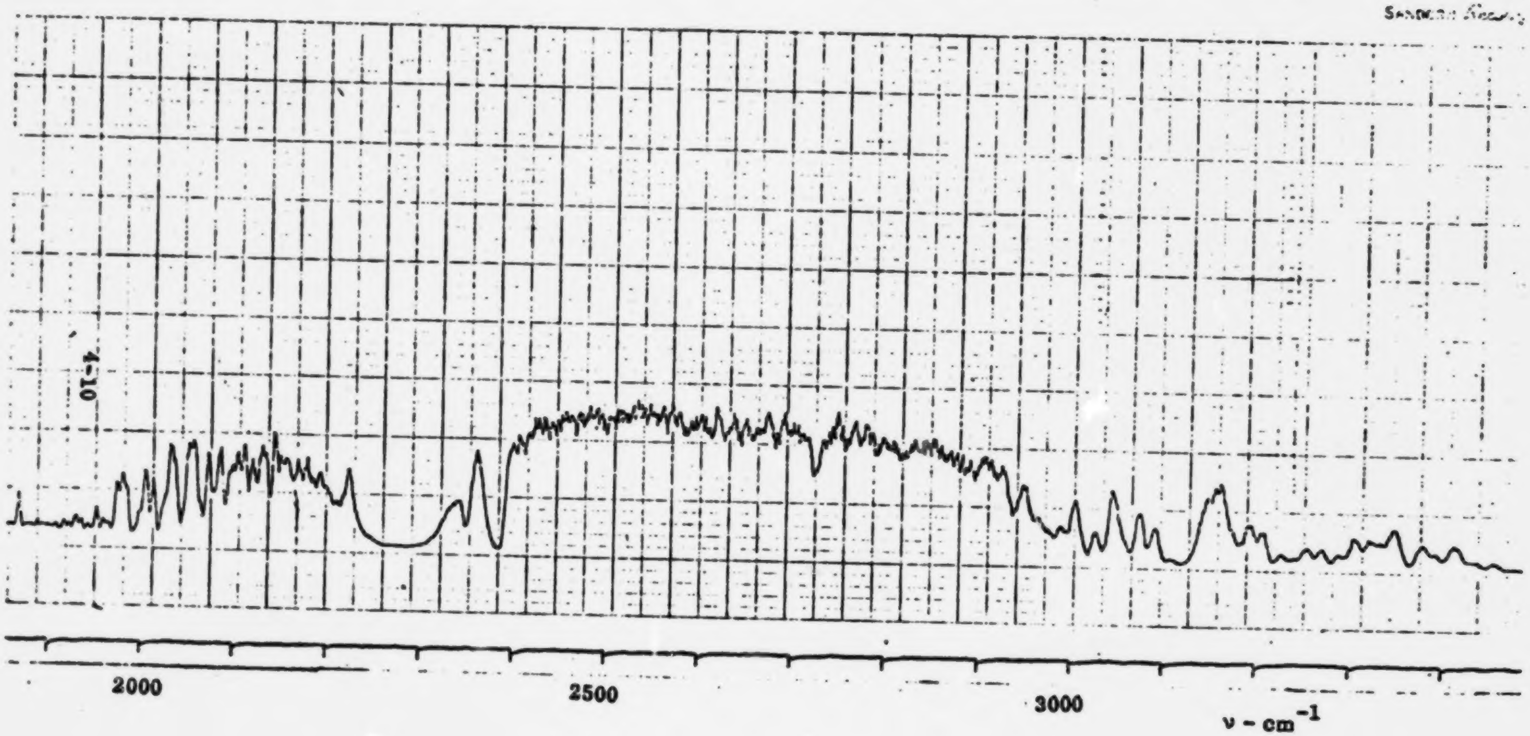

Figure 4-8. 3 to 5 μ I/I_o Scan with One Mile Path, $\Delta \nu_4 = 6$ cm^{-1}

During the week in which the one-mile tests were performed, atmospheric turbidity measurements were made with the Volz sun photometer.* This instrument consists of a small aperture which was aligned so that energy from the sun fell on a filter-detector combination; the detector output was read from a microammeter. The secant of the sun zenith angle associated with the measurement was determined by means of an auxiliary scale and a level. The air mass of the atmosphere was assumed to be equal to the secant of the sun zenith angle (valid for $0° < M < 80°$).

The aerosol optical thickness, τ_{aer}, was determined from the following relation.

$$I = I_o \exp(-(\tau_{aer} + \tau_{atm})M)/f$$

where

I = meter reading of the measurement

I_o = meter reading with zero air mass (=51 with the present instrument, S/N G120).

$M = \sec\theta$ (θ = sun zenith angle)

τ_{atm} = Rayleigh scattering and ozone optical thickness (estimated)

τ_{aer} = aerosol optical thickness

f = a distance correction factor

A series of measurements were made in San Diego which show that the zero air mass deflection (extrapolated to zero air mass) was still equal to the original calibration value of 51 and also show typical variations of the optical thickness during the day, see Figure 4-9.

The results of the photometer measurements made during these field tests are shown on Figure 4-10. For comparison, Elterman's data for clean standard continental air and data taken in San Diego are also shown. Most of the data indicate an optical thickness about twice to three times Elterman's value.

Attempts to correlate τ_{aer} with signal strength were unsuccessful;

---

*F. Volz, Arch.Met. Geophys. Biokl. B, 10 p 100 (1959).

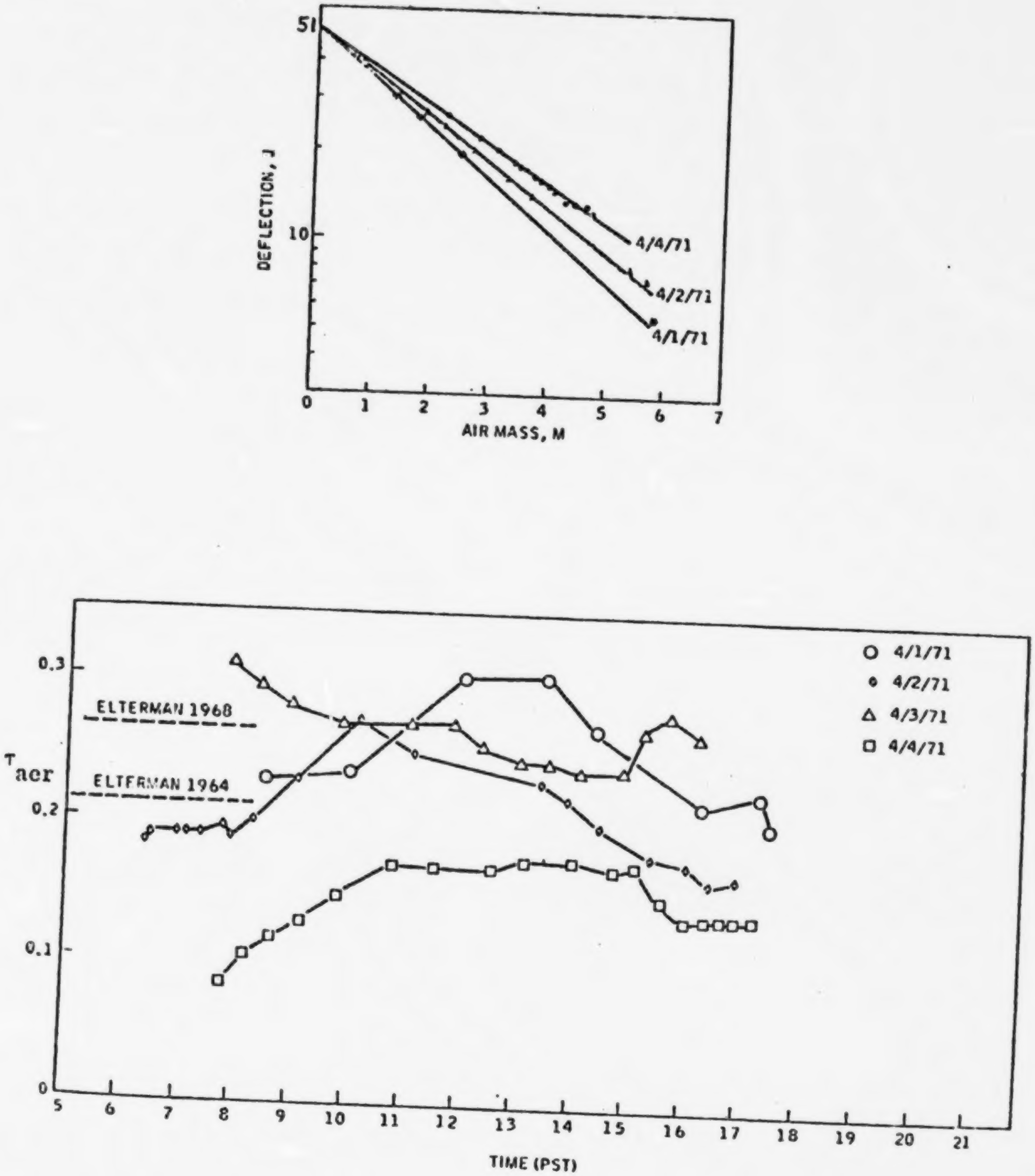

Figure 4-9. Volz Photometer Calibration and Typical Aerosol Optical Thickness Variation in San Diego, California

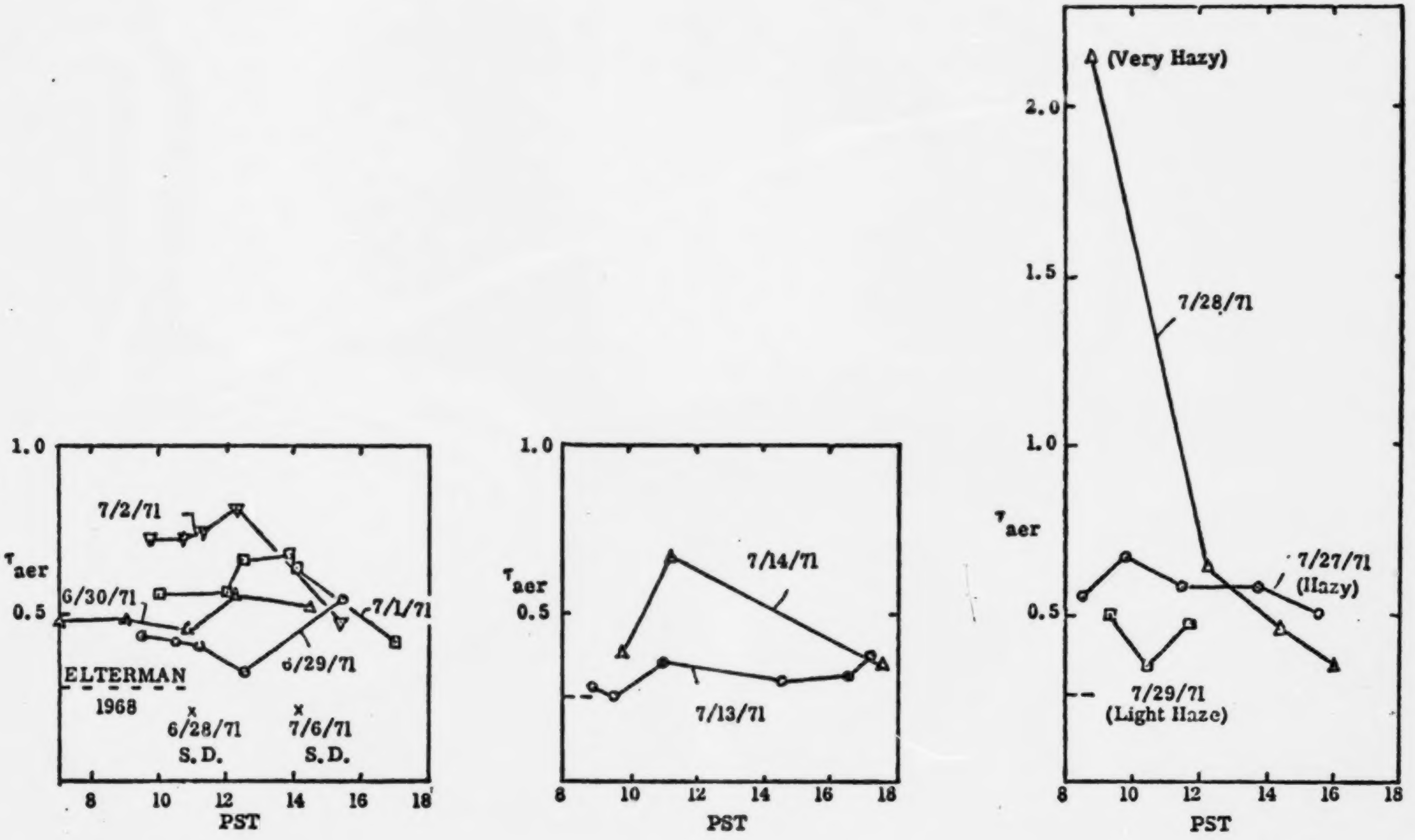

During One-Mile Tests

During Emission Tests

During Two-Mile Tests

Figure 4-10. Volz Photometer Measurements

perhaps the optical thickness value measured with the Volz photometer (which is an altitude integral) does not necessarily represent the horizontal optical thickness required for transmission calculations.

4.2 TWO-MILE MEASUREMENT

A description of the location for these tests is given in Section 1.2 of the Appendix.

In these tests, the receiver telescope was placed in the center of the source beam. A reduction in scintillation noise was expected. However, the fluctuations are again substantial, as shown in Fig. 4-11. The record taken at 10 a.m., shows a signal-to-pp noise ratio of about 9. The time constant was 1 sec, i.e., ten times longer than used in the record of Fig. 4-7, in which a signal-to-pp noise ratio of about 3 is observed. Thus, the apparent "improvement" results mainly from the longer time constant. On the other hand, the atmospheric conditions for the two mile tests were less favorable. A comparison of the relevant parameters is given in Table I.

Table I

	1 Mi	2 Mi
Date	2 July 1971	29 July 1971
Time	9 a.m.	10 a.m.
Air Temperature	72° F	90° F
Relative Humidity	59%	45%

Evidence of the greater stability of the night time atmosphere is clearly visible in the record taken at 9:15 p.m. (Fig. 4-11) in which the signal-to-pp noise ratio is about 26.

A typical spectrum of the transmitted intensity in the spectral range from 8 to 13μ is shown in Fig. 4-12. A time constant of 1 sec was used, which was subsequently determined to be too long for the scan speed employed. Thus, some of the fine structure in the spectrum was lost. Nevertheless, the

Reproduced from best available copy.

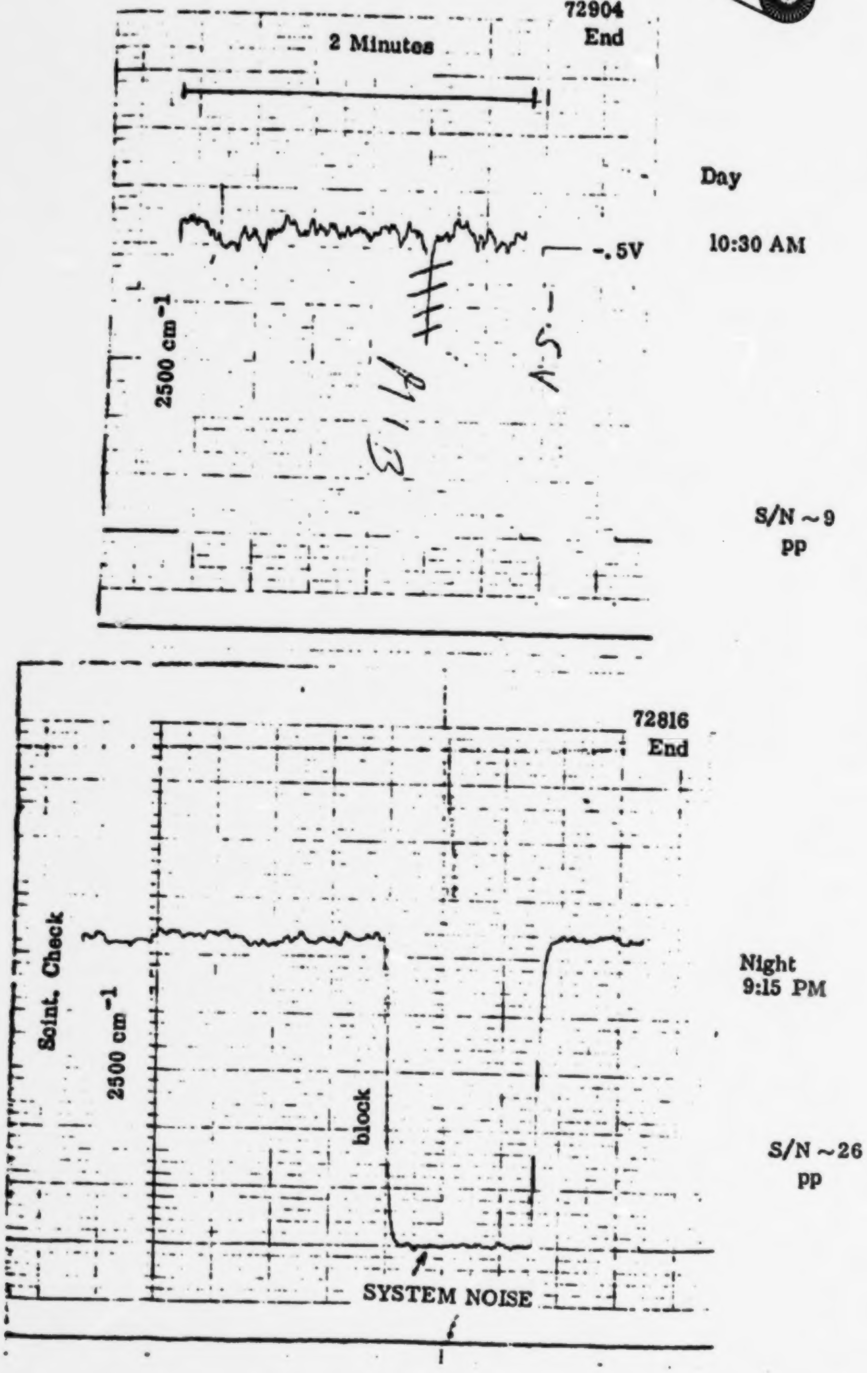

Figure 4-11. Noise at 2500 cm^{-1} with Two Mile Path, $\Delta \nu_4 = 3$ cm^{-1}

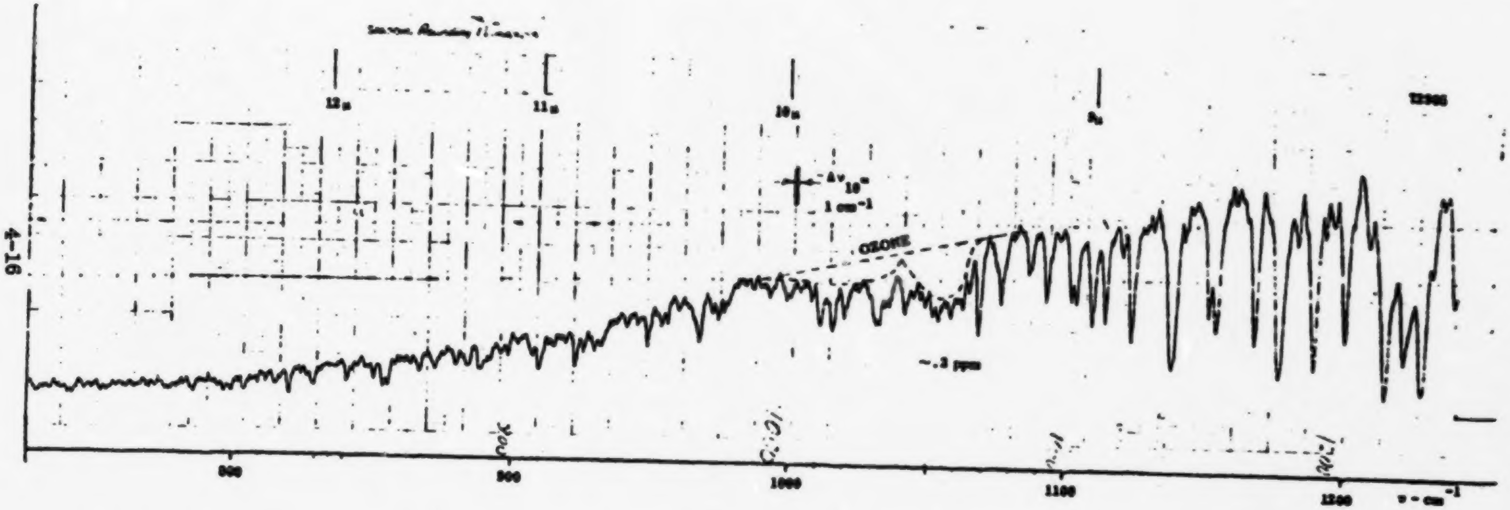

Figure 4-12. 8 to 13 μ Scan with Two Mile Path $-\Delta\nu_s = 1\ \mathrm{cm}^{-1}$

strong water lines throughout the entire spectral range are very well resolved. This becomes especially important in the ozone region, in which the many water lines, if not resolved, would introduce large errors causing an apparent reduction of the ozone concentration. Based upon our present knowledge, the band contour of ozone has been sketched in. Reducing the data obtained during the day of July 28, results in a plot of ozone concentration versus time (see Fig. 4-13). These data are compared with the hourly averaged values taken by the Pomona Station of the Los Angeles APCS (see Table V of the Appendix). The agreement is good. The time shift of about 1 hour between the two traces may be significant, indicating an O_3 build-up near the ground to occur faster than in elevated layers.

A typical spectrum of the transmitted intensity in the spectral range from 3 to 5μ is shown in Fig. 4-14, recorded with a time constant of 1 sec. For the spectral region from 1900 to 2300 cm^{-1} the amplification was higher by a factor of 2 than for the rest of the spectrum. A spectrum produced by the digital system for the CO absorption band is shown on Figure 4-15. The magnetic tape was reformatted and the results plotted on the SC4020 with the frames placed side by side.

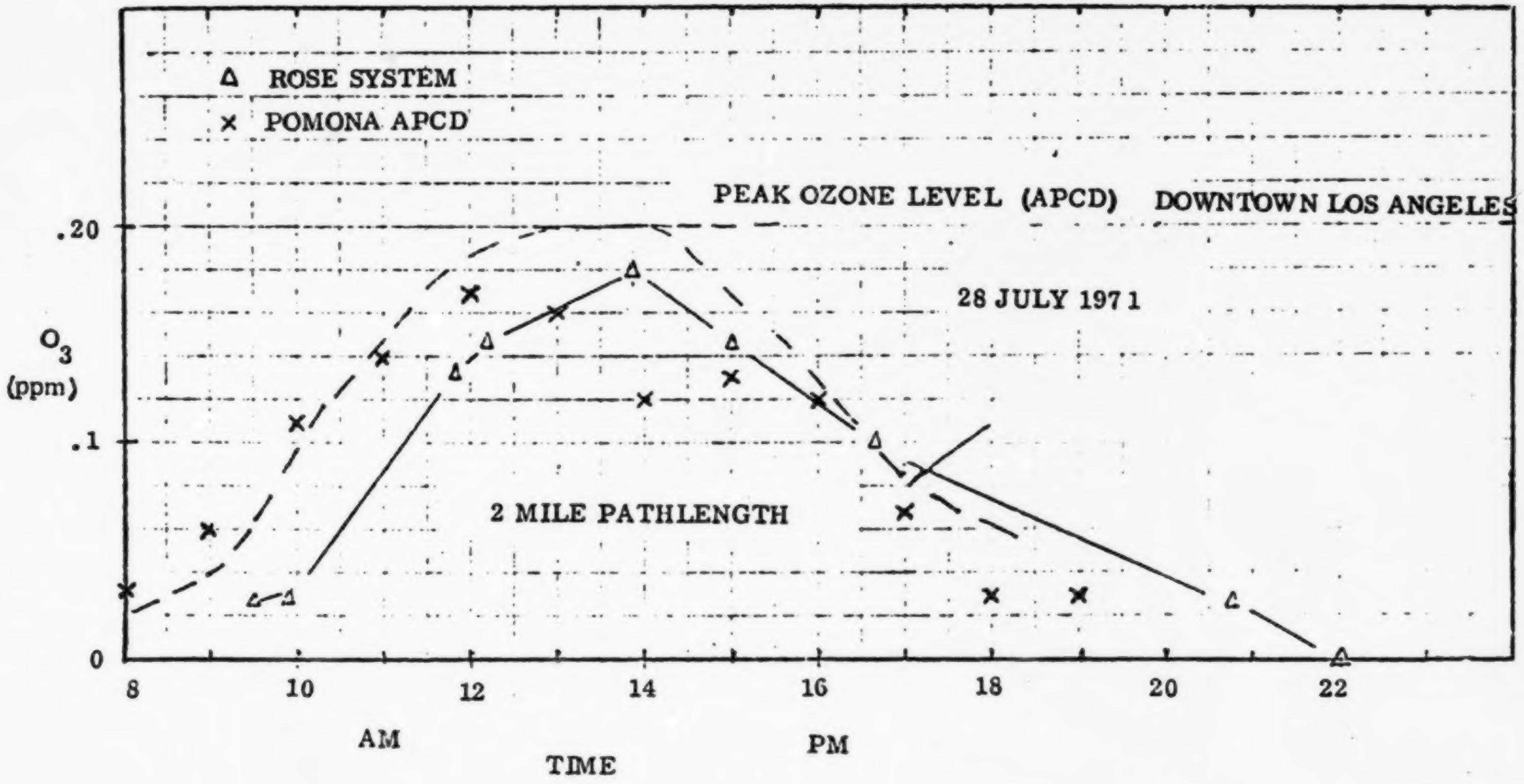

Figure 4-13. Ozone Concentration vs Time - 28 July 1971

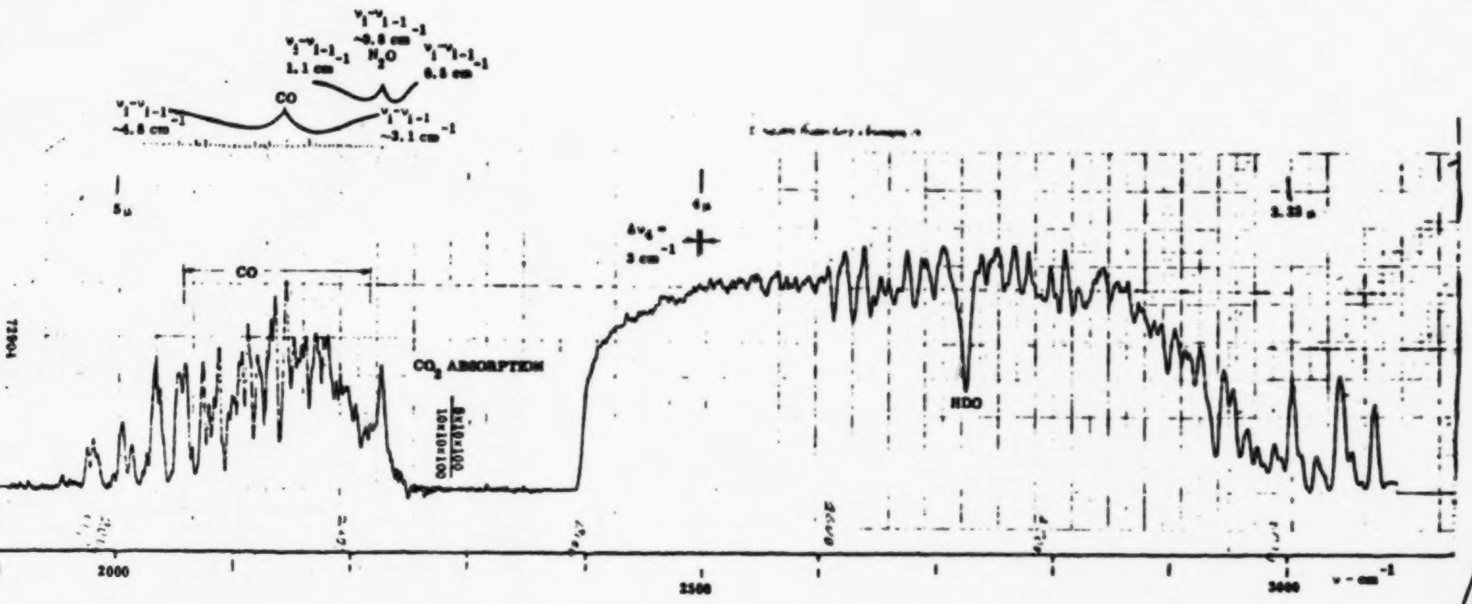

Figure 4-14. 3 to 5 μ Scan with Two Mile Path, $\Delta\nu_s = 3\ cm^{-1}$

Reproduced from best available copy.

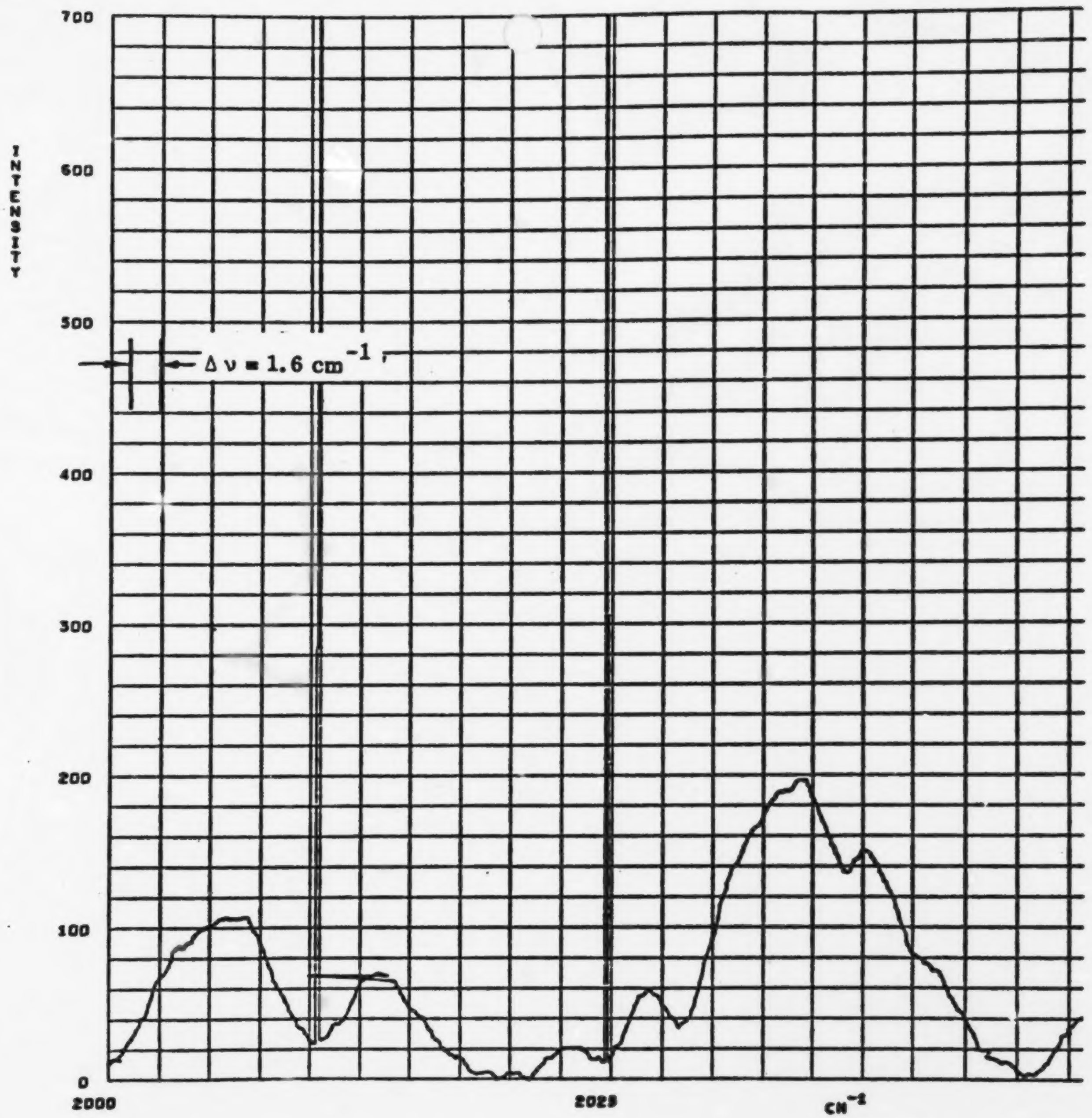

Figure 4-15. Digitized Spectrum of CO Band $\Delta\nu = 1.8\ \text{cm}^{-1}$

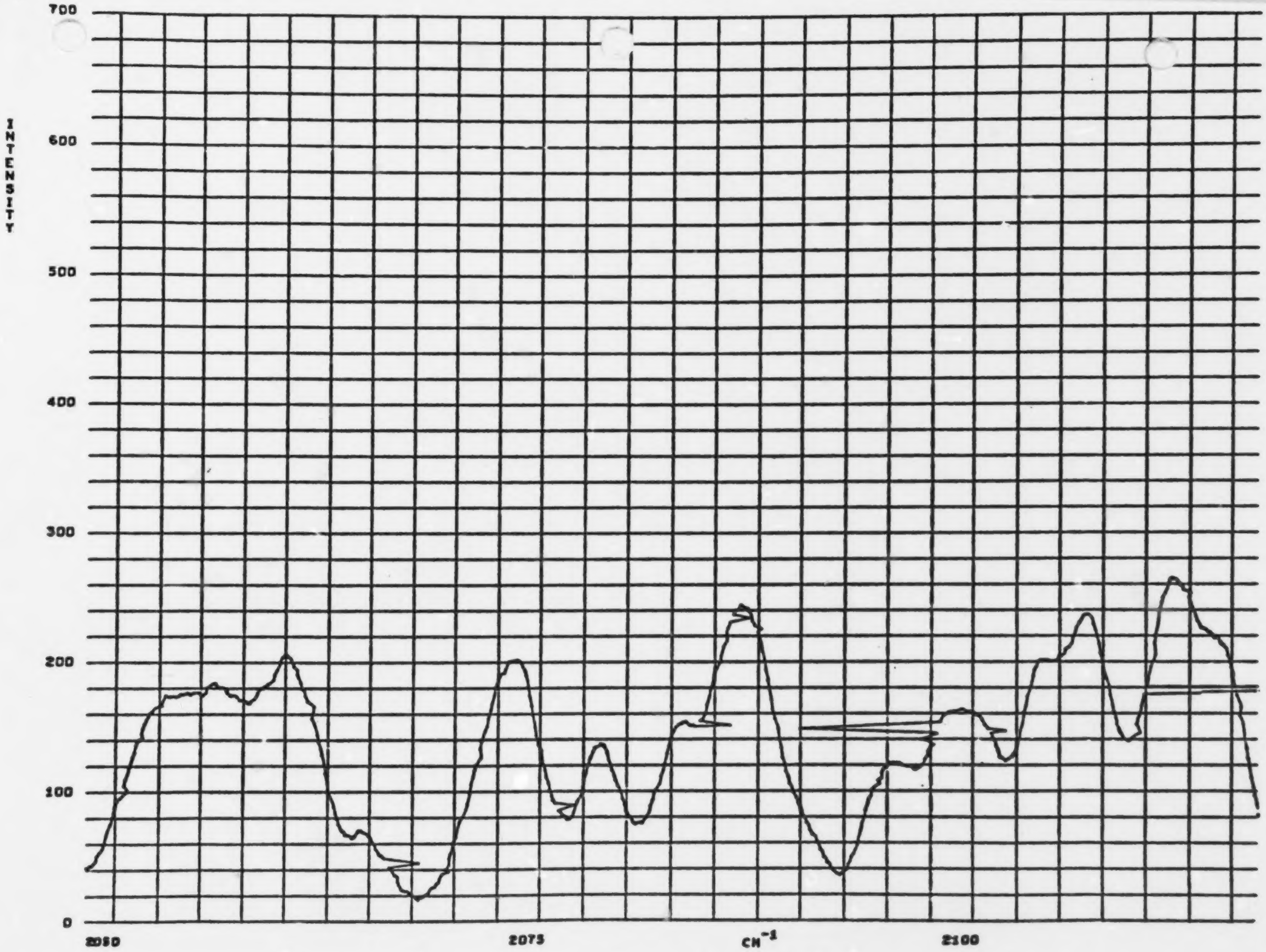

Figure 4-15. (Continued)

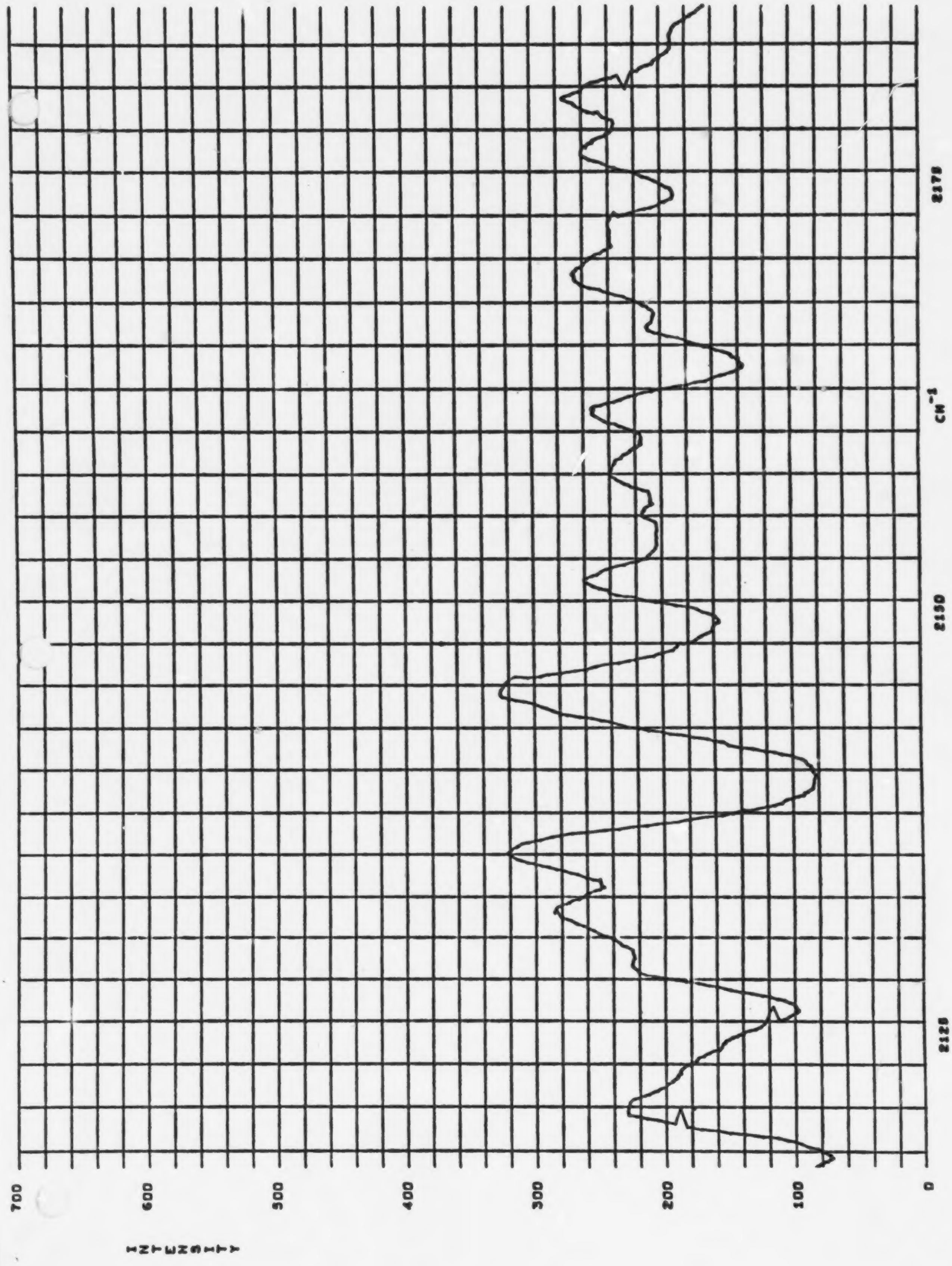

Figure 4-15. (Continued)

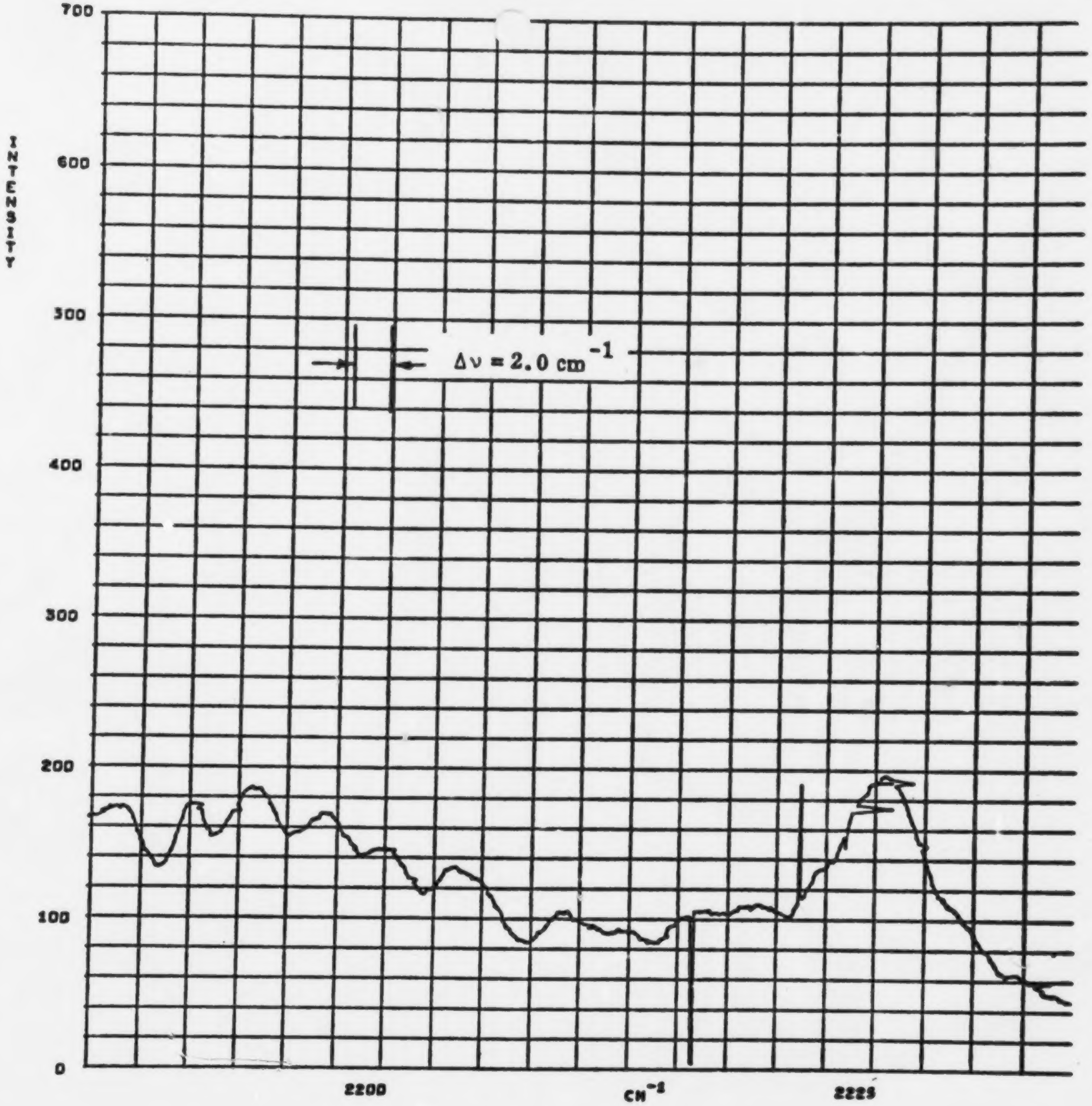

Figure 4-15. (Continued)

5

EMISSION MEASUREMENTS

For each stack, at least two measurements are necessary. One spectrum is taken from the plume, the other one adjacent to the plume to obtain the sky background. The two spectra are then differenced. This is necessary even in the case where the plume fills the field of view of the instrument. For the quantitative determination of the pollutant concentration in the stack plume, the absolute temperature of the plume must be known.

5.1 STEEL MILL

The location and absorption of the stacks of the steel mill selected for these tests are described in Section 2.1 of Appendix I. A typical spectrum of the sky background from 7 - 13μ is shown in Fig. 5-1 and that of the plume emission in Fig. 5-2. In both cases, the spectral resolution was 0.5 to 4.5 cm^{-1}. The reference source was at 106°F. The zero line (no energy difference between target and reference source) is in the center of the recording paper. When the target is colder than the reference source, the deflection is upward; if it is warmer the deflection is downward. In comparison, the two spectra appear to be very similar, except for one obvious region around 7.6μ, where the plume emission shows a rather strong emission. However, even in the regions between 8 and 10.5μ, there are differences which become apparent when the differences between the two spectra are plotted; in Fig. 5-3 the differences are shown. An attempt has been made to identify the species responsible for these bands. Normally, this differencing process is to be done by a computer. However, we experienced difficulties with the electronics and no digital records were taken. The failure of the electronics was attributed to the heat in the equipment, which was located in an unvented van, whose temperature at times reached 112° F.

The most prominent spectral features of the sky emission curve

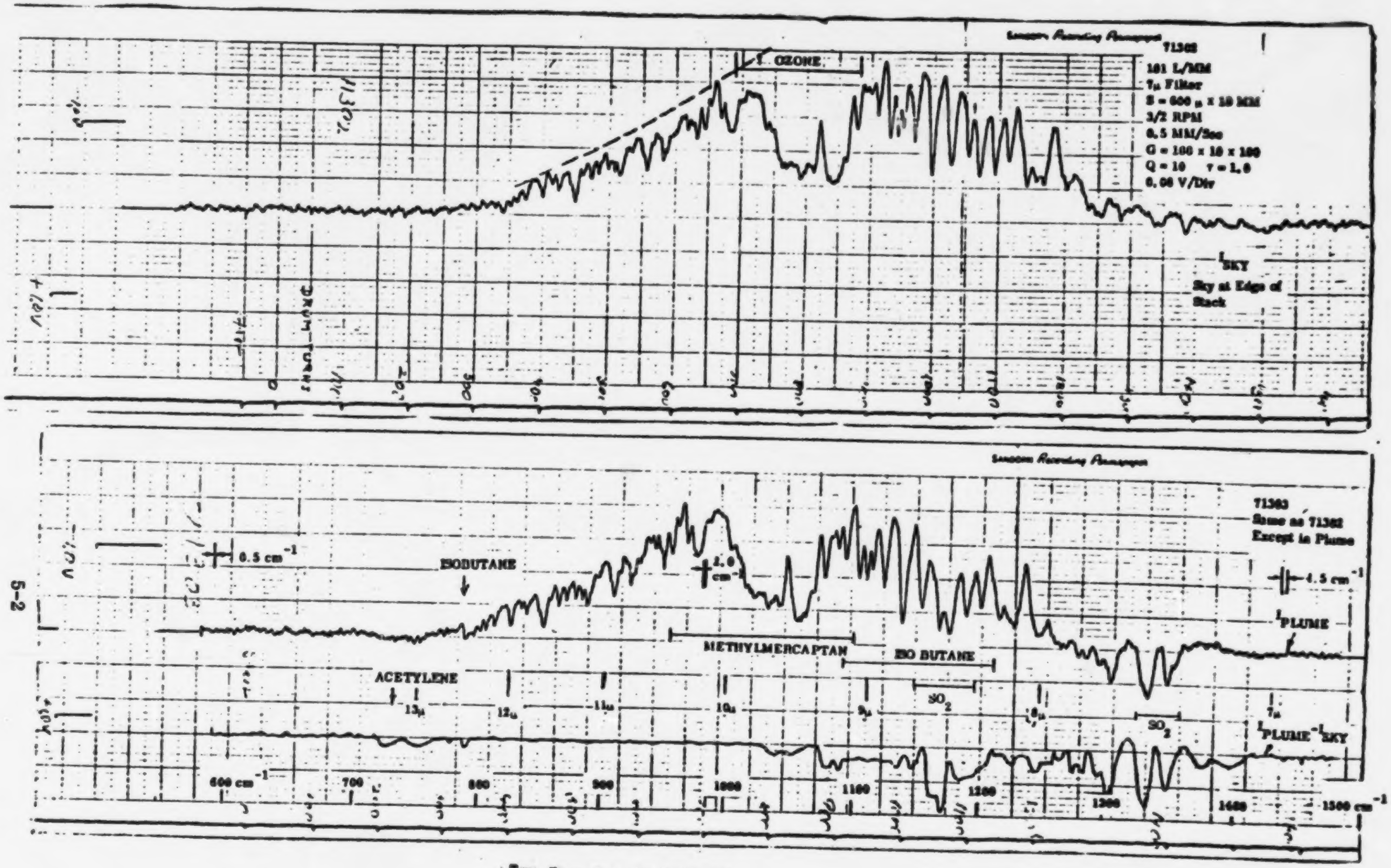

Top: Figure 5-1. Sky Background

Center: Figure 5-2. Coke Oven Plume Emission

Bottom: Figure 5-3. Difference: Plume-Sky shown in Figure 5.1 (71302) are the emission by stratospheric and low-level ozone near 1000 cm^{-1} and the H_2O spectrum.

An estimate of the effective sky radiance may be made as shown below using the final equation from Section 3.3.1 - Emission Mode of Operation, of the final report. (EPA-R2-72-052 or GDC-DBE-72-001 page 3-22).

$$N_s(\lambda, T_s) = \frac{1}{\rho^2} \left[\frac{Sx_r\sqrt{2}}{R_d \tau_c A \Omega_c \Delta\lambda\, G M_z} + N_r^o(\lambda, T_r)\rho^4 \right]$$

Using N_r° for the van temperature of 106° F (314° K) and other values appropriate to the test at $\lambda = 10\mu$,

$$Ns(10\mu, T_s) = \frac{1}{(.90)} \left[\frac{1.9\sqrt{2}}{(12 \times 10^4)(.25)(1.16 \times 10^{-3})(0.021)(10^{5})(0.58)} + 12.42 \times 10^{-4}(.81) \right]$$

$$= 10.5 \times 10^{-4} \omega/cm^2 ster\,\mu$$

for which the equivalent blackbody temperature is

$$T_s = 302° K.$$

The effective temperature difference is thus about 12° C between the van and the atmosphere at an elevation angle of about 5°. The value of sky radiance is 10 to 20% higher than the values cited in the Handbook of Military Infrared Technology (Fig. 5-5 for the clear nighttime sky at Cocoa Beach, Fla., and Fig. 5-8 for a sky with cirrus clouds).

The difference is perhaps due in part to the higher ambient temperatures in Los Angeles and, in part, to the greater pollution particularly at lower levels.

The plume emission shown on Figure 5-2 at first glance looks much the same as the sky background but taking differences as shown in Figure 5-3 reveals important features of the spectrum. A number of candidate pollutants are shown at their respective spectral locations.

A typical example of the plume emission from a steel mill stack from 3 to 5μ is shown in Figure 5-4. The sky background scan and stack wall

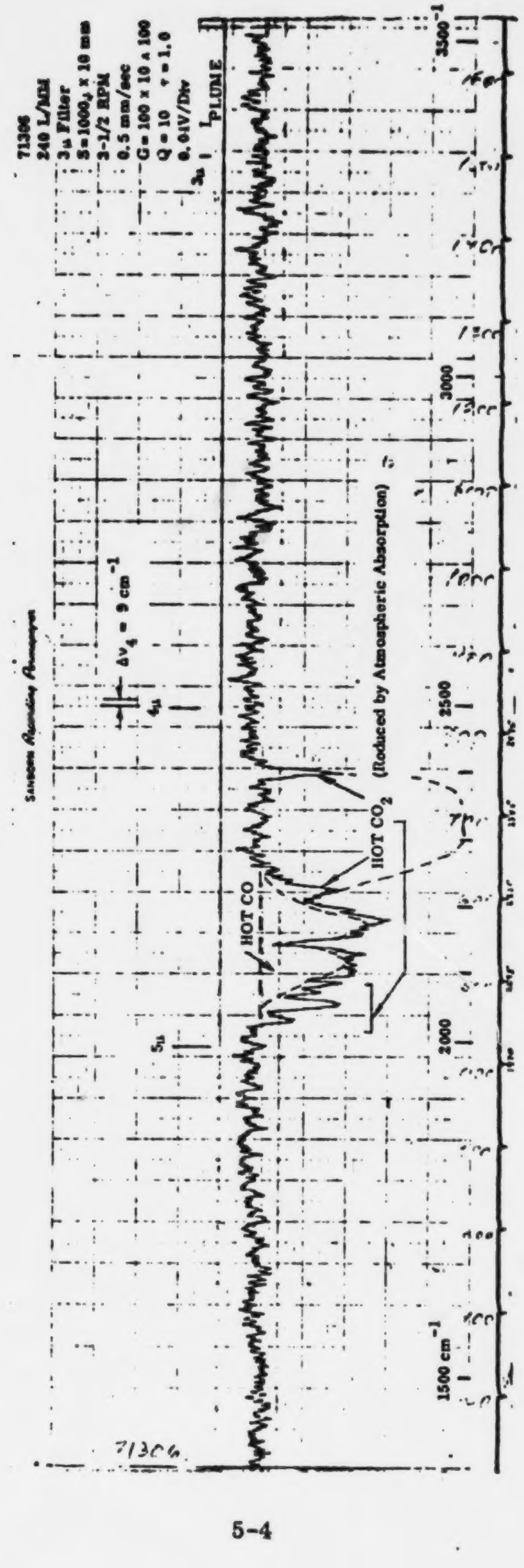

Figure 5-4. Stack Emission - Steel Mill, $\Delta\nu_4 = 9\ cm^{-1}$

scan were similar to Figure 5-4 except there was no spectral features in the CO and CO_2 regions. The spectral slit width at 4μ was about $\Delta \nu_4 = 9 \text{ cm}^{-1}$. The strong emission from hot CO and CO_2 is apparent in Figure 5-4; however, the greater portion of the hot CO_2 band is absorbed by the CO_2 in the atmosphere.

5.2 POWER STATION

The location and description of the studies of a power generating station are described in Section 2.2 of Appendix I. Spectra of both Stack #3 and #1 were taken. A typical spectrum of the emission of Stack #3 in the 7 to 13μ region is shown in Fig. 5-5 along with the sky background and the emission from the stack wall. In these traces, the colder temperatures are recorded downward. The difference between plume and sky emission is shown in Fig. 5-6. Besides SO_2, a number of hydrocarbons are possible contributors to this spectrum as indicated in Fig. 5-6.

A typical spectrum in the 3 - 5μ region is shown in Fig. 5-7 whose prominent feature is the emission from CO_2 and the total lack of CO. An indication of the small fluctuation in the signal is given in Fig. 5-8, which was taken at the peak CO_2 emission at 2475 cm^{-1}. We believe that the absence of large-scale fluctuation is due to the fact that the field-of-view was smaller than the plume but larger than the eddies in the turbulent plume so that a spatial averaging took place.

The emission in the 8 - 13μ region from Stack #1 is very similar to the one from Stack #3, except for the absence of SO_2 emission, which is in agreement with the results obtained with the interferometer.

5.3 HOSPITAL INCINERATOR

A brief description of hospital incinerator stack is given in Section 2.3 of Appendix I. The spectra we observed show great variations both in characteristics and strength. Records taken at one wavelength indicate

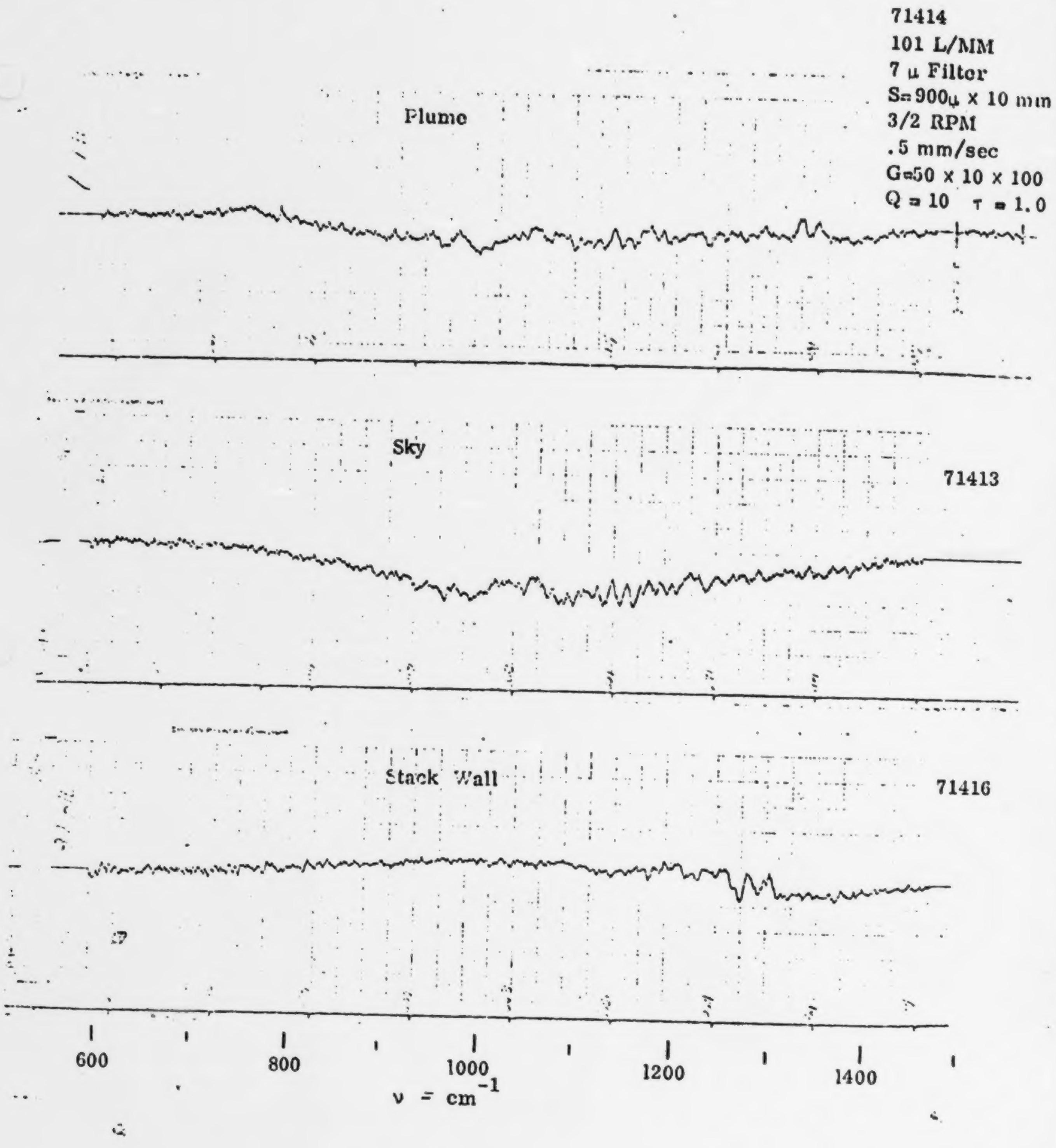

Figure 5-5. Plume, Sky and Stack Scans - Power Station Stack #3, $\Delta\nu_{10} = 3$ cm^{-1}

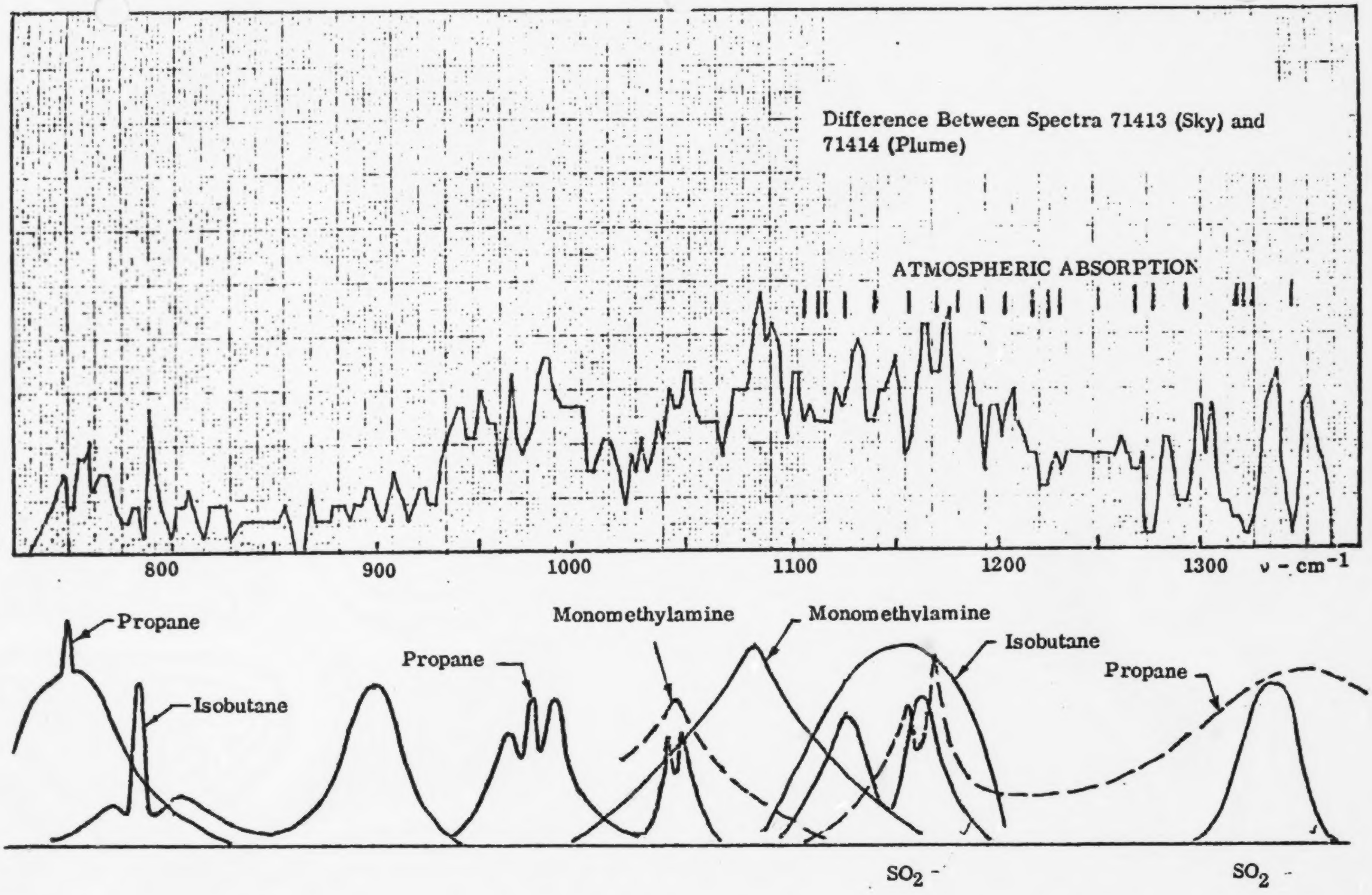

Figure 5-6. Difference Spectrum (Plume - Sky) Power Plant Stack #3

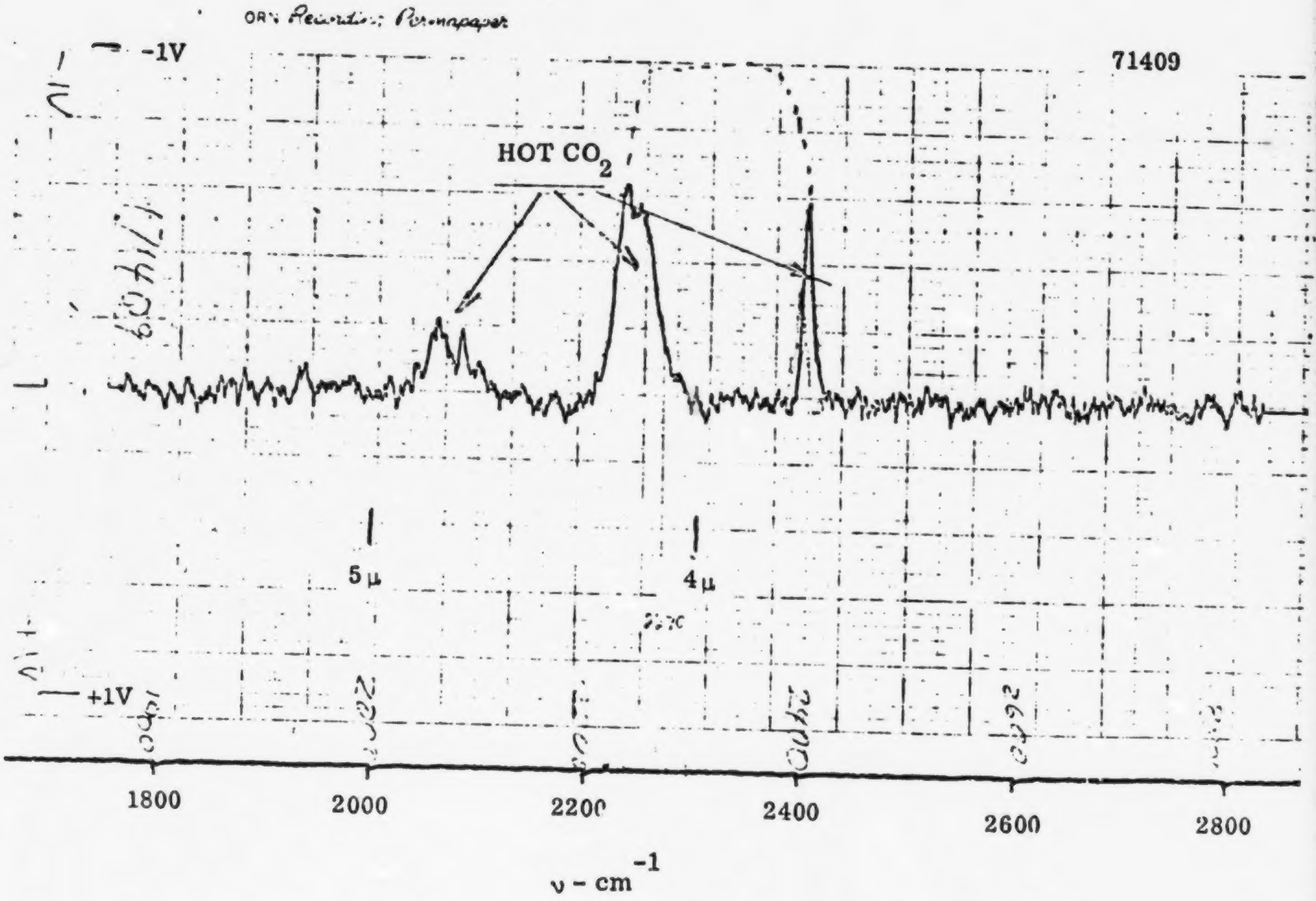

Figure 5-7. Plume Scan, 3 to 5 μ, Power Plant Stack #3

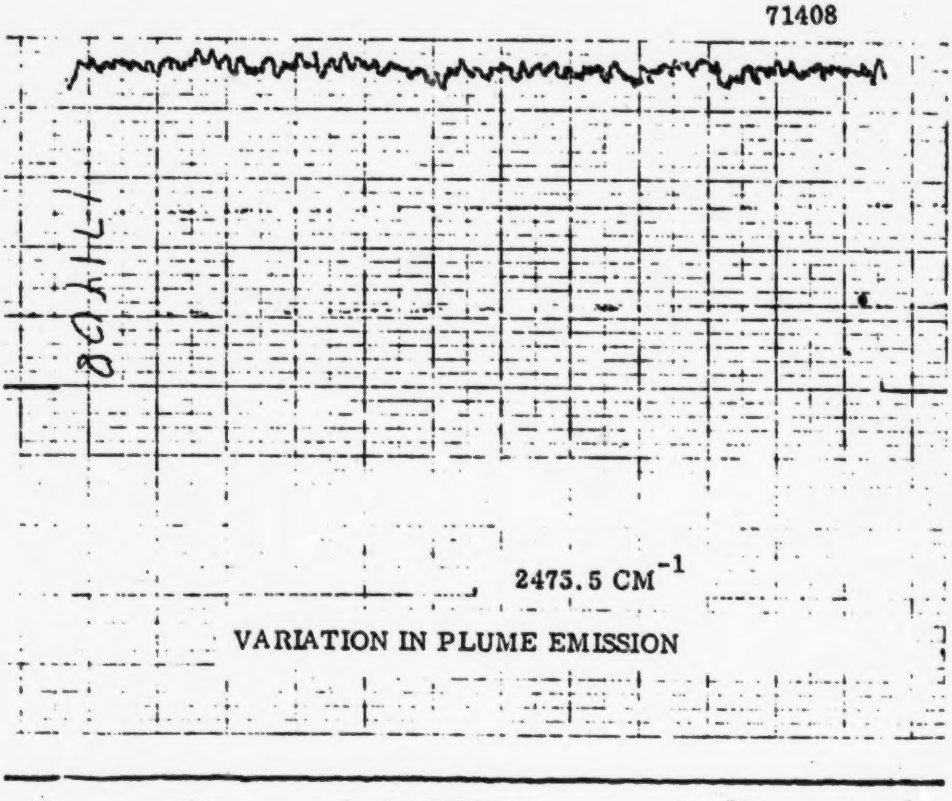

Reproduced from best available copy.

Figure 5-8. Variations in Plume Emission - Power Plant Stack #3

that the variations originate in the plume, an apparent result from the different loadings of the incinerator. A typical trace taken at 2390 cm^{-1} over a period of several minutes is shown in Fig. 5-9.

At another time, the plume appeared visibly rather steady. A comparison of two spectra recorded between 3 and 5μ in a time interval of 2 minutes is shown in Fig. 5-10. The emission between 2600 and 2900 cm^{-1} has changed drastically. The upper curve is indicative of a black body emission from soot particles, while the lower one is indicative of gaseous emission. This is the wavelength region, where H_2S and $HC\ell$ are emitting.

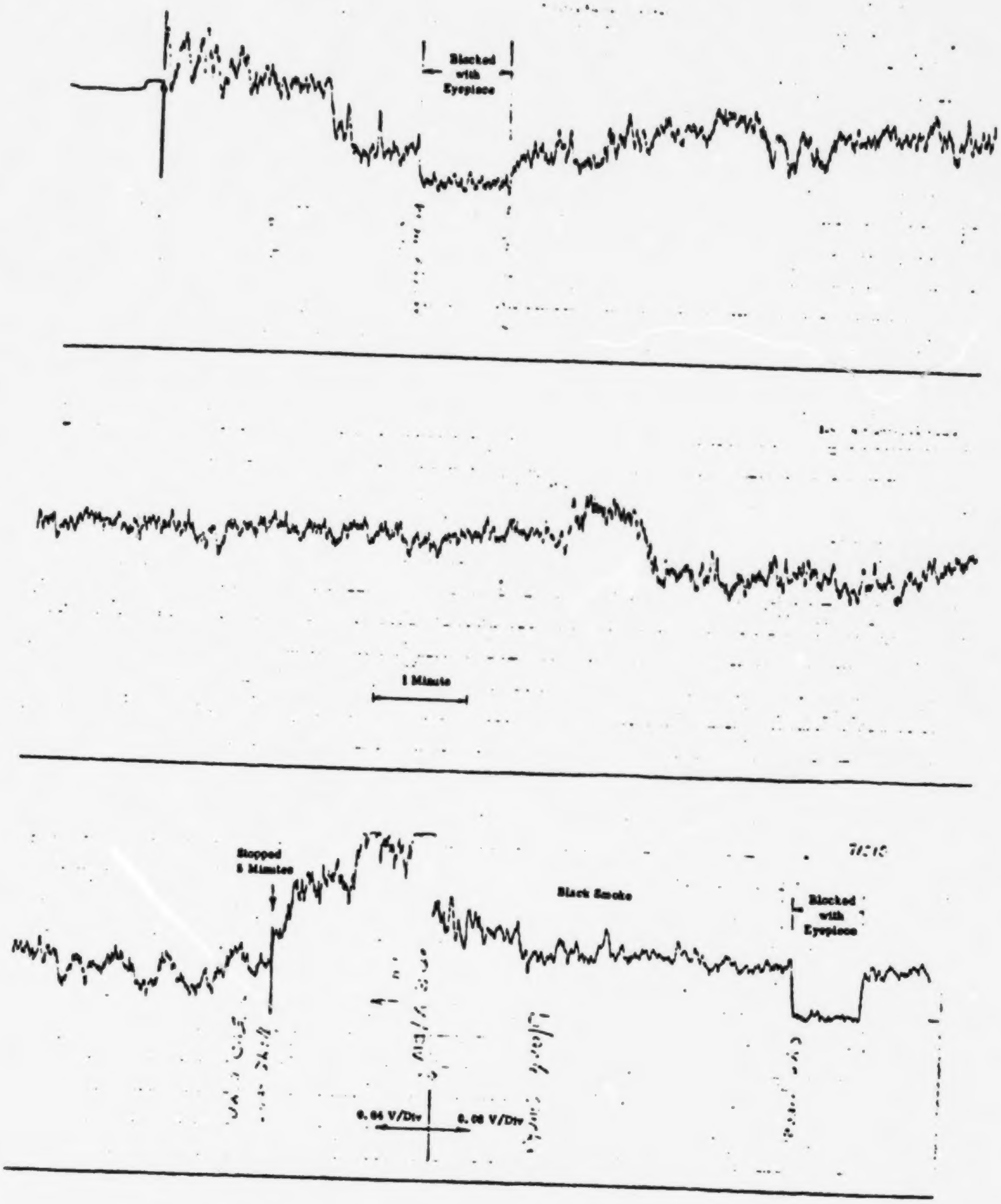

Figure 5-9. Variations of Hospital Incinerator Emission $\nu = 2390\ cm^{-1}$

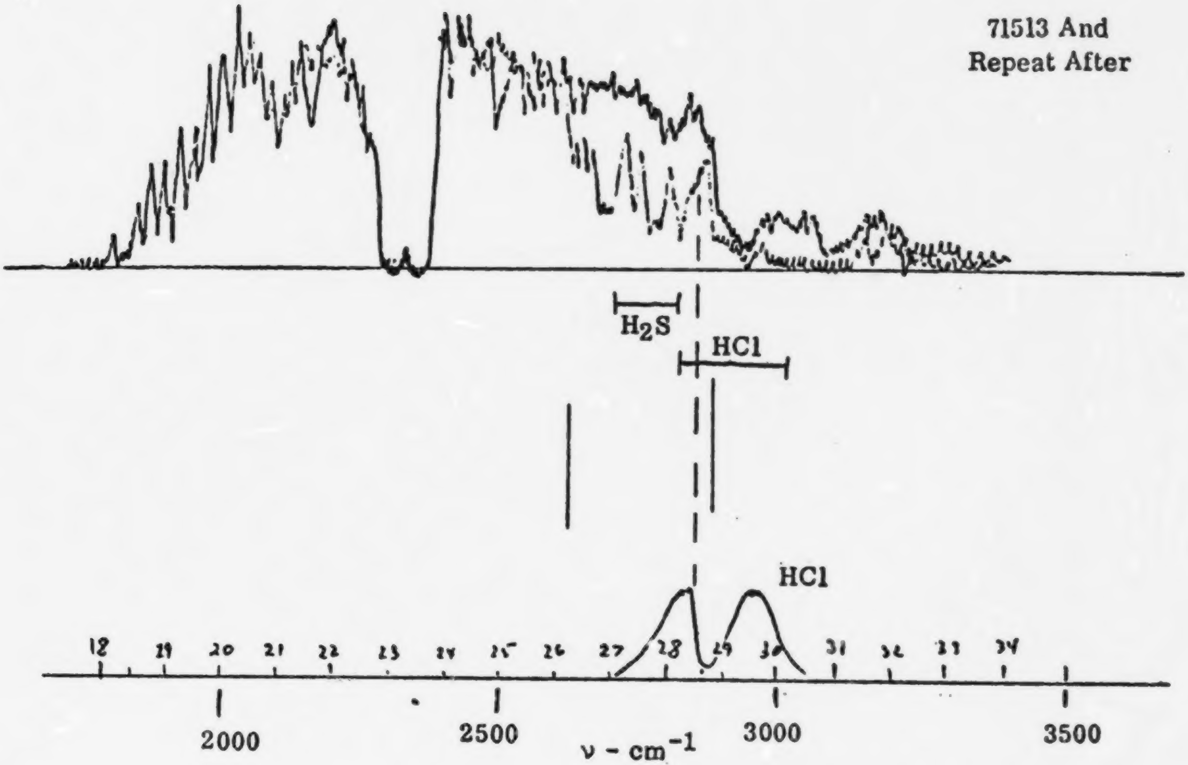

71513 And
Repeat After

Figure 5-10. Comparison of Two Scans, 3 to 5 μ, Hospital Incinerator

6

TRANSMISSION MEASUREMENTS OF EXTENDED SOURCES

Pollutant concentrations in the vicinity of a refinery in Southern California were measured over a pathlength of approximately one quarter mile. Because of prevailing winds from the west a north-south path just inside the eastern boundary of the refinery was chosen. Most of the expected emission was located at the north end of the path near the source; the receiver was located at the south end of the path in a relatively clear area. Although the prevailing wind was from the west, the wind direction varied and, at times, came from the southeast.

At two such times (i.e., with the wind from the southeast) runs were made within about 40 minutes at two different slit widths. These runs clearly show the effect of using a spectral slit width equal to or less than half the spectral line spacing.* The lines of interest here are the CO lines from about 2100 cm^{-1} to 2190 cm^{-1} which have a spacing which varies from about 4.2 to 3.3 cm^{-1}. One run with a spectral slit width at 2150 cm^{-1} of 4.4 cm^{-1} is shown at the top of Figure 6-1 and shows very little, if any, of theCO spectrum. The other run at the bottom of Figure 6-1 with a spectral slit width of 1.3 cm^{-1} shows the CO spectrum quite clearly. Since the wind was blowing toward the refinery the difference was presumably not a result of a CO level change but was a result of setting the spectral slit width less than half the spectral line spacing. An analysis indicates that the CO concentration was about 2 ppm which is about what would be expected for the ambient level.

Later in the afternoon there was a strong west wind. A CO spectrum taken at that time is shown on Figure 6-2 with instrument settings identical

---

*GDCA-DBE-72-001 page 5-16.

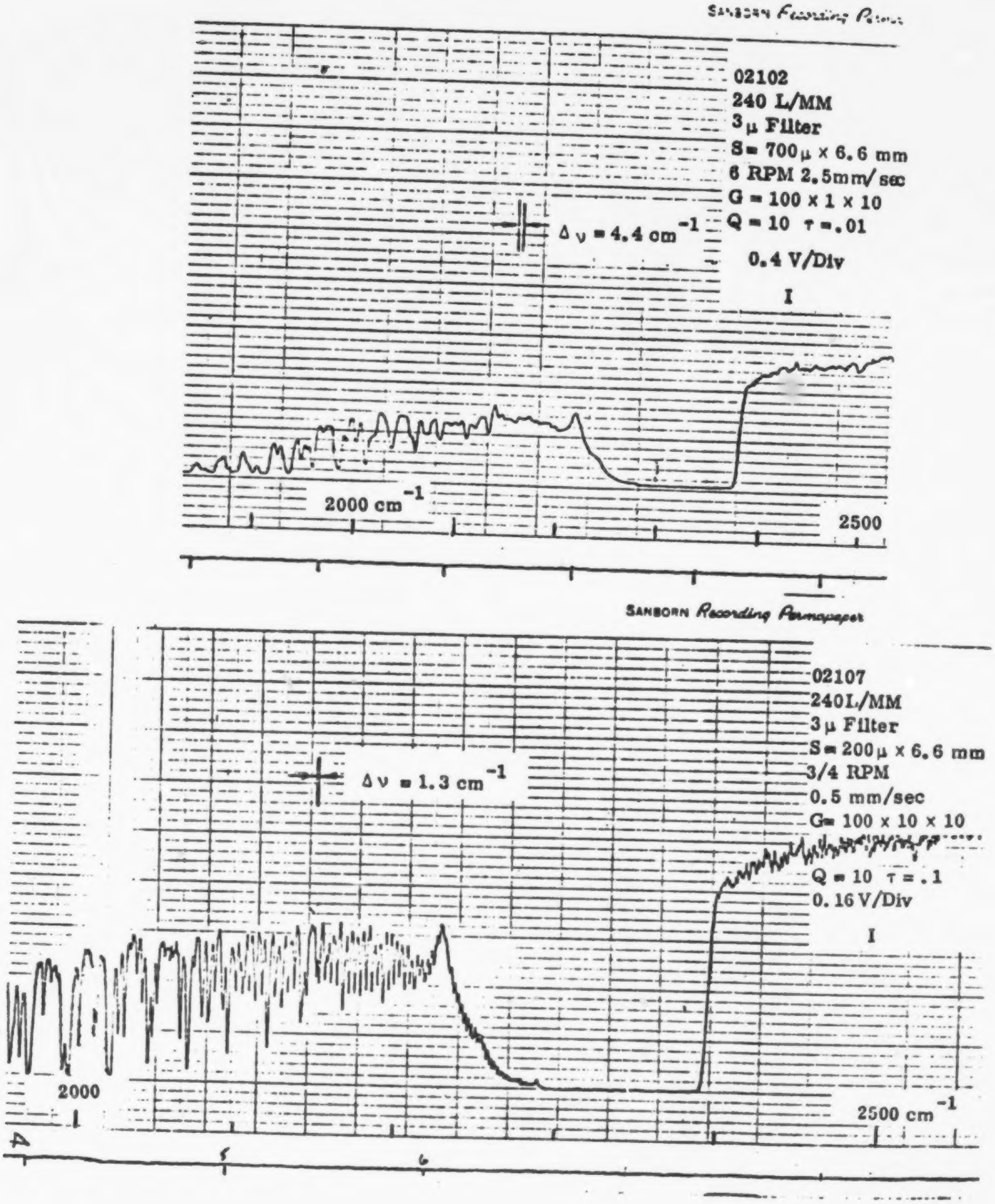

Figure 6-1. Comparison of CO Spectra with $\Delta\nu = 4.4\ \mathrm{cm}^{-1}$ and $1.3\ \mathrm{cm}^{-1}$

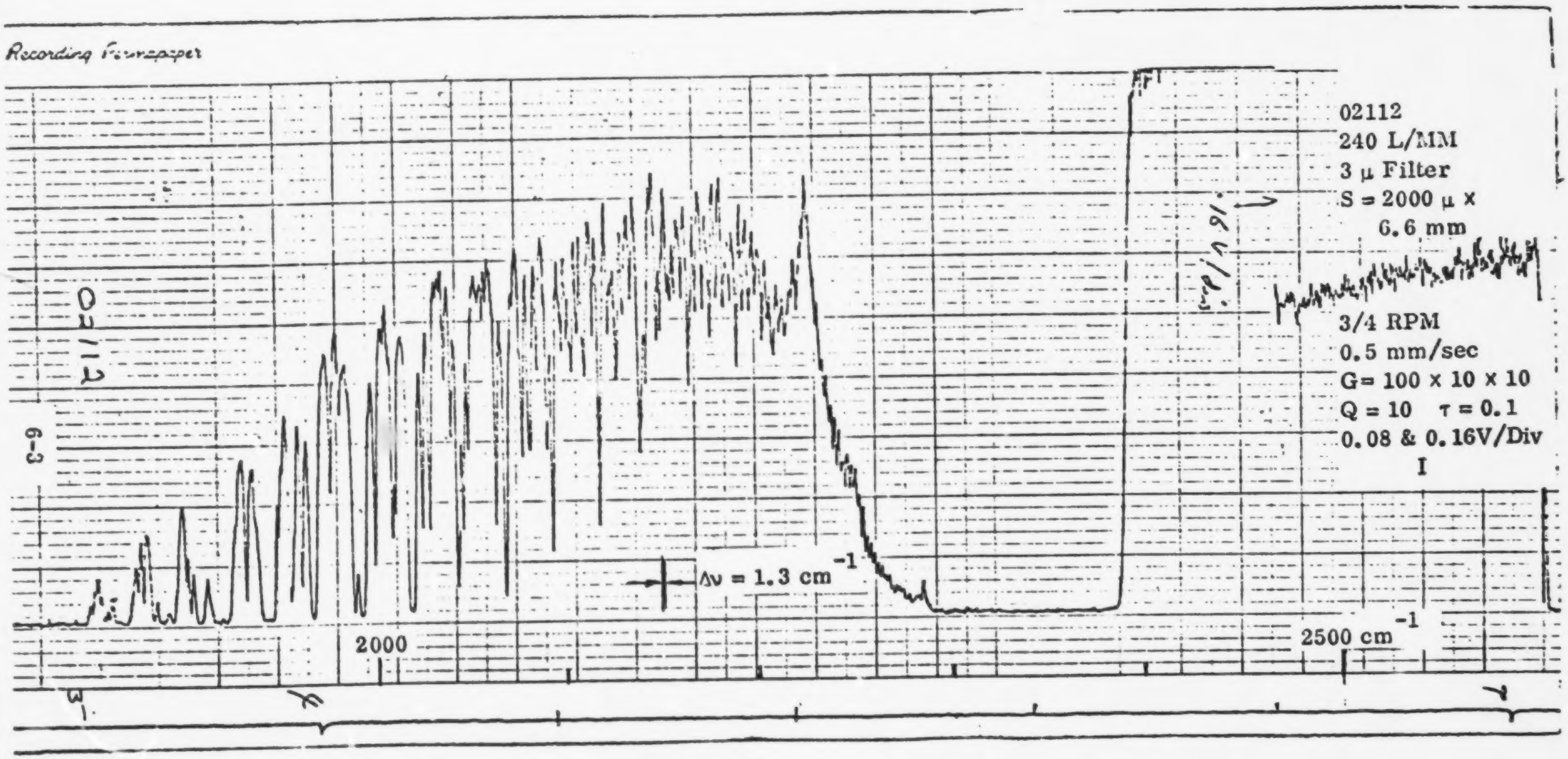

Figure 6-2. CO Spectrum at Refinery, $\Delta\nu = 1.3\ \mathrm{cm}^{-1}$

to that at the bottom of Figure 6-1 (except .08ν/01ν). Comparing the bottom of Figure 6-1 with a southeast wind blowing over a freeway and Figure 6-2 with a west wind blowing across the refinery, the CO level from the refinery is no more, perhaps less, than that from the freeway.

A complete scan with a strong west wind (taken about 15 minutes before Figure 6-2) is shown in Figure 6-3. Although the slit is narrower a longer time constant was used which suppresses line spectra somewhat. Even so, there does not appear to be much CO present. A smell of hydrogen sulfide, H_2S, was noted at the source end of the path at the time the run shown in Figure 6-3 was taken. H_2S absorption would be expected at 1100-1400 cm^{-1}, 3800-4000 cm^{-1} and at 2700-2800 cm^{-1}. No significant absorption was observed probably as a result of only a small portion of the total path containing H_2S.

Figure 6-4 shows a comparison of portions of two runs one with a southeast wind and one with a west wind. The significant difference is two sharp absorptions at 2960 and 2970 cm^{-1} with the west wind from the refinery. There are a large number of hydrocarbons which have absorption at about 3000 cm^{-1} so that positive identification could not be made with the comparison spectra available (R. H. Pierson et al Analytical Chemistry, 28, 1218 (1956)). The spectra were sketched because the absorption features of interest were faint on the original record.

A scan in the 7 to 13μ region is shown on Figure 6-5; a strong west wind was blowing (from the refinery) when this run was made. No evidence of SO_2 absorption in the 1100-1200 cm^{-1} region or other pollutants was observed on this spectrum.

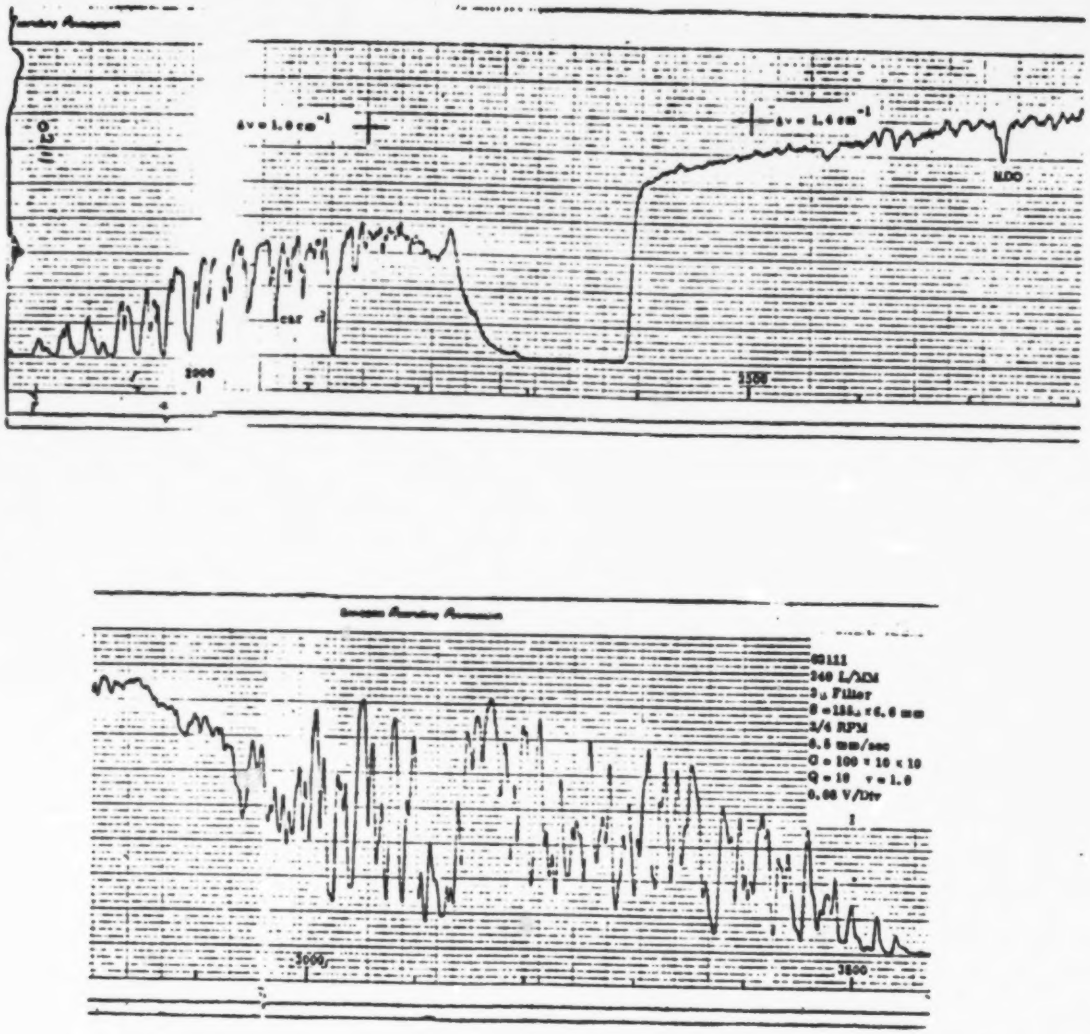

Figure 6-3. 3 to 5 μ Scan at Refinery, $\Delta\nu_4 = 1.4\ \mathrm{cm}^{-1}$

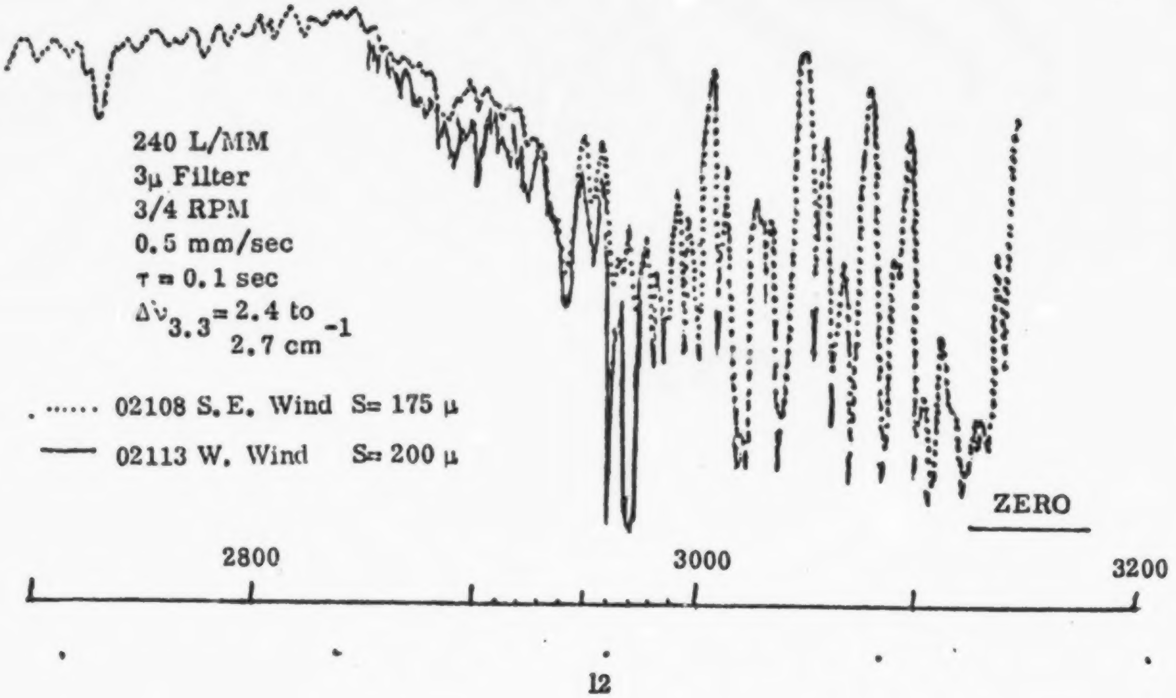

Figure 6-4. Comparison of Spectra near 3000 cm^{-1}

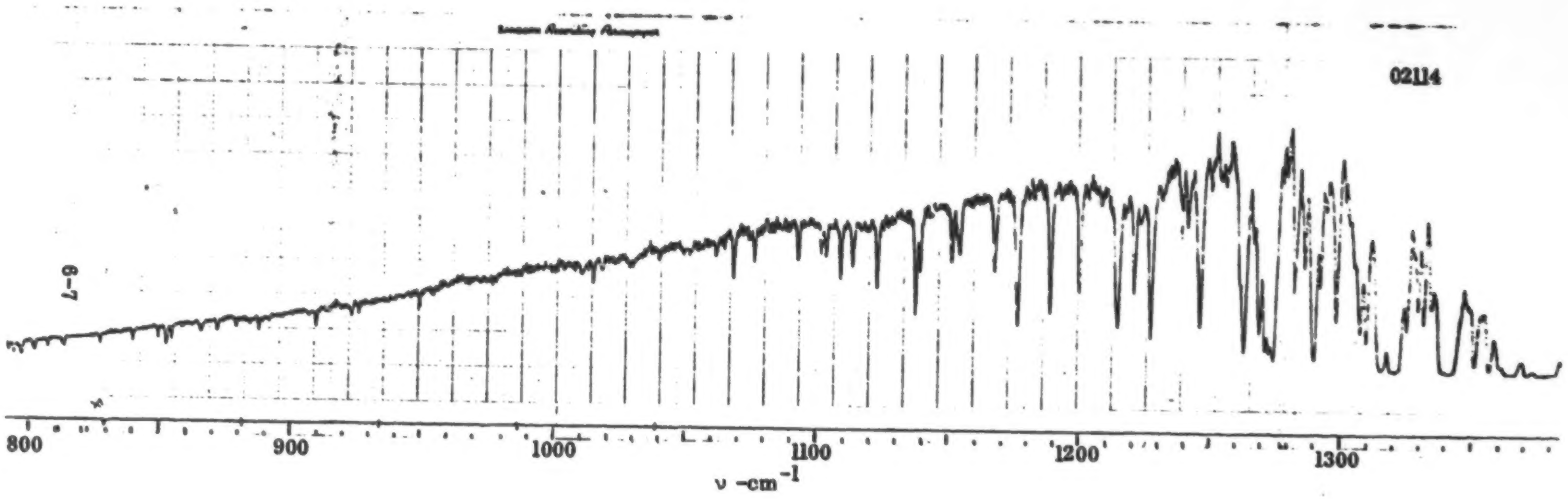

Figure 6-5 7-13μ Scan at Refinery, $\Delta\nu_{10} = 0.65$ cm^{-1}

7

SUPPORTING LABORATORY DATA

7.1 DETECTOR NOISE MEASUREMENTS

During and after the period of the field tests, measurements were made in the laboratory to define more precisely the detector noise and detector plus system noise. Measurements of detector noise were made directly at the preamplifier output with a waveanalyzer. Measurements of the indicated noise of the detector plus system for both the analog and digital systems. Finally, the results of the various measurements are compared.

7.1.1 Wave Analyzer Measurements

The noise of the cold detector with the beam blocked at the entrance slit was measured at the preamplifier output by means of a Hewlitt-Packard 302A waveanalyzer ($\Delta f = 6$ Hz) with an integrator attached to the output. The measured RMS noise voltage, V_κ, was divided by the nominal preamplifier gain to obtain the RMS noise at the detector, V_d. The noise at the detector was divided by $\sqrt{6}$ to obtain $V_d/\sqrt{Hz}$, the RMS voltage at the detector per root-Hertz. Data were taken for a period of about 12 integrator time constants and averaged to obtain the results shown on Figure 7-1. During these tests the source chopper was on and the reference chopper was off.

The wave analyzer output is a current source of 1 ma full scale and use of a 1 K load resistor converts this to a 1 volt full scale voltage source. An RC filter of 1 megohm and 5 μfd was used as an integrator ($\tau = 5$ seconds). The output was read on a CIMRON digital voltmeter ($Z_{in} = 1000$M on 1 V range) which negligibly loads the filter.

Figure 7-1 shows clearly the lower noise resulting from use of the highest preamplifier gain. The lowest noise of about 0.39 $\mu v/\sqrt{Hz}$ is some what less than that measured by the detector manufacturer of 0.44 $\mu v/\sqrt{Hz}$). The highest noise for the preamplifier plus detector is 0.72 $\mu v/\sqrt{Hz}$ which

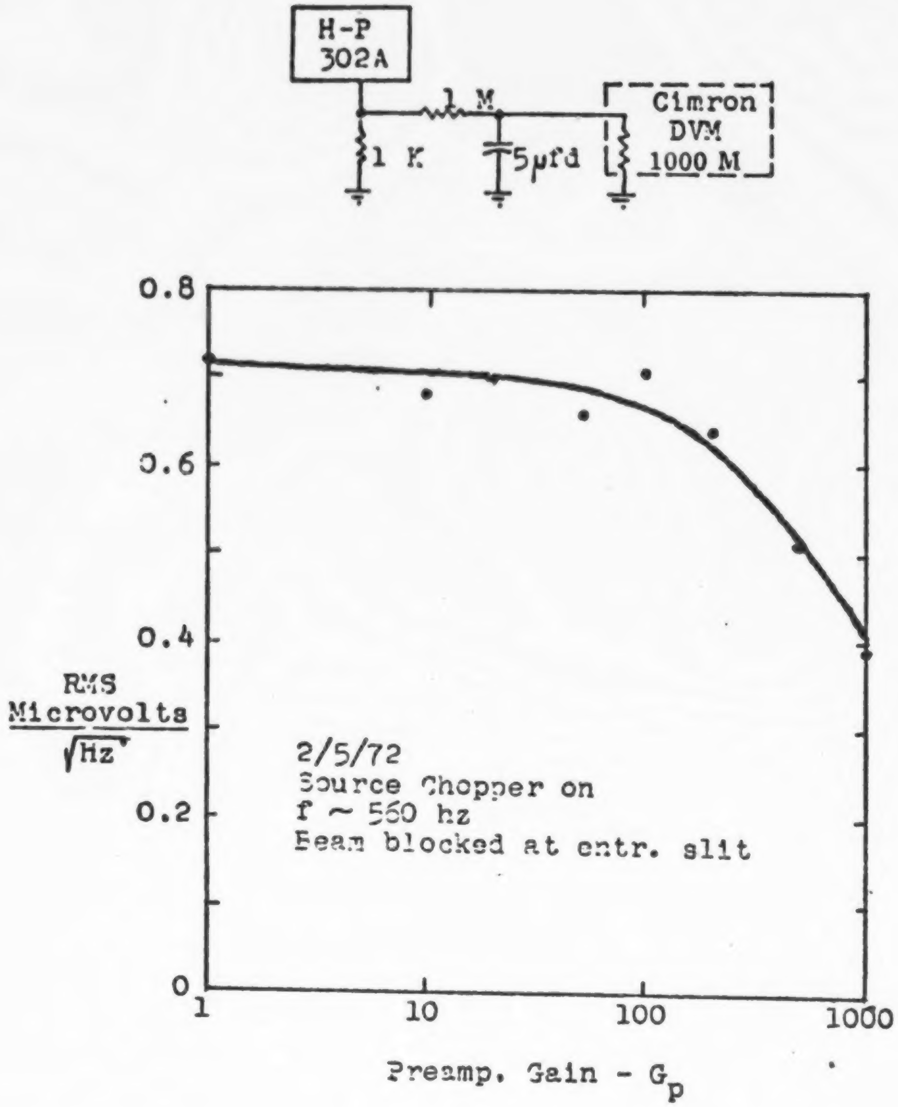

2/5/72
Source Chopper on
f ~ 560 hz
Beam blocked at entr. slit

Figure 7-1. Wave Analyzer Measurements of Detector Noise

is slightly less than that measured previously (0.80 $\mu v/\sqrt{Hz}$). The later measurements are considered more precise than the earlier value because of an improved integrator.

Wave analyzer noise measurements were also made with the preamplifier input open (internal 10K only) and with a 12.7K 1% precision resistor at the preamplifier input to simulate the detector. Data were taken and reduced in a manner similar to that used for the cold detector. With the preamp. input open the noise referred to the input with $G_p = 1000$ and $\Delta f = 6$ was ($35\mu v/1000$) = 35 nv. Thermal noise for a 10K resistance and $\Delta f = 6$ is 31.6 nv which gives a noise figure of 0.6 db. With a 12.7K resistor on the preamp. input the noise was 30 $\mu v/1000$ = 30 nv at $G_p = 1000$ and 3.0 $\mu v/100$ = 30 nv at $G_p = 100$. (At f = 330 Hz the noise was 32 $\mu v/1000$ = 32 nv at $G_p = 1000$). Thus no drop in noise at high preamp gain was observed. The noise per unit bandwidth is thus about 12 $nv/\sqrt{Hz} = 0.012 \mu v/\sqrt{Hz}$ which is small compared to the noise with the cold detector.

7.1.2 Analog System Measurements

During and after the waveanalyzer measurements, records were made with the source channel analog system (f = 560 Hz approx.) consisting of the cold detector, (beam blocked at entrance slit), preamp., selective amplifier, lock-in amplifier compensation amplifier and analog recorder. The source chopper was on and the reference chopper was off. The system was tuned up and calibrated just before the records were made. Record lengths were sufficient to assure that representative values were obtained ($\Delta t/\tau$ ranges from 40 to 170,000 with most of the data between 100 and 10,000.

Because the RMS value of a random signal is difficult to access with precision, the peak to peak values of each record were read. Voltage at the detector (peak to peak) is obtained by dividing the measured value by the overall gain $G = (G_p)(G_{fs})(G_{xs})$. Peak to Peak voltage at the detector per unit bandwidth is calculated by division by $\sqrt{\Delta f} = \sqrt{1/4\tau}$.

The peak to peak results are shown on Figure 7-2 as a function of preamplifier gain. The highest values (between 6 and 7) are occasional peaks and the lowest values (between 1 and 2) are for very small recorder deflections. Except for these, most of the analog data lie between 0.67 and 1.5 of the equivalent peak to peak noise from the wave analyzer measurements indicated by the dashed lines ($= 5\ Vd(RMS)/\sqrt{Hz}$). The scatter is an indication of the difficulty of measuring noise by the peak to peak method. Even considering this scatter the average of the analog data is in resonable agreement with that from the wave analyzer. Note that the lock-in gain, G_{xs} = (DC volts out/RMS volts in), is used for noise calculations.

Also shown on Figure 7-2 is the digital result described in the next section.

7.1.3 Digital System Measurements

Data were taken after the field tests to determine the system noise as indicated by the digital system. Both DVM's were connected to the MONITOR terminal of the reference lock-in amplifier. A signal of about 8 volts was simulated with the lock-in zero suppress circuit. Digital data were taken on paper tape at about 3.3 data points per second and 50 data points were taken. The -010 DVM was on DC so that it measured voltage not ratio.

First, data were taken with the DVMs in the condition in which the field tests were made; i.e., with a filter on the input of the -010 DVM as installed by the manufacturer. It was decided that the system would indicate I/Io more properly if this filter were disconnected. After disconnecting the filter, data were taken again.

Each set of data consisting of 50 data points was analyzed; the (maximum-minimum) gives the peak-to-peak voltage and the RMS value of the deviation from the mean was calculated using the H-P 9100A computer. The results for G = 1K x 1 x 100 with the cold detector (beam blocked at

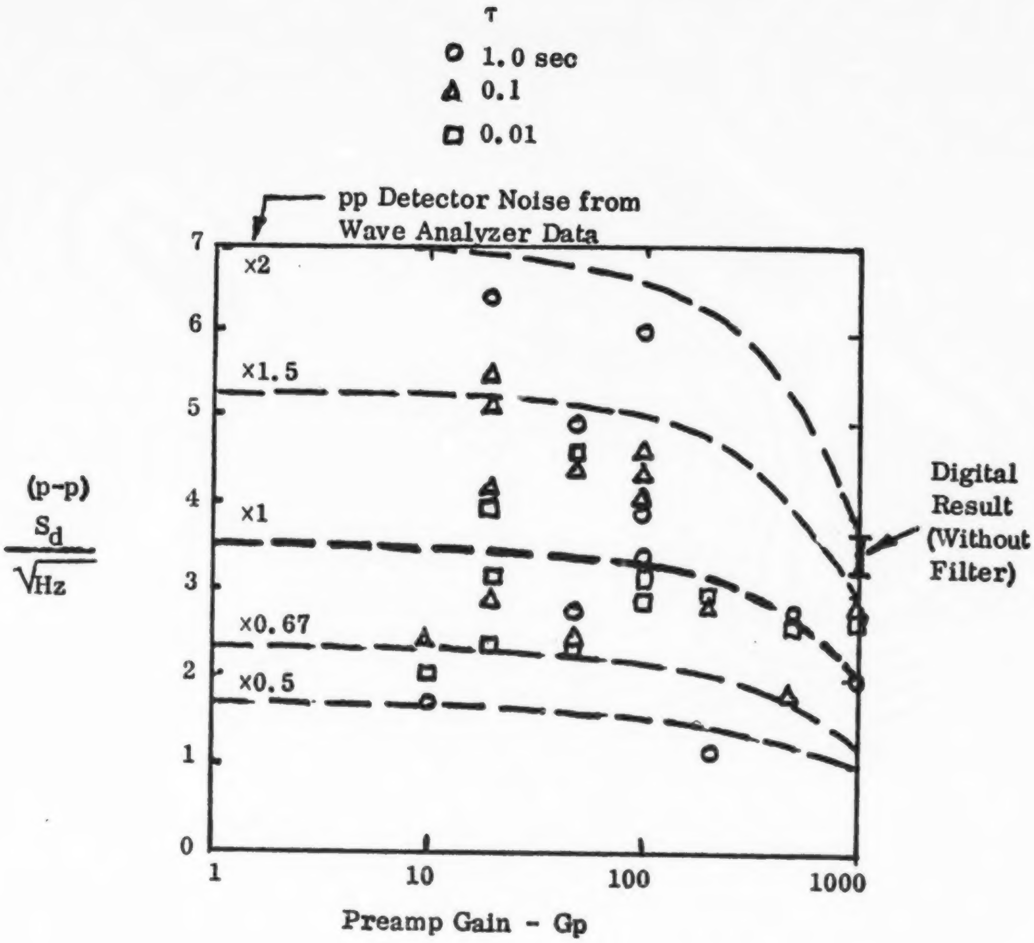

Figure 7-2. Analog Measurements of Noise

the entrance slit) are tabulated below and shown on Figure 7-2. The reference chopper was on during these tests. The voltage at the detector is obtained by dividing the measured lock-in output voltages by the total gain, G, which includes G_{xs}, the normal lock-in gain.

	With Filter - $\mu v/\sqrt{\Delta f}$				Without Filter - $\mu v/\sqrt{\Delta f}$			
τ	-015		-010		-015		-010	
0.01 sec	4.07	0.92	1.34	0.28	6.32	1.09	4.63	0.87
0.03	3.47	0.76	1.93	0.45	3.27	0.73	3.97	0.82
0.1	2.66	0.71	2.20	0.53	3.07	0.63	2.86	0.70
0.3	2.24	0.68	2.50	0.59	2.44	0.54	2.22	0.52
1.0	3.46	0.84	3.16	0.85	2.44	0.70	2.42	0.65
Avg	3.18	0.78	2.23	0.52	3.51	0.74	3.22	0.71
Avg (pp/ RMS)	4.5		4.5		4.6		4.6	

Note that, before removal of the filter on the -010 DVM, the noise (and also the response) is substantially reduced compared to the 015 DVM particularly at the shorter time constants. After removal of the filter, the noise data (and therefore the response) for the two DVM's are much more similar. Note also that the ratio of the (pp/RMS) is very nearly equal to the previously assumed value of 5.

The filter of the -010 DVM was left disconnected to make the response of the two DVM's more nearly equal.

7.2 MONOCHROMATOR CALIBR. - TEMP EFFECTS

Because of the high ambient temperature during some of the field tests (particularly the emission tests) it is appropriate to record the results of a prior check of temperature effects on the wavenumber calibration of the monochromator.

An examination of the approximate effect of temperature on the monochromator wavenumber calibration was made by placing a heat lamp above the monochromator. Time did not permit the elimination of spatial temperature gradients; rather, the monochromator was heated to about 40° C and allowed to cool slowly. The temperature and the wavenumber drum readings for the 5th, 7th and 13th order of a mercury lamp were observed as a function of time. From the drum readings at 40, 35 and 30° C the wavenumber calibration constants were determined:

$$\nu = A + B\ (WD).$$

A is the wavenumber corresponding the zero on the drum and B is the wavenumber interval corresponding to one drum turn (WD is the drum reading in turns). A prior calibration at 25° C is also included for comparison. The total cooling time (to about 29° C) was 5 hours.

Temperatures measured at the center of the top of the cover and at a hole in the base of the monochromator near the Photomultiplier tube agreed within about 1° C, the cover temperature being slightly cooler.

The results of the test are given below:

40° C Order	ν_1	WD	B cm^{-1}/turn	A cm^{-1}
5	3662.3	18.391		
7	2615.9	10.069	125.650	1351.4
13	1408.9	0.454		
35° C				
5		18.376		
7		10.056	125.763	1351.3
13		0.455		
30° C				
5		18.351		
7		10.042	125.938	1351.2
13		0.455		
25° C*				
5		18.334		
7		10.042	126.171	1349.1
13		0.471		

*Calibration the previous day (5/26/70); the monochrometer has since been realigned so that only relative values are important.

$$B = \frac{\nu_5 - \nu_{13}}{WD_5 - WD_{13}}$$

$$A = \nu_7 - \frac{0.454}{B}$$

7.3 DIVIDER BOX

In order to calibrate the system completely from the detector to the DVM it is necessary to insert a divider box (Figure 7-3) ahead of the preamplifier with the divider box having a nominal division ration equal to the nominal preamplifier gain. The lock-in calibration signal is applied to the divider box.

The measured output impedance of the lock-in calibration signal is 52 ohms. The measured input impedance of the preamplifier is 10.01K ohms. These values were used in the calculation of the division ratio. Resistance values were measured on a Cimron 6753 digital multimeter to an accuracy of .005% FS on 0.01% RDG (whichever is greater) on the 1, 10 and 100K ranges and 0.005% FS or 0.02% RDG (whichever is greater) on the 1000K range.

The calculated values of the division ratio, Ei/Eo, agree with the nominal ratio within 1% of the nominal value.

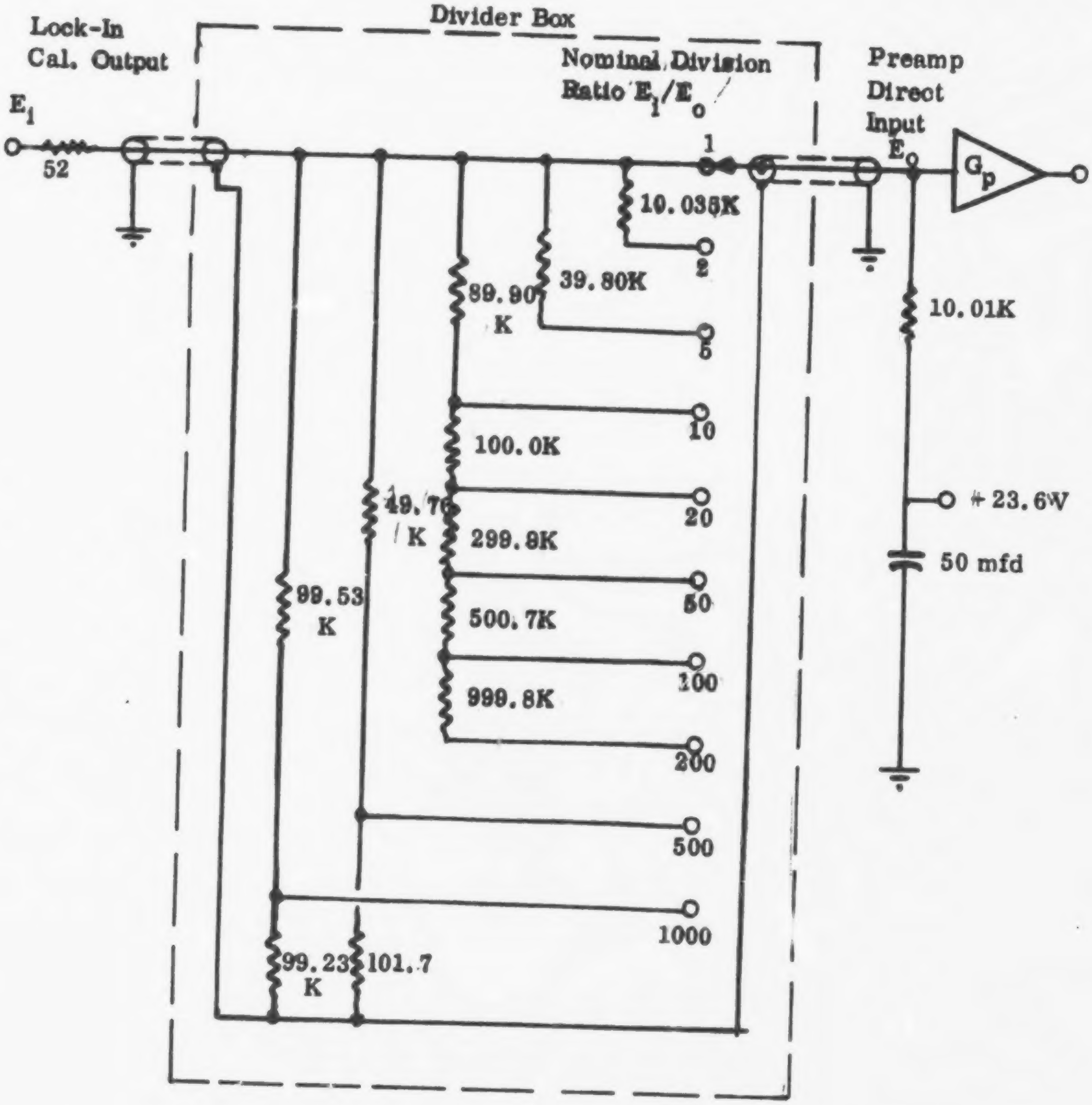
Lock-In
Cal. Output
E_1
52
Divider Box
Nominal Division
Ratio E_1/E_o
1
10.035K
2
39.80K
5
89.90 K
10
100.0K
20
49.76 K
299.8K
50
99.53 K
500.7K
100
999.8K
200
500
1000
99.23 K
101.7
Preamp
Direct
Input
E_o
G_p
10.01K
+23.6V
50 mfd

Nominal Div. Ratio	Actual Div. Ratio (Ei/Eo)	Actual/Nominal
1	1.0068	1.0068
2	2.0108	1.0054
5	4.989	0.9978
10	10.002	1.0002
20	20.008	1.0004
50	50.017	1.0004
100	100.13	1.0013
200	200.16	1.0008
500	496.5	0.9930
1000	1009.1	1.0091

Figure 7-3. Divider Box Schematic

8

RECOMMENDATIONS

1. For emission tests a standard source should be incorporated between the receiver chopper and the receiver telescope to check signal levels.

2. Tweak the detection toroid after each move before testing.

3. In the transmission mode of operation a slit height of about twice h_o would be used to reduce signal noise (from that with height = h_o). Because the relative source to reference signal is reduced, the τ sig control will have to be increased by roughly the same factor of two.

4. The System Operating Log should be expanded (perhaps to 11 × 17) to include the source and reference chopper frequencies (or, at least, if each is on or off) and also the value of τ sig. A section for notes should be included; more copious notes in the field tests would have greatly aided the data analysis.

REFERENCES

1.. Design and Construction of a System for Remote Optical Sensing of Emissions (ROSE System) M. L. Streiff and C. R. Claysmith, EPA-R2-72-052 or GDC-DBE-72-001, January 1972.

2. C. B. Ludwig, Applied Optics 10, 1057 (1971).

3. C. B. Ludwig, M. Griggs, W. Malkmus and R. Bartle, Air Pollution Measurements by Satellite, NASA (in press).

4. C. B. Ludwig, R. Bartle and M. Griggs, NASA CR1380 (July 1969).

5. F. Volz Arch. Met. Geophys. Biokl. B, 10 p. 100 (1959).

6. R. H. Pierson, et al, Analytical Chemistry 28, 1218 (1956).

TM 6-125PH-336
CONTRACT NO. WA-4800

APPENDIX I

AIR POLLUTION MEASUREMENTS IN THE INFRARED

SEPTEMBER 1971

SUBMITTED TO:

GENERAL DYNAMICS
Convair Aerospace Division

BY

GENERAL DYNAMICS
Electro Dynamic Division
P.O. Box 2507, Pomona, California 91766

AIR POLLUTION MEASUREMENTS IN THE INFRARED

FOREWORD

The General Dynamics Electro Dynamics Division, Pomona operation was funded under a subcontract (WA 4800) to General Dynamics, Convair Aerospace Division to assist in conducting a series of infrared spectral measurements for the Environmental Protection Agency, Research Triangle Park, North Carolina.

The primary objectives of these measurements were to demonstrate the feasibility of detecting and identifying air pollutants and to compare measurement data taken with three different instruments. The instruments used in the measurements were:

(1) Convair Grating Spectrometer
(2) Bendix Filter Wheel Spectrometer and
(3) Pomona Operation Interferometer Spectrometers

The Pomona operation acknowledges the cooperation of Mr. G. Rounds of Kaiser Steel Corporation, Fontana, California, Mr. W. Faulkner of the Air Pollution Control District, Los Angeles, California, and Mr. T. Banks of the Pomona Valley Community Hospital, Pomona, California, for providing the Pomona operation with data regarding the concentrations of stack effluents and readings of the APCD Pomona Valley monitoring station.

SUMMARY

The Pomona operation of General Dynamics, in support of the Environmental Protection Agency, provided:

(1) liaison service with various industrial personnel to obtain access to industrial plant property, where required, and analytical data, whenever possible, on concentrations of stack effluents

(2) selection and surveying of sites for performing atmospheric transmission measurements

(3) transmission measurements of an 1800°K blackbody source over 1 and 2 mile paths, and

(4) emission measurements of selected industrial stacks.

For both measurement functions (items 3 and 4), Michelson type interferometer spectrometers covering the spectral region from 716 cm^{-1} to 5000 cm^{-1} were utilized. Both instruments were developed by the Pomona Operation of General Dynamics. A description of the instruments as well as the measurement and data reduction procedures are provided in the Appendices.

The one mile transmission measurements were performed on June 30, July 1 and July 2, while 2 mile measurements were made on July 27 and 28. The spectral data along with concentrations of O_3, NO, NO_2, and CO measured at the Pomona APCD monitoring station obtained through the courtesy of the Public Information Service Department of the Los Angeles County Air Pollution Control District, and meteorological data obtained during the measurements are presented in Section 1.

Spectral measurements of thermally excited gaseous stack effluents at Kaiser Steel Corporation, Fontana, California, Southern California Edison power generating station, Etiwanda, California, and Pomona Valley Community Hospital were made during the week of 12 July. Spectral data, corrected for instrument response, along with available data on concentrations of major pollutants are presented in Section 2.

The transmission and emission measurements demonstrate the efficacy of interferometer type spectrometry in detecting gaseous pollutants in the atmosphere. Transmission data can, for example, readily detect the presence of small quanties of ozone while emission measurements can remotely identify CH_4, SO_2 and CO from stack effluents. The rapid data collection (on the order of 1 sec per spectrum) coupled with the high resolution of the interferometer provides obvious advantages particularly if the source emission shows rapid variations or the source itself is non-stationary (automobiles, airplanes, etc.).

While the present system requires computer reduction for highest resolution, instantaneous data (on the order of 1 sec) can also be obtained at reasonable resolution (8 cm^{-1}), see Figure 20. Moreover, simple state-of-the-art attachments (commercially available) can be utilized to provide highest resolution data (~1 cm^{-1}) for any portion of the spectrum.

Section 1.0

ATMOSPHERIC TRANSMISSION DATA

1.1 ONE MILE MEASUREMENT

One mile transmission measurements with the Pomona operation interferometer spectrometer and the 1800°K blackbody source provided by General Dynamics, Convair were made during the week of June 28, 1971. The location of source and spectrometers are indicated on the map shown in Figure 1. The source was placed at an elevation of approximately 50 feet above the spectrometer location, and the instrumentation was arranged as shown in the photograph of Figure 2.

Hourly average concentrations of NO, NO_2, O_3, and CO (as provided by the local air pollution monitoring station) are presented in Tables I through IV and also in Figures 3 through 6 to indicate the diurnal variations of the concentrations of the pollutants during the week of June 28, 1971. The hourly average concentrations show a maximum ozone concentration during the mid-afternoon hours, while the NO and NO_2 concentrations reach a maximum level during the early morning and late afternoon and evening hours. Carbon monoxide concentrations are relatively constant throughout the day.

The spectral data in Figures 7 through 9 are presented as relative intensitites corrected for instrument response only. The mid-ir region measured with an InSb (pv) detector is shown from 2000 cm^{-1} to 5000 cm^{-1} while the long wavelength information measured with a HgCdTe detector is shown from 720 cm^{-1} to 2000 cm^{-1}. In order to present the spectra in sufficient detail, the entire spectrum was divided into three separate plots. Figure 7 shows the region from 720 to 2000 cm^{-1}, Figure 8 from 2000 to 3500 cm^{-1}, and Figure 9 from 3500 to 5000 cm^{-1}, The relative intensity scales of all three figures are approximately identical, i.e., the actual intensities in Figure 7 (scale values 0 to 8) are considerably lower than those in Figures 8 and 9 (scale values from 0 to 60).

The spectral data clearly indicate the sensitivity of the ozone absorption to changes in concentration. The ozone absorption at 1042 cm^{-1} (ν_3) and 1103 cm^{-1} (ν_1) is of particular interest since it alone of all the gases of interest is relatively unaffected by interference from water vapor, CO_2 and N_2O absorption.

The applicability of transmission data in the determination of ozone concentration in the atmosphere is fully demonstrated in the curves of Figure 10 in which spectra with 3 different ozone concentrations are shown superimposed with the zero levels of relative intensity displaced slightly. The hourly average concentrations of ozone at the time of the measurements were approximately 6, 9 and 13 parts per hundred million and the increased absorption as the concentration increases is readily discernible.

Figure 11 displays the same information but confined to the spectral region primarily affected by ozone. The relative magnitude of the O_3 absorption becomes more apparent in this figure.

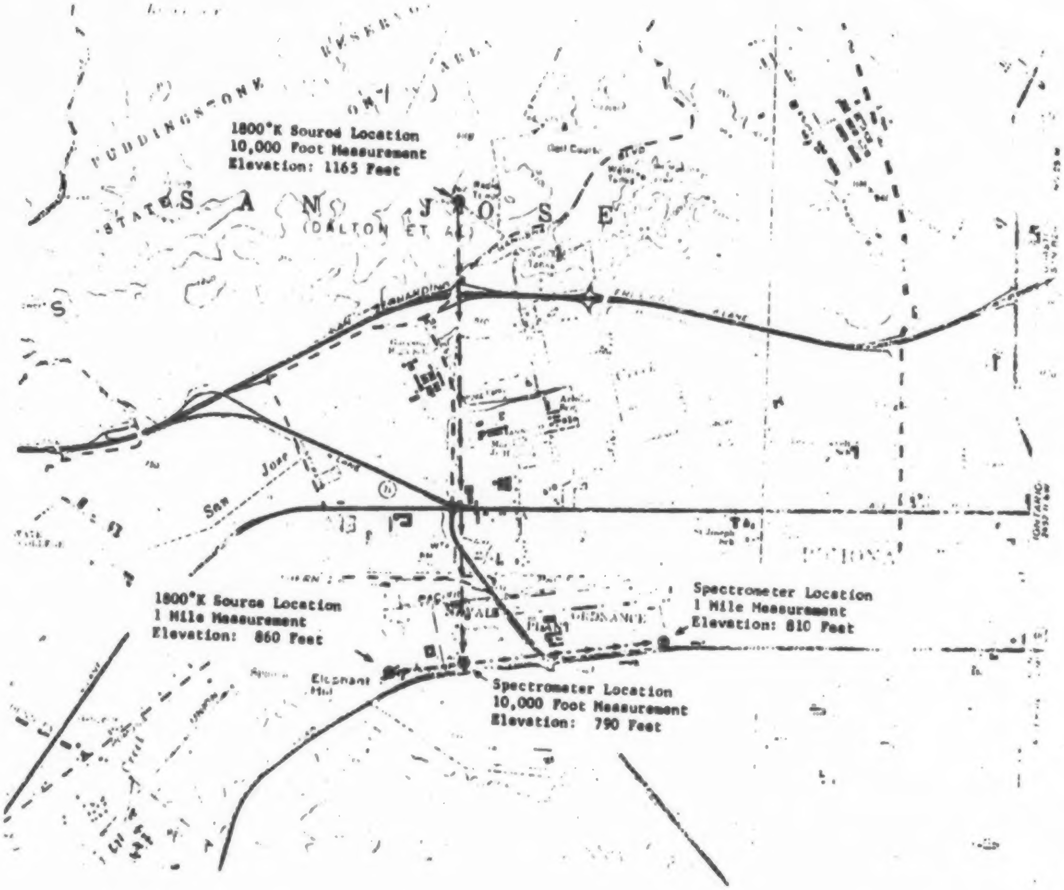
PUDDINGSTONE
1800°K Soured Location
10,000 Foot Measurement
Elevation: 1165 Feet
STATE
S A N J O S E
(DALTON ET AL)
San Jose
POMONA
1800°K Source Location
1 Mile Measurement
Elevation: 860 Feet
NAVAL
ORDNANCE
Elephant Hill
Spectrometer Location
1 Mile Measurement
Elevation: 810 Feet
Spectrometer Location
10,000 Foot Measurement
Elevation: 790 Feet

Figure 1. Map of the Pomona Area Showing Locations of the 1800°K Blackbody Source and the Instrumentation for the One and Two-Mile Transmission Measurements.

Reproduced from best available copy.

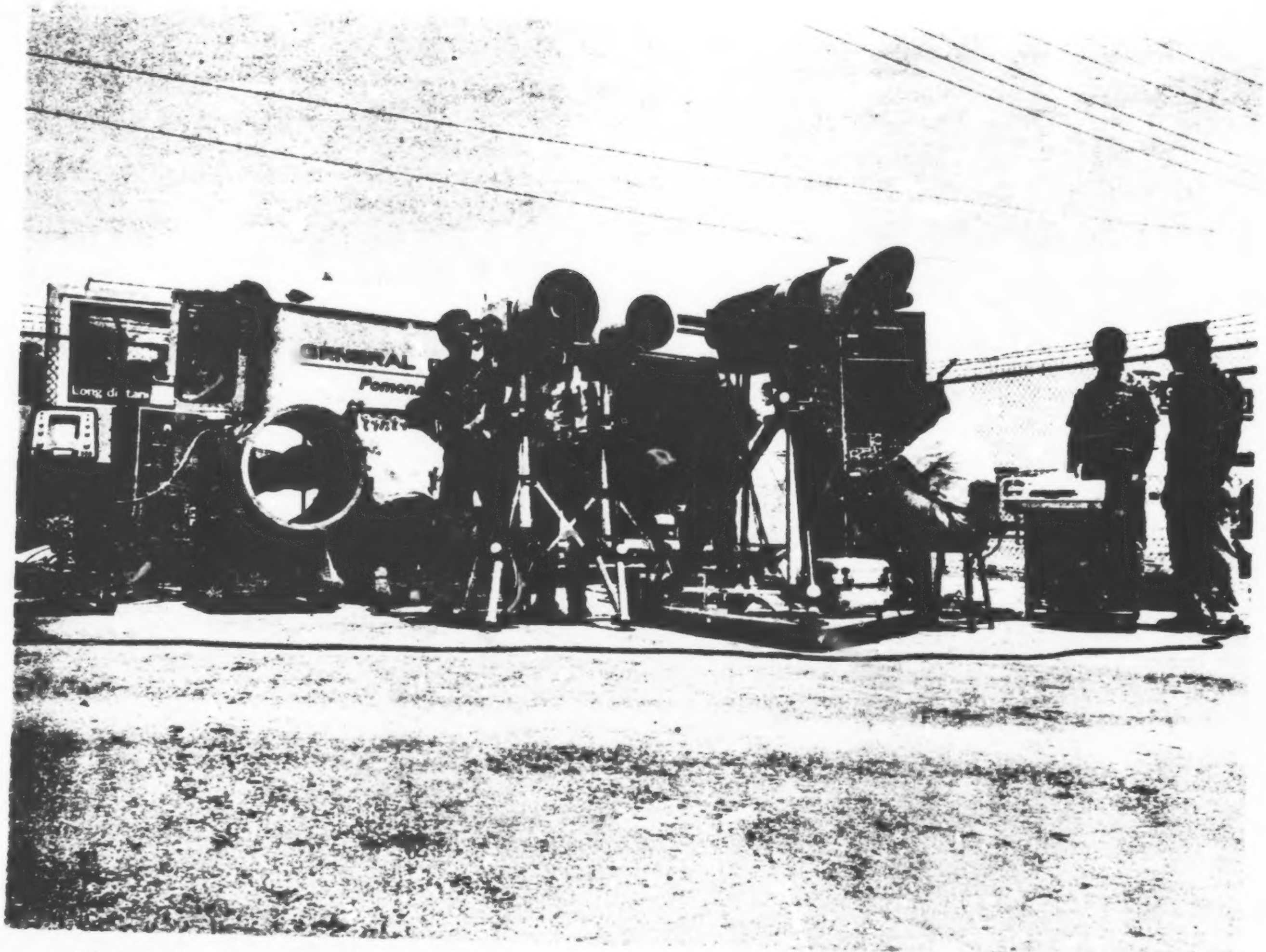

GENERAL
Pomona

Figure 2. Instrumentation Setup for the One-Mile Transmission Measurement.

Table I

HOURLY AVERAGE VARIATION OF OZONE CONCENTRATION (pphm) DURING THE WEEK OF JUNE 28, 1971

Day / Hour	6	7	8	9	10	11	12	13	14	15	16	17	18	19
June 28	2	2	2	2	2	4	5	5	5	4	3	3	2	1
29	1	2	2	4	4	5	8	11	11	11	8	7	5	4
30	1	?	3	5	7	10	13	10	10	11	9	6	4	3
July 1	1	2	4	7	8	11	13	11	9	9	8	6	3	2
2	1	2	3	5	9	13	16	16	9	10	9	6	4	3

Table II

HOURLY AVERAGE VARIATION OF CARBON MONOXIDE CONCENTRATION (ppm) DURING THE WEEK OF JUNE 28, 1971

Day / Hour	6	7	8	9	10	11	12	13	14	15	16	17	18	19
June 28	1	2	3	3	3	3	3	3	3	2	2	2	2	2
29	2	3	2	2	2	2	2	2	2	2	2	3	3	3
30	3	3	3	3	3	3	3	2	2	3	3	3	3	3

Table III

HOURLY AVERAGE VARIATION OF NITRIC OXIDE CONCENTRATION (pphm) DURING THE WEEK OF JUNE 28, 1971

Day Hour	6	7	8	9	10	11	12	13	14	15	16	17	18	19
June 28	2	6	6	7	5	4	-	-	1	1	1	1	1	2
29	8	10	7	4	2	2	-	-	1	1	1	1	1	1
30	12	11	9	-	-	2	1	1	1	1	1	2	3	3
July 1	8	9	4	1	1	1	-	-	-	1	1	1	2	3
2	7	7	5	3	2	1	-	2	2	1	1	1	1	2

Table IV

HOURLY AVERAGE VARIATION OF NITROGEN DIOXIDE CONCENTRATION (pphm) DURING THE WEEK OF JUNE 28, 1971

Day Hour	6	7	8	9	10	11	12	13	14	15	16	17	18	19
June 28	2	3	3	4	4	5	-	-	4	5	5	4	4	4
29	6	7	6	6	5	5	-	-	4	6	7	7	7	9
30	8	9	10	-	-	0	9	8	11	9	10	11	13	14
July 1	8	10	10	8	8	8	-	-	-	12	16	21	26	25
2	11	15	16	15	14	10	-	-	10	12	12	13	12	13

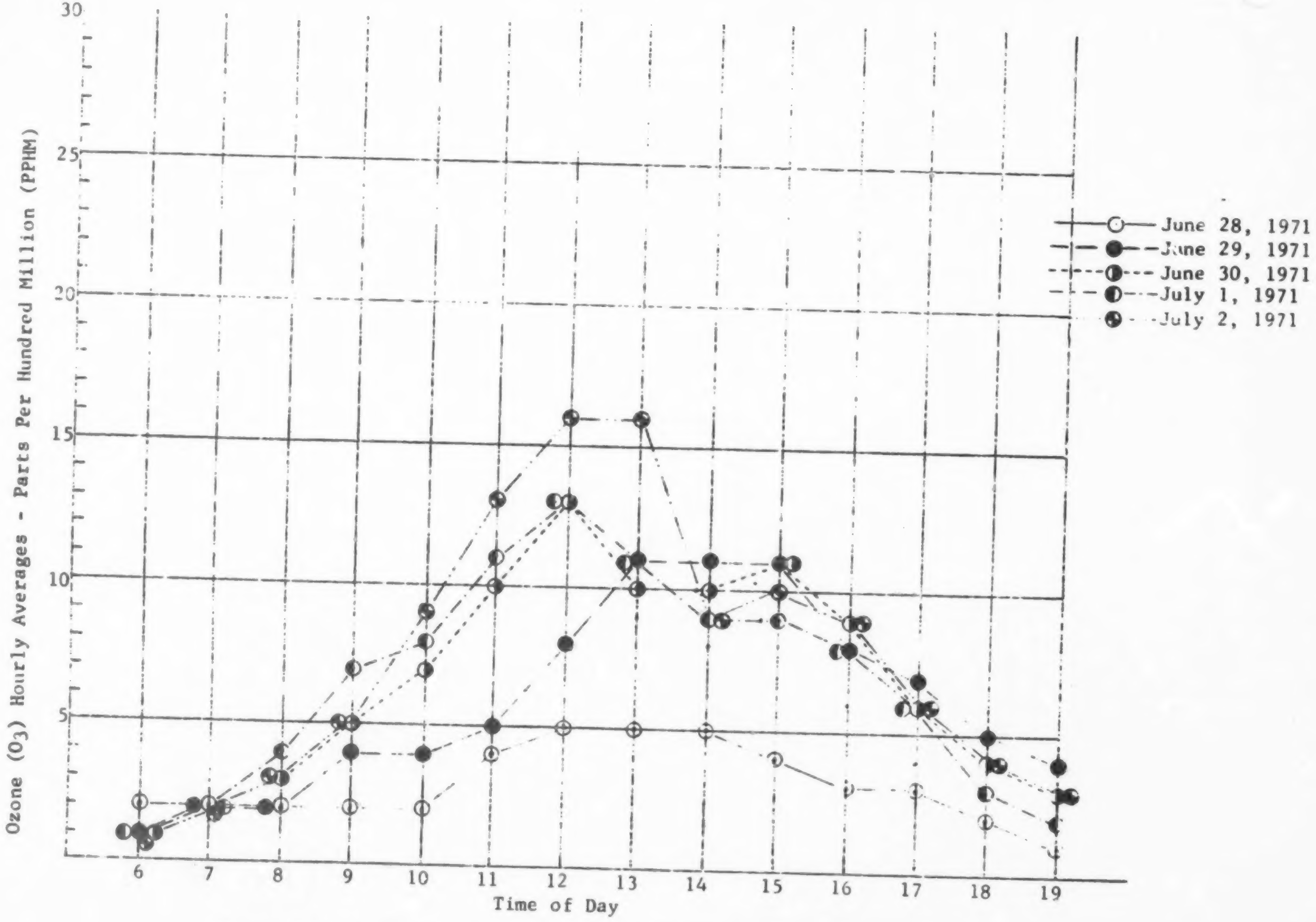

Figure 3. Diurnal Variation of Ozone Measured at the Pomona Station of the Los Angeles County Air Pollution Control District During the Week of June 28, 1971.

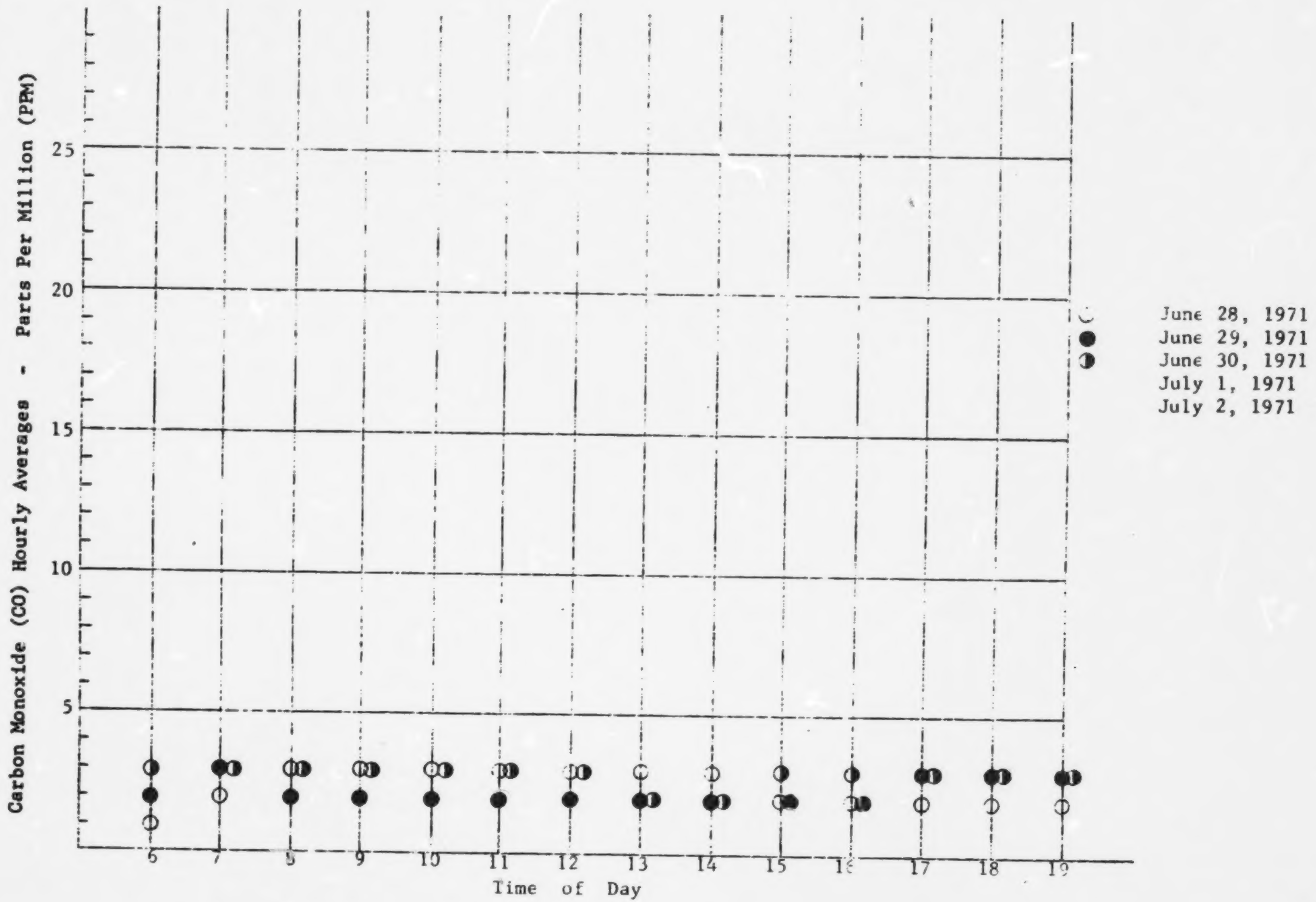

Figure 4. Diurnal Variation of Carbon Monoxide Measured at the Pomona Station of the Los Angeles County Air Pollution Control District During the Week of June 28, 1971.

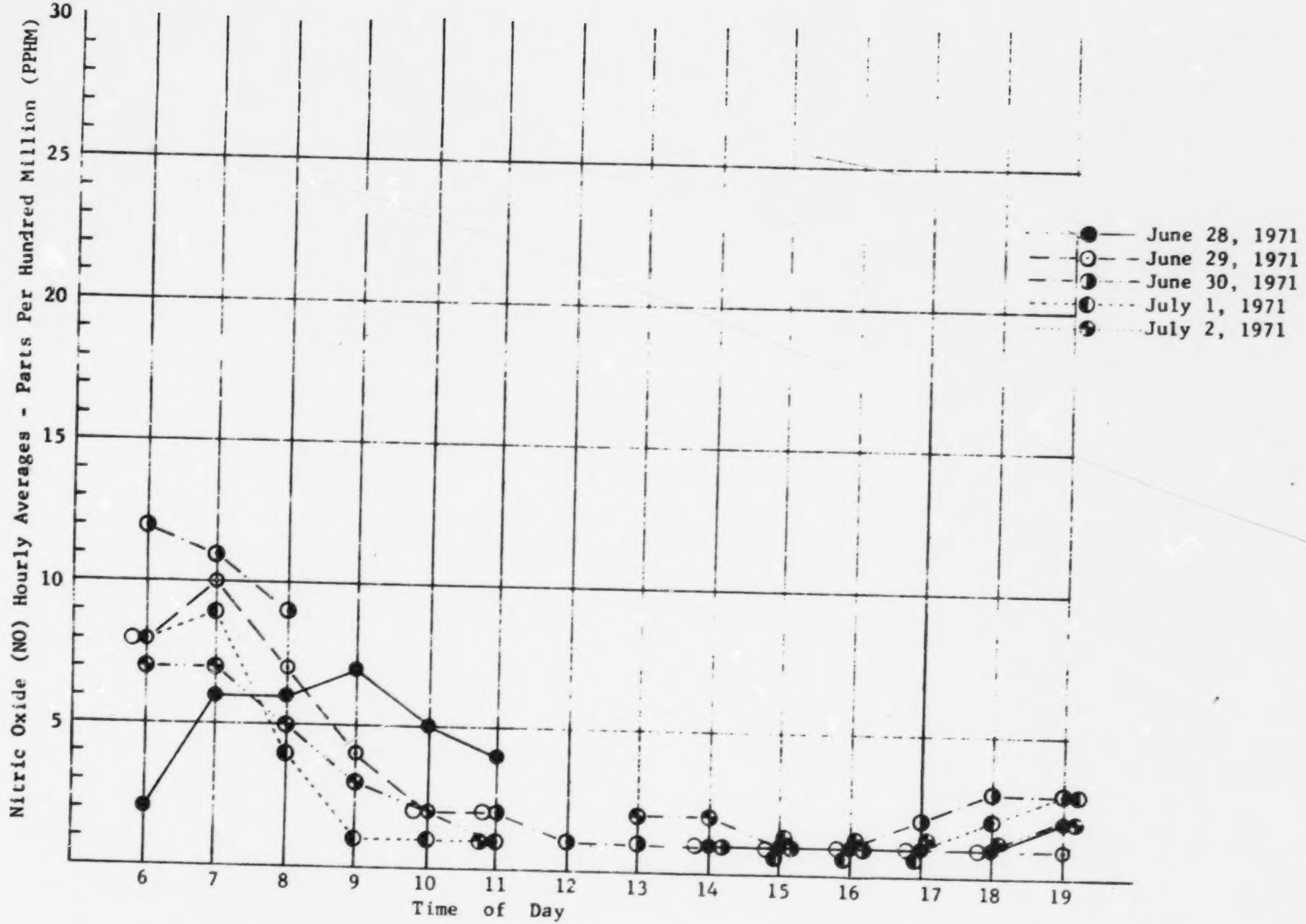

Figure 5. Diurnal Variation of Nitric Oxide Measured at the Pomona Station of the Los Angeles County Air Pollution Control District During the Week of June 28, 1971.

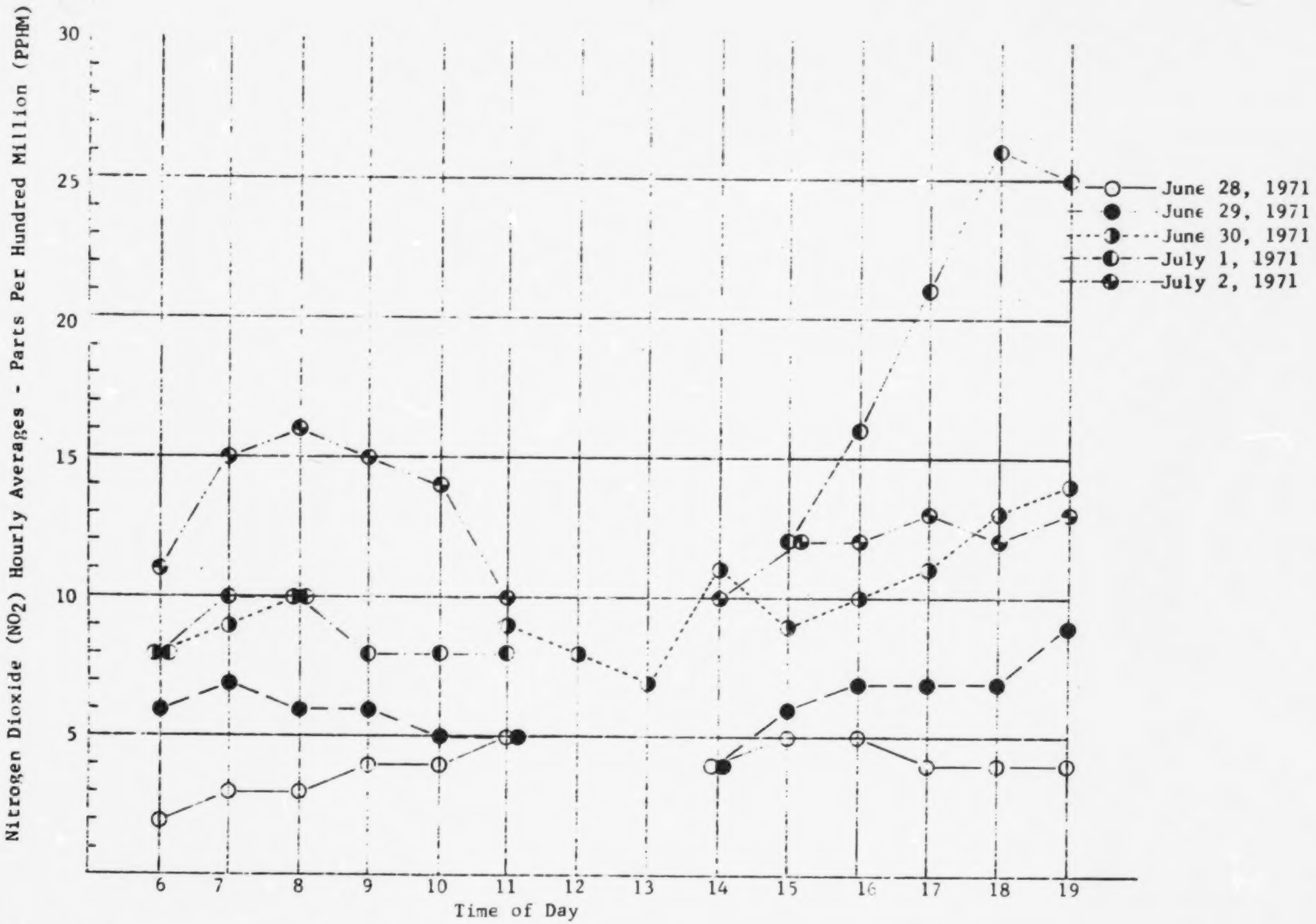

Figure 6. Diurnal Variation of Nitrogen Dioxide Measured at the Pomona Station of the Los Angeles County Air Pollution Control District During the Week of June 28, 1971.

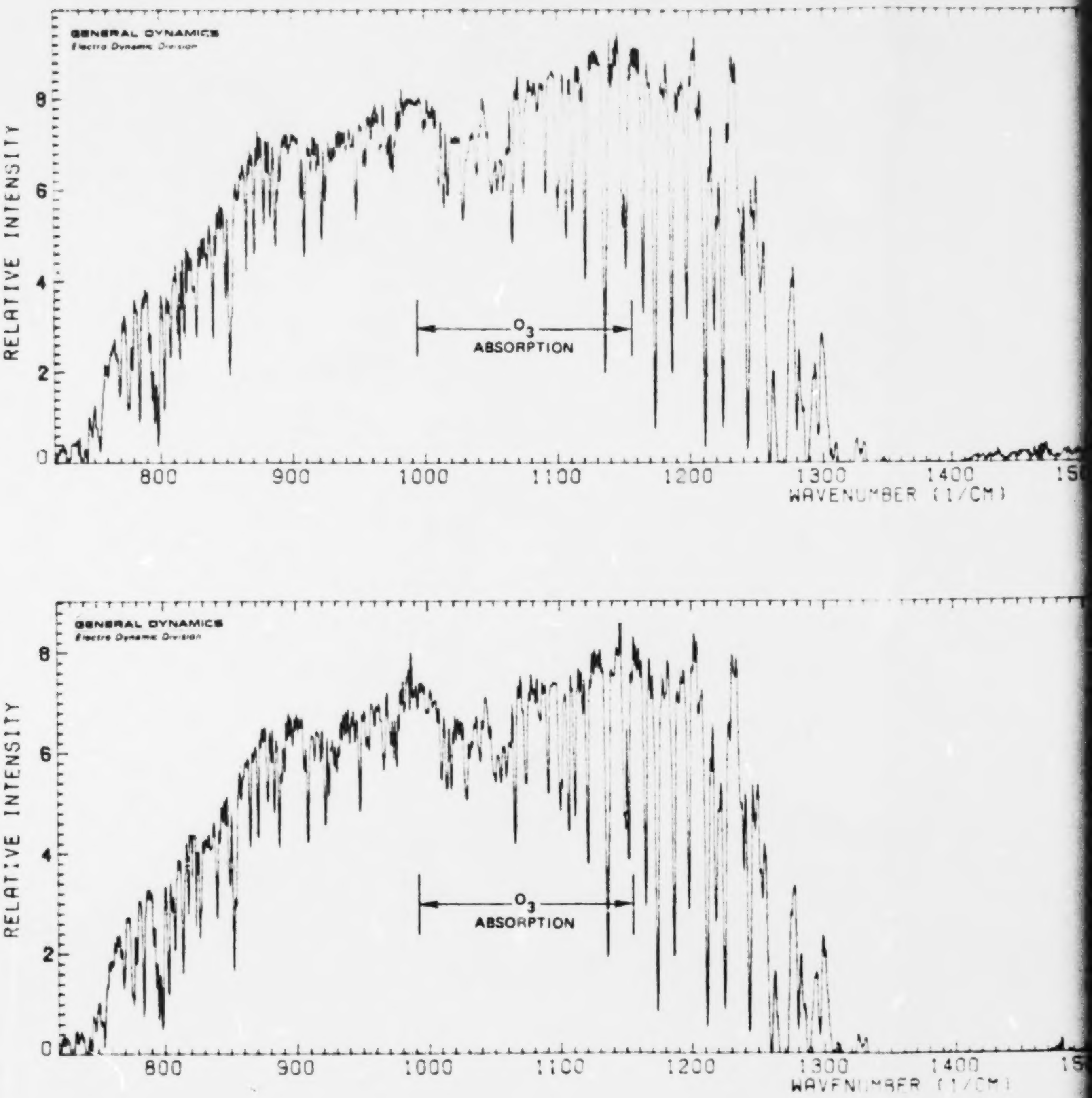

B75721

Figure
Over

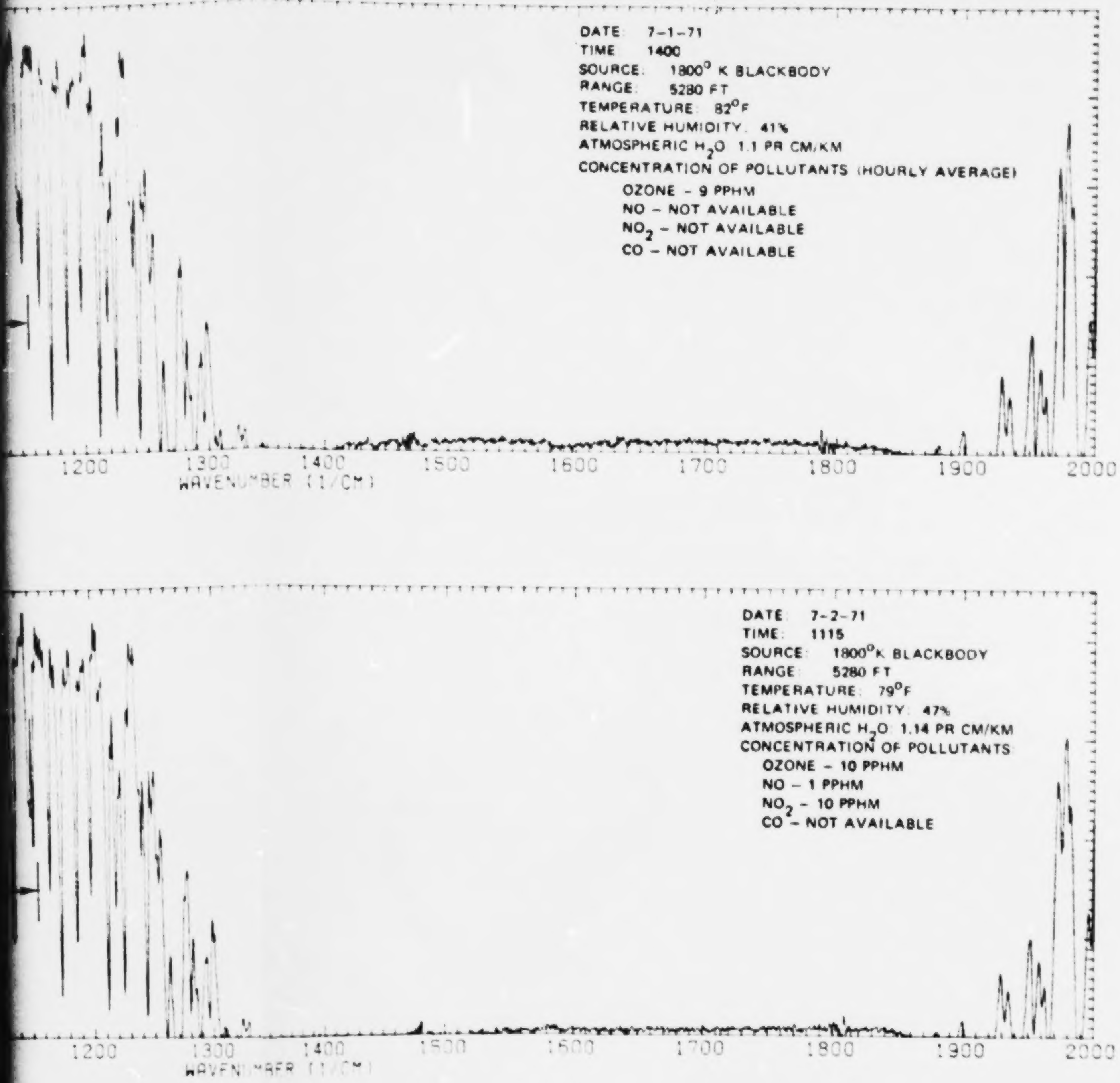

Figure 7. Relative Spectral Intensity of an 1800°K Blackbody Source Over a One-Mile Path in the Interval From 720 to 2000 cm^{-1}.

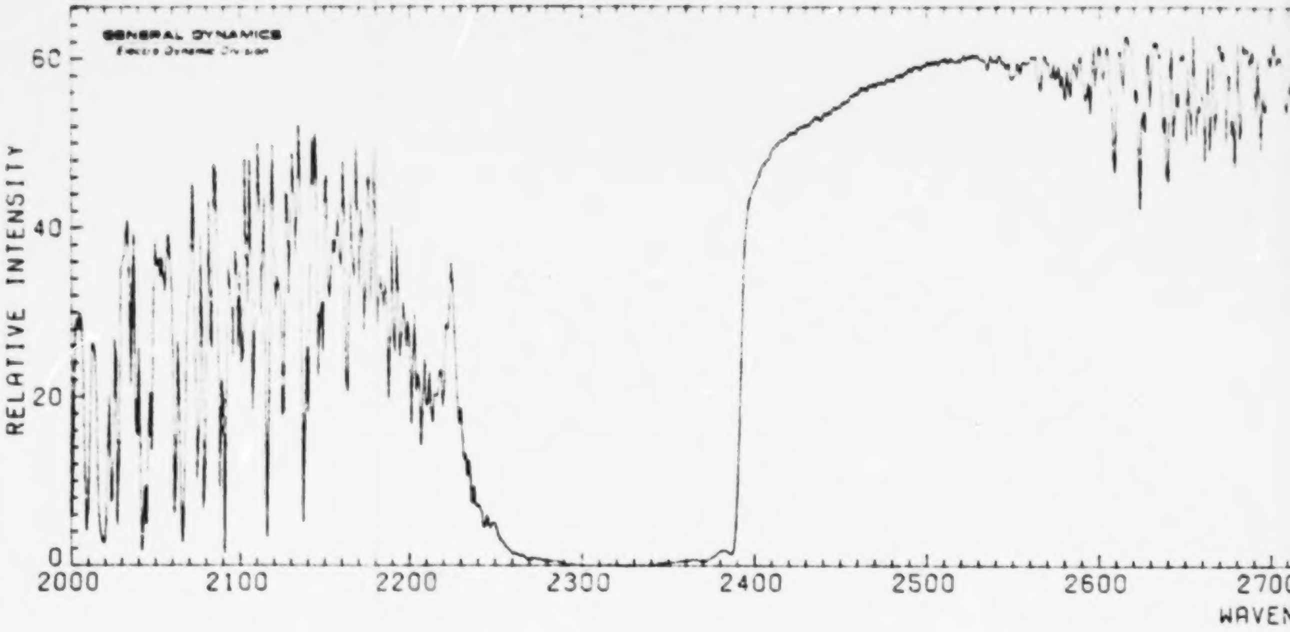
GENERAL DYNAMICS
Electro Dynamic Division
RELATIVE INTENSITY
60
40
20
0
2000
2100
2200
2300
2400
2500
2600
2700
WAVEN

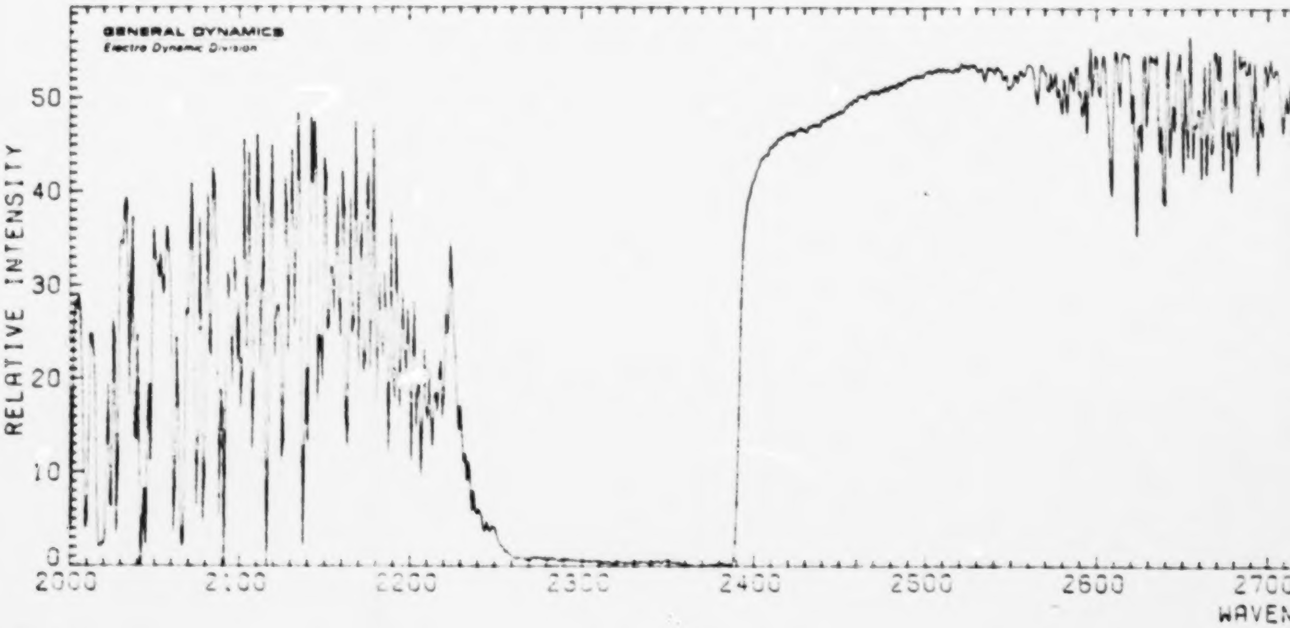
GENERAL DYNAMICS
Electro Dynamic Division
RELATIVE INTENSITY
50
40
30
20
10
0
2000
2100
2200
2300
2400
2500
2600
2700
WAVEN

B75719

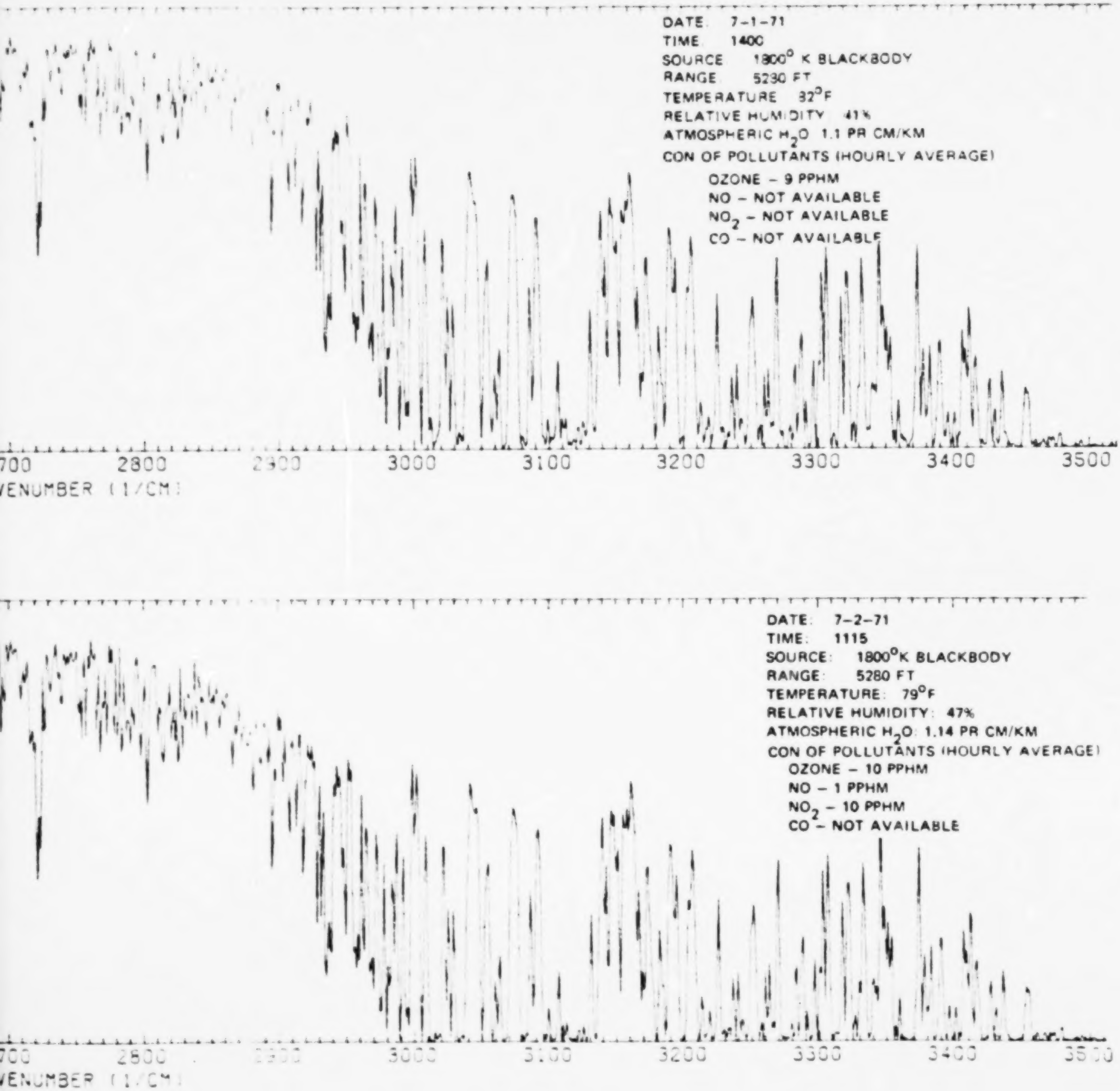

Figure 8. Relative Spectral Intensity of an 1800°K Blackbody Source. Over a One-Mile Path in the Interval From 2000 to 2500 cm^{-1}.

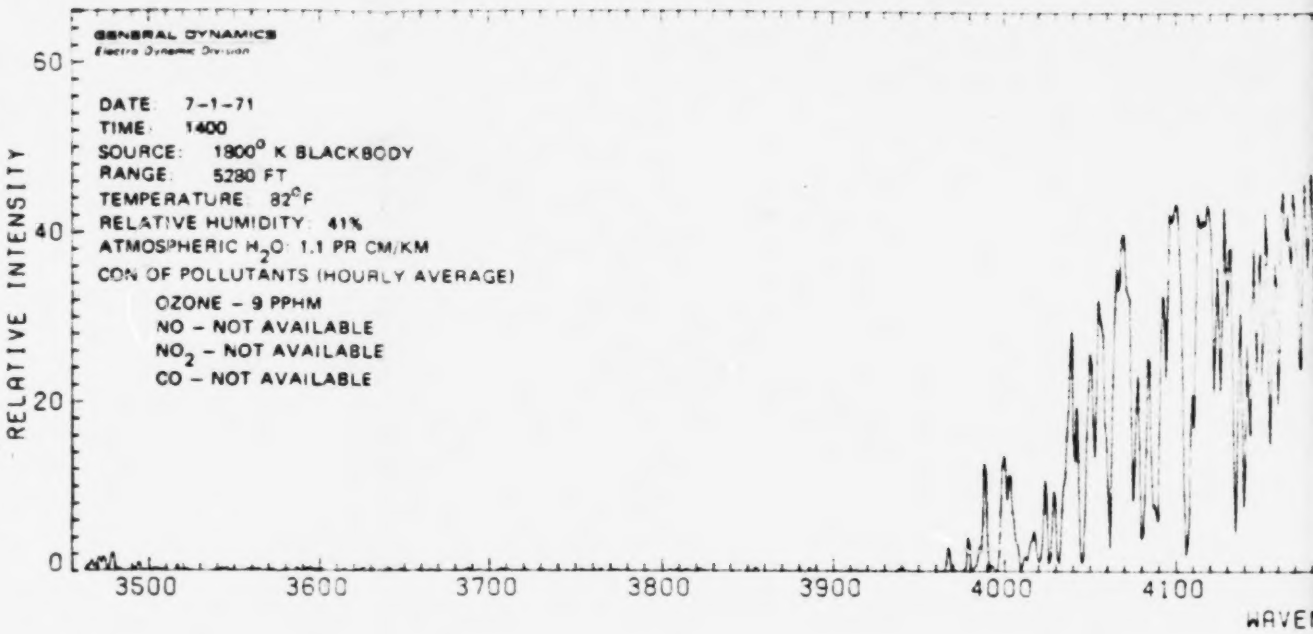
GENERAL DYNAMICS
Electro Dynamic Division
DATE 7-1-71
TIME 1400
SOURCE: 1800° K BLACKBODY
RANGE 5280 FT
TEMPERATURE 82°F
RELATIVE HUMIDITY 41%
ATMOSPHERIC H2O 1.1 PR CM/KM
CON OF POLLUTANTS (HOURLY AVERAGE)
OZONE – 9 PPHM
NO – NOT AVAILABLE
NO2 – NOT AVAILABLE
CO – NOT AVAILABLE
RELATIVE INTENSITY
60
40
20
0
3500
3600
3700
3800
3900
4000
4100
WAVE

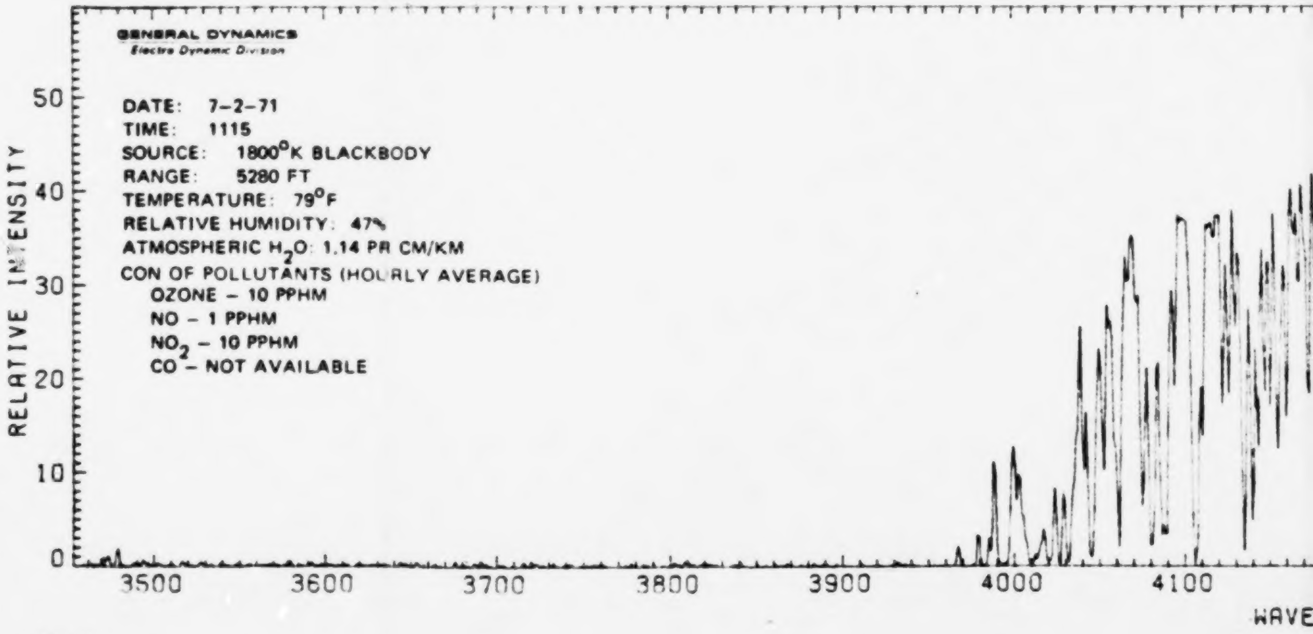
GENERAL DYNAMICS
Electro Dynamic Division
DATE: 7-2-71
TIME: 1115
SOURCE: 1800°K BLACKBODY
RANGE: 5280 FT
TEMPERATURE: 79°F
RELATIVE HUMIDITY 47%
ATMOSPHERIC H2O 1.14 PR CM/KM
CON OF POLLUTANTS (HOURLY AVERAGE)
OZONE – 10 PPHM
NO – 1 PPHM
NO2 – 10 PPHM
CO – NOT AVAILABLE
RELATIVE INTENSITY
50
40
30
20
10
0
3500
3600
3700
3800
3900
4000
4100
WAVE

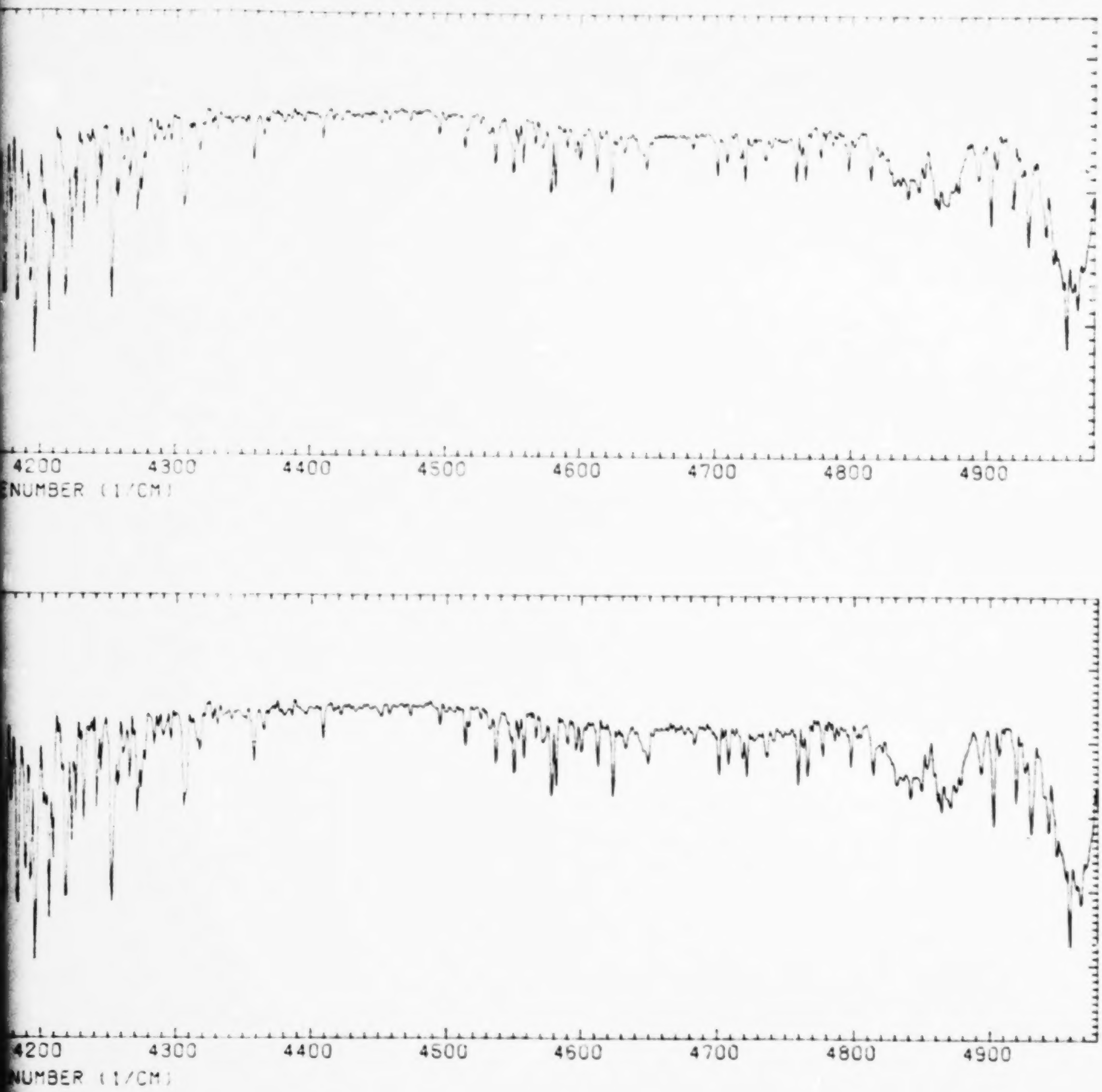

Figure 9. Relative Spectral Intensity of an 1800°K Blackbody Source Over a One-Mile Path in the Interval From 2000 to 2500 cm^{-1}.

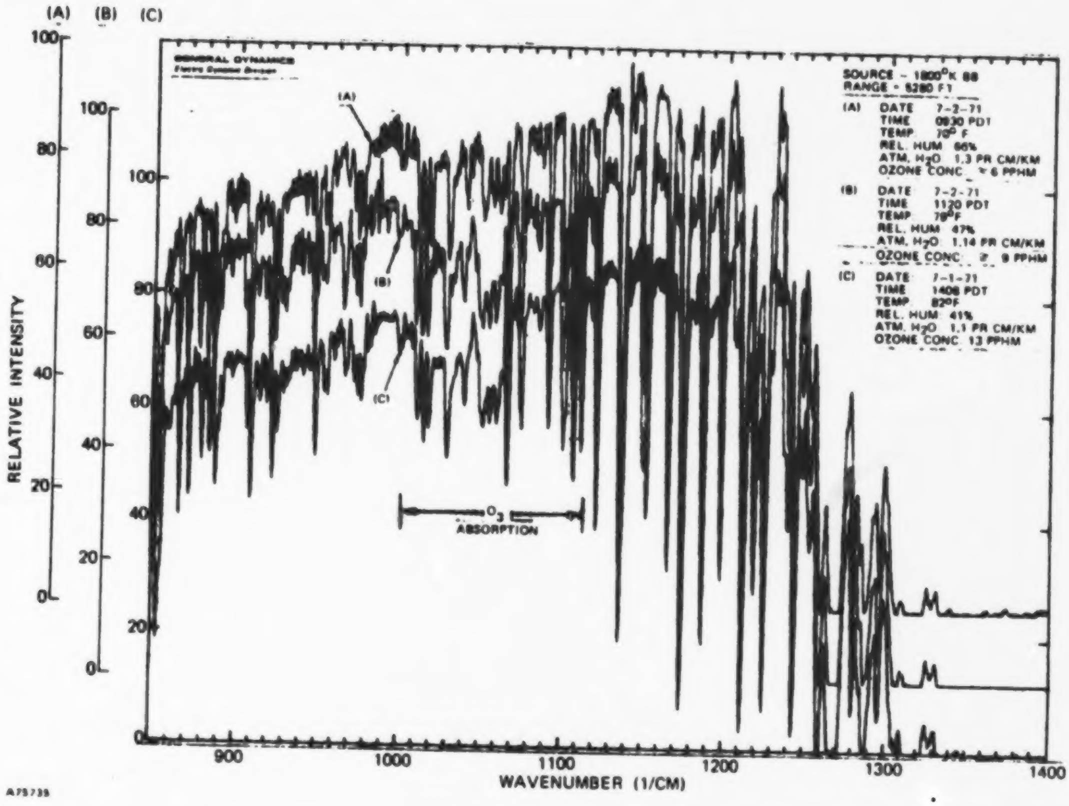

Figure 10. Comparison of the Variation of Ozone Absorption Over a One-Mile Path for Three Levels of Ozone Concentration.

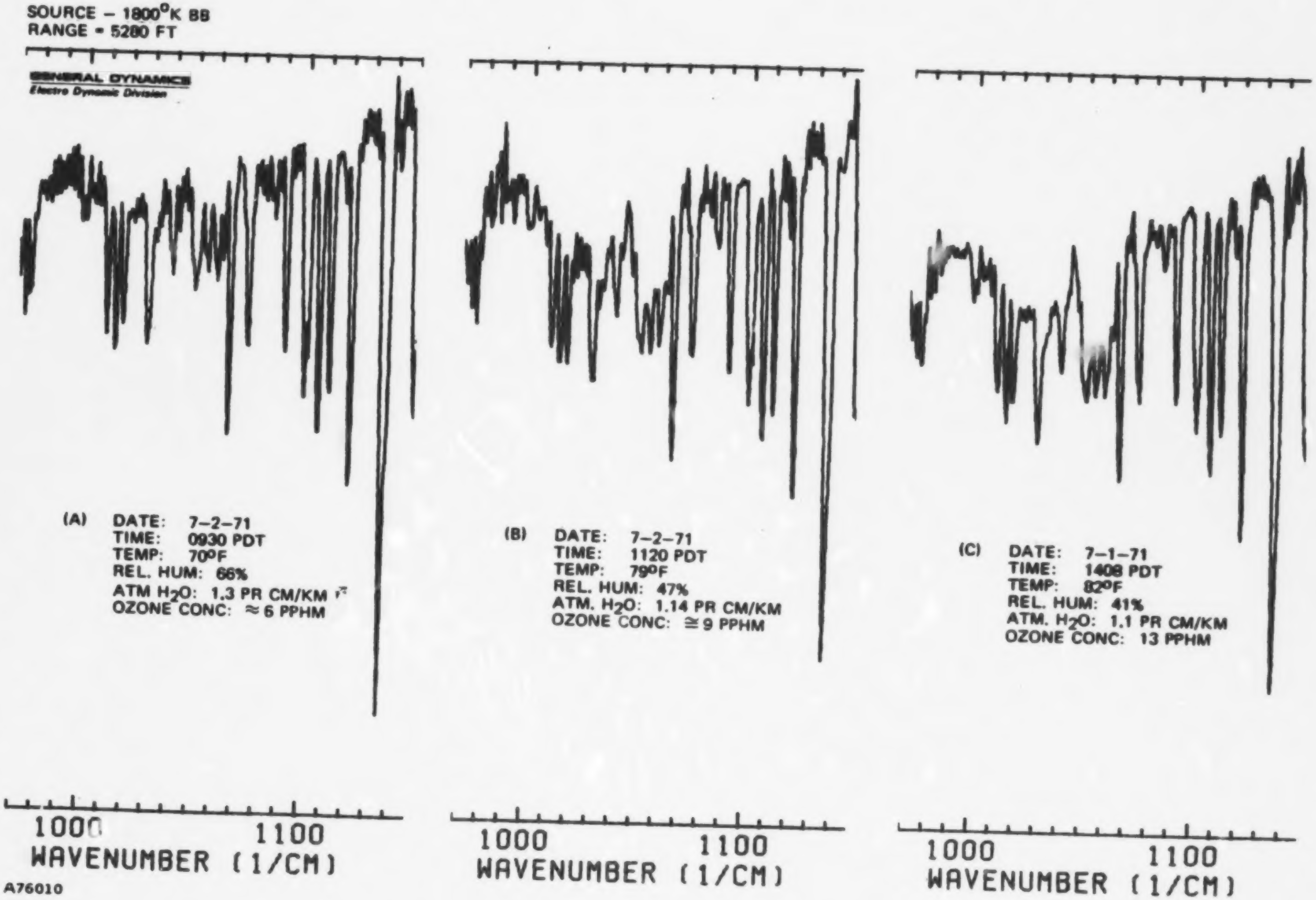

Figure 11. Comparison of the Variation of Ozone Absorption Over a One-Mile Path for Three Levels of Ozone Concentration.

1.2 TWO MILE TRANSMISSION DATA

The two-mile (nominal) transmission measurements were conducted during the week of July 26, with the spectrometric equipment again located on General Dynamics plant property and the 1800°K source located on a hill site approximately 10,000 feet from the spectrometers at an elevation of 470 ft. above the spectrometer location as indicated on the map in Figure 1.

The recorded hourly average concentrations during the week of July 26 are presented in Tables V through VIII and also in graphical form in Figures 12 through 15.

The spectral data for the 2 mile measurements are presented in Figures 16 through 18. The data were again chosen to represent a large variation in ozone concentration. As expected, the 2 mile measurements show a broadening of the absorption in the ozone band, which is more due to the increased contributions of the ν_1 fundamental band of ozone centered at 1103 cm^{-1}, the ν_3 band at 1042 cm^{-1}, and the weak absorption bands of N_2O and CO_2, and the numerous H_2O lines in the same spectral region.

The 10,000 ft atmospheric transmission measurements again clearly indicate the presence of ozone in the atmosphere and the increased absorption as the concentration of ozone increases as illustrated in Figure 19 showing two spectral curves superimposed with a small zero intensity shift.

Other major pollutants such as NO and NO_2 are not as readily observed in long path measurements since the major absorption bands of the NO_x molecules are obscured by atmospheric water vapor absorption.

The use of high resolution reference spectra of pure NO or NO_2 may lead to the determination of the individual vibration rotation lines in the transmission spectra, particularly for NO_2, which has a strong fundamental (ν_3) band at 1260 cm^{-1} and several combination and overtone bands in the 3000 cm^{-1} region. The fundamental of NO at 1887 cm^{-1} lies near the edge of the 6.3 micron water band and is generally obscured in long path measurements. The carbon monoxide fundamental at 2146 cm^{-1} also has interference from various isotopes of CO_2 and from N_2O, although the general band shape of the CO absorption can be observed.

Table V

HOURLY AVERAGE VARIATION OF OZONE CONCENTRATION (pphm) DURING THE WEEK OF JULY 26, 1971

Day / Hour	6	7	8	9	10	11	12	13	14	15	16	17	18	19
July 26	1	2	3	7	10	14	19	24	25	22	19	14	9	4
27	1	2	4	6	11	15	20	22	19	14	14	11	6	3
28	1	-	3	6	11	14	17	16	12	13	12	7	3	3
29	1	2	4	8	9	14	12	9	7	5	6	5	3	2
30	1	1	2	3	5	7	12	7	6	10	6	9	7	3

Table VI

HOURLY AVERAGE VARIATION OF CARBON MONOXIDE CONCENTRATION (ppm) DURING THE WEEK OF JULY 26, 1971

Day / Hour	6	7	8	9	10	11	12	13	14	15	16	17	18	19
July 26	3	3	-	4	3	3	3	4	4	4	4	3	3	3
27	4	5	4	4	4	4	3	3	3	3	3	3	3	3
28	3	4	4	4	4	4	4	3	2	3	3	3	3	3
29	5	5	3	4	3	3	-	3	2	2	3	2	2	2
30	5	5	3	3	3	3	3	3	2	3	3	3	3	4

Table VII

HOURLY AVERAGE VARIATION OF NITRIC OXIDE CONCENTRATION (pphm) DURING THE WEEK OF JULY 26, 1971

Day / Hour	6	7	8	9	10	11	12	13	14	15	16	17	18	19
July 26	5	5	5	3	1	1	-	1	1	1	1	1	1	2
27	14	17	7	4	1	1	-	1	1	1	1	1	2	2
28	9	10	7	5	2	2	-	1	1	1	1	1	2	2
29	17	15	4	2	2	1	-	1	1	1	1	1	2	2
30	16	12	10	4	3	2	-	1	2	1	1	1	1	2

Table VIII

HOURLY AVERAGE VARIATION OF NITROGEN DIOXIDE CONCENTRATION (pphm) DURING THE WEEK OF JULY 26, 1971

DAY / HOUR	6	7	8	9	10	11	12	13	14	15	16	17	18	19
July 26	7	7	7	8	7	7	-	7	7	7	10	8	9	11
27	8	11	15	13	10	11	-	6	8	11	11	12	16	14
28	7	9	11	14	12	11	-	5	5	8	11	11	10	9
29	10	14	13	11	8	7	-	6	7	6	7	4	6	5
30	6	9	7	7	7	7	-	10	6	6	11	10	10	12

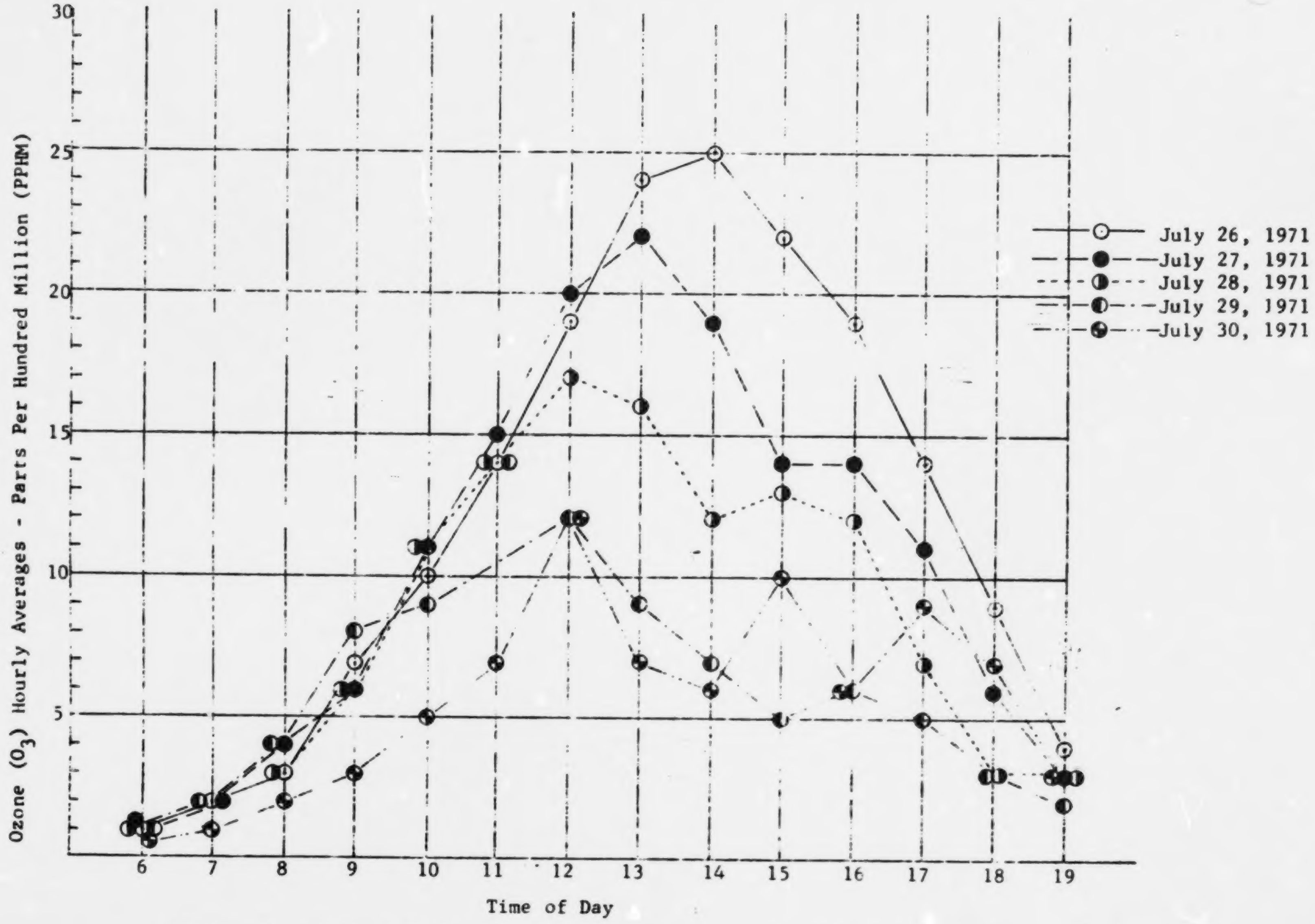

Figure 12. Diurnal Variation of Ozone Measured at the Pomona Station of the Los Angeles County Air Pollution Control District During the Week of July 26, 1971.

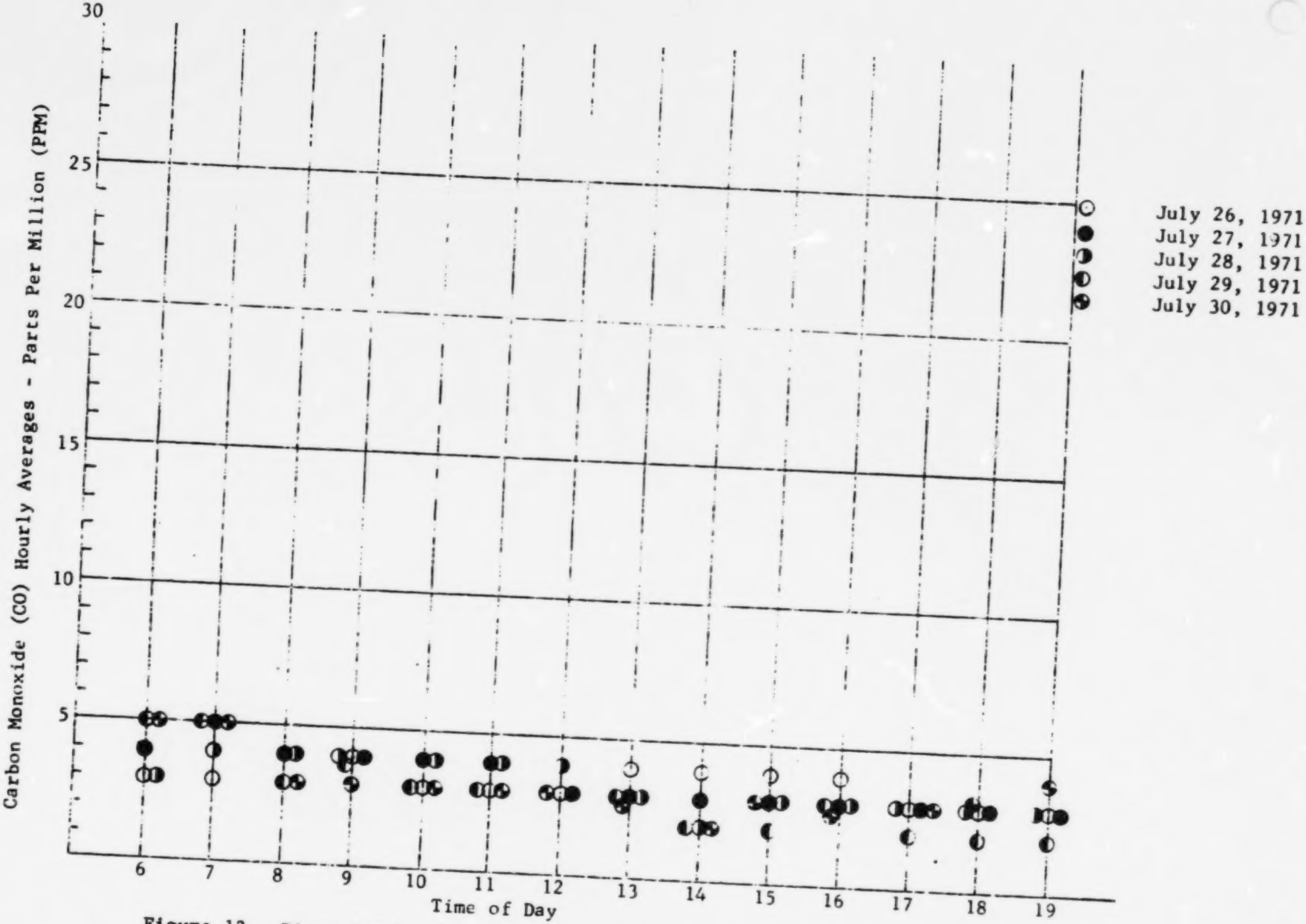

Figure 13. Diurnal Variation of Carbon Monoxide Measured at the Pomona Station of the Los Angeles County Air Pollution Control District During the Week of July 26, 1971.

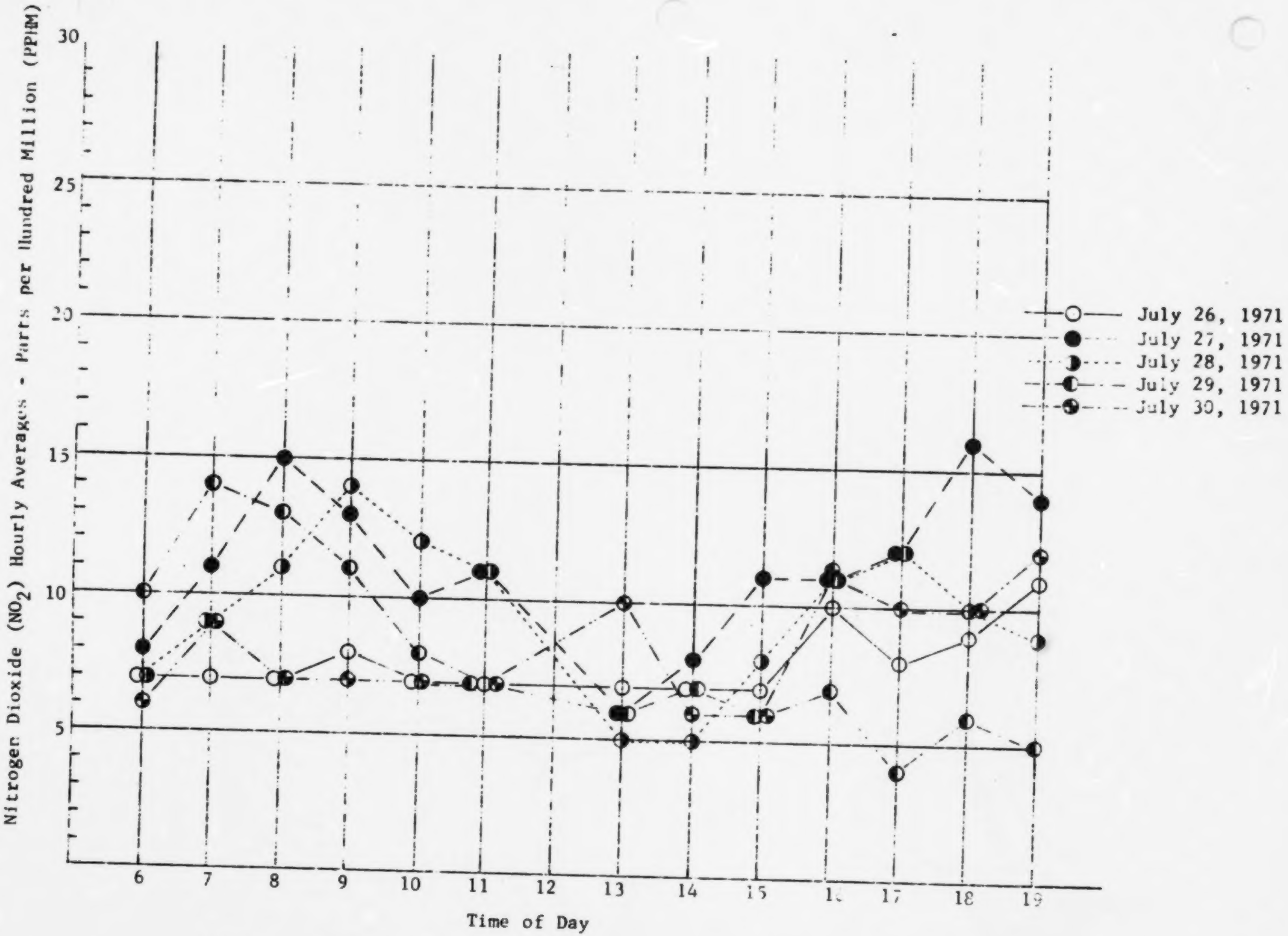

Figure 14. Diurnal Variation of Nitrogen Dioxide Measured at the Pomona Station of the Los Angeles County Air Pollution Control District During the Week of July 26, 1971.

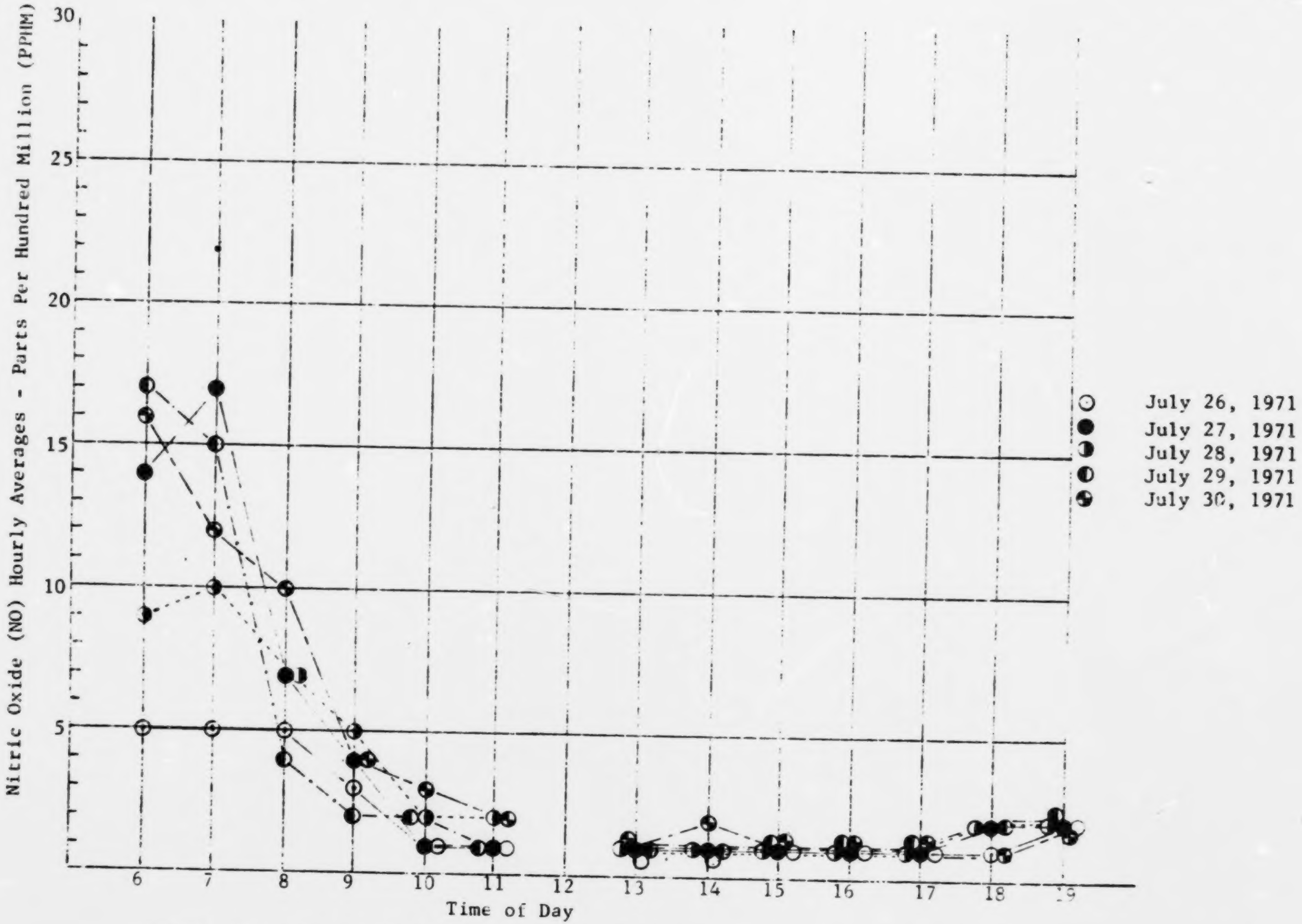

Figure 15. Diurnal Variation of Nitric Oxide Measured at the Pomona Station of the Los Angeles County Air Pollution Control District During the Week of July 26, 1971.

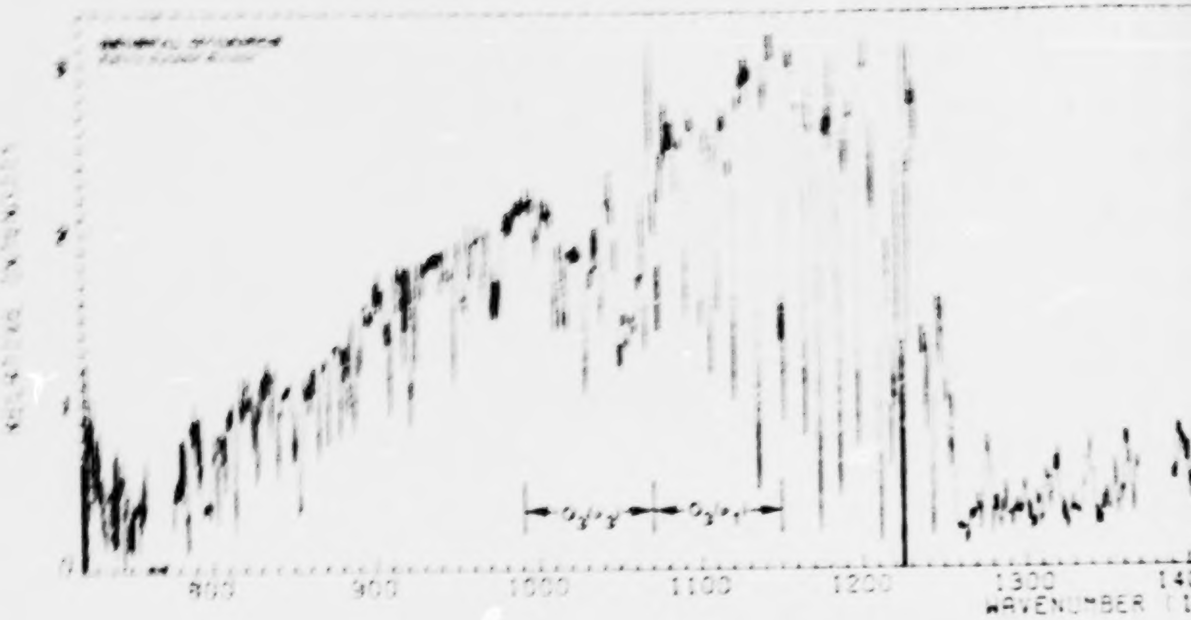
GENERAL DYNAMICS
RELATIVE INTENSITY
3
2
1
0
$O_3(\nu_3)$
$O_3(\nu_1)$
800
900
1000
1100
1200
1300
14
WAVENUMBER (1

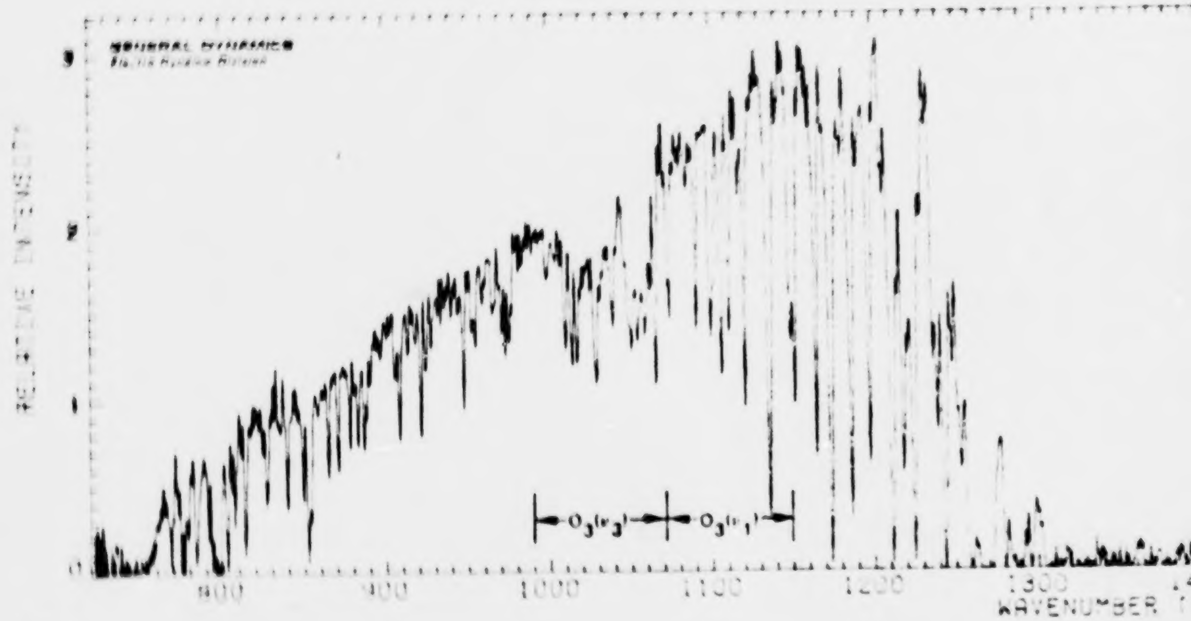
GENERAL DYNAMICS
RELATIVE INTENSITY
3
2
1
0
$O_3(\nu_3)$
$O_3(\nu_1)$
800
900
1000
1100
1200
1300
WAVENUMBER (

Figu

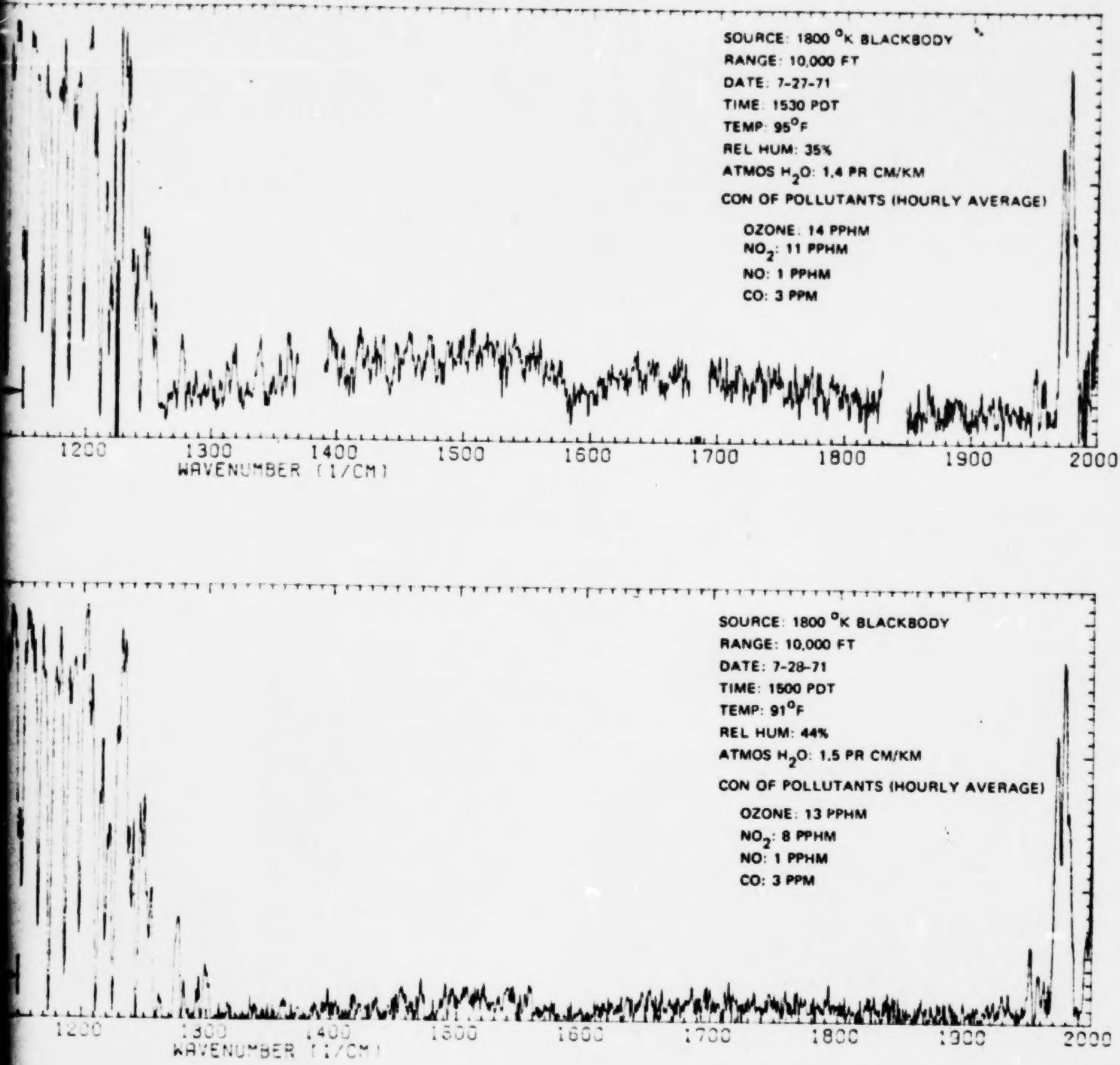

Figure 16. Relative Spectral Intensity of an 1800°K Blackbody Source Over a 10,000-Foot Path in the Interval From 720 to 2000 cm^{-1}.

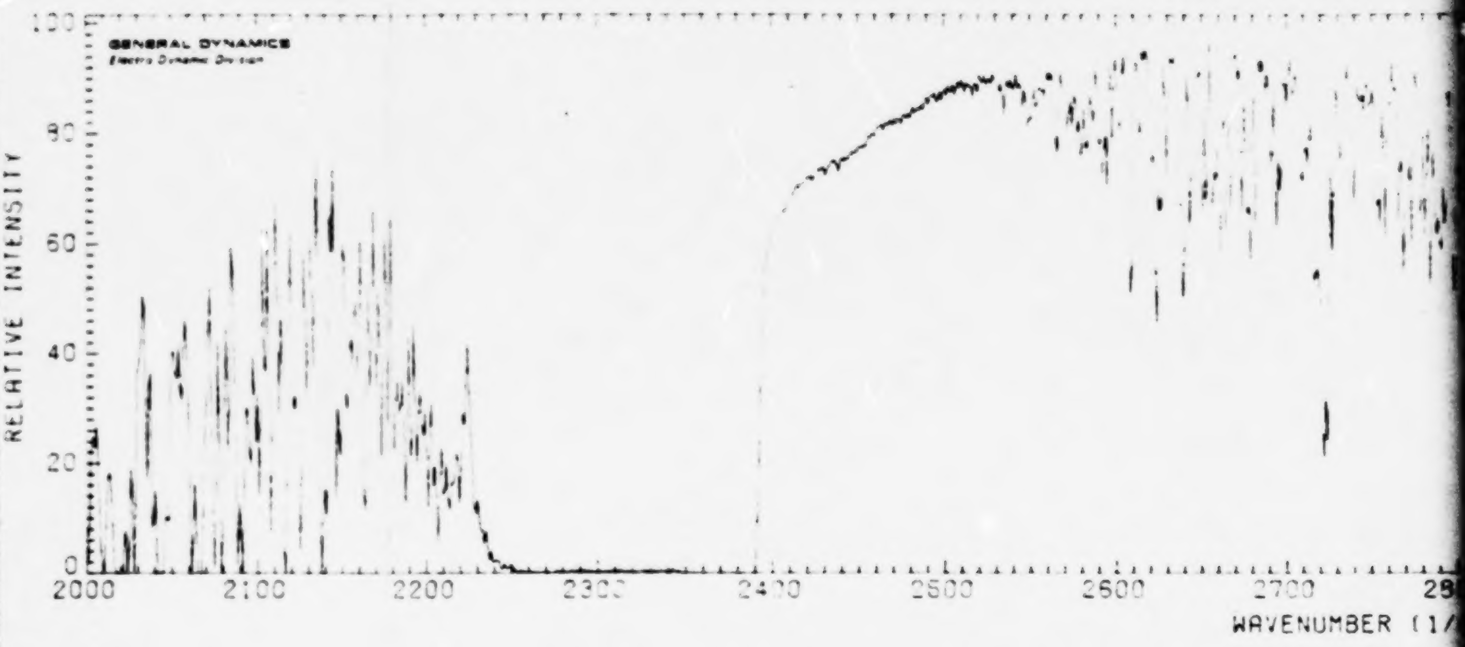
GENERAL DYNAMICS
Electro Dynamic Division
RELATIVE INTENSITY
100
80
60
40
20
0
2000
2100
2200
2300
2400
2500
2600
2700
28
WAVENUMBER (1/

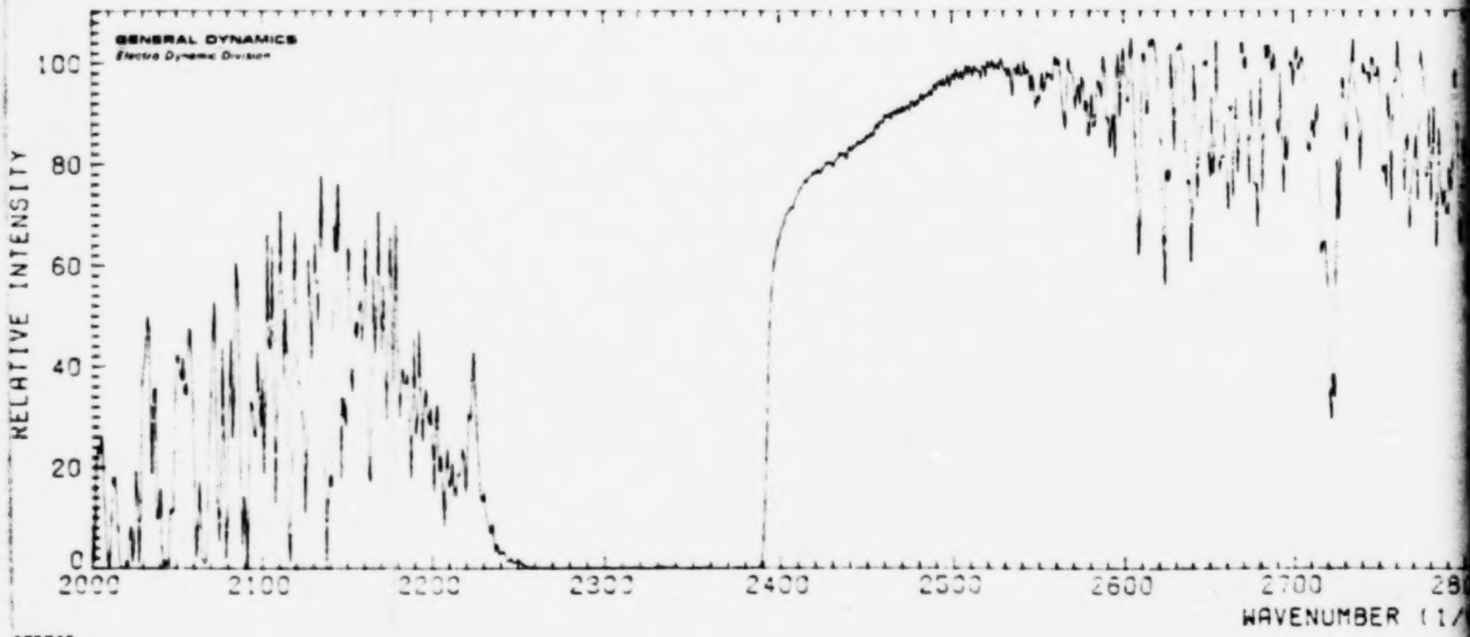
GENERAL DYNAMICS
Electro Dynamic Division
RELATIVE INTENSITY
100
80
60
40
20
0
2000
2100
2200
2300
2400
2500
2600
2700
28
WAVENUMBER (1/

375745

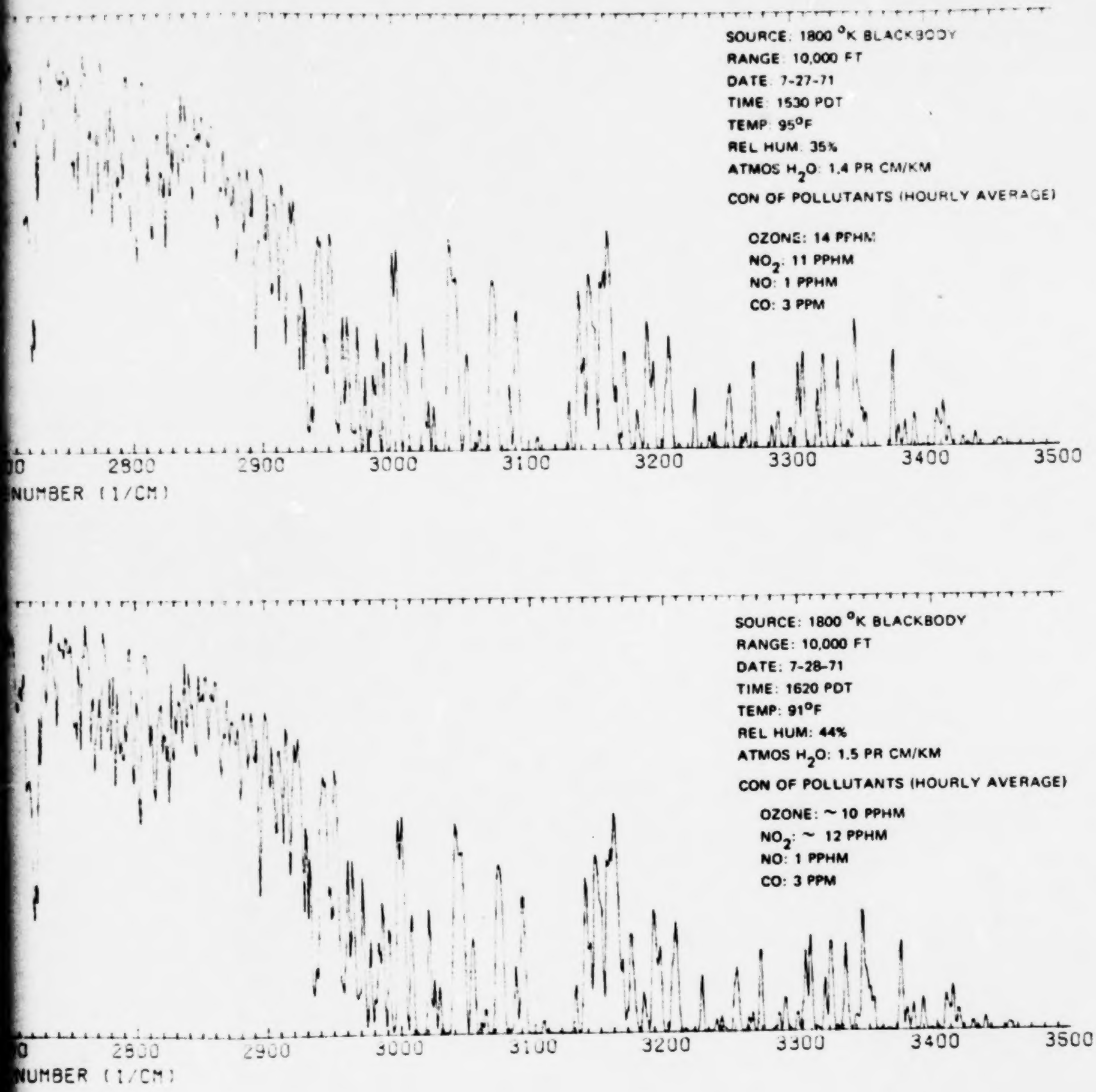

Figure 17. Relative Spectral Intensity of an 1800°K Blackbody Source Over a 10,000-Foot Path in the Interval From 2000 to 2500 cm^{-1}.

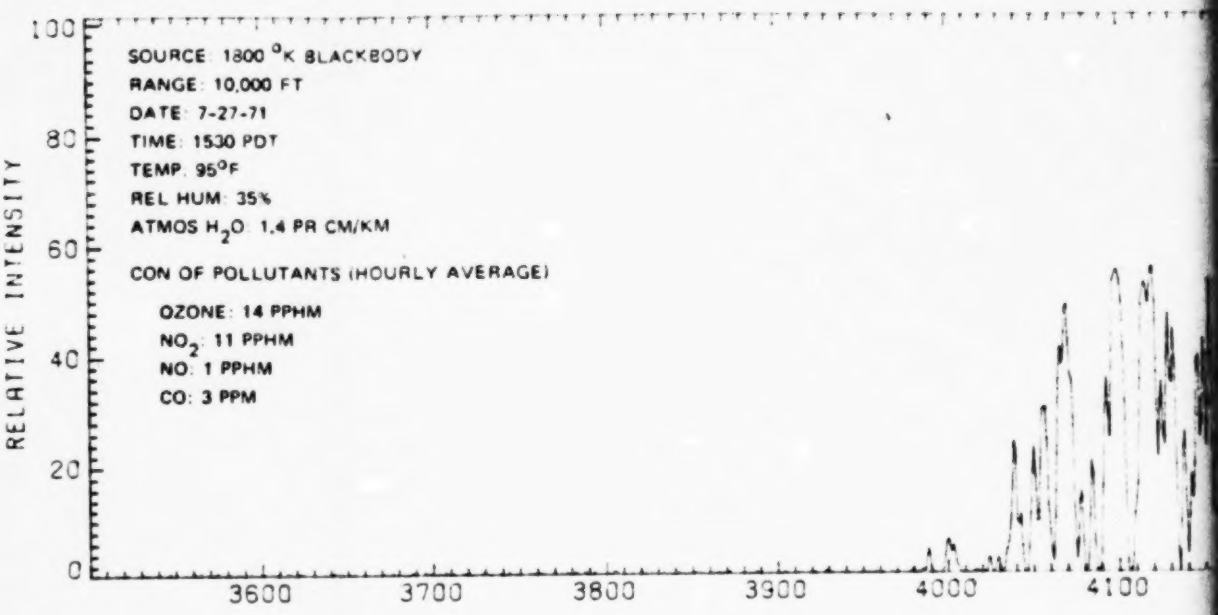

SOURCE: 1800 °K BLACKBODY
RANGE: 10,000 FT
DATE: 7-27-71
TIME: 1530 PDT
TEMP: 95°F
REL HUM: 35%
ATMOS H_2O: 1.4 PR CM/KM

CON OF POLLUTANTS (HOURLY AVERAGE)

OZONE: 14 PPHM
NO_2: 11 PPHM
NO: 1 PPHM
CO: 3 PPM

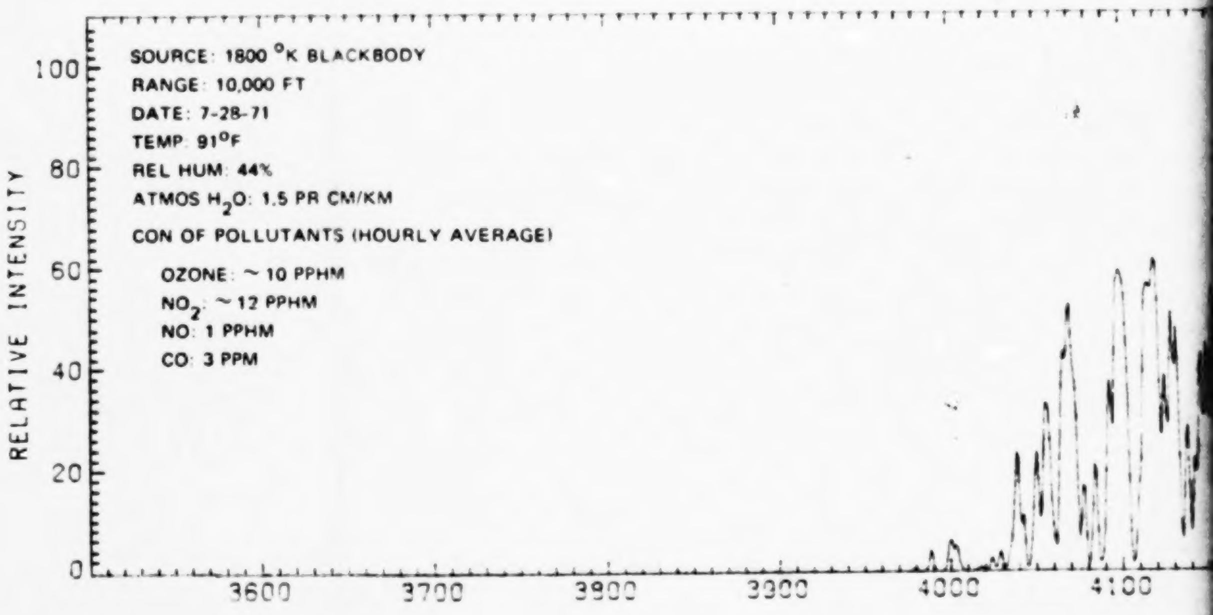

SOURCE: 1800 °K BLACKBODY
RANGE: 10,000 FT
DATE: 7-28-71
TEMP: 91°F
REL HUM: 44%
ATMOS H_2O: 1.5 PR CM/KM

CON OF POLLUTANTS (HOURLY AVERAGE)

OZONE: ~ 10 PPHM
NO_2: ~ 12 PPHM
NO: 1 PPHM
CO: 3 PPM

875746

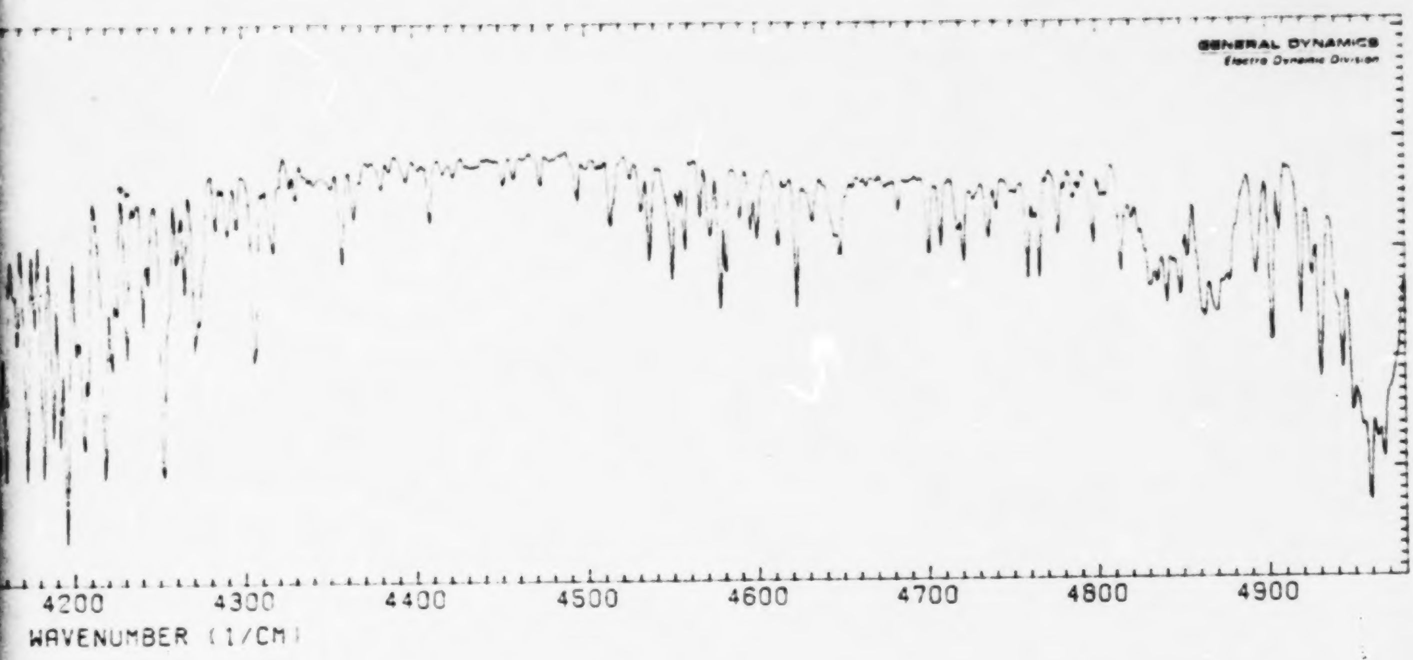

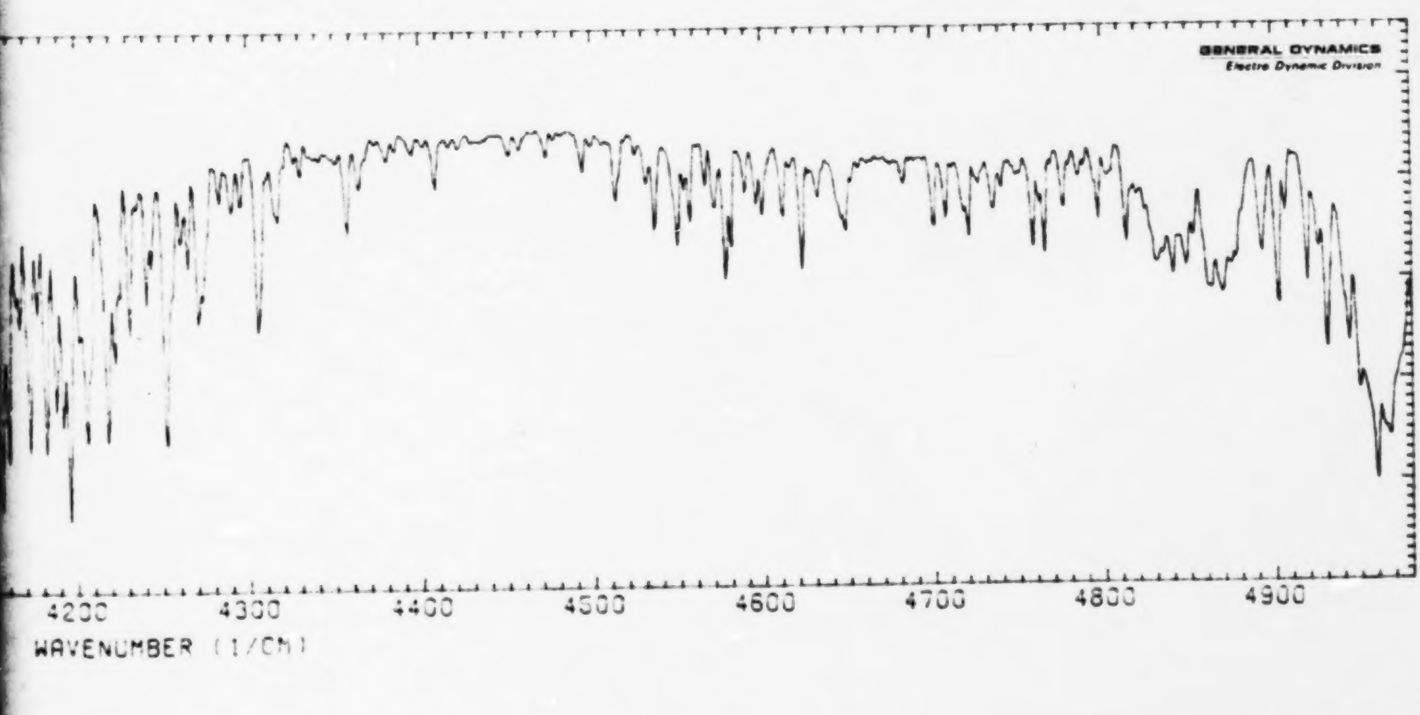

Figure 18. Relative Spectral Intensity of an 1800°K Blackbody Source Over a 10,000-Foot Path in the Interval From 3500 to 5000 cm^{-1}.

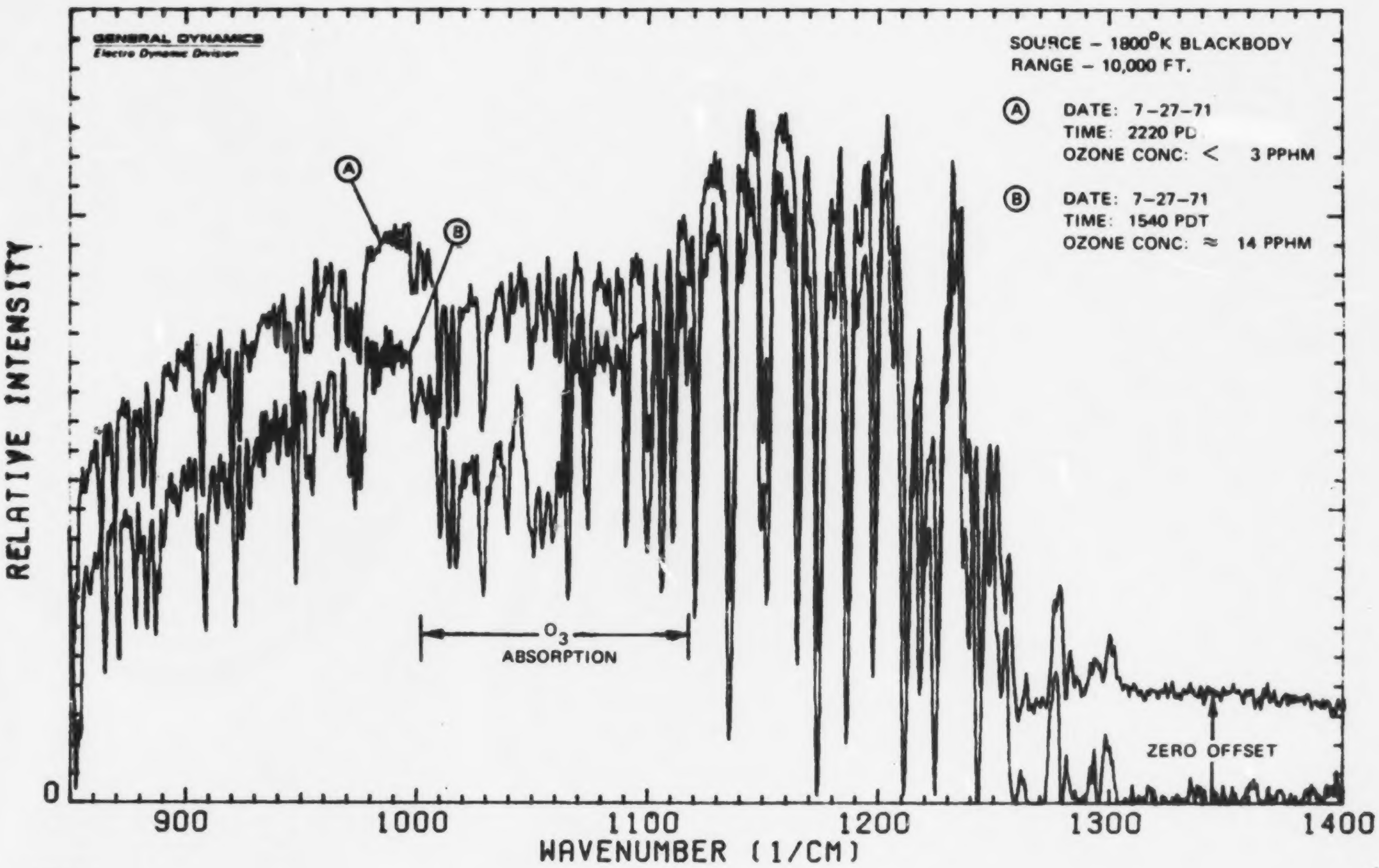

A75722

Figure 19. Comparison of the Variation of Ozone Absorption Over a 10,000-Foot Path for the Levels of Ozone Concentration.

1.3 REAL TIME DATA

In addition to the computer reduced spectral data shown in Figures 16 to 19, an x-y plotter was utilized to obtain "real time" data, presented in Figure 20, from a Federal Scientific "Ubiquitous" Spectrum Analyzer. Computer reduced data are also shown to provide a comparison between the real time data with approximately 8 cm^{-1} resolution and the computer reduced data with 2.5 cm^{-1} and 4.0 cm^{-1} resolution respectively. The spectra in Figure 20 and those previously shown clearly indicate the versatility of the interferometer spectrometer in providing either computer reduced high resolution spectra expanded to any length, or "real time" data obtainable within seconds of the actual measurement using the existing hardware. As indicated earlier, this real time capability can be extended easily to higher resolution (~ 1 cm^{-1}) with commercially available hardware.

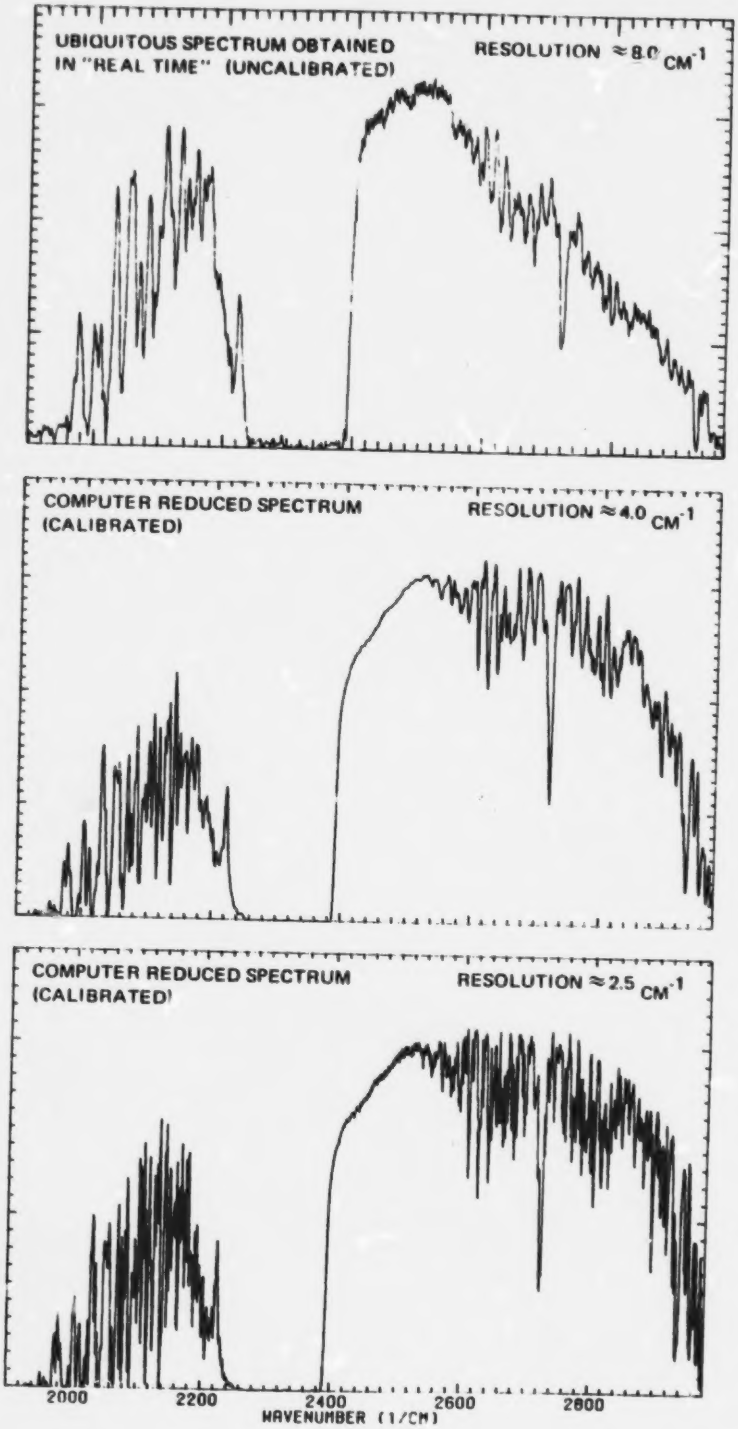

A75551

Figure 20. Spectra of an 1800°K Blackbody as Seen Through 10,000 Feet of Atmospheric Attenuation, Plotted to Three Different Spectral Resolutions.

Section 2.0

EMISSION SPECTRA

Measurements of infrared emission from various stacks in the Pomona area were performed during the week of 7-12-71. The sites selected for measurement were the Kaiser Steel Corporation plant at Fontana, California, the Southern California Edison power generating plant at Etiwanda, California and the Pomona Valley Community Hospital in Pomona, California. The spectral data presented here were generated by measuring the plumes and adjacent sky areas successively, and performing spectral subtractions to obtain contrast spectra between plume plus sky and sky. The spectral subtractions were necessary since the fields-of-view of the instruments were in all cases larger than the plume size.

2.1 KAISER STEEL CORP., FONTANA, CALIFORNIA

A view of the stacks at Kaiser Steel Corporation from the measurement site are shown in the panoramic photograph of Figure 21. The stacks were numbered as a means of identifying the measurements, and identified as to their functions by Mr. G. Rounds of the Kaiser Steel Corporation. Stacks 1, 2, and 13 were measured since each represented a different process. Stack #1 is a coke oven stack, Stack #2 is a blast furnace stack and Stack #13 is the sinter plant stack. The remaining stacks are either blast furnaces, coke ovens, or battery stacks and should have emission spectra similar to those measured. In addition to the panoramic photograph, thermal image photographs of the various stacks were taken with an AGA Thermovision unit operating in the 2-5 micron region to provide a means of quickly identifying the stacks in operation at the time of the measurement. These thermal images are shown above each of the panoramic photographs.

The fuels for the respective stacks are:

(1) Coke oven and battery - primarily methane and air.
(2) Blast furnace - 25 percent CO, 15 percent CO_2, 3-1/2 percent H_2 and 56 percent N_2.
(3) Sinter Plant - Coke breeze (small particles of coke), $CaCO_3$, Fe_2O_3, F_e + oil, and a small amount of sulfur found in the coke and oil.

The combustion products of interest in these measurements were SO_2, H_2S, CO, NO, NO_2, and CH_4.

The spectral data from 720 to 4000 cm^{-1} are presented in Figures 22 and 23. The spectral plots were not continued to 5000 cm^{-1} because none of the measurements indicated any discernible emission beyond about 3500 cm^{-1}. Included with the spectral data are the concentrations of various pollutants determined by chemical

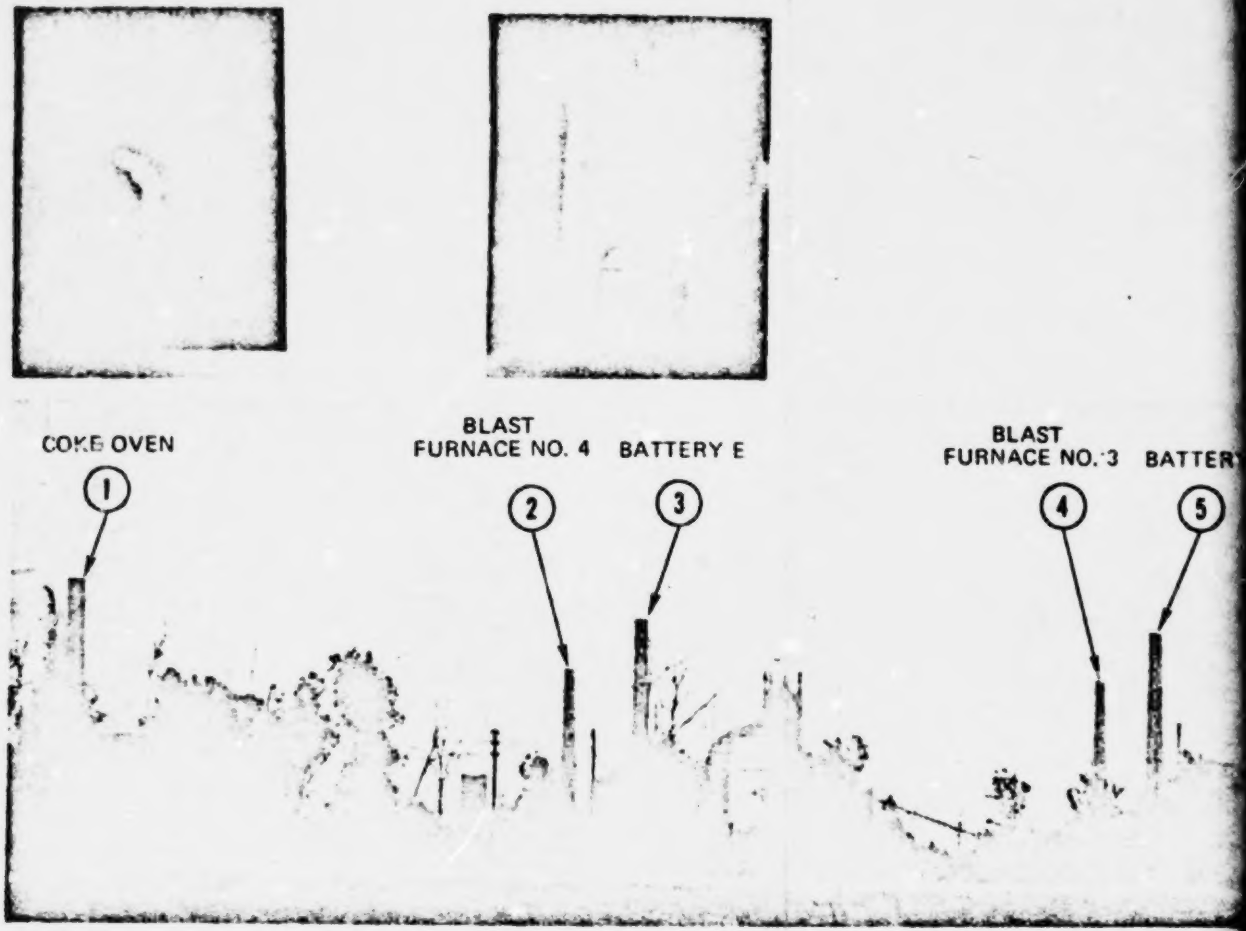
COKE OVEN
①
BLAST FURNACE NO. 4
②
BATTERY E
③
BLAST FURNACE NO. 3
④
BATTERY
⑤

B75468-1

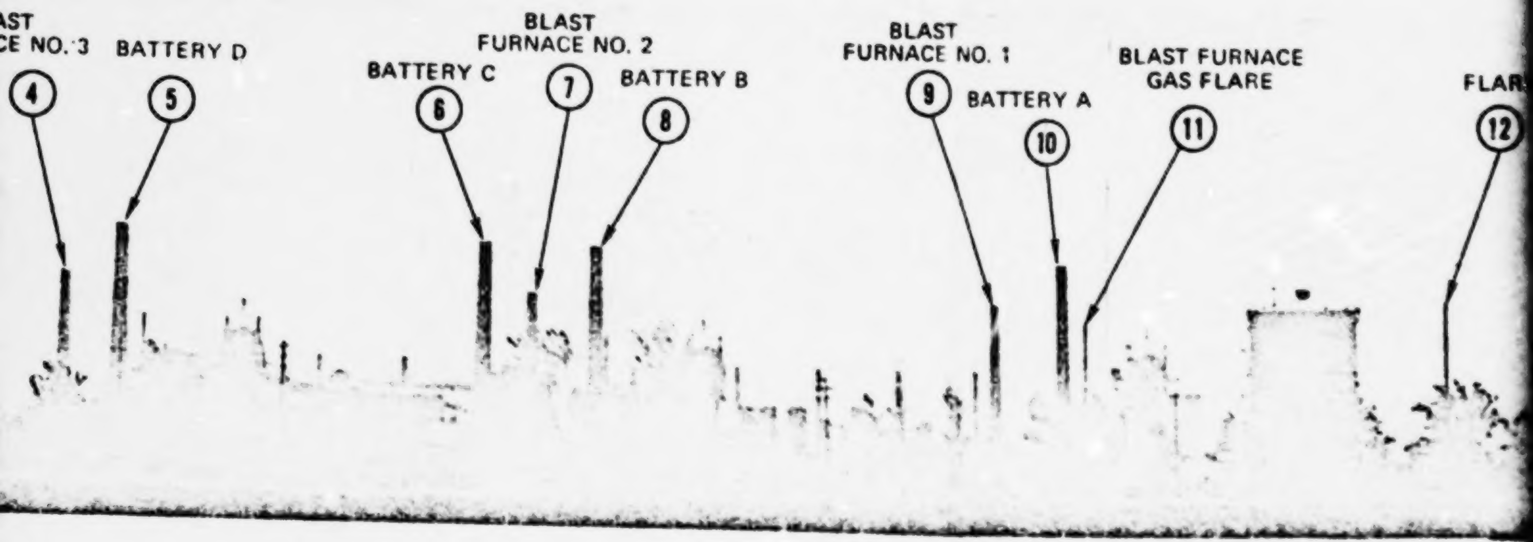
AST
CE NO. 3
4
BATTERY D
5
BATTERY C
6
BLAST
FURNACE NO. 2
7
BATTERY B
8
BLAST
FURNACE NO. 1
9
BATTERY A
10
BLAST FURNACE
GAS FLARE
11
FLAR
12

Figure 21. Kaiser Steel Co

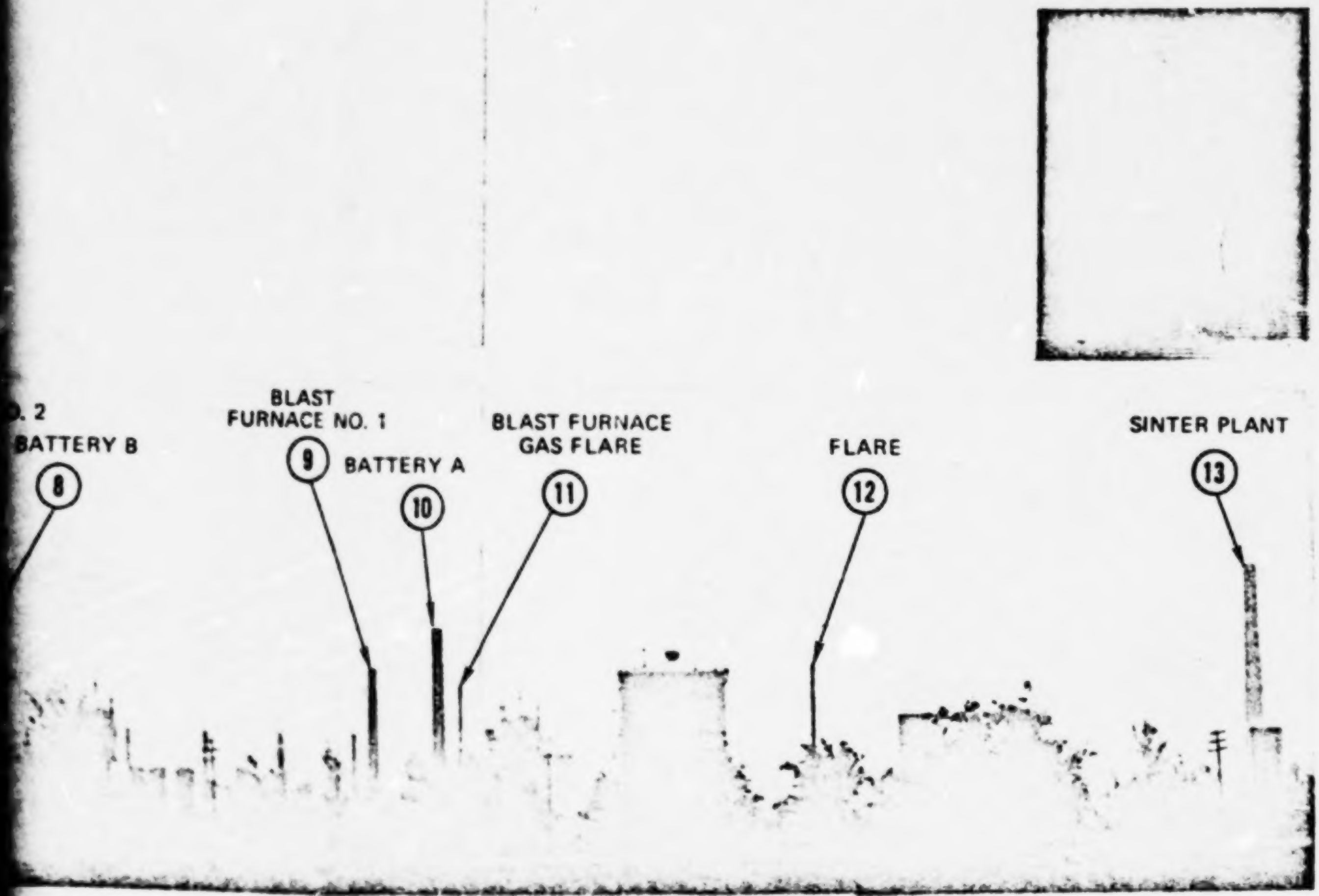

. 2
BATTERY B
8
BLAST FURNACE NO. 1
9
BATTERY A
10
BLAST FURNACE GAS FLARE
11
FLARE
12
SINTER PLANT
13

Figure 21. Kaiser Steel Corporation, Fontana, California.

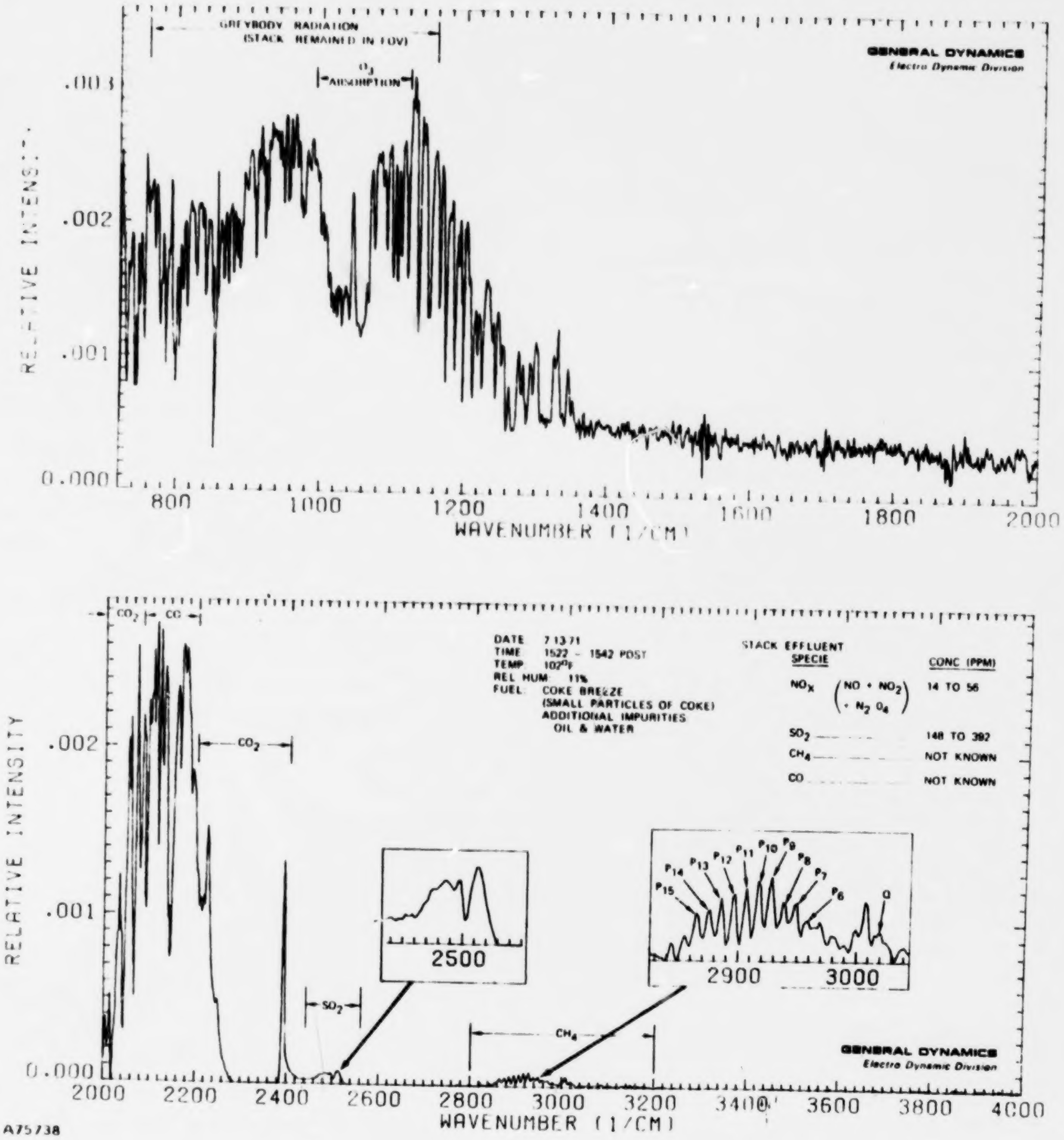

Figure 22. Emission Spectra of the Gaseous Effluents From a Sinter Plant Stack Measured at Kaiser Steel Corporation, Fontana.

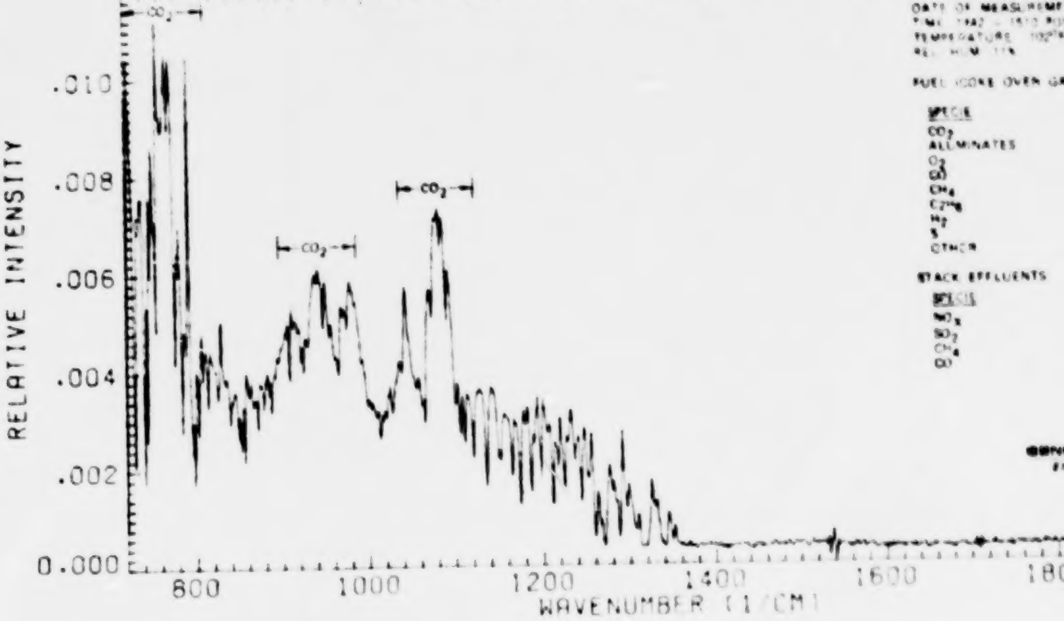
RELATIVE INTENSITY
.010
.008
.006
.004
.002
0.000
800
1000
1200
1400
1600
180
WAVENUMBER (1/CM)
CO2
CO2
CO2
CO2
DATE OF MEASUREMENT
TIME
TEMPERATURE
REL HUM
FUEL (COKE OVEN GA
SPECIE
CO2
ALLUMINATES
O2
CO
CH4
C2H6
H2
S
OTHER
STACK EFFLUENTS
SPECIE
NOx
SO2
CH4
CO

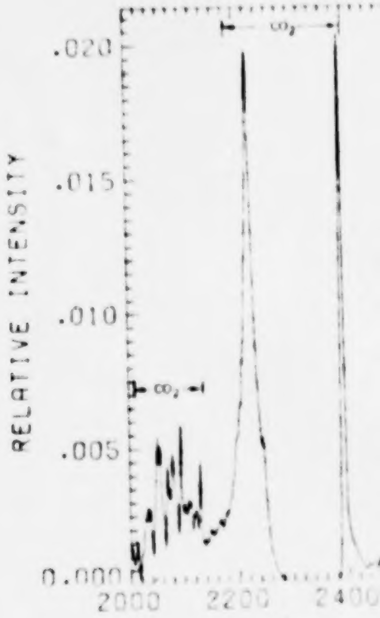
RELATIVE INTENSITY
.020
.015
.010
.005
0.000
2000
2200
2400
CO2
CO2

875737

KE OVEN (STACK NO. 1)

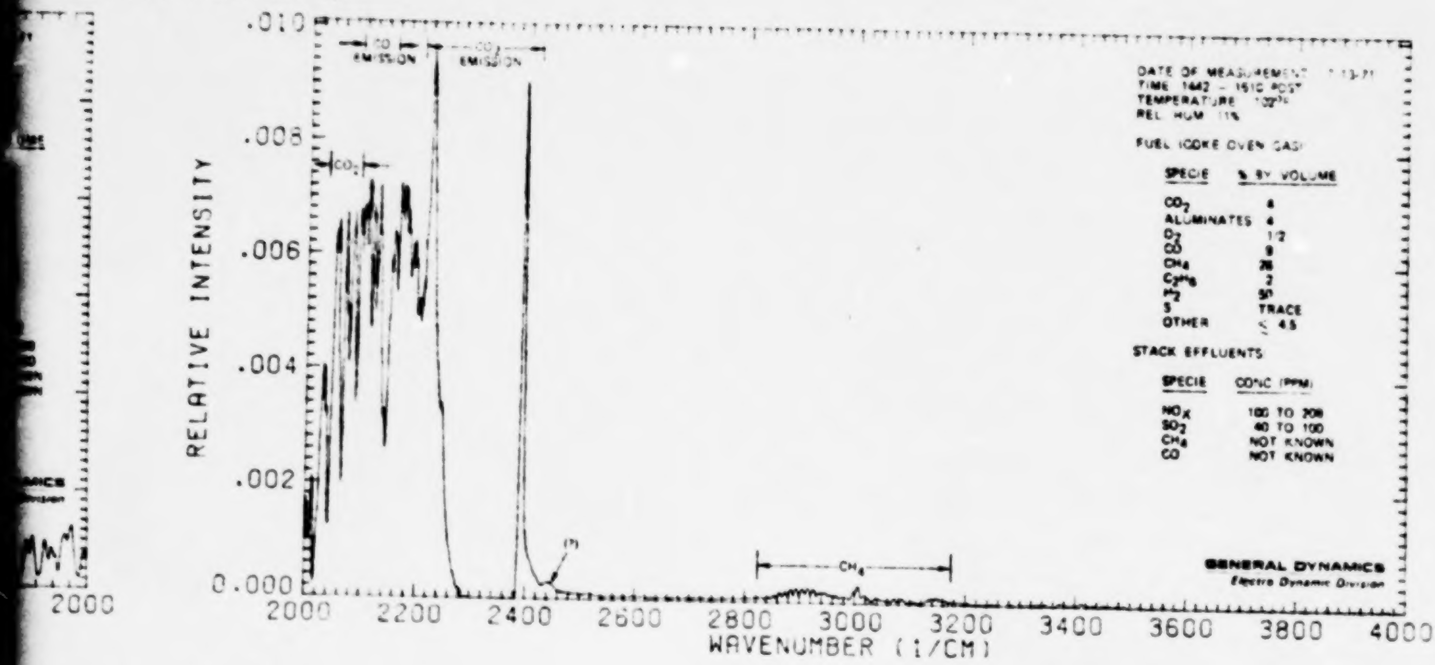

FURNACE (STACK NO. 2)

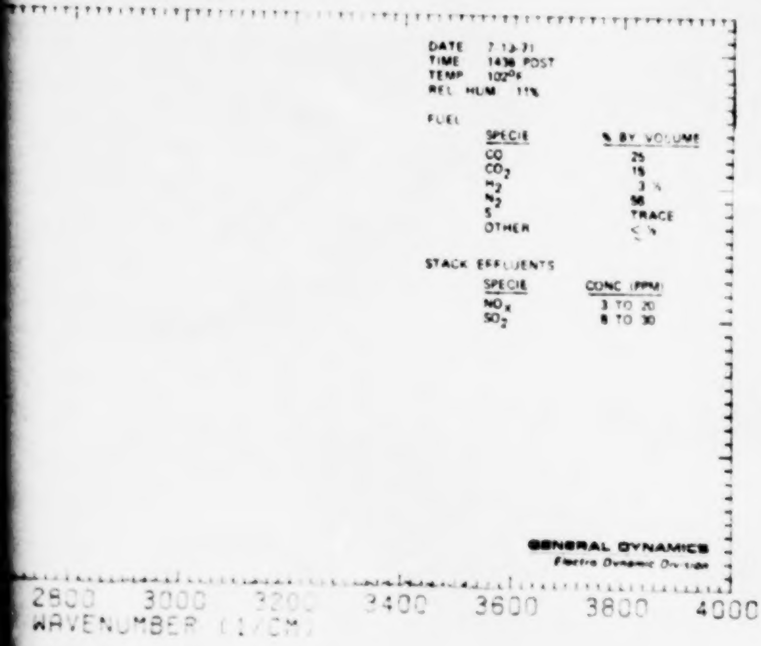

Figure 23. Emission Spectra of the Gaseous Effluents From a Coke Oven Stack and a Blast Furnace Stack Measured at the Kaiser Steel Corporation, Fontana.

analyses, where available. The large number of stacks at Kaiser Steel preclude chemical analysis at a frequency of more than once a year and the data presented are the minimum and maximum values measured for the past several years and not necessarily the concentration at the time of the spectral measurements. The data does, however, provide some indication of the levels present during the measurements.

The measurements at the Kaiser Steel Corporation indicate varying degrees of pollutants from each of the stacks. Particularly noteworthy is the emission from the sinter plant (#13) (Figure 22) which clearly shows the SO_2 ($\nu_1 + \nu_3$) combination band at 2499 cm^{-1}, the CH_4 (ν_3) fundamental band at 3020 cm^{-1}, and the CO fundamental at 2146 cm^{-1}. The inserts in Figure 22 are expanded views of the SO_2 and CH_4 emission clearly indicating the rotation-vibration structure of the CH_4 radiation.

The coke oven stack (#1) measurements (Figure 23) indicate the presence of CH_4 as evidenced by the emission at 3020 cm^{-1}. The blast furnace (#2) measurement (Figure 23) is of interest in that the only species having any significant radiation is CO_2. An anomolous band structure appears in the spectrum of stacks #1 and #2 at 2440 cm^{-1} and it is not known at this time whether this is due to an actual emission component or data processing limitations at the low intensities involved. The anamolous structure is absent in the spectrum of the sinter plant stack (#13). However, the spectrum of the sinter plant stack at 2440 cm^{-1} shows a level greater than zero indicating that the SO_2 and CO_2 radiation are being summed. Examination of the spectrum shows that the CO_2 band "head" near 2440 cm^{-1} is shifted to lower wavenumbers (band narrowed) indicating that the gas temperature of the sinter plant stack is somewhat lower than stacks 1 or 2, which would lead one to surmise that had the gas temperature been somewhat higher, the spectrum of the sinter plant at 2440 cm^{-1} would be quite similar to the spectrum of the Etiwanda power generating station shown in Figure 25, which shows the summation of SO_2 and CO_2 radiation giving a structure at 2440 cm^{-1} similar to that seen in Figure 23. The absence of SO_2 in Figures 22 and 23 does lead one to question whether the low intensity components have somehow been lost in the data reduction or subtraction process since they are very close to the instrument noise limit (the data represent five seconds of actual observation time).

2.2 SOUTHERN CALIFORNIA EDISON POWER GENERATING STATION, ETIWANDA, CALIFORNIA

The Southern California Edison Power Station at Etiwanda, California is shown in the photograph of Figure 24. The stacks measured are numbered 1 and 3, and the spectral data for the respective stacks are included in Figure 25. Information regarding the concentrations of stack effluents were unavailable. It is believed that oil is used as the primary fuel with the resulting combustion products being primarily CO_2, CO, H_2O and a trace of SO_2 depending on the sulfur content of the oil. The spectral data particularly that of Stack #3 (Figure 25) distinctly shows the presence

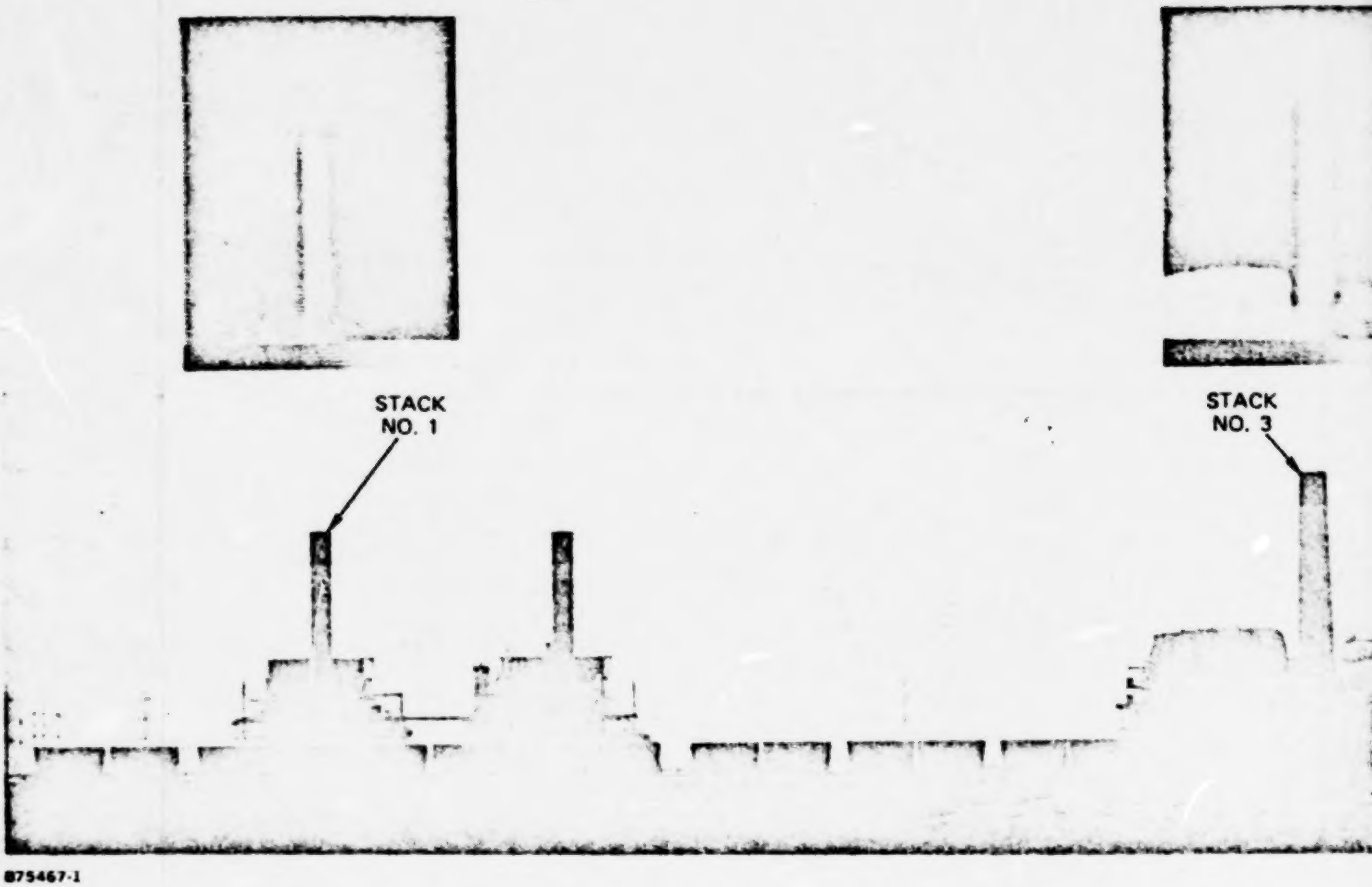
STACK
NO. 1
STACK
NO. 3
875467-1

Figure 24. Southern California

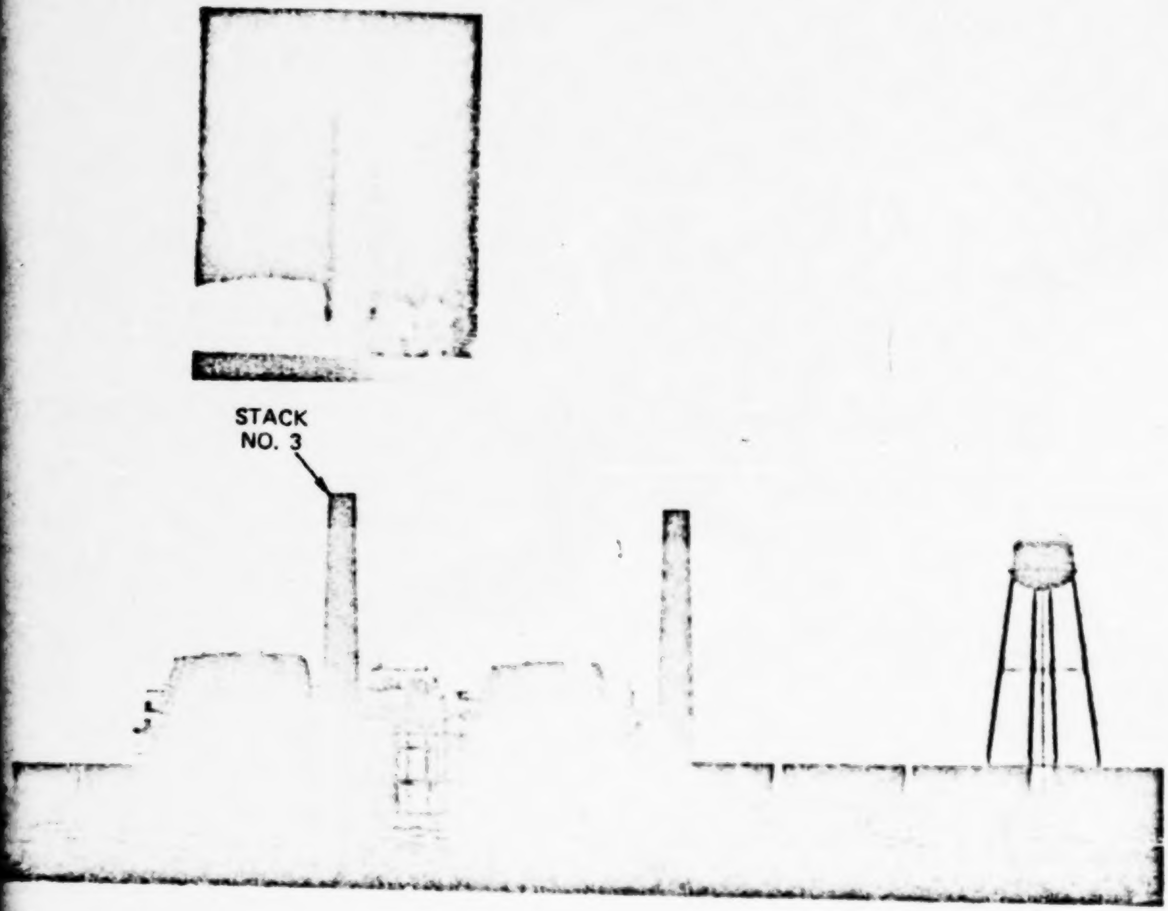

e 24. Southern California Edison Power Generating Station, Etiwanda, California.

Reproduced from best available copy.

STACK NO. 1

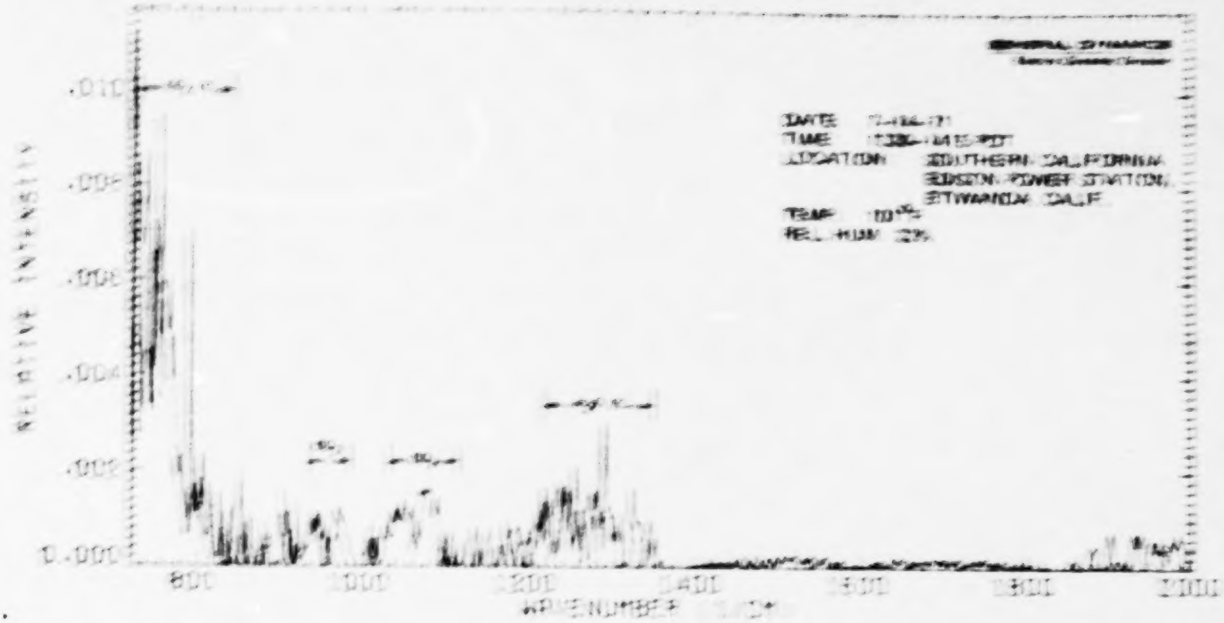

STACK NO. 2

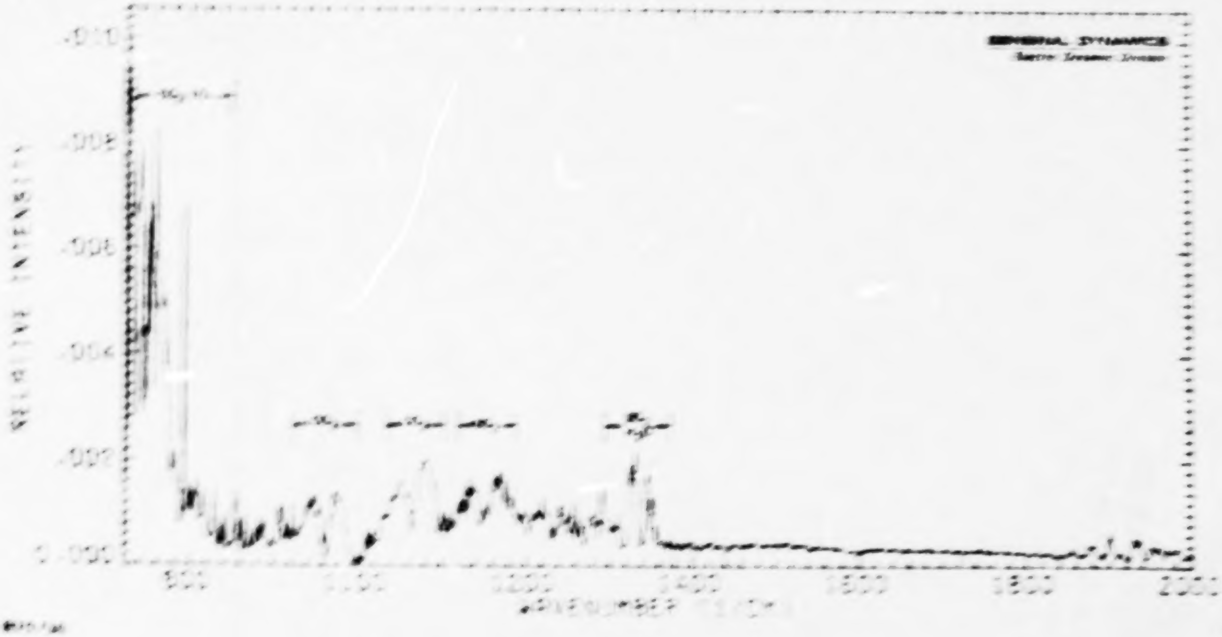

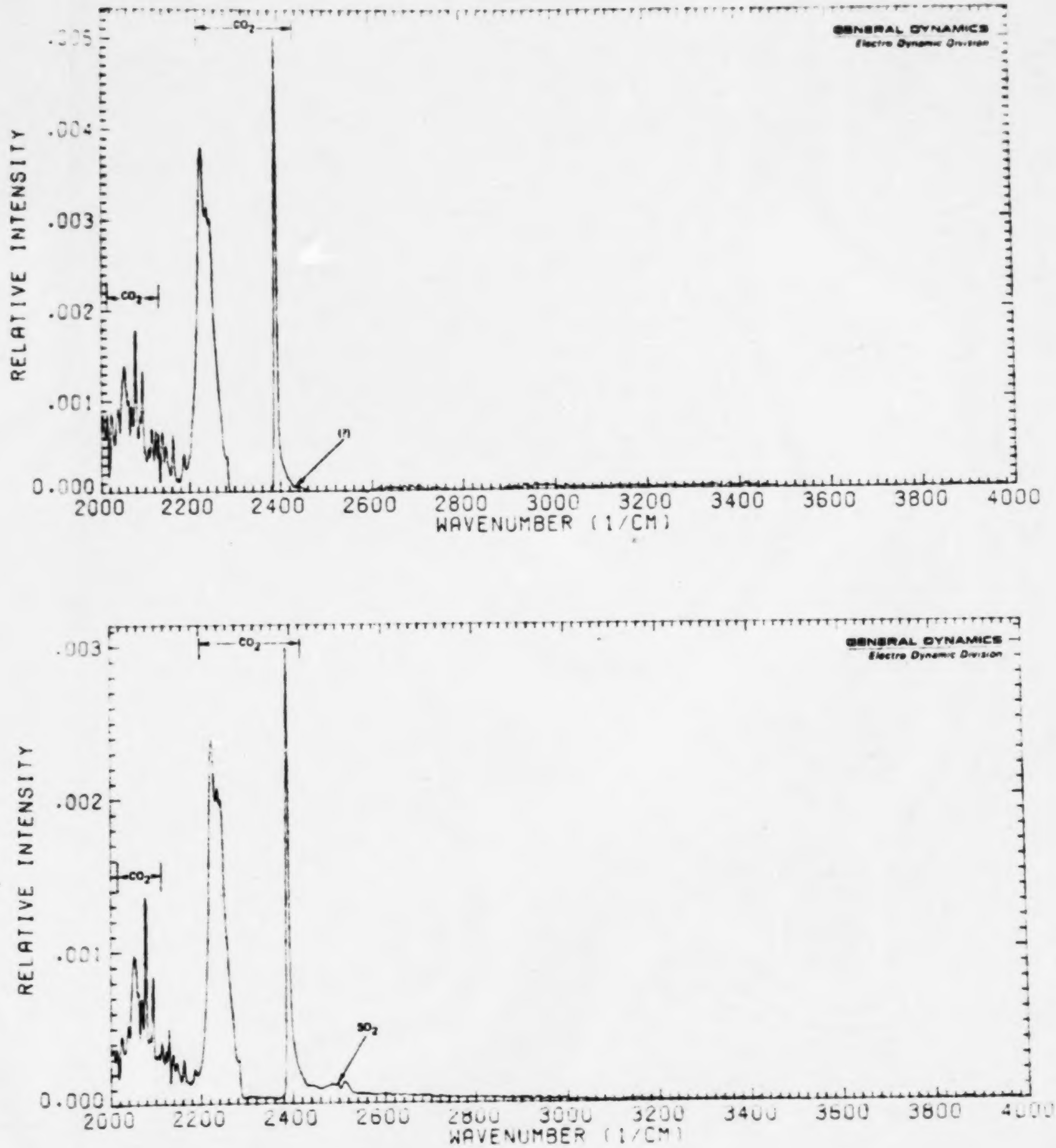

Figure 25. Emission Spectra of Gaseous Effluents From the Southern California Edison Power Generating Station at Etiwanda.

of SO_2. The $(\nu_1 + \nu_3)$ combination band at 2499 cm^{-1} and the ν_1 fundamental band at 1151 cm^{-1} are both easily identified. The emission band near 1350 cm^{-1} is nearly completely masked by water vapor absorption, and not readily identifiable.

The only other species that is readily identifiable in Figure 25 is CO_2. An anamolous band and line structure tentatively identified as CO_2, appears at 760 cm^{-1} and 790 cm^{-1}, identical to that observed in the Kaiser Steel measurements (Figure 22).

2.3 POMONA VALLEY COMMUNITY HOSPITAL

The incinerator and boiler stacks at Pomona Valley Community Hospital were measured on July 15, 1971 primarily to determine whether the burning of plastics in the incinerator could lead to observable emission of gaseous combustion products such as HCl. A photograph of the Pomona Valley Community Hospital stacks is shown in Figure 26. The spectral data are presented in Figure 27. Examination of the data indicates that the HCl fundamental band at 2880 cm^{-1} is not observable in emission. The greybody radiation in the spectrum indicates that portions of the stack remained in the field-of-view of the instruments.

The emission spectra of the stacks at the Pomona Valley Community Hospital are significant for their lack of gas emission other than that due to CO_2.

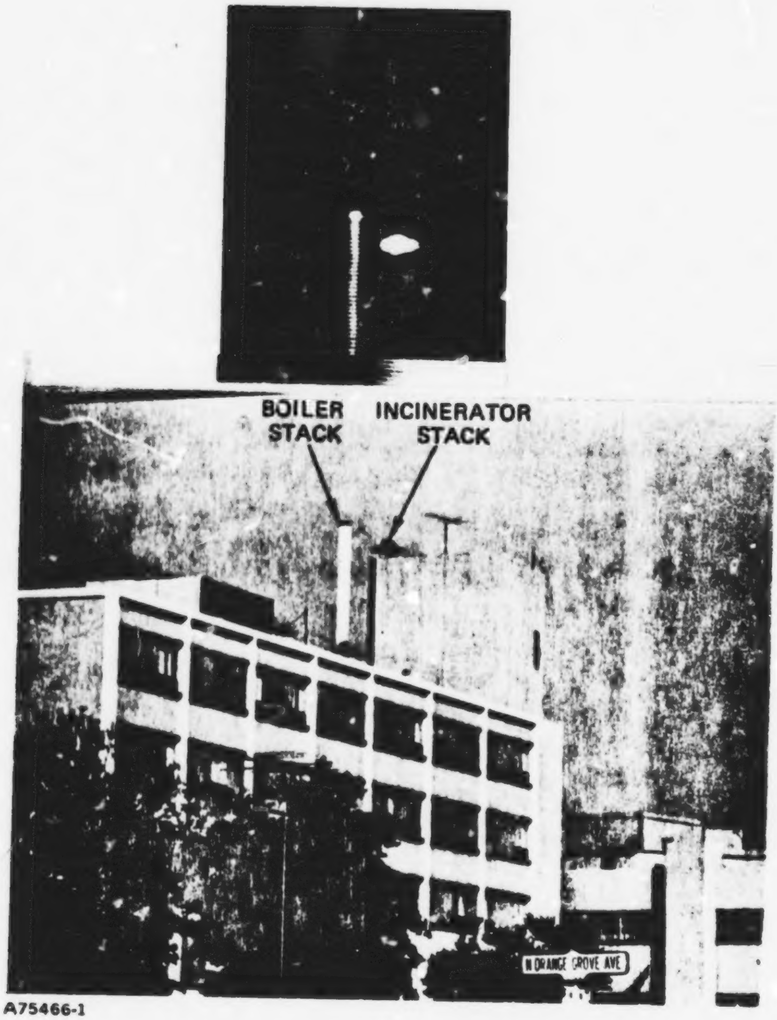
BOILER STACK
INCINERATOR STACK
N ORANGE GROVE AVE
A75466-1

Figure 26. Pomona Valley Community Hosiptal,
Pomona, California.

INCINERATOR

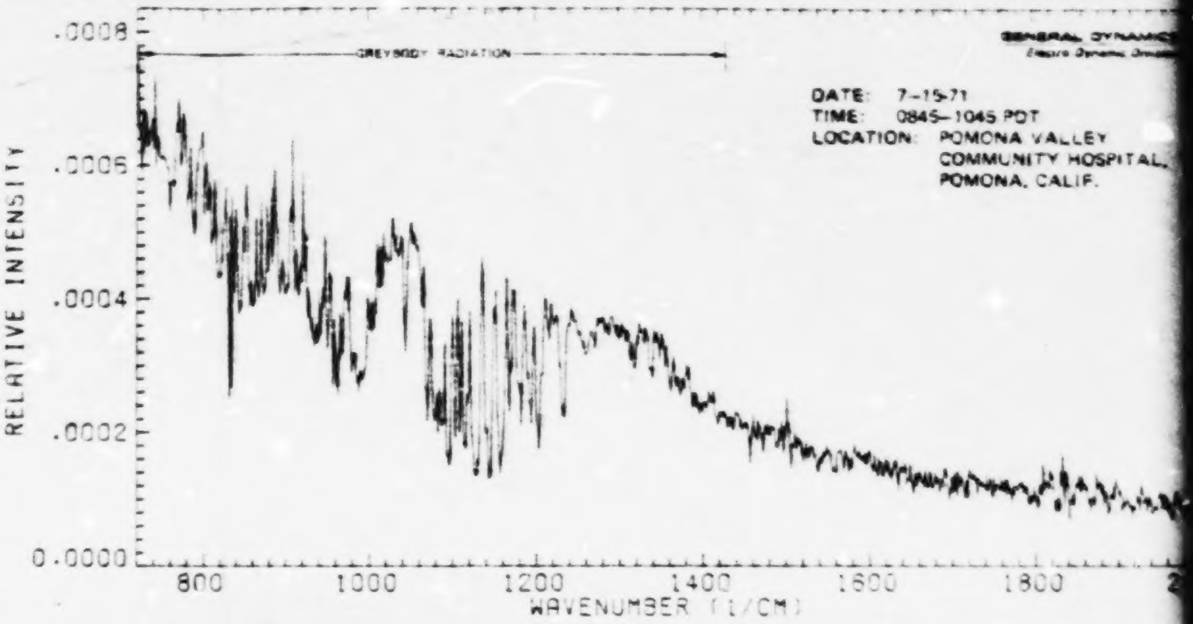

DATE: 7-15-71
TIME: 0845-1045 PDT
LOCATION: POMONA VALLEY
COMMUNITY HOSPITAL,
POMONA, CALIF.

BOILER

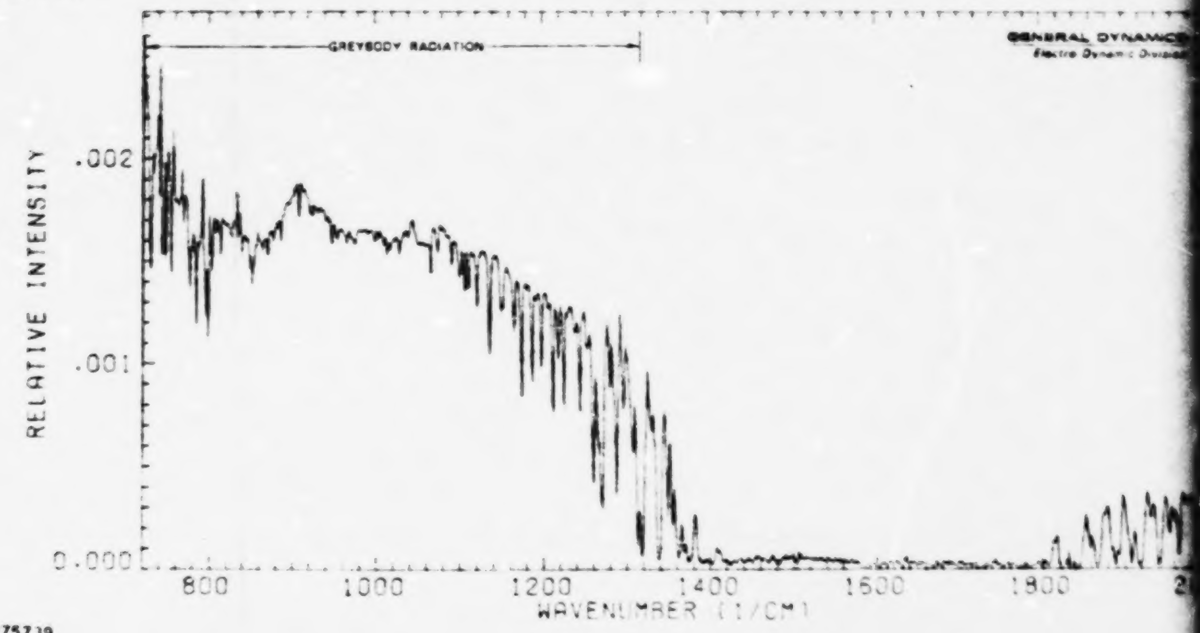

B75739

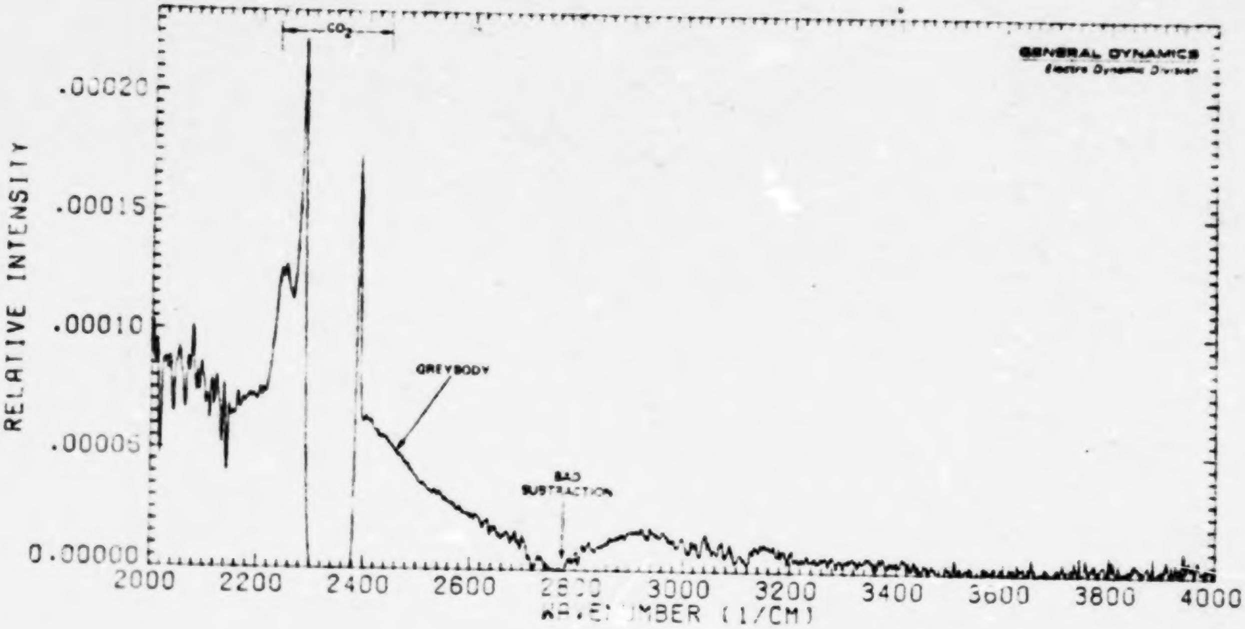

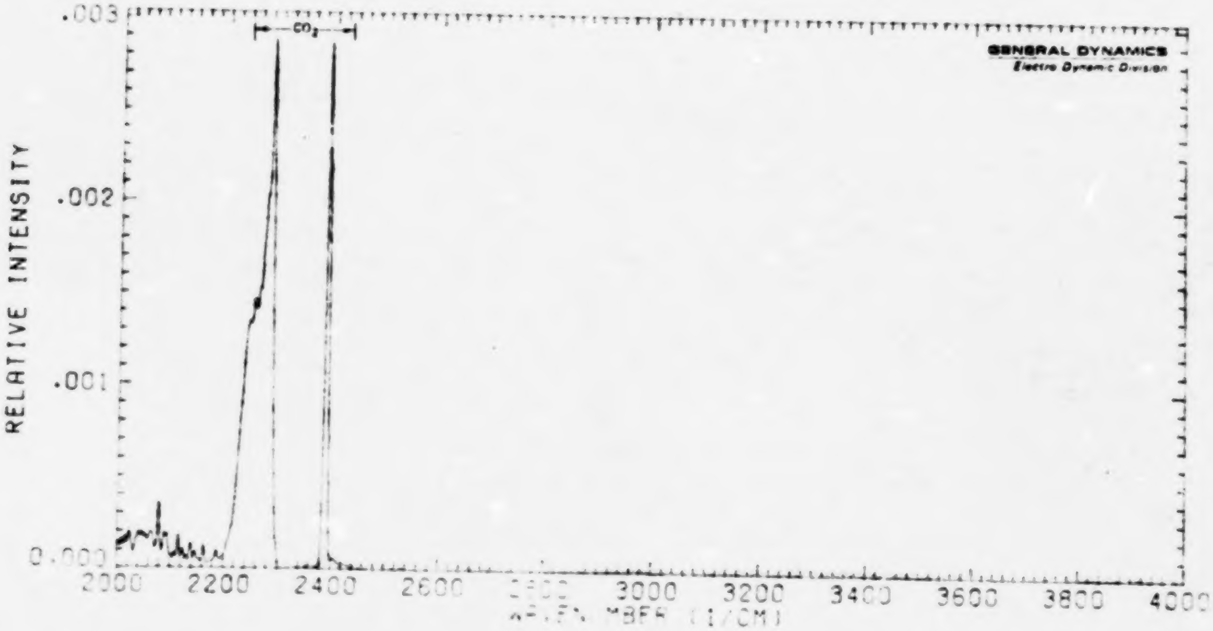

Figure 27. Emission Spectra of the Gaseous Effluents From the Pomona Valley Community Hospital, Pomona.

Section 3.0

CONCLUSION

The infrared transmission spectra at 1 and 2 mile paths and the emission spectra of various industrial stacks clearly demonstrate the applicability of the interferometer spectrometer to air pollution measurements. The rapid data collection combined with high sensitivity and resolution provide for a superior monitoring tool. The one disadvantage of existing systems, namely that the interferograms generated by the instrument require transformation from the time to frequency domain, is easily overcome by the availability of small special purpose computers and spectrum analyzers which can provide real time spectral information much faster than other systems. To a degree this was demonstrated in Figure 20 which shows, even with the existing equipment, sufficient resolution to obtain quantitative data particulary with respect to ozone absorption measurements at 1042 cm^{-1} and 1103 cm^{-1}.

The detection and quantitative determination of ozone concentrations through long path atmospheric transmission measurements in the infrared appear to be highly promising as indicated in the spectral data of Section 1. Less promising is the detection of the oxides of nitrogen other than N_2O. But this is not a shortcoming of the interferometer. The fundamental vibrational frequencies of both nitric oxide and nitrogen dioxide fall within the strong water vapor absorption bands, and neither band nor line structure can be determined with any degree of confidence. The possibility of finding overtone or combination band structure is, however, real, particularly the $(\nu_1 + \nu_3)$ combination band of NO_2 at 2905 cm^{-1} and the $(2\nu_1 + \nu_3)$ combination band of NO_2 at 4180 cm^{-1}. These combination bands will have interference from methane and water vapor, respectively, but are sufficiently removed from the band centers of the interfering gases to possibly permit the identification of rotation-vibration lines with high resolution spectrometers (better than 1 cm^{-1}), or possibly some band structure with lower resolution instruments. In this context, Figures 28 and 29 are included to indicate the possibility that NO_2 absorption of the $(\nu_1 + \nu_3)$ combination band at 2905 cm^{-1} could be responsible for the significant difference in the overlays of 2 sets of spectral curves at ranges of 1 mile and 10,000 ft respectively. There is not, however, conclusive evidence that NO_2 absorption is responsible for the differences, and the curves are presented to suggest the possibility that further study in this particular area may be of value.

The measurements of infrared radiation from industrial stacks also have proved successful in remotely detecting pollutants. Of primary significance in these measurements were the detection of SO_2, CO, and CH_4. The high "through-put" of the interferometer spectrometer is of particular value in detecting the weak $(\nu_1 + \nu_3)$ combination band of SO_2 and the (ν_3) fundamental of methane (CH_4).

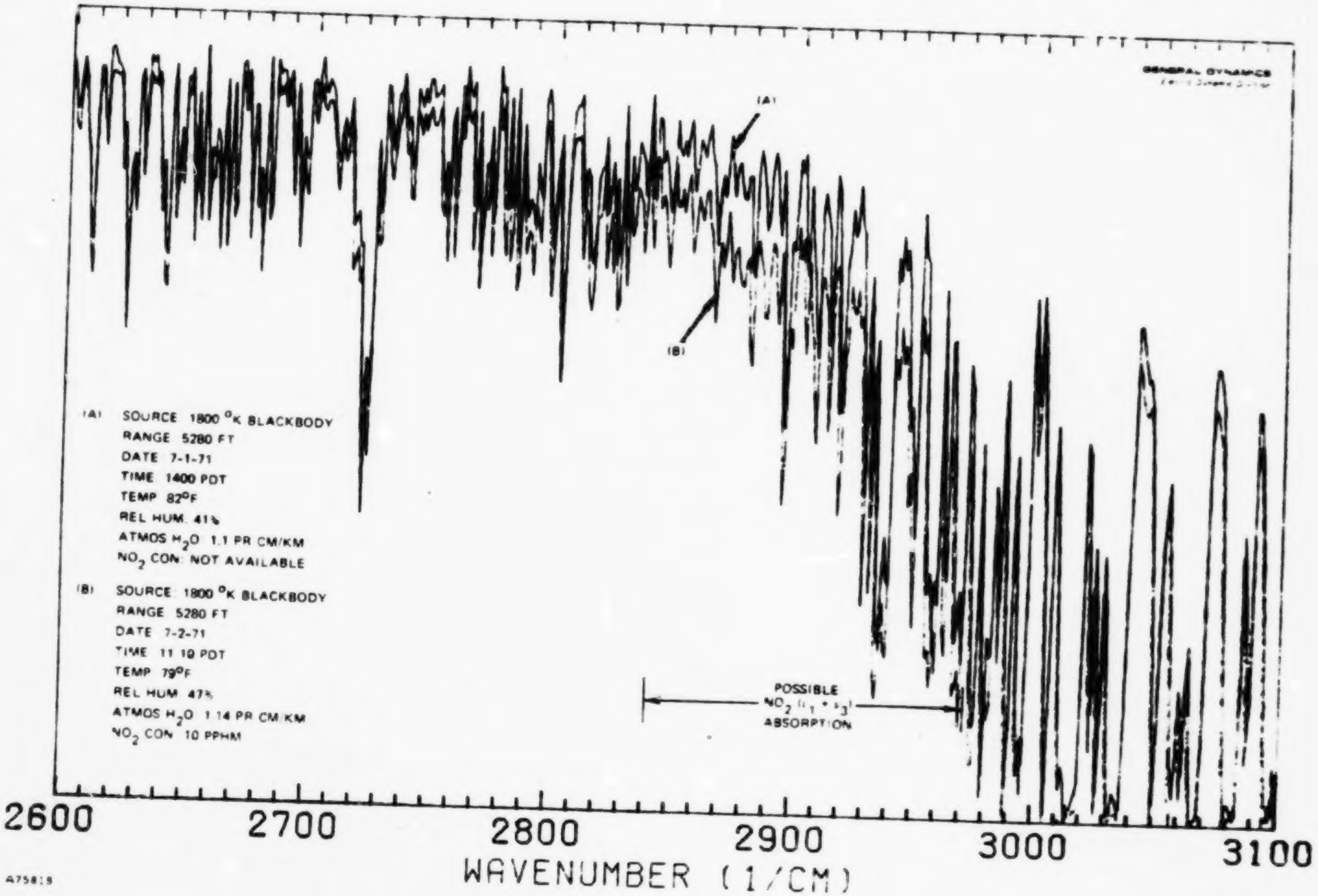

Figure 28. Comparison of the 2900 cm^{-1} Spectral Region for Two Spectral Measurements Over a One-Mile Path.

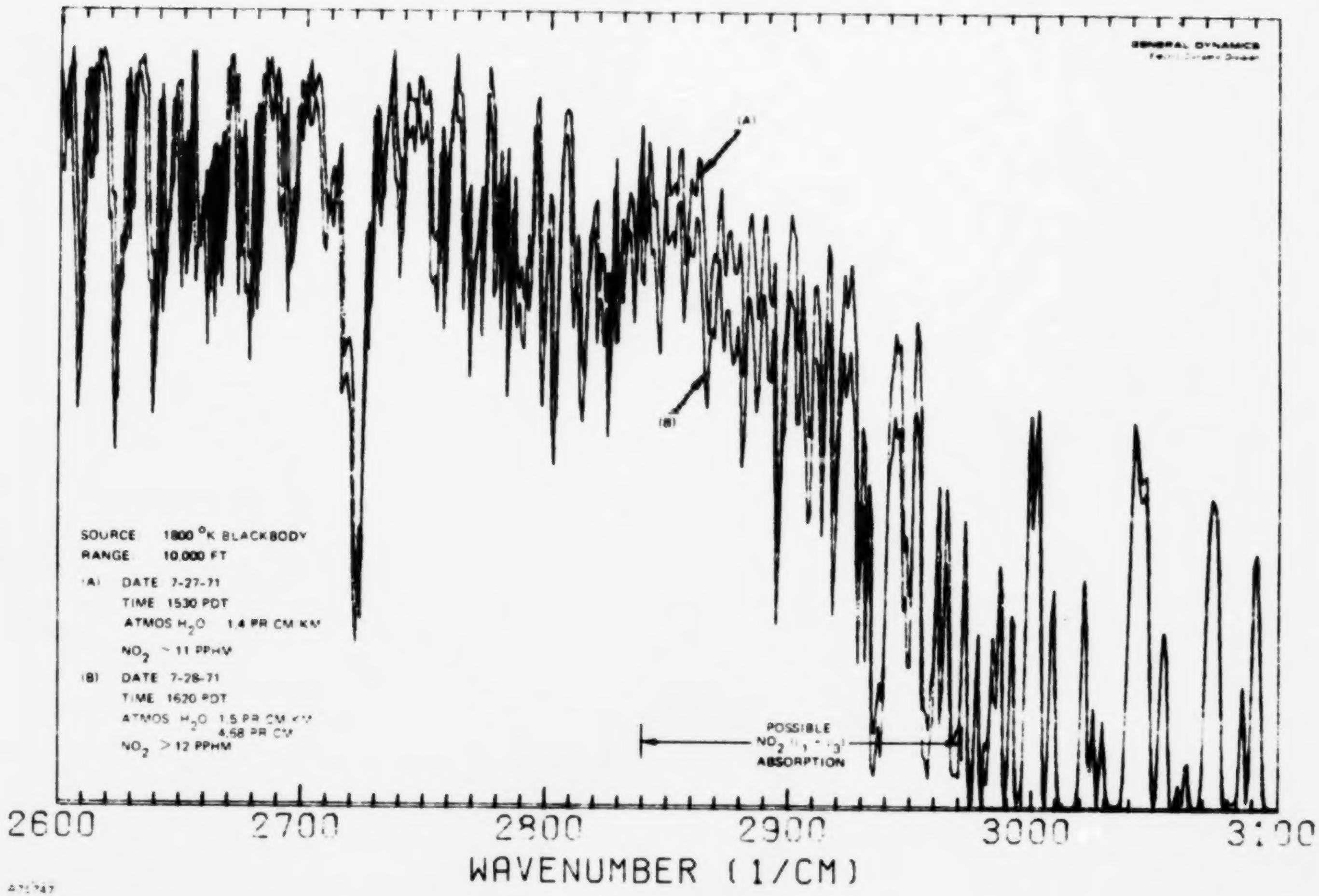

Figure 29. Comparison of the 2900 cm^{-1} Spectral Region for Two Spectral Measurements Over a Two-Mile Path.

APPENDIX

1. INSTRUMENTATION

Two Michelson-type interferometer spectrometers were used to obtain spectral data over the 2 to 14 micron region. One interferometer using an LN2 cooled InSb (PV) detector covered the region from 2-5.4 microns while the second interferometer equipped with an LN2 cooled HgCdTe detector obtained useful data from 3.5 to 14 microns. The characteristics of both interferometers are tabulated in Table A-1.

The principal element in the interferometer is an optical cube consisting of a Pomona operation developed beam splitter, a fixed front surfaced mirror and a moving mirror driven by a servo-controlled system developed by Idealab, Incorporated, in a traingular sweep to obtain linear mirror movement.

The optical cube is shown in schematic form in Figure A-1. As indicated in the schematic, the single cube is used for the information channel, a laser reference and a white light synchronization pulse. The sync pulse is used to locate the exact center of the interferogram for coherent averaging of successive interferograms (when desired). The laser provides the digitizing clock and wavelength reference.

Both instruments were equipped with f/8 collecting optics with the 2-5 micron interferometer having a 10 inch diameter collecting mirror and the 3.5-14 micron interferometer having a 12 inch diameter collecting mirror. A photograph of the 2-5 micron interferometer with associated control and monitoring electronics is shown in Figure A-2. The design allows for variations in the field-of-view from a few milliradian to several degrees by means of quick-change foreoptics elements.

2. DATA ACQUISITION AND REDUCTION PROCEDURE

The data acquisition and reduction procedure is illustrated in Figure A-3. The analog interferogram is converted to digital form and recorded on an HP 3950A wideband FM tape recorder. IRIG timing and voice annotation are also included on separate channels of the recorder. A hybrid digital system has been adopted to eliminate the dominant tape noise in a purely analog recording system at the expense of introducing an additional processing step as opposed to a pure digital system, primarily because of it's high cost and large space requirements. A flow chart of the hybrid system is shown in Figure A-4. The interferogram is sampled by a 15 bit A/D converter and transferred to interface unit 1. The interface unit 1 converts the binary data into a pulse-code modulated (PCM) form which is then recorded on the HP 3950A recorder. The PCM data can be played back into interface unit 2 and either be decoded for monitoring purposes in the field or reformated on digital tape through the IBM 1800 computer for data reduction.

TABLE A-1

PRINCIPAL INTERFEROMETER CHARACTERISTICS

Item	Interferometer #1	Interferometer #2
Model Designation (Drive Mechanism)	IF-3	IF-3
Wavenumber Region of Operation	1850 to 5000 cm^{-1}	716 to 2500 cm^{-1}
Optical Resolution	~ 2.5 cm^{-1}	~ 1 cm^{-1}
Spectrum Recording Rates	1 per 2.5 sec.	1 per 4.5 sec.
Detector	1.0mm dia. InSb (PV)	2 x 2mm HgCdTe
Detector Lens	1/4" dia. silicon	1 1/4" dia. Germanium
Detector Cooling	Liquid Nitrogen	Liquid Nitrogen
Foreoptics/Field-of-View (50%)	10" dia./2m. rad.	12" dia./6m rad.
Wavelength Reference	0.63282μ HeNe Laser	0.63282μ HeNe Laser

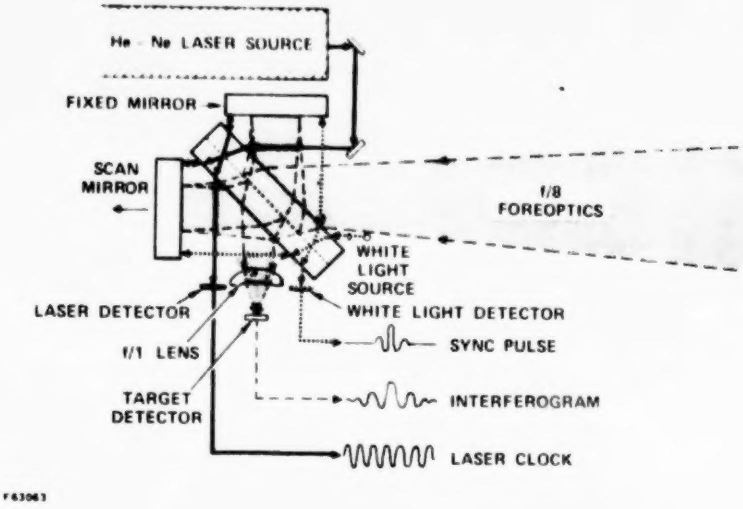
He - Ne LASER SOURCE
FIXED MIRROR
SCAN MIRROR
f/8 FOREOPTICS
WHITE LIGHT SOURCE
LASER DETECTOR
WHITE LIGHT DETECTOR
f/1 LENS
SYNC PULSE
TARGET DETECTOR
INTERFEROGRAM
LASER CLOCK
F63063

Figure A-1. Optical Layout of Michelson Interferometer.

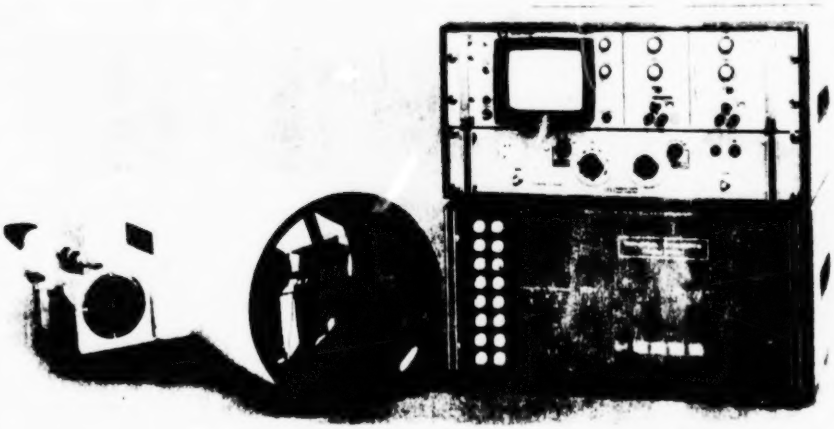

Figure 4-2. Interferometer With Control and Monitor Electronics.

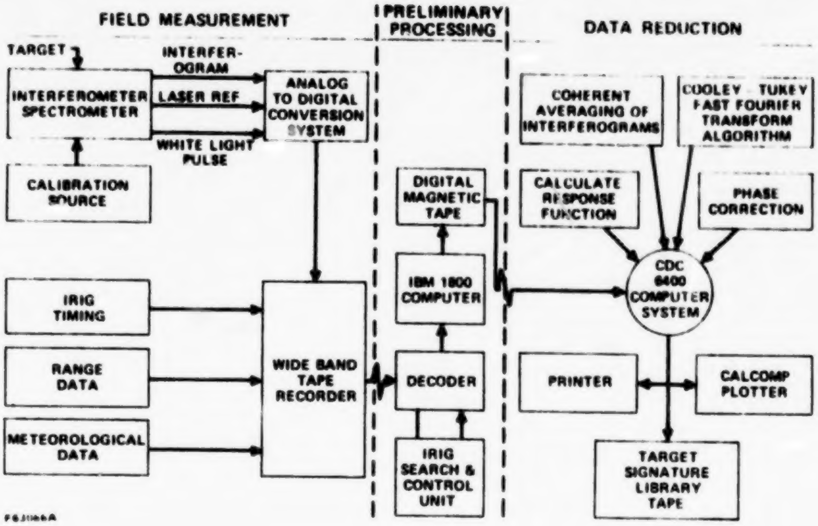
FIELD MEASUREMENT
PRELIMINARY PROCESSING
DATA REDUCTION
TARGET
INTERFEROMETER SPECTROMETER
INTERFEROGRAM
LASER REF
WHITE LIGHT PULSE
ANALOG TO DIGITAL CONVERSION SYSTEM
CALIBRATION SOURCE
IRIG TIMING
RANGE DATA
METEOROLOGICAL DATA
WIDE BAND TAPE RECORDER
DIGITAL MAGNETIC TAPE
IBM 1800 COMPUTER
DECODER
IRIG SEARCH & CONTROL UNIT
COHERENT AVERAGING OF INTERFEROGRAMS
COOLEY - TUKEY FAST FOURIER TRANSFORM ALGORITHM
CALCULATE RESPONSE FUNCTION
PHASE CORRECTION
CDC 6400 COMPUTER SYSTEM
PRINTER
CALCOMP PLOTTER
TARGET SIGNATURE LIBRARY TAPE
F63066A

Figure A-3. Data Acquisition and Reduction and Procedures Block Diagram.

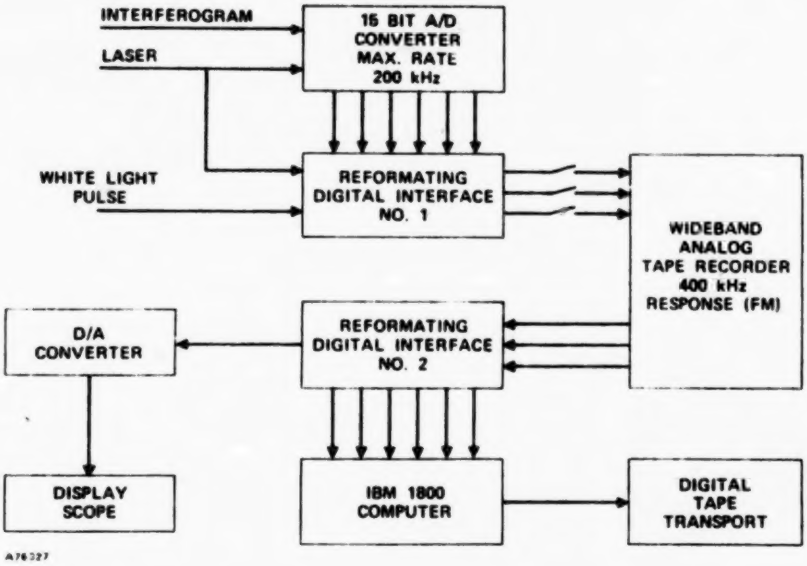
INTERFEROGRAM
LASER
15 BIT A/D CONVERTER MAX. RATE 200 kHz
WHITE LIGHT PULSE
REFORMATING DIGITAL INTERFACE NO. 1
WIDEBAND ANALOG TAPE RECORDER 400 kHz RESPONSE (FM)
D/A CONVERTER
REFORMATING DIGITAL INTERFACE NO. 2
DISPLAY SCOPE
IBM 1800 COMPUTER
DIGITAL TAPE TRANSPORT
A76327

Figure A-4. Hybrid Digital/Analog Recording System Block Diagram.

At the conclusion of the field measurements, the analog tape is decoded and played into an IBM 1800 computer at which time selected portions of the data to be analyzed are put in the proper format on digital tape compatible with the CDC 6400 computer used for the actual data reduction process. The interferograms, single or co-added, are operated on by the Cooley-Tukey fast Fourier transform algorithm to transform the interferograms from the time domain to the frequency domain. Compensation for the non-linear response of the optical and electrical system is achieved by comparing an uncompensated calibration blackbody spectra to Planck's equation at the temperature of the source. The instrument response curve derived by this process is then used to compensate subsequently measured data.

The correspondence between frequency and wavelength or wavenumber is established through the laser reference and used to correctly plot the abscissa scale for all data during the run. The ordinate scale is automatically determined for the calibration and the data by providing the computer with information relating to the calibration source. Plots of spectral data are generated by a Cal-Comp digital plotter. In addition, the spectral data is stored on a library tape for future use in various applications.

APPENDIX II

TABLE A. 1 - BAND STRENGTHS AND BAND-AVERAGED ABSORPTION COEFFICIENTS AND FINE STRUCTURE PARAMETERS OF POLLUTANTS*

Species	λ (μm)	Transition	$\omega_1 - \omega_2$ cm^{-1}	$\Delta\omega$ cm^{-1}	No. Lines	α $cm^{-2}\ atm^{-1}$	$\bar{k}$ $cm^{-1}\ atm^{-1}$	$\bar{a}_0$ atm^{-1}
CO	4.6	0 - 1	1960 - 2240	280	142	217.9	0.7263	0.0093
	2.3	0 - 2	4180 - 4320	140	40	1.99	0.0142	0.0125
CO_2	10.0	$\nu_3 - \nu_1$ $\nu_3 - 2\nu_2$	880 - 1100	220	419	0.0673	0.000306	0.0507
	4.9	$2\nu_1 - \nu_2$ $\nu_1 + \nu_2$	1880 - 2180	300	448	0.9096	0.00303	0.0544
	2.9	$3\nu_2^1 - \nu_2^1 + \nu_3$ $2\nu_2 + \nu_3$	3460 - 3560	100	112	0.8286	0.00829	0.0546
	2.0	$2\nu_1 + \nu_3$	4700 - 5160	460	596	1.597	0.00347	0.0388
SO_2	8.7	ν_1	1040 - 1260	220	6311	99.801	0.4536	1.3534
	4.0	$\nu_1 + \nu_3$	2340 - 2640	300	3073	22.530	0.07510	0.6032
NO_2 **	7.6	ν_1	1200 - 1440	240	2583	105.1	0.438	0.666
	3.4	$\nu_1 + \nu_3$	2800 - 2980	180	1410	62.64	0.3480	0.3833
NO	5.3	0 - 1	1760 - 1980	220	305	110.9	0.504	0.0442
N_2O	8.1	ν_1 $2\nu_2$	1120 - 1340	220	235	249.1	1.132	0.0408
	4.5	ν_3	2140 - 2260	120	942	1746.7	14.556	0.1472
	3.9	$2\nu_1$ $\nu_1 + 2\nu_2$	2460 - 2640	180	210	40.33	0.2240	0.0444
	2.9	$\nu_1 + \nu_3$ $2\nu_2 + \nu_3$	3300 - 3500	200	242	29.13	0.1456	0.0374
NH_3	10.4	ν_2	680 - 1240	560	477	1576.9	2.816	0.0402
	3.0	ν_3	3100 - 3660	560	473	85.53	0.1527	0.0399
HCHO	3.5	ν_4	2620 - 3140	520	1861	299.9	0.577	1.0598
H_2O	9.0		960 - 1260	300	129			0.0119
	5.3		1760 - 1980	220	370			0.0099
	4.7		1980 - 2240	260	186			0.0096
	3.3		2900 - 3140	240	203			0.0323
	3.0		3140 - 3460	320	490			0.0456
	2.4		3980 - 4360	380	321			0.0198
	2.0		4700 - 5160	460	349			0.0199

* This work was supported in part by NASA Contracts NAS-1-10466 and NAS-1-11111.

** The values of α, $\bar{K}$ and $\bar{a}_o$ are now considered to be significantly lower than those listed here.

Table A-2 - Band Model Parameters for CO in 5 and 20 cm^{-1} intervals.

Δω (1/cm)		k(300K) (1/cm-atm)	a_o(300K) (1/atm)
1960	1965	1.160000E-05	7.000000E-03
1965	1970	2.620000E-05	1.344549E-02
1970	1975	4.960000E-05	1.364476E-02
1975	1980	8.720000E-05	1.392088E-02
1960	1980	4.415000E-05	1.126716E-02
1980	1985	1.510000E-04	1.414421E-02
1985	1990	2.560000E-04	1.419167E-02
1990	1995	7.560000E-04	2.294664E-02
1995	2000	8.840000E-04	1.473875E-02
1980	2000	5.117500E-04	1.495969E-02
2000	2005	1.422000E-03	1.477750E-02
2005	2010	2.264000E-03	1.456904E-02
2010	2015	3.572000E-03	1.487009E-02
2015	2020	5.576000E-03	1.478510E-02
2000	2020	3.208500E-03	1.394287E-02
2020	2025	8.678000E-03	1.486012E-02
2025	2030	1.761200E-02	2.320637E-02
2030	2035	2.107200E-02	1.522507E-02
2035	2040	3.086000E-02	1.512884E-02
2020	2040	1.953050E-02	1.614877E-02
2040	2045	4.484000E-02	1.497952E-02
2045	2050	8.034000E-02	2.225785E-02
2050	2055	9.240000E-02	1.472463E-02
2055	2060	2.866400E-01	2.201963E-02
2040	2060	1.260555E-01	1.689605E-02
2060	2065	3.788000E-01	1.888469E-02
2065	2070	3.311000E-01	1.858739E-02
2070	2075	4.033400E-01	1.315909E-02
2075	2080	5.141400E-01	1.282293E-02
2060	2080	4.068450E-01	1.544472E-02
2080	2085	6.533000E-01	1.573729E-02
2085	2090	7.828400E-01	1.184640E-02
2090	2095	2.032954E+00	2.124131E-02
2095	2100	1.259640E+00	1.157379E-02
2080	2100	1.182103E+00	1.464140E-02
2100	2105	1.408760E+00	1.224353E-02
2105	2110	1.523820E+00	1.267373E-02
2110	2115	1.627780E+00	1.559609E-02
2115	2120	3.223820E+00	2.522987E-02
2100	2120	1.947445E+00	1.641082E-02
2120	2125	1.517040E+00	1.733434E-02
2125	2130	1.317840E+00	1.495077E-02
2130	2135	1.036120E+00	1.869465E-02
2135	2140	1.142320E+00	3.011861E-02
2120	2140	1.265830E+00	1.963149E-02
2140	2145	2.538000E-02	1.977818E-02
2145	2150	4.038400E-01	1.755928E-02
2150	2155	1.918710E+00	3.037914E-02
2155	2160	1.429034E+00	1.455675E-02
2140	2160	9.442410E-01	1.628659E-02
2160	2165	1.655178E+00	1.306170E-02
2165	2170	3.712007E+00	2.470612E-02
2170	2175	1.910730E+00	1.204678E-02
2175	2180	3.610112E+00	2.197084E-02
2160	2180	2.722005E+00	1.791142E-02
2180	2185	1.606644E+00	1.051575E-02
2185	2190	1.434266E+00	1.052852E-02
2190	2195	2.308301E+00	1.999320E-02
2195	2200	1.593636E+00	1.913159E-02
2180	2200	1.735712E+00	1.489384E-02
2200	2205	5.660080E-01	9.260309E-03
2205	2210	7.720000E-01	1.877483E-02
2210	2215	2.482000E-01	6.600000E-03
2215	2220	3.090000E-01	1.649928E-02
2200	2220	4.742020E-01	1.271076E-02
2220	2225	1.570000E-01	1.557894E-02
2225	2230	4.160000E-02	7.800000E-03
2230	2235	4.508000E-02	1.434450E-02
2235	2240	1.876000E-02	1.416033E-02
2220	2240	6.436000E-02	1.153738E-02
2240	2245	6.780000E-03	1.377639E-02
2245	2250	2.340000E-03	1.373985E-02
2250	2255	7.500000E-04	1.370900E-02
2255	2260	2.200000E-04	1.369725E-02
2240	2260	2.522500E-03	1.018744E-02

Table A-2 - Band Model Parameters for CO in 5 and 20 cm^{-1} intervals.

Δω (1/atm)		k(300K) (1/cm-atm)	a_o(300K) (1/atm)
4180	4185	2.653846E-03	1.000000E-02
4185	4190	3.771603E-03	1.000000E-02
4190	4195	4.659892E-03	1.000000E-02
4195	4200	1.366755E-02	1.994595E-02
4180	4200	6.290724E-03	1.215339E-02
4200	4205	9.075409E-03	1.000000E-02
4205	4210	1.065622E-02	1.000000E-02
4210	4215	1.219869E-02	1.000000E-02
4215	4220	1.355679E-02	1.000000E-02
4200	4220	1.138103E-02	9.944061E-03
4220	4225	1.472946E-02	1.000000E-02
4225	4230	1.567173E-02	1.000000E-02
4230	4235	1.570526E-02	1.000000E-02
4235	4240	1.533161E-02	1.000000E-02
4220	4240	1.530952E-02	9.998602E-03
4240	4245	2.682928E-02	1.997892E-02
4245	4250	1.013602E-02	1.000000E-02
4250	4255	7.149660E-03	1.000000E-02
4255	4260	3.712673E-03	1.000000E-02
4240	4260	1.195746E-02	1.192743E-02
4260	4265	3.788554E-03	1.000000E-02
4265	4270	7.445104E-03	1.000000E-02
4270	4275	2.437383E-02	1.993241E-02
4275	4280	1.580567E-02	1.000000E-02
4260	4280	1.285329E-02	1.186508E-02
4280	4285	1.731003E-02	1.000000E-02
4285	4290	3.626301E-02	1.999997E-02
4290	4295	3.431369E-02	1.999553E-02
4295	4300	1.523733E-02	1.000000E-02
4280	4300	2.576602E-02	1.438656E-02
4300	4305	2.536465E-02	1.997541E-02
4305	4310	1.830267E-02	1.935587E-02
4310	4315	1.203134E-02	1.993230E-02
4315	4320	7.243012E-03	1.990509E-02
4300	4320	1.574042E-02	1.897163E-02

Table A-3 –Band Model Parameters for CO_2 in 5 and 20 cm^{-1} intervals.

Δω (1/cm)		k(300K) (1/cm-atm)	a_o(300K) (1/atm)
880	865	4.916954E-07	2.795578E-02
885	890	2.036870E-06	6.927074E-02
890	895	4.070596E-06	6.947013E-02
895	900	7.114151E-06	6.964470E-02
880	900	3.438256E-06	5.452399E-02
900	905	1.215480E-05	9.193979E-02
905	910	2.117769E-05	1.092344E-01
910	915	3.204195E-05	1.250205E-01
915	920	3.514707E-05	1.092283E-01
900	920	2.513038E-05	1.055519E-01
920	925	5.788375E-05	1.046969E-01
925	930	6.144504E-05	8.961229E-02
930	935	1.606785E-04	8.733744E-02
935	940	1.690879E-04	7.822484E-02
920	940	1.122738E-04	6.273724E-02
940	945	3.063910E-04	8.977904E-02
945	950	3.319027E-04	7.671395E-02
950	955	2.751116E-04	7.232278E-02
955	960	1.285266E-04	5.981962E-02
940	960	2.604839E-04	7.423433E-02
960	965	9.771268E-05	3.852677E-02
965	970	2.600596E-04	4.181423E-02
970	975	4.491714E-04	5.599443E-02
975	980	3.811069E-04	5.585439E-02
960	980	2.970126E-04	4.650849E-02

Δω (1/cm)		k(300K) (1/cm-atm)	a_o(300K) (1/atm)
980	985	2.270013E-04	5.548925E-02
985	990	1.126177E-04	6.786514E-02
990	995	2.681795E-05	6.631503E-02
995	1000	3.955754E-06	5.324597E-02
980	1000	9.259816E-05	4.435178E-02
1000	1005	2.238974E-06	2.765829E-02
1005	1010	1.001117E-05	4.089040E-02
1010	1015	1.693375E-05	2.776913E-02
1015	1020	3.395262E-05	2.780649E-02
1000	1020	1.578417E-05	2.566877E-02
1020	1025	6.485136E-05	3.520349E-02
1025	1030	1.978487E-04	5.944969E-02
1030	1035	2.356395E-04	4.320074E-02
1035	1040	5.639100E-04	6.167159E-02
1020	1040	2.655624E-04	4.631549E-02
1040	1045	5.444539E-04	5.074378E-02
1045	1050	9.945830E-04	6.623037E-02
1050	1055	1.062078E-03	7.578136E-02
1055	1060	8.046885E-04	7.553358E-02
1040	1060	8.514533E-04	6.668147E-02
1060	1065	3.233264E-04	1.008995E-01
1065	1070	5.555637E-04	8.384374E-02
1070	1075	1.337755E-03	6.824586E-02
1075	1050	1.470025E-03	9.096856E-02
1060	1080	9.216673E-04	8.290743E-02
1080	1085	1.089671E-03	1.045956E-01
1085	1090	6.139384E-04	1.270518E-01
1090	1095	3.068994E-04	1.773993E-01
1095	1100	6.504955E-05	2.032419E-01
1080	1100	5.189395E-04	1.125364E-01

Table A.3 - Band Model Parameters for CO_2 in 5 and 20 cm^{-1} intervals.

Δω (1/cm)		k(300K) (1/cm-atm)	a_o(300K) (1/atm)
1880	1885	0.	1.000000E+00
1885	1890	0.	1.000000E+00
1890	1895	1.994017E-05	5.354093E-02
1895	1900	4.599103E-05	4.136924E-02
1880	1900	1.645790E-05	2.213003E-02
1900	1905	1.047561E-04	4.156243E-02
1905	1910	3.012379E-04	5.519111E-02
1910	1915	[illegible]833997E-04	4.190158E-02
1915	1920	4.[illegible]23317E-04	4.199320E-02
1900	1920	3.204314E-04	4.229724E-02
1920	1925	6.385579E-04	5.591446E-02
1925	1930	7.615096E-04	4.197388E-02
1930	1935	5.260963E-03	3.555155E-01
1935	1940	4.233003E-04	4.170360E-02
1920	1940	1.646153E-03	1.220765E-01
1940	1945	6.006503E-04	4.198117E-02
1945	1950	6.032269E-04	4.199995E-02
1950	1955	4.921961E-04	4.192251E-02
1955	1960	3.295213E-04	4.181175E-02
1940	1960	5.079012E-04	4.136211E-02
1960	1965	1.8[illegible]2184E-04	4.155766E-02
1965	1970	8.9921[illegible]8E-05	4.149460E-02
1970	1975	3.726787E-05	4.129512E-02
1975	1980	1.334332E-05	4.107116E-02
1960	1980	8.171780E-05	3.432409E-02
1980	1985	0.	1.000000E+00
1985	1990	0.	1.000000E+00
1990	1995	0.	1.000000E+00
1995	2000	0.	1.000000E+00
1980	2000	0.	1.000000E+00
2000	2005	0.	1.000000E+00
2005	2010	0.	1.000000E+00
2010	2015	0.	1.000000E+00
2015	2020	0.	1.000000E+00
2000	2020	0.	1.000000E+00
2020	2025	2.6099[illegible]2E-06	1.400000E-02
2025	2030	2.11[illegible]270E-05	4.064729E-02
2030	2035	7.5071[illegible]E-05	4.091006E-02
2035	2040	3.764[illegible]36E-04	5.402410E-02
2020	2040	1.108244E-04	2.865268E-02

Δω (1/cm)		k(300K) (1/cm-atm)	a_o(300K) (1/atm)
2040	2045	8.202241E-04	4.143651E-02
2045	2050	1.778158E-03	4.162105E-02
2050	2055	3.314957E-03	5.397460E-02
2055	2060	7.321276E-03	7.740739E-02
2040	2060	3.308654E-03	5.010615E-02
2060	2065	7.052240E-03	6.567171E-02
2065	2070	6.536904E-03	8.363799E-02
2070	2075	4.566186E-03	1.081142E-01
2075	2080	7.140384E-02	4.039341E-01
2060	2080	2.246479E-02	1.569067E-01
2080	2085	7.010080E-03	1.032869E-01
2085	2090	8.670567E-03	7.734583E-02
2090	2095	2.465065E-02	5.874627E-01
2095	2100	7.4221[illegible]5E-03	1.378407E-01
2060	2100	1.193637E-02	2.202866E-01
2100	2105	5.664181E-03	1.291474E-01
2105	2110	4.376787E-03	1.614844E-01
2110	2115	2.739915E-03	1.726478E-01
2115	2120	1.666631E-03	1.651683E-01
2100	2120	3.629878E-03	1.466217E-01
2120	2125	9.600525E-04	1.621330E-01
2125	2130	3.281512E-03	4.577591E-01
2130	2135	2.156575E-04	1.368414E-01
2135	2140	2.625482E-04	8.928045E-02
2120	2140	1.184942E-03	2.007212E-01
2140	2145	3.106706E-04	5.128562E-02
2145	2150	2.832316E-04	4.197045E-02
2150	2155	2.637703E-04	5.565720E-02
2155	2160	1.080617E-04	4.170155E-02
2140	2160	2.414836E-04	4.643890E-02
2160	2165	5.380447E-05	4.153185E-02
2165	2170	2.301537E-05	4.133536E-02
2170	2175	6.568061E-06	2.779405E-02
2175	2180	0.	1.000000E+00
2160	2180	2.087197E-05	2.516896E-02

Table A.3 - Band Model Parameters for CO_2 in 5 and 20 cm^{-1} intervals.

Δω (1/cm)		k(300K) (1/cm-atm)	a_o(300K) (1/atm)
3460	3465	0.	1.000000E+00
3465	3470	0.	1.000000E+00
3470	3475	5.613639E-05	4.082230E-02
3475	3480	9.786486E-05	2.775244E-02
3460	3480	3.850021E-05	1.622906E-02
3480	3485	2.015276E-04	2.779274E-02
3485	3490	6.906153E-04	4.136595E-02
3490	3495	1.580954E-03	4.155864E-02
3495	3500	1.856743E-03	2.792292E-02
3480	3500	1.082470E-03	3.059104E-02
3500	3505	4.427554E-03	4.181855E-02
3505	3510	6.537214E-03	4.192975E-02
3510	3515	7.927370E-03	4.354302E-02
3515	3520	7.585487E-03	5.737431E-02
3500	3520	6.619400E-03	4.574240E-02
3520	3525	4.657240E-03	6.280731E-02
3525	3530	1.378732E-03	7.611276E-02
3530	3535	7.844144E-03	1.127590E-01
3535	3540	1.183302E-02	1.086935E-01
3520	3540	6.477039E-03	8.400642E-02
3540	3545	1.865778E-02	1.348652E-01
3545	3550	2.271128E-02	1.416281E-01
3550	3555	2.858052E-02	1.328899E-01
3555	3560	3.939894E-02	1.103776E-01
3540	3560	2.721213E-02	1.281068E-01

Table A.3—Band Model Parameters for CO_2 in 5 and 20 cm^{-1} intervals.

Δω (1/cm)		k(300K) (1/cm-atm)	a_o(300K) (1/atm)
4740	4745	4.215487E-05	5.499383E-02
4745	4750	0.	1.000000E+00
4750	4755	3.290388E-05	4.159521E-02
4755	4760	4.563611E-05	4.137265E-02
4740	4760	3.119621E-05	3.429219E-02
4760	4765	5.143166E-05	4.139725E-02
4765	4770	6.766454E-05	8.229514E-02
4770	4775	6.152357E-05	8.338291E-02
4775	4780	1.199370E-04	8.330800E-02
4760	4780	7.512500E-05	7.124722E-02
4780	4785	2.073185E-04	8.362373E-02
4785	4790	2.460264E-04	6.991204E-02
4790	4795	3.541352E-04	6.798161E-02
4795	4800	3.506161E-04	9.331729E-02
4780	4800	2.696476E-04	8.196226E-02
4800	4805	2.542661E-04	1.085886E-01
4805	4810	2.667664E-04	9.806101E-02
4810	4815	4.400544E-04	1.036588E-01
4815	4820	1.103695E-03	1.251322E-01
4800	4820	5.011961E-04	9.951333E-02
4820	4825	1.896671E-03	1.194971E-01
4825	4830	1.811132E-03	7.830026E-02
4830	4835	3.448546E-03	7.631305E-02
4835	4840	4.297422E-03	5.670240E-02
4820	4840	2.851953E-03	7.543347E-02
4840	4845	4.376088E-03	4.199079E-02
4845	4850	3.252666E-03	4.694369E-02
4850	4855	1.171293E-03	5.684686E-02
4855	4860	2.296902E-03	5.171770E-02
4840	4860	2.763222E-03	4.542198E-02
4860	4865	5.893060E-03	7.045053E-02
4865	4870	4.807793E-03	5.265265E-02
4870	4875	5.039944E-03	7.499539E-02
4875	4880	2.859686E-03	7.944571E-02
4860	4880	4.650126E-03	6.737352E-02
4880	4885	1.218336E-03	2.270743E-02
4885	4890	4.219904E-04	9.582105E-02
4890	4895	2.061603E-04	8.647457E-02
4895	4900	3.071357E-04	5.595220E-02
4880	4900	5.383033E-04	7.119148E-02
4900	4905	2.388299E-04	5.591552E-02
4905	4910	1.936167E-04	6.473066E-02
4910	4915	1.390799E-04	1.074626E-01
4915	4920	1.289306E-04	8.837469E-02
4900	4920	1.874143E-04	7.293158E-02
4920	4925	2.563509E-04	7.428924E-02
4925	4930	9.304356E-04	1.061919E-01
4930	4935	1.314668E-03	6.877421E-02
4935	4940	2.590189E-03	8.983731E-02
4920	4940	1.273161E-03	7.493581E-02
4940	4945	4.913484E-03	7.679157E-02
4945	4950	9.146948E-03	8.392789E-02
4950	4955	9.746588E-03	7.371415E-02
4955	4960	1.795418E-02	7.744098E-02
4940	4960	1.071530E-02	7.295232E-02
4960	4965	2.065594E-02	6.305109E-02
4965	4970	1.961626E-02	7.495088E-02
4970	4975	1.343813E-02	9.861278E-02
4975	4980	4.245385E-03	1.300022E-01
4960	4980	[illegible].448893E-02	7.783870E-02
4980	4985	1.781074E-02	1.165578E-01
4985	4990	2.925170E-02	9.648767E-02
4990	4995	2.670216E-02	7.991863E-02
4995	5000	1.709341E-02	7.203785E-02
4980	5000	2.271450E-02	8.965811E-02
5000	5005	9.186800E-03	8.076848E-02
5005	5010	2.697037E-03	1.119716E-01
5010	5015	2.390645E-04	1.222938E-01
5015	5020	7.583970E-06	1.400000E-02
5000	5020	3.032357E-03	5.221165E-02
5040	5045	2.352361E-05	2.768692E-02
5045	5050	5.333970E-05	2.773144E-02
5050	5055	2.079513E-04	4.114917E-02
5055	5060	3.111711E-04	2.783035E-02
5040	5060	1.489964E-04	2.612152E-02
5060	5065	9.763470E-04	4.149806E-02
5065	5070	1.195317E-03	2.791046E-02
5070	5075	2.987375E-03	4.177342E-02
5075	5080	4.681232E-03	4.189716E-02
5060	5080	2.460193E-03	3.537896E-02
5080	5085	6.113701E-03	4.952395E-02
5085	5090	6.367227E-03	5.473697E-02
5090	5095	4.789566E-03	6.144149E-02
5095	5100	1.607208E-03	7.482264E-02
5080	5100	4.719426E-03	5.456615E-02
5100	5105	3.782132E-03	8.760565E-02
5105	5110	6.389617E-03	7.063932E-02
5110	5115	9.495893E-03	8.817157E-02
5115	5120	7.265206E-03	8.635910E-02
5100	5120	6.733212E-03	8.103259E-02
5120	5125	3.909078E-03	7.750350E-02
5125	5130	1.907729E-03	1.177486E-01
5130	5135	1.145349E-03	1.635005E-01
5135	5140	7.000944E-04	1.387208E-01
5120	5140	1.915563E-03	1.020752E-01
5140	5145	5.584206E-04	1.250768E-01
5145	5150	2.403249E-04	1.103607E-01
5150	5155	8.405146E-05	9.614070E-02
5155	5160	0.	1.000000E+00
5140	5160	2.207017E-04	7.570354E-02

Table A.4 - Band Model Parameters for SO_2 in 5 and 20 cm^{-1} intervals.

Δω (1/cm)		k(300K) (1/cm-atm)	a_o(300K) (1/atm)
1040	1045	2.151834E-02	9.119830E-02
1045	1050	1.310995E-02	3.453801E-02
1050	1055	7.465634E-03	5.244718E-02
1055	1060	2.410903E-02	1.125416E-01
1040	1060	1.655079E-02	7.136461E-02
1060	1065	3.806459E-02	2.439590E-01
1065	1070	3.363220E-02	6.994772E-01
1070	1075	3.902193E-02	1.126357E+00
1075	1080	7.905252E-02	1.479112E+00
1060	1080	4.744231E-02	8.459449E-01
1080	1085	1.397075E-01	1.705297E+00
1085	1090	1.648241E-01	1.434754E+00
1090	1095	2.355624E-01	1.282353E+00
1095	1100	3.356223E-01	2.458339E+00
1080	1100	2.189306E-01	1.685906E+00
1100	1105	4.099271E-01	2.127417E+00
1105	1110	5.361855E-01	1.968320E+00
1110	1115	6.420741E-01	1.935790E+00
1115	1120	7.026137E-01	1.877171E+00
1100	1120	5.727001E-01	1.947601E+00
1120	1125	7.426081E-01	2.042507E+00
1125	1130	9.183290E-01	2.239452E+00
1130	1135	9.347560E-01	2.317352E+00
1135	1140	9.934214E-01	2.160237E+00
1120	1140	8.985780E-01	2.186252E+00
1140	1145	8.978266E-01	2.229101E+00
1145	1150	8.170546E-01	2.331354E+00
1150	1155	6.969964E-01	2.179098E+00
1155	1160	1.084347E+00	2.445188E+00
1140	1160	8.740562E-01	2.284538E+00

Δω (1/cm)		k(300K) (1/cm-atm)	a_o(300K) (1/atm)
1160	1165	1.076796E+00	2.364475E+00
1165	1170	1.086842E+00	2.222371E+00
1170	1175	1.074947E+00	2.070205E+00
1175	1180	8.264351E-01	1.749699E+00
1160	1180	1.016254E+00	2.100414E+00
1180	1185	9.776472E-01	1.690513E+00
1185	1190	8.177241E-01	1.798747E+00
1190	1195	6.950115E-01	1.712538E+00
1195	1200	6.276525E-01	1.789129E+00
1180	1200	7.795089E-01	1.788506E+00
1200	1205	5.206751E-01	1.769689E+00
1205	1210	3.735280E-01	1.487231E+00
1210	1215	3.370692E-01	1.405702E+00
1215	1220	2.239230E-01	1.168621E+00
1200	1220	3.637988E-01	1.449949E+00
1220	1225	1.982987E-01	1.156111E+00
1225	1230	1.541947E-01	9.993011E-01
1230	1235	1.097415E-01	9.241392E-01
1235	1240	1.203697E-01	6.145769E-01
1220	1240	1.456512E-01	9.169307E-01
1240	1245	6.178575E-02	7.193671E-01
1245	1250	5.605424E-02	6.139658E-01
1250	1255	5.657581E-02	4.643494E-01
1255	1260	5.202813E-02	3.233667E-01
1240	1260	5.661098E-02	5.227796E-01

Table A.4 - Band Model Parameters for SO_2 in 5 and 20 cm^{-1} intervals.

Δω (1/cm)		k(300K) (1/cm-atm)	a_o(300K) (1/atm)
2340	2345	0.	1.000000E+00
2345	2350	0.	1.000000E+00
2350	2355	3.096098E-04	3.052613E-02
2355	2360	7.292620E-05	1.600000E-02
2340	2360	9.568451E-05	1.127927E-02
2360	2365	1.231665E-04	1.600000E-02
2365	2370	1.495593E-03	4.219651E-02
2370	2375	1.796394E-03	1.600000E-02
2375	2380	3.642956E-04	3.065158E-02
2360	2380	9.406873E-04	2.159481E-02
2380	2385	7.825996E-04	3.191703E-02
2385	2390	0.	1.000000E+00
2390	2395	3.416238E-03	4.183161E-02
2395	2400	2.193621E-03	4.131373E-02
2380	2400	1.598115E-03	2.742373E-02
2400	2405	0.	1.000000E+00
2405	2410	1.628601E-03	3.199090E-02
2410	2415	4.338597E-03	4.325148E-02
2415	2420	4.362732E-03	5.248128E-02
2400	2420	2.582558E-03	3.144897E-02
2420	2425	1.832864E-03	2.191223E-02
2425	2430	7.639305E-03	6.108569E-02
2430	2435	0.	1.000000E+00
2435	2440	1.141301E-02	6.639772E-02
2420	2440	5.221451E-03	3.756566E-02
2440	2445	6.407334E-03	1.099567E-01
2445	2450	1.433933E-02	3.184393E-01
2450	2455	1.530764E-02	6.632604E-01
2455	2460	3.154579E-02	6.391264E-01
2440	2460	1.690082E-02	4.725606E-01
2460	2465	5.270432E-02	1.088783E+00
2465	2470	9.827346E-02	1.222093E+00
2470	2475	1.479137E-01	1.344552E+00
2475	2480	2.452213E-01	1.505669E+00
2460	2480	1.360262E-01	1.235315E+00
2480	2485	3.003053E-01	1.530417E+00
2485	2490	3.807703E-01	1.656309E+00
2490	2495	3.295310E-01	1.699432E+00
2495	2500	7.558317E-01	6.289136E+00
2480	2500	4.414846E-01	2.740953E+00

Δω (1/cm)		k(300K) (1/cm-atm)	a_o(300K) (1/atm)
2500	2505	2.457464E-01	1.393854E+00
2505	2510	5.027689E-01	1.905605E+00
2510	2515	4.936582E-01	2.127517E+00
2515	2520	3.843430E-01	2.406667E+00
2500	2520	4.066796E-01	1.555140E+00
2520	2525	1.775262E-01	2.783076E+00
2525	2530	6.152538E-02	2.294704E+00
2530	2535	3.064289E-02	2.142747E-01
2535	2540	3.050013E-02	9.539228E-02
2520	2540	7.504865E-02	1.226586E+00
2540	2545	2.265153E-02	7.763293E-02
2545	2550	1.572009E-02	5.092004E-02
2550	2555	1.078335E-02	6.233046E-02
2555	2560	2.264143E-02	6.645336E-02
2540	2560	1.794910E-02	6.340592E-02
2560	2565	5.173353E-03	3.557397E-02
2565	2570	1.518827E-02	5.645436E-02
2570	2575	1.175601E-02	6.036945E-02
2575	2580	3.016740E-03	3.181590E-02
2560	2580	8.783592E-03	4.467863E-02
2580	2585	1.269780E-02	5.136001E-02
2585	2590	1.084802E-03	1.600000E-02
2590	2595	9.041922E-03	5.680339E-02
2595	2600	5.056240E-03	3.454066E-02
2580	2600	6.970191E-03	3.657177E-02
2600	2605	6.558353E-03	2.649384E-02
2605	2610	4.849186E-04	1.600000E-02
2610	2615	3.612322E-04	1.600000E-02
2615	2620	1.110743E-02	7.308795E-02
2600	2620	4.627962E-03	2.965926E-02
2620	2625	5.530236E-03	2.187031E-02
2625	2630	0.	1.000000E+00
2630	2635	6.234706E-04	2.929362E-02
2635	2640	2.102527E-04	3.196180E-02
2620	2640	1.590990E-03	1.253591E-02

Table A.5 - Band Model Parameters for NO_2 in 5 and 20 cm^{-1} intervals.

Δω (1/cm)		k(300K) (1/cm-atm)	a_o(300K) (1/atm)
1200	1205	8.620960E-02	8.213305E-01
1205	1210	7.390421E-02	3.564795E-01
1210	1215	7.768848E-02	5.869614E-01
1215	1220	1.468360E-01	6.437247E-01
1200	1220	9.615958E-02	5.863410E-01
1220	1225	1.094817E-01	4.274610E-01
1225	1230	2.425999E-01	8.556429E-01
1230	1235	1.404589E-01	3.495396E-01
1235	1240	1.602911E-01	5.551997E-01
1220	1240	1.632077E-01	5.413509E-01
1240	1245	3.377547E-01	6.795134E-01
1245	1250	2.330276E-01	5.477319E-01
1250	1255	3.240567E-01	7.355857E-01
1255	1260	4.442397E-01	6.362344E-01
1240	1260	3.349975E-01	6.423071E-01
1260	1265	2.815585E-01	4.873144E-01
1265	1270	4.325047E-01	6.104942E-01
1270	1275	6.110820E-01	7.596672E-01
1275	1280	3.427564E-01	6.032684E-01
1260	1280	4.169504E-01	6.117964E-01
1280	1285	8.934598E-01	8.255373E-01
1285	1290	5.022126E-01	7.543224E-01
1290	1295	4.295554E-01	5.543352E-01
1295	1300	7.534405E-01	6.786733E-01
1280	1300	6.446671E-01	6.950697E-01
1300	1305	6.220042E-01	7.012991E-01
1305	1310	3.590968E-01	4.193054E-01
1310	1315	7.408249E-01	5.643225E-01
1315	1320	7.711361E-01	5.509277E-01
1300	1320	6.832655E-01	5.565787E-01

Δω (1/cm)		k(300K) (1/cm-atm)	a_o(300K) (1/atm)
1320	1325	3.397734E-01	5.511240E-01
1325	1330	3.591304E-01	4.012202E-01
1330	1335	8.474156E-01	5.693519E-01
1335	1340	5.375714E-01	6.037167E-01
1320	1340	5.209727E-01	5.621117E-01
1340	1345	7.290039E-01	5.349202E-01
1345	1350	9.657043E-01	7.623634E-01
1350	1355	3.839070E-01	6.793213E-01
1355	1360	5.831324E-01	5.038748E-01
1340	1360	6.654369E-01	6.039723E-01
1360	1365	1.042469E+00	7.937797E-01
1365	1370	4.043430E-01	5.226476E-01
1370	1375	4.652566E-01	4.350597E-01
1375	1380	9.186952E-01	7.206220E-01
1360	1360	7.077412E-01	6.122278E-01
1380	1385	3.098967E-01	4.260096E-01
1385	1390	4.995256E-01	6.771143E-01
1390	1395	6.598895E-01	6.543480E-01
1395	1400	2.807659E-01	3.843510E-01
1380	1400	4.448702E-01	5.327440E-01
1400	1405	3.539553E-01	5.926529E-01
1405	1410	4.973029E-01	5.739233E-01
1410	1415	2.200354E-01	3.656770E-01
1415	1420	3.034190E-01	6.329979E-01
1400	1420	3.436781E-01	5.358796E-01
1420	1425	3.517448E-01	6.287658E-01
1425	1430	1.453927E-01	3.690546E-01
1430	1435	2.269250E-01	6.325053E-01
1435	1440	2.127018E-01	5.563314E-01
1420	1440	2.341911E-01	5.396117E-01

Table A.5 - Band Model Parameters for NO_2 in 5 and 20 cm^{-1} intervals.

Δω (1/cm)		k(300K) (1/cm-atm)	a_o(300K) (1/atm)
2800	2805	2.726722E-04	1.600000E-02
2805	2810	2.439914E-03	2.810323E-02
2810	2615	1.054555E-03	4.417539E-02
2815	2820	1.336027E-03	3.040040E-02
2800	2820	1.275792E-03	2.721058E-02
2820	2825	4.256886E-03	3.105556E-02
2825	2630	6.420719E-03	5.167140E-02
2830	2535	3.742421E-03	2.950333E-02
2835	2640	1.120163E-02	6.543564E-02
2820	2840	6.505415E-03	4.424836E-02
2840	2845	2.004062E-02	2.201452E-01
2845	2850	3.340169E-02	2.821185E-01
2850	2855	5.005520E-02	3.833662E-01
2855	2860	7.751526E-02	4.390413E-01
2840	2860	4.525319E-02	3.263908E-01
2860	2865	1.374496E-01	5.918720E-01
2865	2870	2.484359E-01	6.765592E-01
2870	2875	3.721437E-01	6.231591E-01
2875	2880	5.671012E-01	6.143329E-01
2860	2880	3.313026E-01	5.890527E-01
2880	2685	8.432834E-01	7.920779E-01
2685	2690	1.164414E+00	8.130177E-01
2090	2695	1.080169E+00	8.576145E-01
2895	2900	9.429581E-01	1.090652E+00
2680	2900	1.007706E+00	8.800453E-01
2900	2905	7.906470E-01	1.646614E+00
2905	2910	4.554846E-01	1.129263E+00
2910	2915	1.532684E+00	1.164514E+00
2915	2920	1.307525E+00	1.158148E+00
2900	2920	1.171585E+00	1.169511E+00
2920	2925	1.201004E+00	9.311807E-01
2925	2930	5.709847E-01	6.806681E-01
2930	2935	2.161665E-01	3.347667E-01
2935	2940	1.122653E-01	1.239224E-01
2920	2940	5.251100E-01	5.090197E-01
2940	2945	7.873895E-02	1.152501E-01
2945	2950	4.067645E-02	1.030101E-01
2950	2955	1.623097E-02	6.627097E-02
2955	2960	1.347846E-02	6.102130E-02
2940	2960	3.726871E-02	8.221437E-02
2960	2965	1.169716E-02	7.224161E-02
2965	2970	7.222416E-03	6.113790E-02
2970	2975	6.672055E-04	1.600000E-02
2975	2960	4.106459E-03	4.523010E-02
2960	2980	5.923315E-03	4.734757E-02

Table A.6 - Band Model Parameters for NO in 5 and 20 cm^{-1} intervals.

Δω (1/cm)		k(300K) (1/cm-atm)	a_o(300K) (1/atm)
1760	1765	4.598413E-03	4.905174E-02
1765	1770	6.285940E-03	3.970133E-02
1770	1775	9.556322E-03	3.958669E-02
1775	1780	1.430782E-02	3.967091E-02
1760	1780	8.689623E-03	3.951958E-02
1780	1785	3.909623E-02	5.855177E-02
1785	1790	3.603694E-02	3.870926E-02
1790	1795	7.739046E-02	5.867116E-02
1795	1800	8.211852E-02	3.957017E-02
1780	1800	5.915054E-02	4.637629E-02
1800	1805	1.989554E-01	5.879227E-02
1805	1810	1.721714E-01	3.830976E-02
1810	1815	3.118416E-01	5.867981E-02
1815	1820	2.974341E-01	3.941231E-02
1800	1820	2.451006E-01	4.790636E-02
1820	1825	6.357906E-01	5.833366E-02
1825	1830	4.827254E-01	3.885468E-02
1830	1835	7.665596E-01	5.854457E-02
1835	1840	1.112655E+00	5.674814E-02
1820	1840	7.494400E-01	5.309011E-02
1840	1845	7.443375E-01	3.881786E-02
1845	1850	1.034112E+00	5.819555E-02
1850	1855	1.301225E+00	5.839557E-02
1855	1860	7.215630E-01	3.857706E-02
1840	1860	9.503094E-01	4.839074E-02
1860	1865	1.163906E+00	7.689005E-02
1865	1870	3.721359E-01	3.932427E-02
1870	1875	2.840768E-01	2.502282E-01
1875	1880	4.046734E-01	1.874279E-01
1860	1880	5.561981E-01	1.037701E-01

Δω (1/cm)		k(300K) (1/cm-atm)	a_o(300K) (1/atm)
1880	1885	5.608018E-01	5.695423E-02
1885	1890	5.615086E-01	3.806664E-02
1890	1895	1.503917E+00	7.691200E-02
1895	1900	8.757434E-01	3.869164E-02
1880	1900	8.754928E-01	5.146852E-02
1900	1905	1.833549E+00	7.756226E-02
1905	1910	1.751168E+00	7.767579E-02
1910	1915	1.264344E+00	5.873563E-02
1915	1920	8.692237E-01	5.858478E-02
1900	1920	1.429571E+00	6.768073E-02
1920	1925	1.006325E+00	7.761140E-02
1925	1930	6.938262E-01	7.750816E-02
1930	1935	3.780433E-01	5.883830E-02
1935	1940	2.838681E-01	7.870018E-02
1920	1940	5.917657E-01	6.951515E-02
1940	1945	1.609339E-01	7.869529E-02
1945	1950	8.343249E-02	7.866499E-02
1950	1955	4.030341E-02	7.861267E-02
1955	1960	1.816083E-02	7.854091E-02
1940	1960	7.570767E-02	6.828710E-02
1960	1965	8.420676E-03	9.600770E-02
1965	1970	1.740661E-03	3.941752E-02
1970	1975	0.	1.000000E+00
1975	1980	0.	1.000000E+00
1960	1980	2.540334E-03	3.316746E-02

Table A. 7- Band Model Parameters for N_2O in 5 and 20 cm^{-1} intervals.

Δω (1/cm)		k(300K) (1/cm-atm)	a_o(300K) (1/atm)
1120	1125	0.	1.000000E+00
1125	1130	5.185552E-03	5.543656E-02
1130	1135	1.335698E-02	8.250378E-02
1135	1140	5.431262E-02	9.642334E-02
1120	1140	1.947414E-02	5.291533E-02
1140	1145	9.554190E-02	8.342920E-02
1145	1150	1.548308E-01	8.373795E-02
1150	1155	2.055062E-01	8.394600E-02
1155	1160	2.459817E-01	9.794139E-02
1140	1160	1.754651E-01	8.541930E-02
1160	1165	1.385662E-01	6.297455E-02
1165	1170	3.560152E-02	6.795687E-02
1170	1175	1.243493E-01	8.225949E-02
1175	1180	1.763563E-01	6.991068E-02
1160	1180	1.187189E-01	7.139762E-02
1180	1185	2.375555E-01	8.339767E-02
1185	1190	2.069651E-01	8.388702E-02
1190	1195	1.452267E-01	8.364597E-02
1195	1200	7.392597E-02	6.962416E-02
1180	1200	1.659183E-01	7.797832E-02
1200	1205	4.706623E-02	8.239235E-02
1205	1210	1.789772E-02	6.917082E-02
1210	1215	7.839566E-03	6.892190E-02
1215	1220	0.	1.000000E+00
1200	1220	1.870068E-02	5.021368E-02
1220	1225	2.479049E-03	2.789506E-02
1225	1230	1.486067E-02	6.829324E-02
1230	1235	4.429427E-02	6.851240E-02
1235	1240	1.185583E-01	6.879855E-02
1220	1240	4.505031E-02	4.777157E-02
1240	1245	2.646274E-01	6.936054E-02
1245	1250	6.114521E-01	6.929710E-02
1250	1255	1.171644E+00	6.950676E-02
1255	1260	1.593344E+00	6.968750E-02
1240	1260	1.015267E+00	6.206919E-02
1260	1265	3.707354E+00	8.373657E-02
1265	1270	4.051840E+00	6.996177E-02
1270	1275	5.200834E+00	8.339303E-02
1275	1280	4.073151E+00	8.357540E-02
1260	1260	4.258297E+00	7.995374E-02
1280	1285	1.384579E+00	6.587179E-02
1285	1290	1.956350E+00	7.655794E-02
1290	1295	4.613252E+00	8.353612E-02
1295	1300	5.673476E+00	8.399609E-02
1280	1300	3.406915E+00	7.379887E-02
1300	1305	5.872387E+00	9.784191E-02
1305	1310	3.890340E+00	9.739298E-02
1310	1315	1.999931E+00	9.675432E-02
1315	1320	8.152551E-01	9.596264E-02
1300	1320	3.144479E+00	8.703149E-02
1320	1325	2.837641E-01	1.075150E-01
1325	1330	6.044176E-02	1.057540E-01
1330	1335	8.106079E-03	6.802398E-02
1335	1340	0.	1.000000E+00
1320	1340	8.808299E-02	5.487961E-02

Table A.7 - Band Model Parameters for N_2O in 5 and 20 cm^{-1} intervals.

Δω		k(300K)	a_o(300K)
(1/cm)		(1/cm-atm)	(1/atm)
2140	2145	1.370115E-02	3.903639E-01
2145	2150	3.147045E-02	3.855501E-01
2150	2155	7.582610E-02	4.062745E-01
2155	2160	1.673102E-01	3.982772E-01
2140	2160	7.220197E-02	3.298636E-01
2160	2165	3.434221E-01	3.820376E-01
2165	2170	6.307887E-01	4.172246E-01
2170	2175	1.466835E+00	3.498711E-01
2175	2180	2.829857E+00	3.468126E-01
2160	2180	1.382726E+00	3.243840E-01
2180	2185	5.693340E+00	3.260305E-01
2185	2190	8.001471E+00	2.683256E-01
2190	2195	1.401624E+01	2.347549E-01
2195	2200	2.092456E+01	2.335691E-01
2180	2200	1.215890E+01	2.414566E-01
2200	2205	2.610236E+01	1.961026E-01
2205	2210	2.353002E+01	2.392485E-01
2210	2215	2.941918E+01	1.602552E-01
2215	2220	2.861617E+01	2.629501E-01
2200	2220	2.841693E+01	2.184747E-01
2220	2225	1.182671E+01	3.210736E-01
2225	2230	2.013990E+01	2.444309E-01
2230	2235	4.046403E+01	1.901201E-01
2235	2240	4.319052E+01	1.577362E-01
2220	2240	2.690579E+01	1.572516E-01
2240	2245	3.299479E+01	1.349937E-01
2245	2250	2.275338E+01	1.471367E-01
2250	2255	7.874572E+00	1.273190E-01
2255	2260	1.971160E+00	1.348192E-01
2240	2260	1.639648E+01	1.134965E-01

Table A. 7 - Band Model Parameters for N_2O in 5 and 20 cm^{-1} intervals.

Δω (1/cm)		k(300K) (1/cm-atm)	a_o(300K) (1/atm)
2460	2465	0.	1.000000E+00
2465	2470	0.	1.000000E+00
2470	2475	0.	1.000000E+00
2475	2480	1.359253E-05	5.444794E-02
2460	2480	4.648133E-06	1.361199E-02
2480	2485	6.024518E-05	5.460703E-02
2485	2490	1.173570E-04	4.148910E-02
2490	2495	4.020932E-04	5.486877E-02
2495	2500	1.085382E-03	5.500841E-02
2480	2500	4.162694E-04	4.080117E-02
2500	2505	3.088941E-03	6.833425E-02
2505	2510	7.916225E-03	5.529491E-02
2510	2515	1.712409E-02	5.540940E-02
2515	2520	3.454070E-02	5.551567E-02
2500	2520	1.586749E-02	4.924762E-02
2520	2525	6.767144E-02	6.925521E-02
2525	2530	1.286273E-01	5.577329E-02
2530	2535	2.705949E-01	6.962174E-02
2535	2540	4.266215E-01	6.978263E-02
2520	2540	2.204788E-01	6.108042E-02
2540	2545	5.394511E-01	6.930841E-02
2545	2550	7.023498E-01	6.998658E-02
2550	2555	8.245995E-01	8.394628E-02
2555	2560	5.450515E-01	8.296967E-02
2540	2560	6.653630E-01	7.616528E-02
2560	2565	1.084118E-01	5.309573E-02
2565	2570	5.180476E-01	9.431683E-02
2570	2575	8.419712E-01	6.397643E-02
2575	2580	1.065844E+00	1.039497E-01
2560	2580	6.335667E-01	7.911048E-02
2580	2585	9.467031E-01	1.454343E-01
2585	2590	5.449148E-01	1.745894E-01
2590	2595	2.594071E-01	2.037307E-01
2595	2600	9.904586E-02	2.528762E-01
2580	2600	4.630177E-01	1.547872E-01
2600	2605	2.889199E-02	2.171643E-01
2605	2610	9.141276E-03	1.662176E-01
2610	2615	7.553947E-04	2.794563E-02
2615	2620	0.	1.000000E+00
2600	2620	9.697166E-03	9.716677E-02

Table A. 7 - Band Model Parameters for N_2O in 5 and 20 cm^{-1} intervals.

Δω (1/cm)		k(300K) (1/cm-atm)	a_o(300K) (1/atm)
3300	3305	5.579743E-05	5.507649E-02
3305	3310	1.433565E-04	5.520474E-02
3310	3315	4.550097E-04	6.069268E-02
3315	3320	8.262445E-04	5.546435E-02
3300	3320	3.715265E-04	4.653371E-02
3320	3325	2.134570E-03	6.916311E-02
3325	3330	4.495616E-03	6.938641E-02
3330	3335	6.201173E-03	6.958605E-02
3335	3340	1.325180E-02	6.975364E-02
3320	3340	7.035789E-03	6.305961E-02
3340	3345	1.880796E-02	6.986692E-02
3345	3350	2.311434E-02	6.997624E-02
3350	3355	2.837335E-02	6.397694E-02
3355	3360	2.051177E-02	6.333652E-02
3340	3360	2.270185E-02	7.644111E-02
3360	3365	5.565401E-03	6.524160E-02
3365	3370	1.361043E-02	8.111252E-02
3370	3375	2.685292E-02	6.380154E-02
3375	3380	3.597967E-02	9.799140E-02
3360	3380	2.053767E-02	7.723167E-02
3380	3385	2.925042E-02	1.000023E-01
3385	3390	1.793569E-02	1.017057E-01
3390	3395	9.343346E-03	1.136366E-01
3395	3400	3.285056E-03	1.446663E-01
3380	3400	1.495440E-02	9.660347E-02

Δω (1/cm)		k(300K) (1/cm-atm)	a_o(300K) (1/atm)
3400	3405	1.067034E-03	1.321330E-01
3405	3410	8.042587E-04	9.276684E-02
3410	3415	1.466968E-03	4.164039E-02
3415	3420	4.245147E-03	5.523512E-02
3400	3420	1.996077E-03	6.588255E-02
3420	3425	9.503551E-03	5.535362E-02
3425	3430	1.352177E-02	4.177872E-02
3430	3435	3.292705E-02	5.554132E-02
3435	3440	6.073639E-02	5.563691E-02
3420	3440	2.917219E-02	4.667453E-02
3440	3445	1.041356E-01	5.572362E-02
3445	3450	1.656019E-01	5.580103E-02
3450	3455	3.178602E-01	6.975344E-02
3455	3460	3.509727E-01	5.593742E-02
3440	3460	2.346426E-01	5.663704E-02
3460	3465	5.358745E-01	6.995271E-02
3465	3470	5.793720E-01	6.998643E-02
3470	3475	5.602246E-01	6.372641E-02
3475	3480	2.400502E-01	6.795422E-02
3460	3480	4.846303E-01	7.132496E-02
3480	3485	1.985481E-01	7.729186E-02
3485	3490	5.606456E-01	8.352578E-02
3490	3495	9.820740E-01	1.119659E-01
3495	3500	8.197475E-01	1.116432E-01
3480	3500	6.403036E-01	9.263924E-02

Table A.8 – Band Model Parameters for NH_3 in 5 and 20 cm^{-1} intervals.

Δω (1/cm)		k(300K) (1/cm-atm)	a_o(300K) (1/atm)
680	685	0.	1.000000E+00
685	690	1.075430E-02	1.600000E-02
690	695	2.243199E-02	1.600000E-02
695	700	2.073074E-02	3.193892E-02
680	700	1.347926E-02	1.549829E-02
700	705	4.457161E-02	4.657899E-02
705	710	7.259647E-02	4.186079E-02
710	715	2.643286E-02	1.600000E-02
715	720	7.566970E-02	3.120275E-02
700	720	5.491666E-02	3.230992E-02
720	725	1.728687E-01	9.723796E-02
725	730	1.666653E-01	1.167134E-01
730	735	5.351548E-02	1.600000E-02
735	740	1.761011E-01	3.102552E-02
720	740	1.485379E-01	6.132555E-02
740	745	3.111101E-01	8.905683E-02
745	750	5.057974E-01	1.767480E-01
750	755	2.429092E-01	1.600000E-02
755	760	2.515691E-01	3.700000E-02
740	760	3.278464E-01	7.269475E-02
760	765	6.212162E-01	7.473281E-02
765	770	6.382565E-01	1.230461E-01
770	775	6.436341E-01	3.142037E-02
775	780	1.015093E+00	4.659549E-02
760	780	7.295499E-01	6.268456E-02
780	785	5.107883E-01	3.200000E-02
785	790	1.763516E+00	1.478117E-01
790	795	7.902222E-01	3.194448E-02
795	800	1.884080E+00	4.678758E-02
780	800	1.237152E+00	6.048425E-02
800	805	0.	1.000000E+00
805	810	2.444613E+00	1.236955E-01
810	815	2.043298E+00	3.058187E-02
815	820	2.428978E+00	4.799440E-02
800	820	1.729272E+00	4.708032E-02
820	825	0.	1.000000E+00
825	830	3.650431E+00	1.095898E-01
830	835	4.772876E+00	6.160763E-02
835	840	0.	1.000000E+00
820	840	2.105827E+00	4.095924E-02
840	845	0.	1.000000E+00
845	850	4.052830E+00	7.641310E-02
850	855	6.175769E+00	6.386428E-02
855	860	0.	1.000000E+00
840	860	2.557162E+00	3.429322E-02
860	865	0.	1.000000E+00
865	870	6.049724E+00	7.761371E-02
870	875	2.749911E+00	3.165536E-02
875	880	0.	1.000000E+00
860	880	2.199909E+00	2.730039E-02
880	885	0.	1.000000E+00
885	890	4.568141E+00	4.780485E-02
890	895	2.932717E+00	3.185465E-02
895	900	0.	1.000000E+00
880	900	1.875215E+00	1.993227E-02
900	905	3.737546E-02	1.600000E-02
905	910	4.747914E+00	5.982757E-02
910	915	4.211004E-01	2.911460E-02
915	920	1.249430E+00	5.535641E-02
900	920	1.613955E+00	3.357516E-02
920	925	5.035943E+00	7.097828E-02
925	930	2.308820E+01	1.467822E-01
930	935	3.299013E+01	2.822635E-01
935	940	1.971151E+00	2.519506E-01
920	940	1.597130E+01	1.517218E-01
940	945	5.744636E-02	6.043140E-02
945	950	1.033312E+00	1.600000E-02
950	955	1.191101E+00	1.891728E-02
955	960	1.678452E+00	2.501414E-01
940	960	9.900778E-01	6.131732E-02
960	965	1.849749E+01	3.602077E-01
965	970	4.454779E+01	2.551581E-01
970	975	1.673446E+00	1.600000E-02
975	980	0.	1.000000E+00
960	980	1.617968E+01	1.445092E-01
980	985	0.	1.000000E+00
985	990	0.	1.000000E+00
990	995	6.939210E+00	4.744342E-02
995	1000	0.	1.000000E+00
980	1000	1.734803E+00	1.186085E-02
1000	1005	0.	1.000000E+00
1005	1010	3.871461E+00	3.185501E-02
1010	1015	7.988955E+00	4.755108E-02
1015	1020	0.	1.000000E+00
1000	1020	2.940104E+00	1.982760E-02
1020	1025	0.	1.000000E+00
1025	1030	4.162074E+00	3.165713E-02
1030	1035	1.19917[illegible]E+01	7.761092E-02
1035	1040	0.	1.000000E+00
1020	1040	4.038455E+00	2.723167E-02

Table A.8 - Band Model Parameters for NH_3 in 5 and 20 cm^{-1} intervals (Cont'd)

Δω (1/cm)		k(300K) (1/cm-atm)	a_o(300K) (1/atm)
1040	1045	0.	1.000000E+00
1045	1050	1.159219E+01	7.717927E-02
1050	1055	8.332595E+00	6.225673E-02
1055	1060	0.	1.000000E+00
1040	1060	4.981197E+00	3.483057E-02
1060	1065	0.	1.000000E+00
1065	1070	1.072821E+01	7.643756E-02
1070	1075	4.490932E+00	4.591053E-02
1075	1080	3.784427E+00	4.799933E-02
1060	1080	4.750892E+00	4.195538E-02
1080	1085	1.103748E+01	9.241917E-02
1085	1090	1.642963E+00	2.987264E-02
1090	1095	1.460453E+00	3.199404E-02
1095	1100	3.056401E+00	4.663413E-02
1080	1100	4.299325E+00	4.842969E-02
1100	1105	8.449294E+00	1.045546E-01
1105	1110	3.725461E-01	1.600000E-02
1110	1115	1.703984E+00	4.674591E-02
1115	1120	2.092406E+00	6.221935E-02
1100	1120	3.154558E+00	5.460568E-02
1120	1125	7.157838E+00	1.371139E-01
1125	1130	4.436612E-01	3.198310E-02
1130	1135	6.943463E-01	3.101595E-02
1135	1140	4.472815E+00	1.615352E-01
1120	1140	3.192170E+00	8.689437E-02
1140	1145	8.519628E-01	4.744971E-02
1145	1150	1.203818E-01	1.600000E-02
1150	1155	4.465445E-01	4.659230E-02
1155	1160	3.244951E+00	2.367136E-01
1140	1160	1.165960E+00	8.586188E-02
1160	1165	5.670513E-02	1.600000E-02
1165	1170	1.731642E-01	3.095731E-02
1170	1175	1.873205E-01	4.649670E-02
1175	1180	1.578605E+00	2.328574E-01
1160	1180	4.989987E-01	8.076173E-02
1180	1185	2.687893E-02	1.600000E-02
1185	1190	7.195338E-02	3.079398E-02
1190	1195	6.946081E-01	2.075737E-01
1195	1200	1.625716E-01	1.216977E-01
1180	1200	2.390028E-01	9.046806E-02
1200	1205	2.197763E-02	3.197622E-02
1205	1210	1.609512E-02	1.600000E-02
1210	1215	3.135406E-01	1.973848E-01
1215	1220	1.843696E-02	3.199662E-02
1200	1220	9.301257E-02	6.734778E-02

Table A. 8 - Band Model Parameters for NH_3 in 5 and 20 cm^{-1} intervals.

Δω (1/cm)		k(300K) (1/cm-atm)	a_o(300K) (1/atm)
3100	3105	7.761012E-03	6.361065E-02
3105	3110	5.479422E-04	1.600000E-02
3110	3115	0.	1.000000E+00
3115	3120	1.540336E-02	2.009238E-01
3100	3120	4.678078E-03	6.896190E-02
3120	3125	8.246944E-03	1.232945E-01
3125	3130	0.	1.000000E+00
3130	3135	7.486038E-03	4.773241E-02
3135	3140	4.459650E-02	2.486694E-01
3120	3140	1.508237E-02	1.009736E-01
3140	3145	0.	1.000000E+00
3145	3150	0.	1.000000E+00
3150	3155	3.781295E-02	9.165641E-02
3155	3160	6.256061E-02	1.707464E-01
3140	3160	2.509339E-02	6.554734E-02
3160	3165	0.	1.000000E+00
3165	3170	0.	1.000000E+00
3170	3175	9.701949E-02	1.237947E-01
3175	3180	8.656547E-02	1.079017E-01
3160	3180	4.589624E-02	5.792213E-02
3180	3185	0.	1.000000E+00
3185	3190	0.	1.000000E+00
3190	3195	1.364484E-01	9.362774E-02
3195	3200	1.578601E-01	1.095917E-01
3180	3200	7.357712E-02	5.080434E-02
3200	3205	0.	1.000000E+00
3205	3210	0.	1.000000E+00
3210	3215	2.165016E-01	9.241241E-02
3215	3220	1.802793E-01	7.641474E-02
3200	3220	9.919518E-02	4.220656E-02
3220	3225	0.	1.000000E+00
3225	3230	0.	1.000000E+00
3230	3235	2.189104E-01	6.161398E-02
3235	3240	2.766800E-01	7.761410E-02
3220	3240	1.238976E-01	3.480700E-02
3240	3245	0.	1.000000E+00
3245	3250	0.	1.000000E+00
3250	3255	2.140209E-01	4.788044E-02
3255	3260	2.917096E-01	6.386531E-02
3240	3260	1.264376E-01	2.793564E-02
3260	3265	0.	1.000000E+00
3265	3270	0.	1.000000E+00
3270	3275	0.	1.000000E+00
3275	3280	3.556730E-01	7.904559E-02
3260	3280	8.691825E-02	1.976140E-02
3280	3285	0.	1.000000E+00
3285	3290	0.	1.000000E+00
3290	3295	0.	1.000000E+00
3295	3300	2.089084E-01	4.780029E-02
3280	3300	5.222710E-02	1.195007E-02
3300	3305	0.	1.000000E+00
3305	3310	0.	1.000000E+00
3310	3315	0.	1.000000E+00
3315	3320	5.258979E-02	1.600000E-02
3300	3320	1.314745E-02	4.000000E-03
3320	3325	0.	1.000000E+00
3325	3330	0.	1.000000E+00
3330	3335	4.920651E+00	8.784077E-01
3335	3340	1.718920E+00	3.220163E-01
3320	3340	1.659893E+00	3.000721E-01
3340	3345	6.532596E-02	1.367724E-01
3345	3350	2.939566E-02	5.504914E-02
3350	3355	1.568870E-02	7.287550E-02
3355	3360	6.583729E-02	2.554927E-02
3340	3360	4.406190E-02	6.230249E-02
3360	3365	4.905719E-03	4.425852E-02
3365	3370	5.332754E-04	1.600000E-02
3370	3375	9.370504E-02	2.057110E-02
3375	3380	2.125635E-01	3.185501E-02
3360	3380	7.792609E-02	1.662049E-02
3380	3385	0.	1.000000E+00
3385	3390	0.	1.000000E+00
3390	3395	3.899220E-01	4.744548E-02
3395	3400	2.342023E-01	3.165714E-02
3380	3400	1.557811E-01	1.976331E-02
3400	3405	0.	1.000000E+00
3405	3410	0.	1.000000E+00
3410	3415	1.069935E+00	1.117405E-01
3415	3420	0.	1.000000E+00
3400	3420	2.674837E-01	2.793513E-02
3420	3425	0.	1.000000E+00
3425	3430	0.	1.000000E+00
3430	3435	1.263141E+00	1.392310E-01
3435	3440	0.	1.000000E+00
3420	3440	3.157851E-01	3.480775E-02
3440	3445	0.	1.000000E+00
3445	3450	0.	1.000000E+00
3450	3455	1.220123E+00	1.688307E-01
3455	3460	0.	1.000000E+00
3440	3460	3.050307E-01	4.220992E-02

Table A.8 - Band Model Parameters for NH_3 in 5 and 20 cm^{-1} intervals (Cont'd).

Reproduced from best available copy.

Δω (1/cm)		k(300K) (1/cm-atm)	a_o(300K) (1/atm)
3460	3465	0.	1.000000E+00
3465	3470	4.482409E-01	7.821677E-02
3470	3475	6.426288E-01	1.251681E-01
3475	3480	0.	1.000000E+00
3460	3480	2.727174E-01	5.080698E-02
3480	3485	0.	1.000000E+00
3485	3490	3.859599E-01	1.079114E-01
3490	3495	4.348191E-01	1.236028E-01
3495	3500	0.	1.000000E+00
3480	3500	2.051946E-01	5.792736E-02
3500	3505	0.	1.000000E+00
3505	3510	2.666877E-01	1.244268E-01
3510	3515	2.742416E-01	1.378822E-01
3515	3520	0.	1.000000E+00
3500	3520	1.352314E-01	6.555438E-02
3520	3525	0.	1.000000E+00
3525	3530	1.288850E-01	1.096264E-01
3530	3535	2.098146E-01	1.876500E-01
3535	3540	0.	1.000000E+00
3520	3540	8.467490E-02	7.405293E-02
3540	3545	0.	1.000000E+00
3545	3550	0.	1.000000E+00
3550	3555	1.646220E-01	2.939766E-01
3555	3560	2.086082E-02	3.017044E-02
3540	3560	4.637070E-02	8.094412E-02
3560	3565	0.	1.000000E+00
3565	3570	0.	1.000000E+00
3570	3575	3.747430E-02	1.375454E-01
3575	3580	5.075459E-02	2.000942E-01
3560	3580	2.205722E-02	8.438369E-02
3580	3585	2.962445E-03	1.600000E-02
3585	3590	0.	1.000000E+00
3590	3595	0.	1.000000E+00
3595	3600	1.935961E-02	1.826724E-01
3580	3600	5.580513E-03	4.935732E-02
3600	3605	2.151438E-02	1.830537E-01
3605	3610	2.960283E-03	1.600000E-02
3610	3615	0.	1.000000E+00
3615	3620	0.	1.000000E+00
3600	3620	6.118666E-03	4.953537E-02
3620	3625	5.411217E-03	1.093831E-01
3625	3630	7.854382E-03	1.384094E-01
3630	3635	1.731822E-03	1.600000E-02
3635	3640	6.972575E-04	1.600000E-02
3620	3640	3.923670E-03	6.916354E-02
3640	3645	0.	1.000000E+00
3645	3650	4.243069E-04	1.600000E-02
3650	3655	1.120403E-03	3.154029E-02
3655	3660	6.978049E-04	1.600000E-02
3640	3660	5.606291E-04	1.576444E-02

Table A. 9 -Band Model Parameters for HCHO in 5 and 20 cm^{-1} intervals

Δω (1/cm)		k(300K) (1/cm-atm)	a_o(300K) (1/atm)
2620	2625	4.733933E-04	3.192748E-02
2625	2630	1.131962E-03	6.352645E-02
2630	2635	7.897370E-04	3.192610E-02
2635	2640	1.545539E-03	6.267147E-02
2620	2640	1.000908E-03	4.704324E-02
2640	2645	2.369013E-03	6.317061E-02
2645	2650	4.020274E-03	8.984690E-02
2650	2655	4.454655E-03	7.643067E-02
2655	2660	3.671176E-03	7.252099E-02
2640	2660	3.628768E-03	7.504206E-02
2660	2665	6.312860E-03	7.586226E-02
2665	2670	1.091447E-02	9.929802E-02
2670	2675	1.232839E-02	9.766043E-02
2675	2680	1.496134E-02	1.295906E-01
2660	2680	1.125427E-02	1.003212E-01
2680	2665	1.444031E-02	8.293157E-02
2585	2690	2.518741E-02	9.434348E-02
2690	2695	2.976605E-02	1.183053E-01
2695	2700	3.915227E-02	2.089062E-01
2680	2700	2.688651E-02	1.251012E-01
2700	2705	4.613817E-02	1.060695E-01
2705	2710	6.315084E-02	1.046507E-01
2710	2715	6.062716E-02	2.800110E-01
2715	2720	6.639573E-02	1.013014E-01
2700	2720	5.909298E-02	1.399281E-01
2720	2725	9.312703E-02	1.107336E-01
2725	2730	1.413749E-01	2.072084E-01
2730	2735	1.285226E-01	2.059626E-01
2735	2740	1.317761E-01	1.050586E-01
2720	2740	1.237002E-01	1.545516E-01
2740	2745	1.495605E-01	1.337134E-01
2745	2750	3.425065E-01	3.460118E-01
2750	2755	1.693321E-01	1.137329E-01
2755	2760	2.097456E-01	9.976391E-02
2740	2760	2.177862E-01	1.697523E-01
2760	2765	4.504073E-01	3.418800E-01
2765	2770	4.729124E-01	2.121570E-01
2770	2775	2.792447E-01	1.202614E-01
2775	2780	4.104112E-01	2.350239E-01
2760	2780	4.032439E-01	2.245106E-01
2780	2785	9.058029E-01	3.676909E-01
2785	2790	4.322599E-01	1.371073E-01
2790	2795	3.495528E-01	1.592556E-01
2795	2800	1.376869E+00	4.755664E-01
2780	2800	7.661212E-01	2.839634E-01
2800	2805	5.306059E-01	1.574766E-01
2805	2810	5.709654E-01	1.826280E-01
2810	2815	1.000704E+00	3.594161E-01
2815	2820	1.544515E+00	3.147542E-01
2800	2820	9.266975E-01	2.498936E-01
2820	2825	7.072629E-01	1.865213E-01
2825	2830	7.944371E-01	3.112085E-01
2830	2835	2.618108E+00	4.730949E-01
2835	2840	7.024129E-01	2.101617E-01
2820	2840	1.205555E+00	2.881546E-01
2840	2845	7.854110E-01	2.940537E-01
2845	2850	3.382768E+00	5.212820E-01
2850	2855	6.918175E-01	2.092614E-01
2855	2860	6.347937E-01	2.716160E-01
2840	2860	1.378702E+00	3.093413E-01
2860	2865	2.174626E+00	4.883299E-01
2865	2870	2.547816E+00	3.439945E-01
2870	2875	6.857068E-01	2.753219E-01
2875	2880	1.149864E+00	4.446651E-01
2860	2880	1.639503E+00	3.703191E-01
2920	2925	9.309696E-01	2.102982E-01
2925	2930	1.390880E+00	4.053384E-01
2930	2935	1.538502E+00	2.593133E-01
2935	2940	6.052163E-01	1.494217E-01
2920	2940	1.266392E+00	2.551781E-01
2880	2885	3.980696E+00	4.644716E-01
2885	2890	7.417107E-01	2.540570E-01
2890	2895	9.254837E-01	3.364258E-01
2895	2900	3.946110E+00	5.152331E-01
2880	2900	2.323500E+00	3.705203E-01
2900	2905	7.314618E-01	2.049205E-01
2905	2910	8.861813E-01	2.630051E-01
2910	2915	3.518207E+00	5.516501E-01
2915	2920	8.216312E-01	1.807872E-01
2900	2920	1.489370E+00	2.943532E-01

Table A. 9 - **Band Model Parameters for HCHO in 5 and 20 cm^{-1} intervals (Cont'd).**

Δω (1/cm)		k(300K) (1/cm-atm)	a_o(300K) (1/atm)
2940	2945	1.464374E+00	3.452007E-01
2945	2950	1.855120E+00	3.487781E-01
2950	2955	5.848839E-01	1.246670E-01
2955	2960	7.622234E-01	2.510735E-01
2940	2960	1.166650E+00	2.647055E-01
2960	2965	1.436713E+00	3.521564E-01
2965	2970	6.027342E-01	1.363439E-01
2970	2975	6.583588E-01	1.946095E-01
2975	2980	1.048935E+00	3.698945E-01
2960	2980	9.366852E-01	2.612715E-01
2980	2985	4.813007E-01	1.067291E-01
2985	2990	3.996844E-01	1.453372E-01
2990	2995	5.474445E-01	3.506742E-01
2995	3000	5.564699E-01	1.377455E-01
2980	3000	4.962249E-01	1.761693E-01
3000	3005	2.302254E-01	1.149513E-01
3005	3010	3.318185E-01	3.262460E-01
3010	3015	2.227730E-01	9.728490E-02
3015	3020	2.384782E-01	1.155825E-01
3000	3020	2.708238E-01	1.570393E-01
3020	3025	2.790461E-01	3.001596E-01
3025	3030	1.081934E-01	9.769035E-02
3030	3035	1.480653E-01	1.026042E-01
3035	3040	1.299722E-01	2.268622E-01
3020	3040	1.663193E-01	1.774628E-01
3040	3045	1.075428E-01	1.365010E-01
3045	3050	6.681135E-02	9.997208E-02
3050	3055	6.871896E-02	1.580768E-01
3055	3060	4.920239E-02	1.310099E-01
3040	3060	7.306887E-02	1.283701E-01
3060	3065	4.195006E-02	1.102839E-01
3065	3070	3.599504E-02	1.218331E-01
3070	3075	2.485553E-02	9.919845E-02
3075	3080	1.716114E-02	9.293775E-02
3060	3080	2.999069E-02	1.044214E-01
3080	3085	1.860007E-02	1.145134E-01
3085	3090	1.206333E-02	8.751000E-02
3090	3095	6.431222E-03	9.466814E-02
3095	3100	5.541345E-03	7.536370E-02
3080	3100	1.116399E-02	9.080406E-02
3100	3105	6.817508E-03	1.043484E-01
3105	3110	3.566443E-03	7.466702E-02
3110	3115	2.238173E-03	6.175460E-02
3115	3120	1.811493E-03	6.241978E-02
3100	3120	3.606404E-03	7.403968E-02
3120	3125	1.754351E-03	7.877905E-02
3125	3130	6.084417E-04	3.192802E-02
3130	3135	2.753297E-04	1.600000E-02
3135	3140	0.	1.000000E+00
3120	3140	6.470306E-04	3.151418E-02

Table A. 10 - **Band Model Parameters for H_2O in 5 and 20 cm^{-1} intervals.**

Δω (1/cm)		k(300K) (cm^2/gm)	a_o(300K) (1/atm)
960	965	0.	1.000000E+00
965	970	0.	1.000000E+00
970	975	0.	1.000000E+00
975	980	2.170000E-02	1.306000E-02
960	980	5.425000E-03	3.265000E-03
980	985	0.	1.000000E+00
985	990	0.	1.000000E+00
990	995	0.	1.000000E+00
995	1000	1.270000E-02	1.226000E-02
980	1000	3.175000E-03	3.065000E-03
1000	1005	2.538000E-02	2.160924E-02
1005	1010	0.	1.000000E+00
1010	1015	9.898000E-02	2.413211E-02
1015	1020	4.846000E-02	1.952380E-02
1000	1020	4.321000E-02	1.536228E-02
1020	1025	0.	1.000000E+00
1025	1030	9.148000E-02	4.403440E-02
1030	1035	1.332000E-02	2.239563E-02
1035	1040	1.178000E-02	1.064000E-02
1020	1040	2.914500E-02	1.821603E-02
1040	1045	0.	1.000000E+00
1045	1050	2.796000E-02	1.393000E-02
1050	1055	2.130000E-02	1.382000E-02
1055	1060	2.388000E-02	2.166923E-02
1040	1060	1.953500E-02	1.224815E-02
1060	1065	5.316000E-02	2.316476E-02
1065	1070	2.210600E-01	1.388999E-02
1070	1075	8.964000E-02	1.807273E-02
1075	1080	1.000000E-02	9.600000E-03
1060	1080	9.346500E-02	1.321003E-02
1080	1085	0.	1.000000E+00
1085	1090	1.468000E-02	1.254000E-02
1090	1095	1.106600E-01	1.134000E-02
1095	1100	8.862000E-02	1.318000E-02
1080	1100	5.349000E-02	8.082099E-03
1100	1105	1.305000E-01	1.374000E-02
1105	1110	2.616800E-01	1.134000E-02
1110	1115	2.320800E-01	1.810318E-02
1115	1120	1.270000E-02	1.226000E-02
1100	1120	1.592400E-01	1.189874E-02
1120	1125	2.939600E-01	2.597169E-02
1125	1130	0.	1.000000E+00
1130	1135	0.	1.000000E+00
1135	1140	1.084000E+00	3.023772E-02
1120	1140	3.444900E-01	1.307198E-02
1140	1145	1.398000E-02	1.239000E-02
1145	1150	2.468400E-01	1.280000E-02
1150	1155	2.456800E-01	2.622524E-02
1155	1160	0.	1.000000E+00
1140	1160	1.266250E-01	1.105150E-02
1160	1165	0.	1.000000E+00
1165	1170	4.008200E-01	4.772146E-02
1170	1175	2.330880E+00	2.392463E-02
1175	1180	0.	1.000000E+00
1160	1180	6.829250E-01	1.283201E-02
1180	1185	4.248000E-02	2.493297E-02
1185	1190	1.658680E+00	2.007523E-02
1190	1195	2.152000E-02	4.360561E-02
1195	1200	9.489400E-01	1.786948E-02
1180	1200	6.679050E-01	1.322067E-02
1200	1205	0.	1.000000E+00
1205	1210	4.712000E-02	8.498496E-02
1210	1215	2.832360E+00	3.153891E-02
1215	1220	8.670400E-01	3.000248E-02
1200	1220	9.366300E-01	1.828349E-02
1220	1225	6.307400E-01	5.684659E-02
1225	1230	2.229960E+00	4.337197E-02
1230	1235	7.940000E-03	7.690000E-03
1235	1240	3.857600E-01	4.244758E-02
1220	1240	8.136000E-01	3.109495E-02
1240	1245	2.938580E+00	4.007291E-02
1245	1250	1.481600E-01	3.818537E-02
1250	1255	3.021600E-01	1.036377E-01
1255	1260	6.795600E-01	4.546467E-02
1240	1260	1.017115E+00	3.653765E-02

Table A.10 - Band Model Parameters for H_2O in 5 and 20 cm^{-1} intervals.

Δω (1/cm)		k(300K) (cm^2/gm)	a_o(300K) (1/atm)
1760	1765	0.	1.000000E+00
1765	1770	0.	1.000000E+00
1770	1775	0.	1.000000E+00
1775	1780	1.941998E+01	2.274773E-02
1760	1780	4.854970E+00	5.686032E-03
1780	1785	4.182225E+02	7.325240E-02
1785	1790	6.051960E+00	6.157870E-02
1790	1795	9.472365E+02	3.679286E-02
1795	1800	3.057601E+02	7.398713E-02
1780	1800	4.193200E+02	4.207307E-02
1800	1805	2.011017E+02	2.903736E-02
1805	1810	4.750410E+01	3.730237E-02
1810	1815	1.799126E+02	3.243615E-02
1815	1820	3.726922E+01	2.502440E-02
1800	1820	1.164469E+02	2.753228E-02
1820	1825	1.070604E+01	3.353651E-02
1825	1830	4.467748E+02	4.593317E-02
1830	1835	3.448316E+02	2.703129E-02
1835	1840	5.350678E+01	4.684149E-02
1820	1840	2.155548E+02	2.871490E-02
1840	1845	7.617215E+02	3.779761E-02
1845	1850	9.643022E+01	6.416238E-02
1850	1855	2.630440E+00	2.975850E-02
1855	1860	1.557865E+01	5.603416E-02
1840	1860	2.190902E+02	2.345553E-02
1860	1865	1.155430E+01	4.517320E-02
1865	1870	4.947534E+02	5.659126E-02
1870	1875	1.589272E+01	1.274090E-02
1875	1880	4.592000E+00	4.774316E-02
1860	1880	1.317006E+02	2.292195E-02
1880	1885	1.461742E+01	2.334611E-02
1885	1890	1.746575E+02	2.091129E-02
1890	1895	2.490060E+00	6.190777E-02
1895	1900	5.494126E+01	2.949685E-02
1880	1900	6.167380E+01	1.754990E-02
1900	1905	9.408720E+00	4.073146E-02
1905	1910	6.318754E+01	3.909347E-02
1910	1915	9.590200E-01	3.999346E-02
1915	1920	2.558971E+02	2.470790E-02
1900	1920	8.234959E+01	1.807519E-02
1920	1925	1.014953E+02	3.337627E-02
1925	1930	3.379900E-01	3.640187E-02
1930	1935	5.301690E+00	2.941643E-02
1935	1940	6.781900E-01	8.703336E-02
1920	1940	2.693077E+01	1.554030E-02

Δω (1/cm)		k(300K) (cm^2/gm)	a_o(300K) (1/atm)
1940	1945	1.784669E+02	3.538673E-02
1945	1950	2.581154E+01	4.326648E-02
1950	1955	7.327520E+00	2.682454E-02
1955	1960	1.726600E+00	7.254751E-02
1940	1960	4.403168E+01	2.414530E-02
1960	1965	5.167660E+00	1.975295E-02
1965	1970	6.070570E+01	2.684536E-02
1970	1975	2.464909E-02	1.256030E-02
1975	1980	9.354800E-01	3.189832E-02
1960	1980	1.670837E+01	1.193724E-02

Reproduced from best available copy.

Table A. 10 - Band Model Parameters for H_2O in 5 and 20 cm^{-1} intervals.

Δω (1/cm)		k(300K) (cm^2/gm)	a_0(300K) (1/atm)
1980	1985	2.879200E-01	7.820005E-02
1985	1990	1.934264E+01	1.628879E-02
1990	1995	7.416360E+01	3.022176E-02
1995	2000	4.304860E+00	1.999866E-02
1980	2000	2.452475E+01	1.638143E-02
2000	2005	5.386000E-02	6.447633E-02
2005	2010	3.724120E+00	3.708239E-02
2010	2015	6.000000E-02	6.376716E-02
2015	2020	3.733950E+01	4.179331E-02
2000	2020	1.029435E+01	1.841400E-02
2020	2025	2.560100E+00	1.730125E-02
2025	2030	2.004660E+00	3.690753E-02
2030	2035	3.315400E-01	3.397646E-02
2035	2040	2.838000E-01	3.611100E-02
2020	2040	1.295030E+00	2.345304E-02
2040	2045	1.443164E+01	3.662225E-02
2045	2050	6.188600E-01	2.767460E-02
2050	2055	7.776000E-02	6.681421E-02
2055	2060	5.720000E-03	1.102000E-02
2040	2060	3.783545E+00	1.487414E-02
2060	2065	1.361988E+01	2.602473E-02
2065	2070	3.011420E+00	1.295135E-02
2070	2075	1.163040E+00	3.141695E-02
2075	2080	3.231200E-01	2.586659E-02
2060	2080	4.529365E+00	1.595904E-02
2080	2085	2.118000E-01	1.282000E-02
2085	2090	1.408400E+00	3.101801E-02
2090	2095	4.036300E+00	1.765944E-02
2095	2100	3.403400E-01	2.727027E-02
2080	2100	1.499210E+00	1.625542E-02
2100	2105	4.103000E-01	1.280000E-02
2105	2110	3.992400E-01	3.807856E-02
2110	2115	6.439000E-01	4.493301E-02
2115	2120	1.075100E+00	1.491402E-02
2100	2120	6.321350E-01	2.398076E-02
2120	2125	4.389800E-01	7.458217E-02
2125	2130	0.	1.000000E+00
2130	2135	0.	1.000000E+00
2135	2140	2.060020E+00	6.111795E-02
2120	2140	6.247500E-01	2.871665E-02
2140	2145	4.738000E-02	3.400730E-02
2145	2150	5.432200E-01	4.576554E-02
2150	2155	2.805000E-01	2.678050E-02
2155	2160	1.143600E-01	2.222714E-02
2140	2160	2.463650E-01	2.845357E-02
2160	2165	4.880800E-01	2.586469E-02
2165	2170	7.820000E-03	1.136000E-02
2170	2175	1.330600E-01	2.406459E-02
2175	2180	1.820000E-02	3.437020E-02
2160	2180	1.618100E-01	1.598536E-02
2180	2185	1.974200E-01	2.383690E-02
2185	2190	1.615600E-01	3.859526E-02
2190	2195	4.256000E-02	2.363975E-02
2195	2200	9.500000E-03	1.978000E-02
2180	2200	1.027600E-01	2.265335E-02
2200	2205	5.010000E-02	8.800000E-03
2205	2210	2.262800E-01	4.100347E-02
2210	2215	1.062600E-01	7.024402E-02
2215	2220	5.608000E-02	4.590258E-02
2200	2220	1.101800E-01	3.696153E-02
2220	2225	0.	1.000000E+00
2225	2230	3.168000E-02	4.597181E-02
2230	2235	5.924000E-02	1.948819E-02
2235	2240	3.812000E-02	6.091813E-02
2220	2240	3.226000E-02	2.805174E-02

Table A. 10 - Band Model Parameters for H_2O in 5 and 20 cm^{-1} intervals.

Δω (1/cm)		k(300K) (cm^2/gm)	a_o(300K) (1/atm)
2900	2905	1.710000E-02	1.564000E-02
2905	2910	4.776000E-02	1.780000E-02
2910	2915	4.638000E-02	2.315529E-02
2915	2920	8.200000E-03	1.550000E-02
2900	2920	2.386500E-02	1.678658E-02
2920	2925	8.000000E-03	6.769000E-03
2925	2930	0.	1.000000E+00
2930	2935	4.236600E-01	7.076811E-02
2935	2940	3.904400E-01	4.479433E-02
2920	2940	2.055250E-01	2.974545E-02
2940	2945	5.820000E-03	7.180000E-03
2945	2950	7.146000E-02	2.555437E-02
2950	2955	3.169800E-01	2.128604E-02
2955	2960	2.789000E-01	7.595645E-02
2940	2960	1.682900E-01	2.847301E-02
2960	2965	2.870400E-01	3.125480E-02
2965	2970	6.591400E-01	4.389671E-02
2970	2975	1.143000E+00	3.170059E-02
2975	2980	1.173740E+00	3.304648E-02
2960	2980	6.157500E-01	3.258237E-02
2980	2985	8.877000E-01	8.308683E-02
2985	2990	1.423560E+00	3.961383E-02
2990	2995	2.094850E+00	5.136008E-02
2995	3000	3.766200E-01	1.452569E-02
2980	3000	1.195695E+00	4.338372E-02
3000	3005	1.910620E+00	5.727028E-02
3005	3010	3.973800E-01	2.726058E-02
3010	3015	7.070140E+00	9.283212E-02
3015	3020	2.112380E+00	1.698901E-02
3000	3020	2.872630E+00	4.476869E-02
3020	3025	7.330200E-01	3.117127E-02
3025	3030	2.233960E+00	2.785103E-02
3030	3035	1.254778E+01	8.844314E-02
3035	3040	1.195140E+00	2.167732E-02
3020	3040	4.177475E+00	3.902247E-02
3040	3045	1.628000E-02	2.867783E-02
3045	3050	3.781880E+00	5.076429E-02
3050	3055	7.870000E-02	6.211927E-02
3055	3060	7.199900E+00	5.570041E-02
3040	3060	2.769190E+00	3.052522E-02
3060	3065	6.582840E+00	2.188949E-02
3065	3070	5.735560E+00	3.563131E-02
3070	3075	6.440000E-03	7.120000E-03
3075	3080	6.384340E+00	6.947279E-02
3060	3080	4.677295E+00	3.024308E-02
3080	3085	4.056500E+00	5.051840E-02
3085	3090	8.019200E-01	2.371092E-02
3090	3095	1.496580E+00	3.761542E-02
3095	3100	1.037412E+01	6.475515E-02
3080	3100	4.182280E+00	4.056022E-02
3100	3105	9.413160E+00	5.604365E-02
3105	3110	3.161200E+00	6.374782E-02
3110	3115	4.828060E+00	1.009373E-01
3115	3120	1.291956E+01	8.656706E-02
3100	3120	7.580500E+00	7.082258E-02
3120	3125	8.470000E+00	6.497553E-02
3125	3130	5.630340E+00	1.126016E-01
3130	3135	8.380140E+00	3.050693E-02
3135	3140	1.074000E-02	1.788000E-02
3120	3140	5.622805E+00	4.705790E-02

Table A. 10 - Band Model Parameters for H_2O in 5 and 20 cm^{-1} intervals.

Δω (1/cm)		k(300K) (cm^2/gm)	a_o(300K) (1/atm)
3140	3145	0.	1.000000E+00
3145	3150	0.	1.000000E+00
3150	3155	4.448400E-01	5.707469E-02
3155	3160	5.764000E-02	4.192277E-02
3140	3160	1.256200E-01	2.162818E-02
3160	3165	1.471400E-01	3.818435E-02
3165	3170	8.328700E-01	1.017799E-01
3170	3175	2.151800E-01	8.870563E-02
3175	3180	9.280040E+00	2.633084E-02
3160	3180	2.617545E+00	2.374819E-02
3180	3185	1.649720E+00	5.050077E-02
3185	3190	3.922840E+00	2.589892E-02
3190	3195	1.634000E-02	2.131325E-02
3195	3200	1.133434E+01	6.265894E-02
3180	3200	4.230810E+00	3.186893E-02
3200	3205	2.778600E-01	6.006676E-02
3205	3210	8.248440E+00	2.607892E-02
3210	3215	9.528220E+00	3.142576E-02
3215	3220	9.177380E+00	4.210724E-02
3200	3220	6.807975E+00	2.849647E-02
3220	3225	4.010300E+00	4.678618E-02
3225	3230	8.515340E+00	6.449138E-02
3230	3235	4.315680E+00	7.846444E-02
3235	3240	4.044160E+00	2.590940E-02
3220	3240	5.221370E+00	5.177888E-02
3240	3245	1.458964E+01	6.012836E-02
3245	3250	1.607280E+00	4.088451E-02
3250	3255	9.128220E+00	2.293227E-02
3255	3260	3.974600E+00	3.392579E-02
3240	3260	7.324935E+00	3.473668E-02
3260	3265	4.063460E+00	5.255033E-02
3265	3270	3.128140E+00	4.185840E-02
3270	3275	1.327948E+01	8.306299E-02
3275	3280	1.014236E+01	5.995489E-02
3260	3280	7.653360E+00	5.752169E-02
3280	3285	4.926780E+00	8.749814E-02
3285	3290	4.177440E+00	3.884275E-02
3290	3295	1.065558E+01	1.007616E-01
3295	3300	4.045600E+00	5.966249E-02
3280	3300	5.951850E+00	7.027819E-02
3300	3305	9.396900E-01	4.782782E-02
3305	3310	9.988160E+00	4.983652E-02
3310	3315	7.391400E+00	6.215151E-02
3315	3320	1.236220E+00	5.791961E-02
3300	3320	4.888865E+00	4.382508E-02
3320	3325	3.776480E+00	6.762981E-02
3325	3330	3.280340E+00	9.400655E-02
3330	3335	1.712460E+00	2.522301E-02
3335	3340	6.647600E+00	6.249317E-02
3320	3340	3.854220E+00	5.934592E-02
3340	3345	1.761800E+00	5.256264E-02
3345	3350	9.728200E-01	6.844199E-02
3350	3355	2.047280E+00	7.647100E-02
3355	3360	3.520600E+00	8.320767E-02
3340	3360	2.075625E+00	6.768372E-02
3360	3365	9.480220E+00	1.263572E-01
3365	3370	1.587156E+01	8.339692E-02
3370	3375	6.570400E-01	6.901627E-02
3375	3380	1.742960E+00	6.726448E-02
3360	3380	6.812945E+00	6.922867E-02
3380	3385	3.636000E+00	4.685170E-02
3385	3390	6.283440E+00	3.366906E-02
3390	3395	1.347260E+01	6.623492E-02
3395	3400	1.018380E+00	6.498648E-02
3380	3400	6.107605E+00	4.407896E-02
3400	3405	4.723920E+00	9.937204E-02
3405	3410	1.173480E+00	6.467432E-02
3410	3415	1.133160E+00	5.074792E-02
3415	3420	5.225160E+00	7.358328E-02
3400	3420	3.063930E+00	6.760604E-02
3420	3425	2.235618E+01	7.410374E-02
3425	3430	1.523220E+00	4.781374E-02
3430	3435	5.221740E+00	8.043255E-02
3435	3440	2.773140E+00	2.171435E-01
3420	3440	7.968570E+00	6.970130E-02
3440	3445	1.530296E+01	9.431856E-02
3445	3450	2.067378E+01	1.063442E-01
3450	3455	2.754000E-02	1.292000E-02
3455	3460	0.	1.000000E+00
3440	3460	1.098857E+01	5.000069E-02

Table A.10 – Band Model Parameters for H_2O in 5 and 20 cm^{-1} intervals.

Δω (1/cm)		k(300K) (cm^2/gm)	a_o(300K) (1/atm)
3980	3985	1.398596E+01	6.773658E-02
3985	3990	1.049524E+01	5.041934E-02
3990	3995	2.194140E+01	6.693676E-02
3995	4000	1.429798E+01	7.460738E-02
3980	4000	1.515514E+01	6.407850E-02
4000	4005	3.900740E+00	1.236323E-01
4005	4010	3.179608E+01	3.815846E-02
4010	4015	8.048140E+00	6.265781E-02
4015	4020	1.406664E+01	9.839532E-02
4000	4020	1.442790E+01	5.845969E-02
4020	4025	5.852000E-01	4.055709E-02
4025	4030	1.702744E+01	3.949627E-02
4030	4035	4.785400E+00	6.388479E-02
4035	4040	6.017400E-01	5.935423E-02
4020	4040	5.749565E+00	3.216364E-02
4040	4045	1.443256E+01	4.273756E-02
4045	4050	8.152240E+00	2.313270E-02
4050	4055	1.530220E+00	3.221405E-02
4055	4060	6.826600E-01	1.739902E-02
4040	4060	6.199420E+00	2.434819E-02
4060	4065	4.665940E+00	3.831239E-02
4065	4070	1.477200E-01	2.112999E-02
4070	4075	2.502320E+00	3.777456E-02
4075	4080	5.702920E+00	3.869164E-02
4060	4080	3.274725E+00	3.033566E-02
4080	4085	2.790240E+00	4.234074E-02
4065	4090	7.320600E+00	4.716274E-02
4090	4095	3.459000E-01	3.027278E-02
4095	4100	0.	1.000000E+00
4080	4100	2.614185E+00	2.554330E-02
4100	4105	3.537560E+00	2.774423E-02
4105	4110	9.787140E+00	5.151048E-02
4110	4115	4.736000E-02	2.516774E-02
4115	4120	0.	1.000000E+00
4100	4120	3.343015E+00	2.092084E-02
4120	4125	9.234200E-01	2.515386E-02
4125	4130	7.449800E-01	3.856715E-02
4130	4135	4.309080E+00	3.769435E-02
4135	4140	2.648080E+00	2.727268E-02
4120	4140	2.206390E+00	2.853490E-02
4140	4145	9.116000E-01	2.111480E-02
4145	4150	1.410160E+00	5.436328E-02
4150	4155	1.142460E+00	2.792154E-02
4155	4160	1.053320E+00	3.999775E-02
4140	4160	1.129355E+00	3.536683E-02
4160	4165	2.356000E-02	1.146000E-02
4165	4170	4.109800E-01	2.378892E-02
4170	4175	1.085620E+00	2.464935E-02
4175	4180	7.480000E-02	2.595780E-02
4160	4180	3.987400E-01	1.634860E-02
4180	4185	1.118360E+00	1.532037E-02
4185	4190	7.540200E-01	1.578784E-02
4190	4195	1.343180E+00	4.738973E-02
4195	4200	3.397600E-01	3.038429E-02
4180	4200	8.888300E-01	2.480224E-02
4200	4205	9.340400E-01	2.173745E-02
4205	4210	3.649400E-01	3.443246E-02
4210	4215	9.932000E-02	2.428103E-02
4215	4220	5.198400E-01	3.950425E-02
4200	4220	4.795350E-01	2.604197E-02
4220	4225	3.170200E-01	3.840487E-02
4225	4230	0.	1.000000E+00
4230	4235	2.513600E-01	2.651494E-02
4235	4240	7.134000E-02	2.408377E-02
4220	4240	1.599300E-01	2.129421E-02
4240	4245	1.003800E-01	3.555871E-02
4245	4250	0.	1.000000E+00
4250	4255	6.524400E-01	5.798760E-02
4255	4260	1.675400E-01	2.780157E-02
4240	4260	2.300900E-01	2.825177E-02
4260	4265	5.618000E-02	1.148000E-02
4265	4270	1.372000E-01	9.980000E-03
4270	4275	2.081800E-01	3.887755E-02
4275	4280	1.072600E-01	1.392000E-02
4260	4280	1.272050E-01	1.792496E-02
4280	4285	3.936000E-02	1.583755E-02
4285	4290	1.778000E-02	2.125943E-02
4290	4295	2.794000E-02	1.890998E-02
4295	4300	0.	1.000000E+00
4280	4300	2.127000E-02	1.334655E-02
4300	4305	6.178000E-02	2.570590E-02
4305	4310	1.550000E-01	1.68[illegible]390E-02
4310	4315	2.452000E-02	1.260000E-02
4315	4320	1.364000E-02	8.920000E-03
4300	4320	6.373500E-02	1.404361E-02
4320	4325	0.	1.000000E+00
4325	4330	1.374000E-02	1.835152E-02
4330	4335	0.	1.000000E+00
4335	4340	1.510000E-02	1.288000E-02
4320	4340	7.210000E-03	7.710974E-03

Table A. 10 - Band Model Parameters for H_2O in 5 and 20 cm^{-1} intervals.

Δω (1/cm)		k(300K) (cm^2/gm)	a_o(300K) (1/atm)
4700	4705	0.	1.000000E+00
4705	4710	1.514000E-02	2.083090E-02
4710	4715	0.	1.000000E+00
4715	4720	1.338000E-02	3.807495E-02
4700	4720	7.130000E-03	1.427225E-02
4720	4725	3.664000E-02	1.998000E-02
4725	4730	0.	1.000000E+00
4730	4735	0.	1.000000E+00
4735	4740	2.118000E-02	4.023075E-02
4720	4740	1.445500E-02	1.364638E-02
4740	4745	0.	1.000000E+00
4745	4750	0.	1.000000E+00
4750	4755	0.	1.000000E+00
4755	4760	5.252000E-02	3.471327E-02
4740	4760	1.313000E-02	8.678318E-03
4760	4765	4.776000E-02	5.546265E-02
4765	4770	0.	1.000000E+00
4770	4775	0.	1.000000E+00
4775	4780	2.438000E-02	1.922000E-02
4760	4780	1.807500E-02	1.852540E-02
4780	4765	9.700000E-03	1.940000E-02
4785	4790	0.	1.000000E+00
4790	4795	0.	1.000000E+00
4795	4800	2.480000E-02	1.924000E-02
4780	4800	8.625000E-03	9.164008E-03
4800	4805	0.	1.000000E+00
4805	4810	6.420000E-03	1.262000E-02
4810	4815	2.752000E-02	3.597515E-02
4815	4820	6.500000E-03	1.898000E-02
4800	4820	1.013500E-02	1.643862E-02
4820	4825	5.760000E-03	1.342000E-02
4825	4830	1.804000E-02	2.761683E-02
4830	4835	0.	1.000000E+00
4835	4640	0.	1.000000E+00
4820	4840	5.950000E-03	1.015798E-02
4840	4845	2.498000E-02	2.665541E-02
4845	4850	8.040000E-03	1.769000E-02
4850	4855	2.818000E-02	3.341523E-02
4855	4860	1.522000E-02	2.874497E-02
4840	4860	1.910500E-02	2.610766E-02
4860	4865	2.340000E-02	1.769000E-02
4865	4870	6.000000E-03	1.776000E-02
4870	4875	0.	1.000000E+00
4875	4880	2.034000E-02	3.354385E-02
4860	4880	1.243500E-02	1.620595E-02
4880	4885	0.	1.000000E+00
4885	4890	0.	1.000000E+00
4890	4895	1.528000E-02	2.746261E-02
4895	4900	0.	1.000000E+00
4880	4900	3.820000E-03	6.865654E-03
4900	4905	5.160000E-02	4.776003E-02
4905	4910	1.792000E-02	1.622000E-02
4910	4915	0.	1.000000E+00
4915	4920	4.852000E-02	3.669602E-02
4900	4920	2.951000E-02	2.511121E-02
4920	4925	1.514000E-02	2.853148E-02
4925	4930	5.280000E-02	5.397257E-02
4930	4935	3.770000E-02	4.366997E-02
4935	4940	3.542000E-02	2.510242E-02
4920	4940	3.551500E-02	3.712056E-02
4940	4945	3.106000E-02	1.466000E-02
4945	4950	3.930000E-02	3.196763E-02
4950	4955	5.872000E-02	4.022194E-02
4955	4960	2.156600E-01	1.000397E-01
4940	4960	8.618500E-02	4.614595E-02
4960	4965	1.233200E-01	4.524400E-02
4965	4970	1.075000E-01	3.026894E-02
4970	4975	0.	1.000000E+00
4975	4980	0.	1.000000E+00
4960	4980	5.770500E-02	1.879706E-02
4980	4985	2.577200E-01	4.921115E-02
4985	4990	4.624400E-01	7.411647E-02
4990	4995	1.650400E-01	2.991456E-02
4995	5000	8.092000E-02	2.034794E-02
4980	5000	2.415450E-01	4.330209E-02
5000	5005	4.052000E-01	3.993905E-02
5005	5010	1.564400E-01	2.791070E-02
5010	5015	7.382000E-01	4.743236E-02
5015	5020	0.	1.000000E+00
5000	5020	3.249600E-01	2.712954E-02
5020	5025	7.791600E-01	5.058759E-02
5025	5030	1.408600E-01	4.150631E-02
5030	5035	7.217200E-01	4.236620E-02
5035	5040	2.766600E-01	2.527967E-02
5020	5040	4.796000E-01	3.731458E-02
5040	5045	3.166400E-01	4.110362E-02
5045	5050	5.117600E-01	7.422455E-02
5050	5055	1.793520E+00	4.776309E-02
5055	5060	6.716000E-02	4.915356E-02
5040	5060	6.722750E-01	4.038952E-02

Table A. 10 - Band Model Parameters for H_2O in 5 and 20 cm^{-1} intervals (Cont'd).

Δω (1/cm)		k(300K) (cm^2/gm)	a_o(300K) (1/atm)
5060	5065	2.950600E-01	9.075015E-02
5065	5070	7.833200E-01	7.947063E-02
5070	5075	2.150200E+00	5.786203E-02
5075	5080	8.354000E-02	1.592761E-02
5060	5060	8.280350E-01	4.857689E-02
5080	5065	7.048200E-01	6.973457E-02
5085	5090	9.139600E-01	8.597215E-02
5090	5095	3.656020E+00	7.637437E-02
5095	5100	3.668129E+00	6.142457E-02
5080	5100	2.235735E+00	6.387123E-02
5100	5105	1.965260E+00	6.382954E-02
5105	5110	3.152340E+00	1.034877E-01
5110	5115	3.754440E+00	8.609766E-02
5115	5120	7.978900E+00	4.610853E-02
5100	5120	4.212735E+00	6.545165E-02
5120	5125	8.451200E-01	8.819241E-02
5125	5130	2.823600E+00	1.306756E-01
5130	5135	7.008680E+00	9.514976E-02
5135	5140	3.271049E+00	1.080296E-01
5120	5140	3.507160E+00	9.395874E-02
5140	5145	1.816410E+01	1.148952E-01
5145	5150	1.323260E+00	5.231989E-02
5150	5155	1.065332E+01	1.473064E-01
5155	5160	3.630416E+01	9.774202E-02
5140	5160	1.661121E+01	8.829245E-02

TABLE A.11 - BAND STRENGTHS AND FINE STRUCTURE PARAMETERS OF POLLUTANTS NOT INCLUDED IN TABLE D-3

Species		$\omega_1 - \omega_2$ cm^{-1}	α $cm^{-2}\ atm^{-1}$	$\overline{a}_0$ atm^{-1}
HCl	3.5 μm	2200-3200	143	.003
HF	2.5	3000-4400	450	.0015
CH_4	7.8	1195-1667	418	.01
	3.3	2700-3200	270	.01
	2.3	4082-4552	(80)	.01
C_2H_4	10.5	813-1149	365	.03
	3.2	2939-3187	(4500)	.03
PAN	12.3	757- 847	(1600)	.5
	8.3	1111-1333	(4200)	.5
C_6H_6	9.6	1007-1064	(950)	.08
	3.2	3011-3150	(9600)	.08
O_3	9.6	1006-1063	400	.05

NOTE: Values of α in parenthesis are integrals of absorption coefficients derived from limited laboratory data and may be of low accuracy.

Table A. 12 - **Absorption Coefficients for HCl**

1/CM	MICRON	K(300° K) (atm^{-1} cm^{-1})	K(600° K) (atm^{-1} cm^{-1})
2200.	4.545	.000E-32	.562E-06
2225.	4.494	.000E-32	.431E-05
2250.	4.444	.000E-32	.806E-05
2275.	4.395	.000E-32	.118E-04
2300.	4.347	.000E-32	.155E-04
2325.	4.301	.000E-32	.918E-04
2350.	4.255	.000E-32	.168E-03
2375.	4.210	.000E-32	.244E-03
2400.	4.166	.722E-07	.320E-03
2425.	4.123	.451E-05	.139E-02
2450.	4.081	.896E-05	.247E-02
2475.	4.040	.134E-04	.354E-02
2500.	4.000	.176E-04	.462E-02
2525.	3.960	.112E-03	.140E-01
2550.	3.921	.207E-03	.235E-01
2575.	3.883	.105E-02	.330E-01
2600.	3.846	.191E-02	.424E-01
2625.	3.809	.767E-02	.852E-01
2650.	3.773	.134E-01	.127E 00
2675.	3.738	.411E-01	.170E 00
2700.	3.703	.668E-01	.213E 00
2725.	3.669	.154E 00	.280E 00
2750.	3.636	.240E 00	.348E 00
2775.	3.603	.375E 00	.380E 00
2800.	3.571	.509E 00	.412E 00
2825.	3.539	.566E 00	.370E 00
2850.	3.508	.465E 00	.260E 00
2875.	3.478	.168E 00	.867E-01
2900.	3.448	.255E 00	.129E 00
2925.	3.418	.644E 00	.339E 00
2950.	3.389	.815E 00	.493E 00
2975.	3.361	.720E 00	.555E 00
3000.	3.333	.469E 00	.515E 00
3025.	3.303	.272E 00	.386E 00
3050.	3.278	.756E-01	.257E 00
3075.	3.252	.390E-01	.156E 00
3100.	3.225	.240E-02	.547E-01
3125.	3.200	.120E-02	.289E-01
3150.	3.174	.596E-05	.320E-02
3175.	3.149	.298E-05	.160E-02
3200.	3.125	.693E-10	.129E-04

Table A. 13 - **Absorption Coefficients for HF**

1/CM	MICRON	K(300°K) (atm^{-1} cm^{-1})	K(600°K) (atm^{-1} cm^{-1})
3000.	3.333	.112E-12	.684E-06
3025.	3.305	.266E-09	.115E-04
3050.	3.279	.532E-09	.224E-04
3075.	3.252	.799E-09	.333E-04
3100.	3.225	.106E-08	.441E-04
3125.	3.200	.133E-06	.550E-04
3150.	3.174	.159E-06	.659E-04
3175.	3.149	.186E-06	.768E-04
3200.	3.125	.213E-06	.877E-04
3225.	3.100	.137E-05	.765E-03
3250.	3.076	.274E-05	.146E-02
3275.	3.053	.411E-05	.218E-02
3300.	3.030	.549E-05	.287E-02
3325.	3.007	.686E-05	.357E-02
3350.	2.985	.823E-05	.427E-02
3375.	2.962	.961E-05	.497E-02
3400.	2.941	.109E-04	.566E-02
3425.	2.919	.125E-02	.496E-02
3450.	2.898	.252E-02	.425E-02
3475.	2.877	.378E-02	.354E-02
3500.	2.857	.504E-02	.284E-02
3525.	2.836	.629E-02	.213E-02
3550.	2.816	.755E-02	.142E-02
3575.	2.797	.881E-02	.721E-03
3600.	2.777	.100E-01.	.144E-04
3625.	2.758	.996E-01	.106E 00
3650.	2.739	.169E 00	.215E 00
3675.	2.721	.278E 00	.323E 00
3700.	2.702	.368E 00	.431E 00
3725.	2.684	.458E 00	.539E 00
3750.	2.666	.547E 00	.647E 00
3775.	2.649	.637E 00	.755E 00
3800.	2.631	.726E 00	.863E 00
3825.	2.614	.772E 00	.824E 00
3850.	2.597	.817E 00	.784E 00
3875.	2.580	.863E 00	.744E 00
3900.	2.564	.909E 00	.704E 00
3925.	2.547	.954E 00	.664E 00
3950.	2.531	.100E 01	.625E 00
3975.	2.515	.104E 01	.585E 00
4000.	2.500	.109E 01	.545E 00
4025.	2.484	.119E 01	.722E 00
4050.	2.469	.130E 01	.899E 00
4075.	2.453	.141E 01	..07E 01
4100.	2.439	.152E 01	.125E 01
4125.	2.424	.117E 01	.107E 01
4150.	2.409	.835E 00	.886E 00
4175.	2.395	.490E 00	.703E 00
4200.	2.380	.145E 00	.519E 00
4225.	2.366	.109E 00	.398E 00
4250.	2.352	.728E-01	.277E 00
4275.	2.339	.366E-01	.156E 00
4300.	2.325	.477E-03	.359E-01
4325.	2.312	.357E-03	.269E-01
4350.	2.298	.238E-03	.180E-01
4375.	2.285	.119E-03	.904E-02
4400.	2.272	.163E-06	.719E-04

Table A.14 -**Absorption Coefficients for CH4**

1/CM	MICRON	K (300°K) (atm^{-1} cm^{-1})	1/CM	MICRON	K(300°K) (atm^{-1} cm^{-1})
1195.	8.368	.857E-01	2925.	3.419	.570E 00
1216.	8.223	.420E 00	2940.	3.401	.900E 00
1234.	8.103	.133E 01	2957.	3.382	.100E 01
1246.	8.026	.322E 01	2975.	3.361	.860E 00
1250.	8.000	.101E 01	2985.	3.350	.670E 00
1256.	7.960	.201E 01	2993.	3.341	.442E 00
1263.	7.915	.485E 01	3000.	3.333	.750E 00
1266.	7.900	.322E 01	3010.	3.322	.267E 01
1277.	7.828	.121E 01	3020.	3.311	.400E 01
1288.	7.762	.209E 01	3030.	3.300	.930E 00
1293.	7.736	.734E 01	3037.	3.293	.505E 00
1299.	7.697	.946E 01	3050.	3.279	.900E 00
1305.	7.664	.689E 00	3060.	3.268	.114E 01
1314.	7.610	.246E 00	3075.	3.252	.135E 01
1325.	7.550	.195E 01	3086.	3.240	.140E 01
1333.	7.500	.366E 01	3095.	3.231	.137E 01
1341.	7.455	.443E 01	3100.	3.226	.131E 01
1351.	7.400	.379E 01	3110.	3.215	.110E 01
1352.	7.395	.555E 01	3125.	3.200	.740E 00
1370.	7.300	.205E 01	3150.	3.175	.262E 00
1389.	7.200	.143E 00	3160	3.164	.150E 00
1404.	7.125	.264E-01	3175.	3.150	.680E-01
1429.	7.000	.323E-01	3200.	3.125	.100E-01
1449.	6.900	.353E-01	4082.	2.450	.143E-01
1471.	6.800	.304E-01	4132.	2.420	.312E-01
1493.	6.700	.157E-01	4153.	2.408	.545E-01
1504.	6.650	.122E-01	4172.	2.397	.901E-01
1515.	6.600	.989E-02	4186.	2.389	.124E 00
1527.	6.550	.762E-02	4195.	2.384	.183E 00
1541.	6.489	.412E-01	4203.	2.379	.249E 00
1563.	6.400	.604E-02	4209.	2.376	.305E 00
1575.	6.350	.573E-02	4227.	2.366	.422E 00
1587.	6.300	.673E-02	4294.	2.329	.305E 00
1613.	6.200	.940E-02	4354.	2.297	.249E 00
1639.	6.100	.103E-01	4390.	2.278	.183E 00
1667.	6.000	.757E-02	4435.	2.255	.124E 00
2700.	3.704	.150E-01	4456.	2.244	.901E-01
2800.	3.571	.400E-01	4496.	2.224	.545E-01
2850.	3.509	.720E-01	4498.	2.223	.312E-01
2885.	3.466	.152E 00	4552.	2.197	.143E-01
2900.	3.448	.253E 00			
2915.	3.431	.400E 00			

Table A. 15 - **Absorption Coefficients for C_2H_4**

1/CM	MICRON	K(300°) (atm^{-1} cm^{-1})
813.	12.300	.828E+00
819.	12.200	.969E+00
826.	12.100	.142E+01
833.	12.000	.289E+01
840.	11.900	.517E+01
847.	11.600	.899E+01
854.	11.700	.138E+02
862.	11.600	.208E+02
869.	11.500	.293E+02
877.	11.400	.404E+02
884.	11.300	.460E+02
892.	11.200	.549E+02
900.	11.100	.612E+02
909.	11.000	.657E+02
917.	10.900	.702E+02
925.	10.800	.654E+02
934.	10.700	.109E+03
943.	10.600	.261E+03
946.	10.563	.731E+03
952.	10.500	.226E+03
955.	10.468	.182E+03
961.	10.400	.101E+03
970.	10.300	.872E+02
980.	10.200	.778E+02
990.	10.100	.717E+02
1000.	10.000	.633E+02
1010.	9.900	.552E+02
1020.	9.800	.430E+02
1030.	9.700	.279E+02
1041.	9.600	.172E+02
1052.	9.500	.114E+02
1063.	9.400	.782E+01
1075.	9.300	.406E+01
1066.	9.200	.255E+01
1098.	9.100	.176E+01
1111.	9.000	.825E+00
1123.	8.900	.567E+00
1136.	8.800	.393E+00
1149.	8.700	.329E+00
2939.	3.402	.352E+01
3022.	3.309	.184E+02
3108.	3.217	.303E+02
3158.	3.166	.184E+02
3187.	3.137	.352E+01

Table A. 16 - Absorption Coefficients for PAN

1/CM	MICRON	K(300°) $(atm^{-1}\ cm^{-1})$
757.	13.200	.663E+00
763.	13.100	.131E+01
769.	13.002	.226E+01
775.	12.900	.416E+01
781.	12.800	.117E+02
787.	12.700	.448E+02
793.	12.600	.790E+02
800.	12.500	.296E+02
806.	12.400	.106E+02
811.	12.330	.965E+01
819.	12.200	.124E+02
826.	12.100	.990E+01
833.	12.000	.868E+01
840.	11.900	.496E+01
847.	11.800	.826E+00
1111.	9.000	.630E+00
1123.	8.900	.119E+01
1136.	8.800	.777E+01
1149.	8.700	.462E+02
1165.	9.580	.138E+03
1176.	8.500	.428E+02
1190.	6.400	.138E+01
1204.	8.300	.119E+01
1250.	8.000	.239E+01
1265.	7.900	.144E+02
1263.	7.790	.978E+02
1298.	7.700	.546E+02
1315.	7.600	.153E+02
1333.	7.500	.113E+02

Table A. 17 - C_6H_6 - BENZENE

1/CM	MICRON	K(300° K) (atm^{-1} cm^{-1})
1007.	9.923	.923E+00
1013.	9.867	.471E+01
1018.	9.821	.150E+02
1023.	9.773	.226E+02
1029.	9.712	.183E+02
1035.	9.659	.464E+02
1036.	9.648	.590E+02
1038.	9.629	.464E+02
1040.	9.610	.150E+02
1042.	9.588	.905E+01
1046.	9.559	.150E+02
1047.	9.524	.188E+02
[illegible]	9.490	.150E+02
[illegible]	9.427	.471E+01
1064.	9.397	.923E+00
3011.	3.321	.923E+00
3030.	3.300	.471E+01
3037.	3.292	.150E+02
3042.	3.287	.464E+02
3058.	3.270	.170E+03
3124.	3.201	.464E+02
3139.	3.185	.150E+02
3147.	3.177	.471E+01
3150.	3.174	.923E+00

Table A. 18-O_3 - OZONE

1/CM	MICRON	K(300° K) (atm^{-1} cm^{-1})
1006.	9.940	.235E+01
1010.	9.900	.345E+01
1017.	9.830	.500E+01
1024.	9.770	.615E+01
1028.	9.722	.915E+01
1036.	9.650	.585E+01
1042.	9.590	.405E+01
1049.	9.530	.790E+01
1054.	9.490	.950E+01
1057.	9.460	.865E+01
1063.	9.400	.405E+01